



| | |
|----------------------------------|--|
| Publication Year | 2019 |
| Acceptance in OA | 2020-12-30T14:48:40Z |
| Title | What is a globular cluster? An observational perspective |
| Authors | GRATTON, Raffaele, BRAGAGLIA, Angela, CARRETTA, Eugenio, D'ORAZI, VALENTINA, LUCATELLO, Sara, SOLLIMA, ANTONIO LUIGI |
| Publisher's version (DOI) | 10.1007/s00159-019-0119-3 |
| Handle | http://hdl.handle.net/20.500.12386/29384 |
| Journal | THE ASTRONOMY AND ASTROPHYSICS REVIEW |
| Volume | 27 |

What is a Globular Cluster?

An observational perspective

Raffaele Gratton¹ · Angela Bragaglia² ·
Eugenio Carretta² · Valentina D'Orazi^{1,3} · Sara
Lucatello¹ · Antonio Sollima²

Received: date / Accepted: date

Abstract Globular clusters are large and dense agglomerate of stars. At variance with smaller clusters of stars, they exhibit signs of some chemical evolution. At least for this reason, they are intermediate between open clusters and massive objects such as nuclear clusters or compact galaxies. While some facts are well established, the increasing amount of observational data is revealing a complexity that has so far defied the attempts to interpret the whole data set in a simple scenario. We review this topic focusing on the main observational features of clusters in the Milky Way and its satellites. We find that most of the observational facts related to the chemical evolution in globular clusters are described as being primarily a function of the initial mass of the clusters, tuned by further dependence on the metallicity – that mainly affects specific aspects of the nucleosynthesis processes involved – and on the environment, that likely determines the possibility of independent chemical evolution of the fragments or satellites where the clusters form. We review the impact of multiple populations on different regions of the colour-magnitude diagram and underline the constraints related to the observed abundances of lithium, to the cluster dynamics, and to the frequency of binaries in stars of different chemical composition. We then re-consider the issues related to the mass budget and the relation between globular cluster and field stars. Any successful model of globular clusters formation should explain these facts.

Keywords Globular Clusters · Open Clusters · The Galaxy

Contents

| | | |
|---|-------------------------------------|---|
| 1 | Introduction | 3 |
| 2 | Chemical anomalies in GCs | 6 |

¹INAF-Osservatorio Astronomico di Padova, Vicolo dell'Osservatorio 5, 35122 Padova (Italy), Tel.: +39-049-661303, E-mail: raffaele.gratton@inaf.it · ²INAF-Osservatorio di Astrofisica e Scienza dello Spazio, via P. Gobetti 93/3, 40129 Bologna (Italy) · ³Monash Centre for Astrophysics, School of Physics and Astronomy, Monash University, Melbourne, Clayton 3800, Australia.

| | | |
|-------|---|-----|
| 2.1 | Basics of multiple stellar populations in GCs | 6 |
| 2.2 | Observational approaches | 7 |
| 2.3 | A mechanism to rule them all | 13 |
| 2.4 | Neutron-capture elements | 16 |
| 2.5 | Some caveats | 17 |
| 3 | What is a GC | 18 |
| 3.1 | Relation between anti-correlations | 18 |
| 3.2 | Cluster masses | 21 |
| 3.3 | Small clusters | 24 |
| 3.4 | Type I and Type II clusters | 25 |
| 3.5 | Metallicity dependence | 28 |
| 3.6 | Is there an age dependence? | 29 |
| 4 | Impact of chemical anomalies on stellar evolution | 31 |
| 4.1 | The main sequence | 31 |
| 4.2 | RGB bump | 32 |
| 4.3 | The horizontal branch | 34 |
| 4.4 | Asymptotic giant branch stars vs red giant stars | 36 |
| 5 | Lithium | 40 |
| 5.1 | Lithium and mixing | 40 |
| 5.2 | Lithium and multiple populations: observations | 40 |
| 5.3 | Lithium and multiple population: some considerations | 44 |
| 6 | Evidence from dynamics | 45 |
| 6.1 | Gas dynamics | 45 |
| 6.2 | Stellar dynamics | 48 |
| 7 | Binaries | 52 |
| 7.1 | Overall frequency of binaries GCs | 53 |
| 7.1.1 | Observational evidence | 53 |
| 7.1.2 | Evolution of binary systems in GCs | 54 |
| 7.2 | Frequency of binaries in different stellar populations | 54 |
| 7.3 | Toy model and the different populations | 56 |
| 7.4 | Blue stragglers, CH/Ba stars, and the contribution of binaries to the fraction of stars with chemical anomalies | 57 |
| 8 | GCs and the halo | 59 |
| 8.1 | Mass budget | 59 |
| 8.1.1 | The case of Type I GCs | 59 |
| 8.1.2 | The case of Type II GCs | 63 |
| 8.1.3 | Conclusions about mass budget | 65 |
| 8.2 | GC stars in the field | 66 |
| 9 | Conclusions and open issues | 69 |
| 10 | Appendix 1: Summary of data for Milky Way GCs | 99 |
| 11 | Appendix 2: Summary of data for MC clusters | 100 |

“16. Of Globular Clusters of Stars.

The objects of this collection are of a sufficient brightness to be seen with any good common telescope, in which they appear like telescopic comets, or bright nebulae, and under this disguise, we owe their discovery to many eminent astronomers; but in order to ascertain their most beautiful and artificial construction, the application of high powers, not only of penetrating into space but also of magnifying are absolutely necessary; and as they are generally but little known and are undoubtedly the most interesting objects in the heavens, I shall describe several of them, by selecting from a series of observations of 34 years some that were made with each of my instrument, that it may be a direction for those who wish to view them to know what they may expect to see with such telescopes as happen to be in their possession.”

Herschel, W. 1814, Philosophical Transactions, 104, 248

1 Introduction

Globular clusters (GCs: [Herschel 1814](#)) are usually considered as a class of stellar agglomerates characterized by being compact (half-light radius up to a few tens of pc, with more typical values of about 3 to 5 pc), bright (mean absolute visual magnitude around $M_V = -7$), old (in most cases, ages around 10 Gyr), and (within the Milky Way - MW) to be representative of the halo, thick disk and bulge, but being absent in the thin disk¹. Being abundant in the halo and thick disk, they are often metal-poor and have quite extreme kinematics. There is evidence that the peak of the formation of GCs pre-dates most of the stellar formation in galaxies and that they may have played an important role in the early formation of galaxies and even in re-ionization (see e.g. the discussion in [Renzini 2017](#)). However, at a closer scrutiny the classical definition of GCs becomes a bit vague and there are many objects that are classified as GCs based on only a few of these criteria. About ten years ago, [Carretta et al. \(2010c\)](#) proposed a new definition of GCs, that is related to the chemical inhomogeneities that are characteristic of these objects, and that differentiate them from the less massive open clusters: genuine GCs are stellar systems showing anti-correlations among the abundances of light-elements, whose main and most widespread example is the Na-O anticorrelation. While classification according to this criterion is still not perfect, it has the advantage to shift the attention to a fundamental characteristics of GCs, that is their complex formation scenarios and the clear signatures of a chemical evolution within them. In this sense, GCs are objects intermediate between normal stellar clusters and the blue compact galaxies, as indicated by their location in the

¹ Globular clusters may have been formed in-situ or have been accreted, see the classical paper by [Searle and Zinn \(1978\)](#) and the recent results coming out from the Gaia mission, as presented e.g. in [Gaia Collaboration et al. \(2018\)](#); [Myeong et al. \(2018c\)](#); [Helmi et al. \(2018\)](#).

mass-to-light ratio versus luminosity plane (Dabringhausen et al. 2008; Forbes et al. 2008). While how a GC forms and what are its very early phases are still strongly debated topics, we have at least in theory the possibility of separating chemically, and in some case dynamically, quite pure populations, sharing very similar chemical composition reflecting single nucleosynthesis effects. In this environment, stars form with very peculiar chemical composition, that are very rarely observed in the main population of galaxies, where we generally see the combination of many different nucleosynthesis processes.

It is then not surprising that since their discovery from low resolution spectra and intermediate band photometry in the '70s, chemical “inhomogeneities” in individual GCs raised a considerable interest. Reviews of very early results can be found in Kraft (1979) and of later progress obtained mainly thanks to echelle spectrographs on 4m telescopes in Kraft (1994). The availability of high quality spectroscopic data for large samples of stars in many individual clusters allowed by multi-fiber high-resolution spectrographs on 8m class telescopes and the exquisite photometry provided by HST have provided an important breakthrough in the first decade of the new millennium, with the acknowledgment that the “inhomogeneities” are due to a distinct chemical evolution within the GCs that seem to be characterized by multiple stellar populations. Reviews of the progress, more focused on the observational side, were given by Gratton et al. (2004); Piotto (2010); Gratton et al. (2012a).

In the mean time, a number of discussions were rather more focused on the scenarios that may explain the multiple populations (see e.g. Renzini 2008; Schaerer and Charbonnel 2011; Krause et al. 2013; Renzini et al. 2015; Bastian and Lardo 2015; D’Antona et al. 2016; D’Ercole et al. 2016; Bastian et al. 2015a; Prantzos et al. 2017; Bastian and Lardo 2018; Gieles et al. 2018). The conclusion of the review by Bastian and Lardo (2018) is that there is not a unique simple scenario able to explain the variety of issues related to the multiple population problem. This suggests that GCs are likely not a homogeneous sample of objects, but rather may include different histories. This fact should be perhaps considered not too surprising for objects that represent transitions between single episodes of star formation - characteristics of open clusters - and more continuous stories of star formation - characteristics of galaxies.

Notwithstanding these difficulties, in this review we will generally assume that the different populations are indeed different generations of stars. As already discussed in the previous reviews Gratton et al. (2004, 2012a), there are various arguments supporting this assumption. A successful scenario should not only explain enrichment in some element such as He or Na - this is relatively easy to achieve also in alternative scenarios because it may be obtained by integrating in a star a small fraction of polluted material - but also the large depletion of quite robust nuclei such as O and Mg, that are observed in a significant fraction of the GC stars. This depletion can only be obtained by having stars that are mainly composed of the ejecta of previous generations, in spite of the fact that only a small fraction of the ejecta of a generation of stars are expected to be actually depleted of these elements. In fact, alternative schemes such as selective chemical enrichment during star formation and deep mixing fail completely to reproduce either the observed abundance pattern or the fact that the abundance anomalies are observed in a similar way throughout the whole

colour-magnitude diagram. Finally, in many cases - though possibly not in all cases - discrete populations can be clearly discerned. However, we concur with [Bastian and Lardo \(2018\)](#) that the scenarios based on multiple generations considered so far have major difficulties and that we should be open to other possible explanations.

In this review we present an update of the field, exploiting the new look that is provided by additional spectroscopic data, both at high and low-resolution, that is accumulating (see the review by [Bastian and Lardo 2018](#)), by the extensive UV photometry obtained with HST-WFC3 (e.g. [Piotto et al. 2015](#), for the MW, [Niederhofer et al. 2017a](#), for the MW satellites) and by the estimates of the initial cluster masses (e.g. [Baumgardt et al. 2019](#)) that are now possible thanks to the orbital parameters extracted from the Gaia DR2 data ([Gaia Collaboration et al. 2018](#)), as well as a large number of other important contributions. This impressive amount of data is revealing a complex scenario, with different types of clusters likely having different evolution, that left traces imprinted in the chemistry of their stars. An help can be given by the so-called “chromosome map”, first introduced by [Milone et al. \(2012e, 2017a\)](#), for several tens of GCs (see Fig. 1). In the following, we will make extensive use of their notation of Type I and II clusters, based on this diagram (see Section 3.3), even if we alert that exact classification of some GC may be questioned.

Due to space limitations, we have to operate a selection on topics, privileging the observer’s “route” and focusing on papers discussing large samples. In addition, we will not speak of the wide main sequence turn off (MSTO) of young and intermediate age clusters in the MCs. This had been originally considered as an evidence for multiple populations with large age differences in these clusters too (e.g. [Bertelli et al. 2003](#); [Milone et al. 2009](#); [Goudfrooij et al. 2014](#)). However, recent developments seem rather to indicate a combination of spread in stellar rotation and possibly presence of binaries as an explanation (e.g. [Dupree et al. 2017](#); [D’Antona et al. 2017](#); [Milone et al. 2018a](#); [Marino et al. 2018a](#); [Bastian et al. 2018](#); [Lim et al. 2019](#)), as originally proposed by [Bastian and de Mink \(2009\)](#). We will also not describe the evidence from variable stars (in particular, RR Lyrae) for which we refer to [Catalan \(2009\)](#); [Gratton et al. \(2010a\)](#), and [Jang et al. \(2014\)](#). In addition, we will limit our analysis to the meta-Galaxy, that is the MW and its close satellites; reviews of the properties of GCs in further galaxies can be found in [Brodie and Strader \(2006\)](#); [Kruijssen \(2014\)](#); [Grebel \(2016\)](#).

Finally and more importantly, we will not discuss the vast literature on models of cluster formation and evolution and will only touch upon some scenarios for explaining the multiple population phenomenon (for this, see [Bastian and Lardo 2018](#) and more recent papers).

In Section 2 we will introduce the chemical anomalies usually seen in GCs. In Section 3 we will describe the main observed dependencies considering various classes of GCs. In Section 4 we will review the impact of chemical anomalies on the stellar evolution. In Section 5, 6 and 7 we will discuss three important pieces of information, often neglected in the discussion of GCs: that is, the evidence that concern Lithium abundances, dynamics, and binarity. In Section 8 we will revisit the connection existing between GCs and the general field. Finally, we draw some conclusions in Section 9. Relevant data used throughout this review are collected in the Appendices.

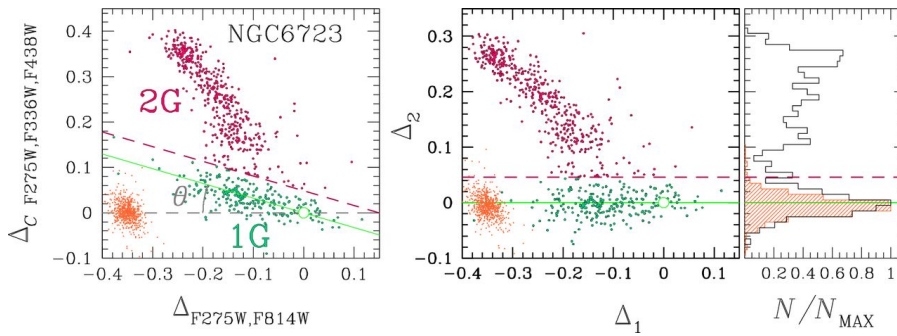


Fig. 1 Example of a chromosome map as taken from Milone et al. (2017a). As explained in the caption of the figure of their paper, this map is used to identify the two samples of bona-fide first-generation (indicated as 1G, FG in the present text) and second-generation (2G in the figure, SG in this text) stars in NGC 6723. The left-hand panel shows Δ_C (F275W, F336W, F438W) versus Δ_1 (F275W, F814W). The green line through the origin of the frame is a fit to the sequence of candidate 1G=FG stars. The middle panel shows the Δ_2 versus Δ_1 plot where these new coordinates have been obtained by a suitable rotation of the plot in the left-hand panel. The histogram in the right-hand panel shows the distributions of the Δ_2 values. The orange points in the left-hand and middle panels show the distribution of the observational errors and their Δ_2 distribution is represented by the shaded orange histogram in the right-hand panel. The dashed magenta lines separate the selected 1G=FG and 2G=SG stars, which are coloured aqua and magenta, respectively, in the left-hand and middle panels.

2 Chemical anomalies in GCs

The simplest and clearer way to define multiple stellar populations in GCs is through their opposite. A *simple* stellar population (SSP) is an ensemble of coeval (single) stars with the same initial chemical composition. Thus, when we see stellar systems hosting stars of different starting chemistry and with (even small) age differences we observe multiple stellar populations.

2.1 Basics of multiple stellar populations in GCs

Almost a century may have gone by since pioneering observations pointed out that star-to-star abundance variations existed among stars of otherwise mostly chemically homogeneous GCs (see the nice historical notes in Smith and Briley 2006). By comparing elemental abundances in field and cluster stars (e.g. Gratton et al. 2000; Smith and Martell 2003; see the review by Gratton et al. 2004) it is immediately evident what is observed for the multiple population phenomenon, in what stellar systems, and at which evolutionary phase.

Large abundance variations are mostly seen among light elements, starting from the elusive He up to Sc. The GC NGC 2808 is the ideal “showroom” for all involved elements in mono-metallic GCs, because it was extensively studied with spectroscopy at different evolutionary phases: red giant branch (RGB)/red horizontal branch (RHB): Norris and Smith (1983); Carretta et al. (2003); blue hook: Moehler et al. (2004); RGB: Carretta et al. (2004); Carretta (2006); Carretta et al. (2006); Pasquini et al. (2011); Carretta (2014); Mucciarelli et al. (2015a); D’Orazi et al. (2015); Carretta

et al. (2015, 2018); blue horizontal branch (BHB): Pace et al. (2006); main sequence (MS): Bragaglia et al. (2010b); horizontal branch (HB): Gratton et al. (2011a); Marino et al. (2014); RGB/asymptotic giant branch (AGB): Wang et al. (2016); AGB: Marino et al. (2017). If we add also the indirect evidence provided by photometry on the MS (e.g. D’Antona et al. 2005; Piotto et al. 2007; Milone et al. 2019a) we see that the multiple population phenomenon concerns stars in *all* the stages of their lifetime, from very low-mass dwarfs to giants.

Abundance variations are not randomly distributed. By looking at the relationships summarized in Fig. 2 and Fig. 3 and made using the same sample of stars, we can appreciate that the star-to-star variations are all linked by (anti)correlations with each other. Moreover, the examples of NGC 2808 and of almost all GCs studied so far show that the “direction” of these (anti)correlations is uniquely determined: the departures from the level imprinted by supernova nucleosynthesis all go in the same sense. Oxygen abundances may only be depleted, there is no observed star with [O/Fe] enhanced much above the plateau given by SN II ejecta, nor is Na found much below the level observed in field stars of similar metallicity, its abundance can be only enhanced above this level. This is crucial to understand the origin of the chemical pattern observed in GCs.

Multiple populations are found in almost all Galactic GCs, regardless of their Galactic parent population (halo, disk, bulge); for an updated list see Bragaglia et al. (2017) and the Appendix. Both those GCs formed *in situ* and those thought to have formed in external galaxies and later accreted by the Milky Way are found to host multiple populations. The phenomenon is ubiquitous in “tiny” GCs as well as in the most massive ones (probably former nuclear clusters of dwarf galaxies, like ω Cen=NGC 5139 and M 54=NGC 6715), in mono-metallic (intended as overall metal abundance [Fe/H]) as well as iron complex GCs. In the last, the multiple populations are simply repeated in each individual metallicity component. Multiple populations are not found among field stars of dwarf galaxies (e.g. Sgr, Fornax, Large Magellanic Cloud - LMC) but only observed in their associated old² GCs (e.g. Carretta et al. 2010b,a; Letarte et al. 2006; Johnson et al. 2006; Mucciarelli et al. 2009; Larsen et al. 2014). Finally, no anti-correlation among light elements was ever observed in open clusters, whose average abundances follow the pattern of other field thin disc stars (see e.g. de Silva et al. 2009; Bragaglia et al. 2014; MacLean et al. 2015) and Sect. 3.3.

2.2 Observational approaches

Since the finding by Lindblad (1922) of giant stars with anomalously weak CN bands in NGC 6205=M 13, observations of abundance variations in GCs were performed either through spectroscopy or photometry. Of course, spectroscopy is the privileged method, because the essence of multiple stellar populations resides in abundance differences. However, we may think that photometry in different bands is equivalent to very low resolution spectroscopy and it allows access to large samples in a short observing time and better handling of crowded regions close to the cluster center.

² See, however, Sect. 3.6 for the recent extension to lower ages.

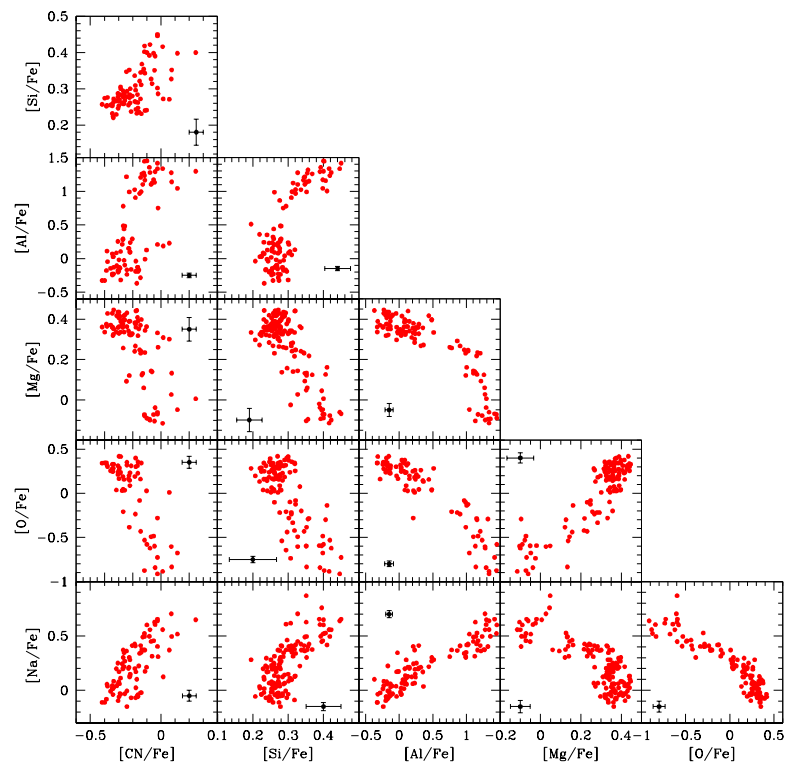


Fig. 2 Run of abundance ratios for light elements in RGB stars in NGC 2808. O, Na, Si, Mg are from Carretta (2015), Al and CN abundances from Carretta et al. (2018). The figure is adapted from the invited review by Carretta (2016).

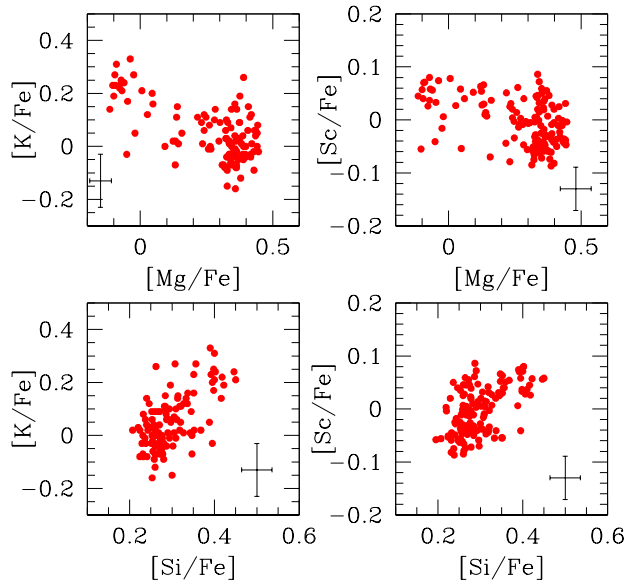


Fig. 3 As in previous figure for Mg, Si, Sc from [Carretta \(2015\)](#) and K abundances from [Mucciarelli et al. \(2015a\)](#).

The information accessible via the different techniques on the various involved species is principally dictated by the spectral resolution. At low resolution, lines are blended in spectra. This implies resorting to spectral synthesis and/or line indices to extract the information on abundances. Traditionally, this is the most followed approach to detect differences between populations based on the molecular features of CN and CH (and, less often, NH). To obtain detailed estimates of C and N, calibration through spectral synthesis is required (see the review by [Smith 1987](#); [Gratton et al. 2004, 2012a](#) for references on early and following works using this technique). The gain in observing time due to the low spectral resolution is exploited in particular for stars with severe flux limitations, either because they are intrinsically faint (as the case of unevolved stars in Galactic GCs, e.g. [Briley et al. 2004](#); [Harbeck et al. 2003](#); [Pancino et al. 2010](#)) or distant, as giants in old clusters in the LMC (e.g. [Hollyhead et al. 2019](#)). The chief drawback is that there is no indicator of O abundance from low resolution spectroscopy, though, interestingly, O abundance variations can be seen using UV photometry. This fact in turn generates uncertainties in the determination

of C and N abundances, since their derivation from molecular CH and CN features requires the knowledge of O abundance, in particular for bright giants, where the CO formation is favoured. On the other hand, the strength of molecular bands decreases in warmer stars (such as dwarfs near the turn-off), with a bias against low metallicity clusters, where features of bi-metallic molecules like CN may become vanishingly weak. Despite these limitations, low resolution spectroscopy is widely used to detect “first-pass” evidence of abundance variations in C/N for moderately large sample of stars in many Galactic and extra-galactic GCs, in particular when multi-object spectroscopy is feasible. Only a few heavier elements can be measured with this technique. The atomic lines visible even at low resolution allow to compute e.g. the Lick indexes, that are essentially expressing the overall metallicity (see Fig. 9 in Kim et al. 2016), or to derive abundances of species like Cr, Sr, Ba, and Mg using spectrum synthesis (e.g. Gratton et al. 2012c; Dias et al. 2016). The calibration of low resolution spectroscopic observations of Ca features are also frequently used. In the near-IR the reduced equivalent width of the Ca II triplet is considered (see Olszewski et al. 1991; Armandroff and Da Costa 1991; and Rutledge et al. 1997; Da Costa 2016 for extensive applications), whereas in the near-UV spectral region, the calcium index HK’ (Lim et al. 2015) based on the Ca II H & K resonance lines provides metallicity estimates from a set of calibrating GCs with [Fe/H] determined from high resolution spectroscopy. In the last case, all these Ca (and Mg) lines are among the strongest lines in the stellar spectra; although the origin of multiple population is not supposed to be related primarily to polluting source altering the Fe content, the growing number of iron complex GCs makes useful to have methods for a quick first screening of the cluster overall metallicity and dispersion, in particular for distant objects.

Blending of lines is more easy to deal with high-resolution spectroscopy, and accurate equivalent widths of many transitions for numerous elements may be obtained, provided the spectral coverage is large enough. Abundances of many different species are then simultaneously derived, in particular those for elements that differ in multiple stellar populations. Abundance ratios may be then constructed for all the relevant species³. In other words, with high-resolution spectroscopy we are measuring the concentration of atoms of different species in the atmosphere of stars of different stellar populations. With respect to lower resolution spectra, the chief disadvantage is that, for a given magnitude, less flux is available per resolution element and thus longer integration times are required to achieve high signal-to-noise ratios (SNR). The problem is partly alleviated by using modern multi-object spectrographs mounted at 8-10 m class telescopes. Nevertheless, despite the multiplex advantage, the increased observing times forcibly reduces the sample size. Good statistics is routinely possible only for RGB and AGB stars, is more limited for HB stars (mainly for concerns related to abundance analysis in hot objects), and for dwarf stars is more or less limited to nearby GCs (such as 47 Tuc=NGC 104, M 4=NGC 6121, NGC 6397, NGC 6752, ω Cen=NGC 5139).

A particular care must be applied for He, since the direct determination of its abundance is plagued by the lack of photospheric lines in cool stars. Therefore, only

³ For most elements, we adopt the usual spectroscopic notation, *i.e.* $[X]=\log X_{\text{star}} - \log X_{\odot}$ for any abundance quantity X, and $\log \epsilon(X) = \log N_X/N_H + 12.0$ for absolute number density abundances. For Helium, we use Y, that is the fraction of He in mass.

a handful of giants have He abundances derived from the near IR line at 10,830 Å. Moreover, this line forms in the upper chromosphere, in non-LTE conditions and the analysis requires using complex chromospheric models, and even accounting for spherical geometry of the atmosphere (see [Pasquini et al. 2011](#); [Dupree and Avrett 2013](#)). The only other direct He determinations are based on the weak He I triplet at 5875.6 Å discovered in the spectra of late-type stars by [Wilson and Aly \(1956\)](#). This line is vanishingly weak in stars cooler than about 8000 K and cannot be safely used above 11500 K. In warmer stars the measured He content is not the original one of the star at birth, but the value resulting from sedimentation caused by diffusion and element stratification (e.g. [Behr et al. 1999, 2000](#); [Behr 2003](#)). For these reasons, He is only measured directly in HB stars in this limited temperature range (e.g. [Villanova et al. 2009](#); [Gratton et al. 2014](#)), and its abundance in GCs is mainly obtained by indirect estimates based on photometry. Apart from He and related problems, high-resolution spectroscopy is a powerful tool to study multiple stellar populations because the measured indicators are directly related to the stellar composition, i.e., to the essence of multiple populations. Age differences of a few or a few tens of Myr expected in most scenarios of multiple populations are not detectable in colour-magnitude diagrams. On the other hand, the abundance differences related to these scenarios, several tenths of a dex in the abundances of elements such as C, N, Na, O, Mg, Al, are well measurable from spectra. These differences cannot be produced within the currently observed low mass stars.

Finally, the photometric approach consists in tracing the abundance variations through their effects (flux variations) in selected band-passes where some molecular features of CNO elements are located. As such, panoramic photometry can be considered as spectroscopy at very low resolution and with very high multiplexing gain. Investigation of multiple stellar populations is possible with any photometric system including some filters (located in the UV/blue regions) whose band-passes cover features of interest (essentially CN, NH, OH, CH molecular bands). Broad band (Sloan: [Lardo et al. 2011](#); Johnson-Cousins: e.g. [Monelli et al. 2013](#); HST: e.g. [Piotto et al. 2015](#); [Larsen et al. 2014](#); intermediate band Strömgren: e.g. [Grundahl et al. 1998](#); [Yong et al. 2008a](#); [Carretta et al. 2011b](#), and narrow band systems such as Ca-photometry: [Anthony-Twarog et al. 1991](#); [Lee et al. 2009b,a](#); [Lee 2015](#)) have all been used to detect variations in light-elements abundances, separate different populations on colour-magnitude diagrams, and trace their radial distribution thanks to the large statistics possible with photometry. The dichotomy low/high resolution is partially reproduced also for photometric observations, since the crowded cores of GCs can be only resolved with space-based photometry. However, this is possible at the price of a limited spatial coverage, and this occurrence may give some problems when radial gradients in the distribution of the population ratios are present (e.g. [Lee 2019](#)), unless they are combined with ground-based data (e.g. [Milone et al. 2012e](#); [Savino et al. 2018](#)). Also, the definition of what are the multiple populations may differ somewhat according to the study and the adopted photometric system, although in most cases there is a reasonable agreement between spectroscopy and photometry classification (see the discussions in [Carretta et al. 2011b](#); [Savino et al. 2018](#); [Lee 2019](#) and [Marino et al. 2019](#)).

Due to the above limitations related to spectroscopic detection of He, photometry is the most used approach to estimate the He abundance and variations, by exploiting the prediction of stellar evolution for He-enhanced models (e.g. Salaris et al. 2006). Even if the absolute He abundance cannot be given by these methods, relative estimates can be provided by differences in magnitude of RGB-bump stars and in colour of RGB stars (Bragaglia et al. 2010a, e.g.), colour spreads on the main-sequence (Norris 2004; Piotto et al. 2007; Gratton et al. 2010a, e.g.), and comparison of multi-wavelength HST photometry with synthetic spectra (e.g. Milone et al. 2018c). An additional drawback of photometry is that the accessible pattern of multiple population is limited to the lightest elements (He, C, N). Oxygen can be estimated only when the HST filter F275W is available, and this introduces the same degree of uncertainty as seen for low dispersion spectroscopy of CN and CH bands. No indicator is available for heavier elements, apart from Ca (see Lee 2019 and references therein), measuring the Ca II H & K lines through narrow band photometry (Anthony-Twarog et al. 1991; Lim et al. 2015).

Further improvements of photometric methods can come from the upcoming survey J-PAS (see Benitez et al. 2014 and <http://www.j-pas.org/> for information), which will observe about 8000 deg² of the Northern sky with 56 narrow band filters (about 150 Å each, covering the $\sim 3750 - 8100$ Å interval) which will hopefully permit to measure different light element abundances. A tentative separation of the upper RGB of NGC 7078=M 15 has already been presented by Bonatto et al. (2019) who use J-PLUS data (J-PLUS is meant to calibrate J-PAS and uses a combination of 12 wide, intermediate, and narrow band filters).

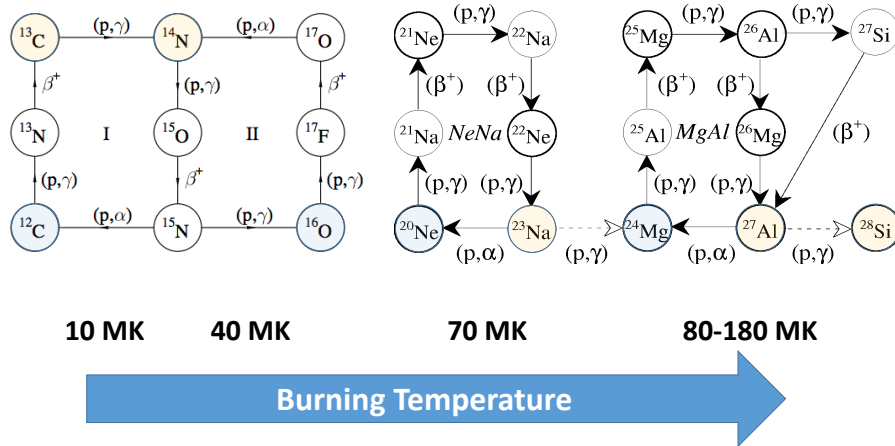


Fig. 4 The upper part of the figure shows the main p-capture cycles considered in this review: from left to right the CNO-cycle, the Ne-Na cycle, and the Mg-Al cycle. We marked in light orange/light blue those nuclei considered in this review that are produced/destroyed by the various cycles. The lower part of the figure shows the values of the temperature at which the various cycles become efficient. These temperatures are indicative; they depend on the evolutionary phase where the burning occurs. Adapted from Salaris et al. (2002)

2.3 A mechanism to rule them all

To understand the nature and origin of multiple stellar populations in GCs, the abundance ratios represent our privileged investigation tool, because they provide an unique source of *thermometers* and *chronometers* to get insights on this phenomenon. Different elements are forged/destroyed at different temperatures, hence by looking at abundance ratios we have an accurate description of the temperature stratification of the sites where these species were altered (e.g. Prantzos et al. 2007, 2017; D'Antona et al. 2016). Moreover, stars of different masses are able to reach different inner temperature, and mass simply means different evolutionary times. Of course, this picture is schematic because the material from which stars of the second generation forms likely comes from stars of the first generation in a range of masses that mix together, possibly blurring and making more confuse the picture.

Simply by looking at the full set of abundance ratios, (anti-)correlated to each other, as observed e.g. in NGC 2808, we may understand several key facts. In the vast majority of GCs (those also classified as Type I GCs, see Sect. 3.4), the main nucleosynthesis mechanism is very likely proton-capture reactions in H-burning at high temperature (Denisenkov and Denisenkova 1989; Langer et al. 1993); see Fig. 4. In the H-burning of main sequence stars, the conversion of C \rightarrow N proceeds at fusion temperature $\geq 10 \times 10^6$ K, while the activation of the ON branch of the CNO cycle requires higher inner temperatures ($\geq 40 \times 10^6$ K). The Na-O anti-correlation, widely observed in almost all GCs, simply results from this conversion of O and the simultaneous production of Na from the NeNa chain, operating at the same temperatures. Higher temperatures ($\geq 70 \times 10^6$) allow Al to be produced from Mg, whereas $T > 80 \times 10^6$ and $> 180 \times 10^6$ are necessary to produce Si and K, respectively (see Prantzos et al. 2017), that are observed in a fraction of the GCs. Temperatures are even higher when considering hot bottom burning (see e.g. D'Antona et al. 2016). Armed with these basics thermometers, an ESO Large Program led Gratton et al. (2001) to change once and for all the paradigm of GCs as simple stellar population. They found a clear Mg-Al anti-correlation among unevolved stars in NGC 6752. Currently observed low mass stars cannot reach the temperature threshold required to activate the Mg \rightarrow Al conversion, thus this nuclear burning must have occurred in more massive stars, already evolved and dead, of a first stellar generation. The (anti-)correlation among light elements are simply a manifestation of the multiple stellar populations.

There are still problems for theoretical models to quantitatively reproduce the observations (Bastian et al. 2015b). This led these authors to suggest that possibly the observed pattern cannot be attributed to nucleosynthesis and that alternative scenarios not invoking nuclear burning must be explored. Unluckily, no practical alternative scenario has been found so far. Let us recall the most relevant facts.

- We know since long time that C and N are anti-correlated in GC stars, but at the same time the sum C+N increases as C decreases, already in unevolved stars (e.g. Briley and Cohen 2001; Briley et al. 2004). Either the conversion of O into N must be happening or we are seeing a variable level of N. However, when the trio C, N, O is simultaneously available, the sum C+N+O is found to be quite constant in the majority of GCs, both in dwarfs (Carretta et al. 2005) and in giants (e.g. Ivans

et al. 1999; Smith et al. 2005; Yong et al. 2008b, 2015; Mészáros et al. 2015). Notably, there are exceptions to this rule, that is, clusters where the sum C+N+O is not constant; we will come back to this point Section 3.4.

- The Na-Al correlation mimics the Na-O anti-correlation, in the sense that links two chains (Ne-Na and Mg-Al) sampling different temperature ranges. Moreover, the sum Al+Mg does not vary in most GCs (Mészáros et al. 2015).
- In other GCs, while the sum Mg+Al does not stay constant, the sum Mg+Al+Si does, as in NGC 6388 (Carretta and Bragaglia 2018). This agrees with the findings that in very metal-poor and/or massive GCs Si is anti-correlated with Mg and/or correlated with Al abundances (e.g. Yong et al. 2015; Carretta et al. 2009c; Mészáros et al. 2015), an occurrence explained by leakage of Mg on Si bypassing the Al production, when interior temperatures exceed $\sim 65 \times 10^6$ K (Karakas and Lattanzio 2003).
- Star-to-star abundance variations can be traced up to the heavier elements like K and Sc. Abnormal abundances of these elements are actually observed only in about 10-15% of stars in peculiar GCs such as NGC 2419 and NGC 2808 (Mucciarelli et al. 2012a, 2015a; Carretta et al. 2015); they are however robustly documented and explained as the output of the Ar-K chain, that bypasses Al production for temperatures in excess of 150 MK (Ventura et al. 2012; Prantzos et al. 2017).
- Finally, there is no correspondence between the observed anti-correlations and either the temperature of condensation on grains or the sensitivity to radiation pressure and sedimentation, the only other selective effects that are known to affect the chemical composition of main sequence stars. For instance, in both cases we should expect that the abundances of CNO are correlated with each other, and Li with Na (Meléndez et al. 2009; Behr et al. 1999); these patterns are at odds with what is required to explain abundances in GC stars.

All these observations show not only the effects of complete CNO cycling, but also that all possible chains of proton-capture reactions (Ne-Na, Mg-Al, Ar-K) were active: the resulting abundances all go in the sense predicted by stellar nucleosynthesis (some being depleted, some produced) in the proton-capture reactions occurring during H-burning, with a few exceptions. Other nucleosynthesis processes such as triple- α , s -process, and explosive nucleosynthesis should be considered for a minority of GCs (also classified as Type II, see Sect. 3.4). In addition, we know that the gas polluted by these ejecta was not simply accreted to the surface of forming stars (Gratton et al. 2001; Cohen et al. 2002; Briley et al. 2004), but went into the formation of the whole star. This conclusion stems from the observation that the same chemical patterns (e.g. the Na-O anti-correlation), are found with very similar extent in both dwarf and giant stars (e.g. Dobrovolskas et al. 2014 and Cordero et al. 2014 for 47 Tuc=NGC 104), despite very different stellar structures (negligible convective envelopes in MS *versus* convection extended to more than half of star on the RGB) and H-burning mode (p-p in core burning on the MS and CNO-shell burning along the RGB).

Differences in the multiple stellar populations are due to the ashes of nuclear burning. However, this is not the whole story. Both theory and observations strongly

suggest that a majority of the stellar populations following the first burst of star formation must be composed by a mix of nuclearily processed ejecta and gas with pristine composition. First, since star formation is far from being a 100% efficient process (e.g. [Lada and Lada 2003](#)) there should be gas leftover from the first star formation burst, available for new episodes of stellar formation until pushed out from the cluster. At the same time, if GCs form in high pressure discs of high redshift galaxies (e.g. [Kruijssen 2015](#)), some fresh gas may be also re-collected from the surrounding ambient medium (see [D’Ercole et al. 2016](#)). More importantly, most of the proposed candidate polluters of first generation (FG) are not able to provide more than a few percent of their mass in the chemical feedback process, not enough to reproduce the observed change in chemical composition of second generation (SG) stars (e.g. [de Mink et al. 2009](#)). Dilution with unprocessed gas is mandatory for some kind of polluters, like the AGB stars, fast rotating massive stars and supermassive stars, to turn their correlated O and Na yields into the observed anti-correlation (e.g. [D’Ercole et al. 2010, 2011, 2012](#)). Finally, the observations show the presence of Li in second generation stars (e.g. [Pasquini et al. 2005](#); [D’Orazi et al. 2015](#)). Since Li is destroyed at much lower temperature than those experienced in hot-H-burning, either fresh Li must be provided by some class of polluters (see [Ventura et al. 2009](#)) or dilution with unprocessed matter must be taken into account (as first suggested by [Prantzos et al. 2007](#)), or both. We will come back on Lithium in Section 5.

A dilution model where processed material is mixed with variable amounts of gas with primordial composition may easily explain the run of the observed negative and positive correlations among light-elements (see the discussions in [Carretta et al. 2009c,b](#)). In this case, two other complications must be considered. First, there is the difficulty to distinguish between SG stars formed by pure processed ejecta and those including a minimum amount of unprocessed matter, as well as to reliably separate FG stars from SG stars affected by large amount of dilution. In turn, the translation of the observed correlations into a temporal sequence may be not trivial or unambiguous (see e.g. the complex sequence devised by [D’Antona et al. 2016](#) to explain NGC 2808). Second, when large samples of polluted, second (and possibly further) generation stars are scrutinized in details with spectroscopy, discrete (as opposed to continuous) distributions are detected along the anti-correlations in a growing number of GCs (e.g. M 4=NGC 6121, 47 Tuc=NGC 104, M 28=NGC 6626, NGC 6752, NGC 5986, NGC 2808, NGC 6388, NGC 6402). This pairs with the observations of very common multiple sequences in the colour-magnitude diagram (see e.g. [Bedin et al. 2004](#); [Piotto et al. 2007](#)) and multiple groups in the photometric chromosome map ([Milone et al. 2017a](#)). Note however that these different groups may be not exactly homogeneous and that the match between groups selected from spectroscopy and photometry is not always exact (see [Carretta et al. 2015](#) for the exemplary case of NGC 2808). For several GCs a single dilution model is not adequate to reproduce simultaneously the components with extreme and intermediate composition, leading to the conclusion that the operation of different classes of FG polluters is likely required to fit all the observations ([Carretta et al. 2012](#); [Johnson et al. 2017a](#); [Carretta et al. 2018](#); [Carretta and Bragaglia 2018](#); [Johnson et al. 2019](#)). Alternatively, we might perhaps consider the possibility that the whole scenario of multiple generations is incorrect, or at least, complicated by the presence of other mechanisms too.

Strictly connected to the above issues of yields from FG polluters and dilution another observation at present seems very difficult to reconcile with model prediction. Even if large amounts of uncontaminated gas were available at early times in the lifetime of GCs the most popular scenarios for self-enrichment are seen to clash with the observed number ratios of SG stars. Since these stars must include in their composition matter ejected by only a small fraction of FG stars, and their fraction represent the majority of current cluster stars (as tagged from both spectroscopy and photometry) most scenarios are confronted with a sort of paradox. This problem is known as the mass-budget problem, discussed below (see Section 8.1). The most common way out has been to assume that current GCs are only a small remnant of their starting mass, and were able to get rid of most of their FG components in early times, in particular during the phase of expansion driven by the loss of SNe II ejecta (e.g. [D’Ercole et al. 2008a](#)).

Closing this discussion, we note that according to most models, the extra-He observed in the SG stars is produced during the main sequence phase and brought to the surface of the polluter by the second dredge-up; on the other hand, if the massive AGB stars are considered as polluters, the anti-correlations described above are produced by hot bottom burning during the early AGB phase, that is a later evolutionary phase. The correlation between the production of He and other elements then depends on details of the models, such as the efficiency of convection and mass-loss.

2.4 Neutron-capture elements

Trans-iron elements are produced via two main mechanisms, involving neutron capture processes because of the high Coulomb barriers: the *slow* neutron capture process (the *s*-process) and the *rapid* neutron capture process (the *r*-process), where slow and rapid are defined with respect to the β decay timescale. The exact site of the *r*-process is still controversial, however due to the necessary conditions of high neutron density and high temperature, core collapse supernovae and neutron star mergers are the most likely candidates (see e.g., [Qian and Woosley 1996](#), [Freiburghaus et al. 1999](#), and the recent review by [Cowan et al. 2019](#)).

The majority of the *s*-process elements between Fe and Sr ($60 < A < 90$) are produced in massive stars (with initial mass $M > 8 M_{\odot}$), defining the *weak s* component ([Käppeler 1999](#)). In these stars, the main neutron source is provided by the $^{22}\text{Ne}(\alpha, n)^{25}\text{Mg}$ reaction, activated at the end of the convective He-burning core ([Prantzos et al. 1990](#)) and in the following convective C-burning shell (e.g., [Raiteri et al. 1991](#)). The ^{22}Ne abundance available in the He core is produced from the initial CNO isotopes, which are converted to ^{14}N during the H-burning phase, and then to ^{22}Ne by two α -captures (see [Pignatari et al. 2010](#) and references therein).

For $A > 90$, the *s*-process elements are produced in AGB stars ($\approx 1.3\text{--}8 M_{\odot}$) forming the *main s*-component (see [Karakas and Lattanzio 2014](#) for an updated review on the nucleosynthesis of low-mass and intermediate single stars). In AGB stars, carbon and *s*-process elements are produced during the thermal pulse (TP) phase and brought to the surface by mixing episodes known as third dredge-up events. The *s*-process elements are produced via the capture of neutrons on Fe seeds, with neu-

trons released both during the H-burning phases, within a so-called ^{13}C “pocket” by the $^{13}\text{C}(\alpha, n)^{16}\text{O}$ reaction at temperatures in the order of 100 MK, and during the TPs by the $^{22}\text{Ne}(\alpha, n)^{25}\text{Mg}$ reaction, if the temperature reaches above 300 MK (Cristallo et al. 2009). In AGB stars of relatively low mass ($\lesssim 4M_{\odot}$) the temperature barely reaches 300 MK, and the ^{13}C nuclei are the predominant neutron source, at variance with higher masses for which ^{22}Ne neutron is the main mechanism. The ^{13}C and ^{22}Ne neutron source produce different s -process paths, implying that isotopes beyond the first s -process peak can be reached (up to Pb at low metallicity) at lower burning temperatures (smaller masses) while a significant Rb production is only predicted with high temperature burning (larger masses).

In general, GCs are homogeneous as far as n-capture elements are concerned (e.g., Armosky et al. 1994; James et al. 2004; D’Orazi et al. 2010a), with the exception of “anomalous” (or Type II) clusters (e.g., Yong and Grundahl 2008; Marino et al. 2015), where variations in the s -process content are detected in conjunction with iron, CNO and p-capture element abundances (see dedicated discussion of these GCs in Section 3.4). An interesting case in this framework is represented by the metal-poor GC NGC 7078=M 15, where Sneden et al. (1997) first detected a Ba variation simultaneous with Eu, suggesting an r -process enrichment within this cluster. This trend was later confirmed by Otsuki et al. (2006). As for the primordial composition, GC stars exhibit a typical r -process rich pattern, which reflects pollution episodes (before the cluster formation) related to massive star nucleosynthesis. Interesting enough, in some cases the n-capture primordial abundance is conversely s -process rich: e.g. NGC 6121=M 4 displays an average s -process element content significantly larger than other GCs (including its *twin* NGC 5904=M 5), with an enrichment more than a factor of two larger than typical values for field stars of similar metallicity (Ivans et al. 1999, D’Orazi et al. 2010a, 2013).

2.5 Some caveats

When considering the various abundance anomalies observed in GCs, a few facts should be considered. First, the spread is typically expressed as a logarithm of the variation, essentially because this is how observational errors scale, and the O-Na anti-correlation that we observe in virtually all GCs is due to the transformation of previously existing (from cluster formation) O and Ne into N and Na, respectively. Similarly, the Mg-Al anti-correlation is due to the transformation of already existing Mg into Al. Destruction and production are then proportional to the initial chemical composition, and the spread (expressed in the logarithm) is quite independent of the original metal abundance of the cluster, save for the possible dependence of the burning temperature on the chemical composition. The situation is different for the variation of the total content of CNO and of Fe, observed in a fraction of the clusters (called Type II clusters by Milone et al. 2017a or iron-complex clusters by Johnson et al. 2015; see Section 3.4), where newly produced metals sum up to the existing ones. In this case, much more production is required to obtain the same spread in the logarithm of the abundance in metal-rich clusters than in metal-poor ones. For instance, while the ejecta of a few SNe are enough to cause detectable star-to-star vari-

ations in the Fe abundance of a cluster with $[\text{Fe}/\text{H}]=-1.7$ (such as M 2=NGC 7089), about 15 times more SNe are required to produce the same (logarithmic) change in a cluster with $[\text{Fe}/\text{H}]=-0.5$ (such as NGC 6388), even if the two clusters likely had a similar original mass. The case for He is simpler, first because the He abundances are not measured in logarithmic units, and second because all GCs have similar original values of the Y abundance.

An additional important point concerns the sensitivity of observations to abundance variations. We note here that a variation of $dY = 0.01$, that is detectable on the colour-magnitude diagram e.g. considering HB stars, implies an He abundance variation of only 4%, that is ~ 0.017 dex that is not detectable through spectroscopy, neither for He nor for other elements. This should be considered in particular when considering the correlation of a spread in He abundances derived from photometry with spreads for other elements obtained from spectroscopy (see e.g. [Cabrera-Ziri et al. 2019](#)), especially in a context where we expect a strong dilution effect is present.

3 What is a GC

The aim of this section is to provide a basic classification of GCs, useful to understand the relative roles of origin vs environment/evolution.

3.1 Relation between anti-correlations

While representative of a unique broad phenomenon (see e.g. the good correlations between different element distributions in Fig. 2, and the extensive discussion in [Marino et al. 2019](#)), the various anti-correlations are not strictly identical with each other. In Fig. 5 we compare the index of the spread of the N abundances from HST photometry ([Milone et al. 2017a](#)) with the interquartile of the $[\text{Na}/\text{O}]$ and $[\text{Al}/\text{Mg}]$ ⁴ distribution from the literature (see Appendix 1). The index of spread of N abundances is the value of $\Delta_{\text{F275W,F336W,F438W}}$, subtracted by the best fit straight line with metallicity for the clusters with absolute visual magnitude $M_V > -7.3$, as given by the same paper. We first notice that, due to observational errors (typically of the order of 0.1-0.2 dex), the interquartiles are always positive, even when no real spread exists. We will then hereinafter assume that an interquartile value smaller than 0.2 dex is compatible with no spread at all. Second, there is no reason to think that $\Delta_{\text{F275W,F336W,F438W}} = 0$ implies no spread in N abundances. Rather, a comparison with the internal spread in N abundances considered in [Milone et al. \(2018c\)](#) indicates that the clusters with the smaller values of $\Delta_{\text{F275W,F336W,F438W}}$ still have a spread in N abundances as large as ~ 0.2 dex, while those with the larger values have a spread as large as ~ 1.2 dex. In addition, the removal of the metallicity dependence using a simple offset from a reference line may be simplistic, so that $\Delta_{\text{F275W,F336W,F438W}}$ should only be considered as a proxy for the N abundances.

⁴ The interquartile of a distribution is the range of values including the middle 50% of the distribution, leaving out the highest and lowest quartiles.

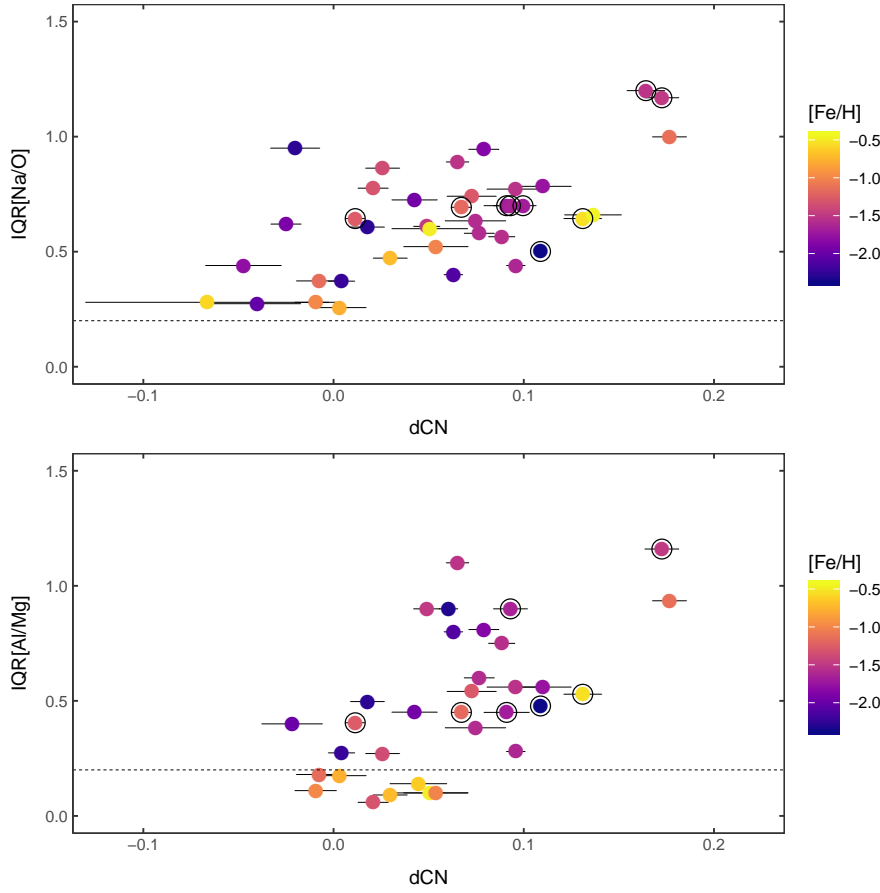


Fig. 5 Upper panel: run of the interquartile IQR[Na/O] of the distribution of [Na/O] abundance ratios within a cluster (see compilation in Appendix 1) and the spread in CN as derived from the spread in UV colours along the RGB $\mathcal{A}_{F275W,F336W,F438W}$ from Milone et al. (2017a). Lower panel: the same, but for the interquartile IQR[Al/Mg] of [Al/Mg] abundance ratios. Circled dots are for Type II clusters according to the classification by Milone et al. (2017a). In both panels, points below the dashed lines are actually consistent with no spread at all because they corresponds to the observational errors. Colours code metallicity (see scale on the right of the plot)

Once this is taken into account, there is a roughly linear relation between the spread in N abundances and the interquartile of the [Na/O] ratio. On the other hand, the Al/Mg relation is offset with respect to the two others: only clusters with positive values of $\mathcal{A}_{F275W,F336W,F438W}$ - that implies a spread in N abundances larger than 0.5 dex - have a significant spread in the Al/Mg ratio. In addition, only a small fraction of the metal-rich clusters ($[\text{Fe}/\text{H}] > -0.8$) exhibits a spread in Al/Mg. We will come back on this point later, but the different behaviour of the O-Na and Mg-Al anticorrelations was first noted by Carretta et al. (2009b) and later confirmed by other studies (see e.g. Nataf et al. 2019).

The variation of $\Delta_{F275W,F814W}$ at nearly constant $\Delta_{F275W,F336W,F438W}$ in FG stars observed in many clusters is discussed at length in [Marino et al. \(2019\)](#) (and references therein). While this might in principle be an indication of a spread in He abundances without a corresponding spread in N, they argue that the most probable explanation is rather a small spread in the Fe abundances that should likely be primordial. On the other hand, while star-to-star differential reddening is corrected while deriving the chromosome map, it is also possible that some residuals may remain: this also may contribute to this spread.

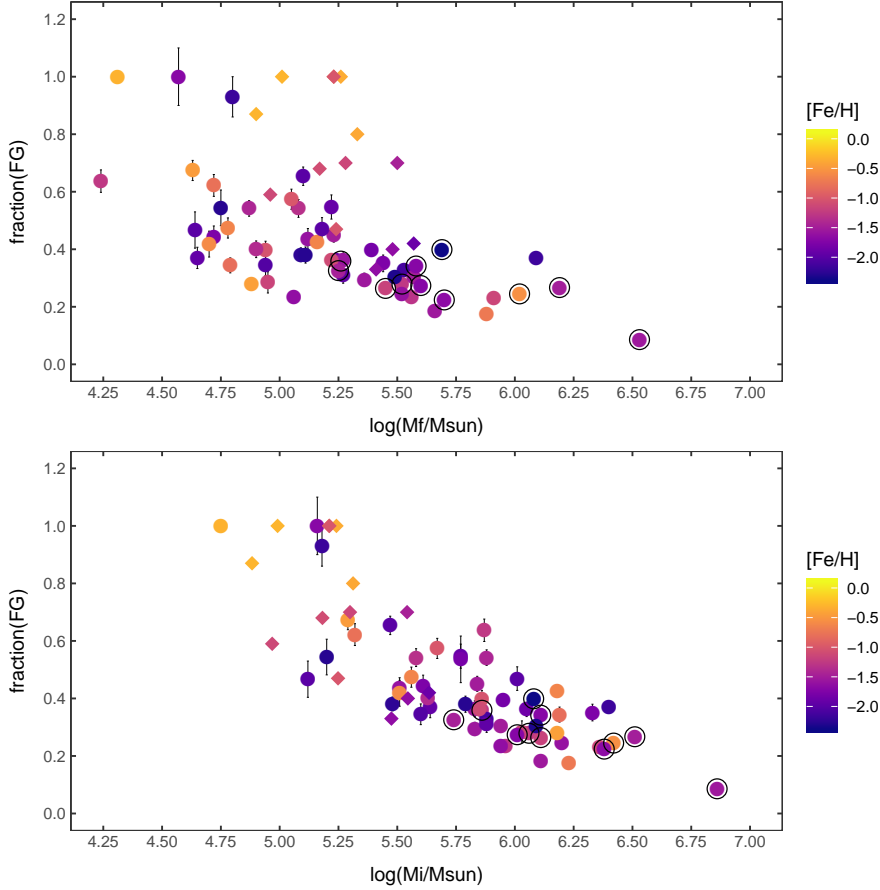


Fig. 6 Upper panel: run of the fraction of first generation stars within a cluster ([Milone et al. 2017a](#)) and the cluster mass from [Baumgardt et al. \(2019\)](#). Lower panel: the same, but using the initial mass from [Baumgardt et al. \(2019\)](#). Circled dots are for Type II clusters according to the classification by [Milone et al. \(2017a\)](#). Diamonds are clusters in the MCs (see Appendix for references). Note that for the latter in case of unknown metallicity $[\text{Fe}/\text{H}]=-1$ was adopted for the sake of the figure. Colours code metallicity (see scale on the right of the plot)

3.2 Cluster masses

Arguably, the most important parameter determining the chemical evolution within a cluster is its original mass. This may be largely different from the current mass because the clusters have a substantial dynamical evolution, and several attempts have been done in the past to better estimate this quantity. Very recently, [Baumgardt et al. \(2019\)](#) published new estimates for the current and original mass of MW GCs based on extensive comparisons between observational data for the surface luminosity and internal velocity distribution and N-body computations, and exploiting the Gaia DR2 data to better estimate distances and 3-d motion of the clusters. The original masses reported by these authors neglect many processes possibly occurring during the early stage of evolution (like e.g. gas expulsion, remnant retention, collisions with giant molecular clouds, etc. [D’Ercole et al. 2008a](#); [Giersz et al. 2019](#)) which could determine important amount of mass loss. Nevertheless, they represent the first attempt to account for the slow mass loss process occurred during the last Gyrs of dynamical evolution. We will then use them to estimate the masses at the end of the very complex formation phase of GCs. We will come back on this point in Section 8.1. In [Fig. 6](#) we compare the run of the fraction of first generation stars from [Milone et al. \(2017a\)](#) with the values for the present and original mass of the clusters from [Baumgardt et al. \(2019\)](#). The scatter of points is substantially reduced when we use the initial rather than the present masses. This suggests that while uncertainties are still not negligible, the initial masses are now reliable enough that we may use them in the present discussion. We notice that using the initial rather than present mass implies to take into consideration the environment where the GC formed, at least at first order.

In addition to the results for the MW, we considered the case of clusters in the Magellanic Clouds (MCs), to enlarge the sample ranges both in mass and age. Estimates of the present mass have been provided by [Mackey and Gilmore \(2003a\)](#) and [Mackey and Gilmore \(2003b\)](#) for a large number of clusters in the Large and SMCs⁵. Of course, when comparing the properties of the MC clusters with those of the MW ones, we should consider the mass loss by the MC clusters as was done by [Baumgardt et al. \(2019\)](#) for the Galactic clusters. Unluckily, we are not aware of a systematic determination of initial masses for clusters in the MCs similar to that described above. In general, mass loss from MC clusters is considered to be small but it is likely not entirely negligible (see e.g. the discussion in [Baumgardt et al. 2013](#) and [Piatti and Mackey 2018](#)). Hereinafter, we only considered the minimum mass loss that is due to the combination of stellar evolution ([Lamers et al. 2010](#)) and of the evaporation related to the two-body relaxation (neglecting then tidal effects, disk shocks, and encounters with giant molecular clouds). Both of them are function of age, and the second one also of the cluster relaxation time (that is presently of the order of 500 Myr for most of the clusters of interest here: see [Piatti and Mackey 2018](#)). With these assumptions, the oldest clusters in the MCs have lost at least 30% of their original

⁵ Alternative estimates of the current masses for MC clusters are provided by other studies, e.g. by [McLaughlin and van der Marel \(2005\)](#); while these last authors did not list values for all the clusters considered here, whenever available the masses agree very well with those given by [Mackey and Gilmore \(2003a\)](#) and [Mackey and Gilmore \(2003b\)](#), but for the single case of NGC 2257.

mass, while those about 2 Gyr old only about 10%. We corrected the points relative to the MC clusters for these effects on the lower panel of Fig. 6. However, it is very possible that the initial masses determined in this way are underestimated for some of the oldest clusters (see Baumgardt et al. 2013).

We can compare these masses with the fraction of FG stars. Initial values of these quantities were derived by Carretta et al. (2010c) from spectroscopic surveys, that call Primordial (or P) the FG stars. Carretta et al. (2010c) found a quite uniform value of the fraction of FG stars in GCs of 30%, although with cluster-to-cluster variations within quite large error bars. These values, with some addition from later papers, were used e.g. in the discussion by Bastian and Lardo (2015). However, the separation between FG and SG stars according to Carretta et al. (2009c) might be affected by small number statistics and the presence of outliers. The locus of FG stars was individuated by comparing the P components in GCs to the field halo stars of similar metallicity, as shown e.g. in Fig. 10 of Carretta (2016), where it is evident that the estimate of a typical value of about 30% of FG stars in GCs is likely correct. However, due to the adopted methodology, a fraction of the SG stars with moderate excess of Na may be disguised as FG stars, an effect that may depend on the actual shape of the distribution of Na abundances. A better statistics to derive the frequency of stars in the different populations in individual GCs is now possible thanks to the HST photometry, see Milone et al. (2017a): these are not directly abundance determinations but rather qualitative labeling based on indices that can be determined accurately for large samples of stars. Inspection of the figures in their paper shows that while in the majority of cases the distinction is clear and the measured fractions yield a clear statistical meaning, there are a few cases where the separation of stars in different populations might be questioned (e.g. NGC 5272=M 3 and a few more): care should then be taken in order not to over-interpret data. As a further note of caution, in some cases slightly different filters and procedures may result in large variations of the estimated fraction of FG and SG stars. The case of NGC 2419 (admittedly the most distant Galactic GC) is a good example. Using the same approach as Milone et al. (2017a), Zennaro et al. (2019) estimated a fraction of $37 \pm 1\%$ of FG stars, as listed in our Table 8, while Larsen et al. (2019) obtained a much higher value of 55% for this component in the same GC. Both studies are based on HST magnitudes through filters sensitive to CNO absorption features.

Fig. 6 indicates that there is a close (anti-)correlation between the initial masses of the cluster and the fraction of FG stars as found using the HST photometry by Milone et al. (2017a), in disagreement of a uniform value. The lower panel indicates that an initial mass in the range between 8×10^4 and $\sim 2 \times 10^5 M_{\odot}$ is likely required for the multiple population phenomenon⁶. In this mass range, there is actually a considerable cluster-to-cluster scatter in the fraction of first/second generation stars. This might possibly be simply an effect of the uncertainties existing in the determination of the masses and of the fraction of FG stars in small clusters, where also the samples

⁶ The sample of clusters in Milone et al. (2017a) may suffer from a selection bias, because only rather nearby and massive GCs have been targeted (the selection is essentially that of the ACS Survey by Sarajedini et al. 2007). On the other hand, these are also those GCs for which more precise data can be obtained. A similar bias can of course be present in case spectroscopy is used to define the populations fractions. It would be interesting to extend the same kind of studies to a sample fully representative of all MW GCs.

available from photometry become limited in size; however, we cannot exclude that some parameter(s) other than mass is (are) also important. As a matter of fact, it is not even exactly clear what we mean for initial mass in the framework of a multiple population scenario. We also notice that the fraction of FG stars is not strongly dependent on cluster metallicity.

Finally, [Baumgardt and Hilker \(2018\)](#) also found a quite close (anti-)correlation between the fraction of FG stars from [Milone et al. \(2017a\)](#) and the escape velocity from the cluster, supporting an early suggestion by [Georgiev et al. \(2009\)](#). This suggests that the correlation with cluster mass may actually be due to a higher capability of massive cluster to retain a larger fraction of the ejecta from FG stars, that may be used to produce next generations ([Vesperini et al. 2010](#)). However, this issue may be more complex, as we will see in Section 8.1.

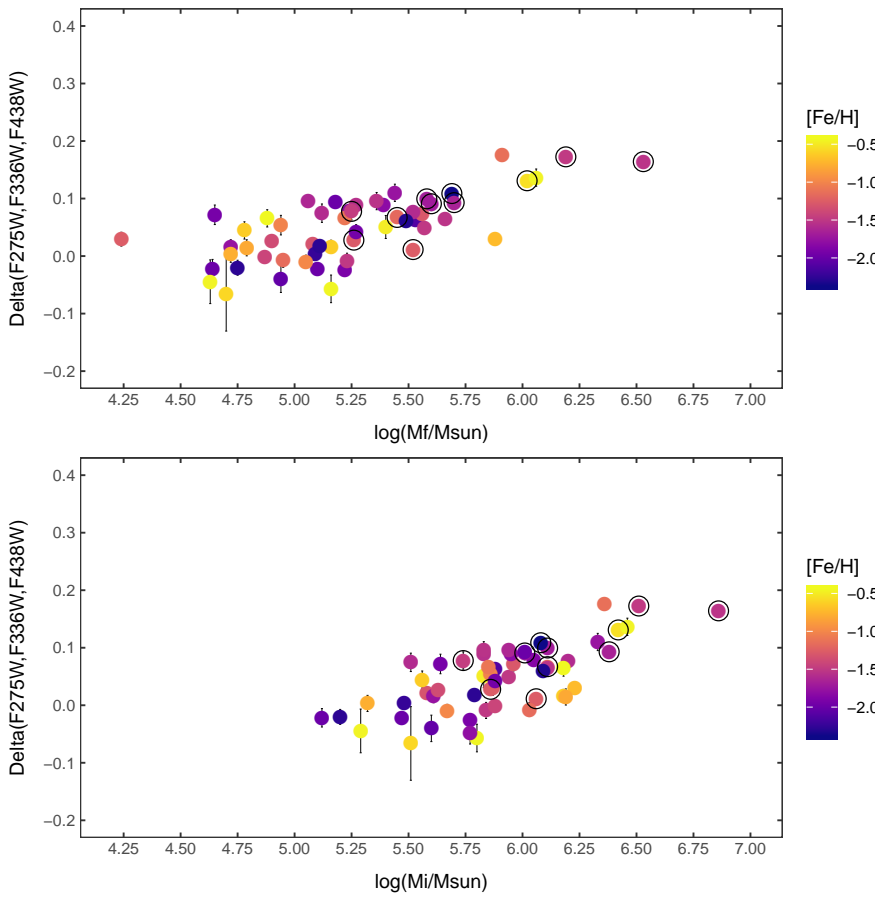


Fig. 7 Run of the spread of UV colours $\Delta_{F275W,F336W,F438W}$ within a cluster ([Milone et al. 2017a](#)) with final and initial cluster mass from [Baumgardt et al. \(2019\)](#). Circled symbols are for Type II clusters according to the classification by [Milone et al. \(2017a\)](#). Colours code metallicity (see scale on the right of the plot)

3.3 Small clusters

Establishing that a cluster does not have MPs is not easy, because “lack of evidence” does not necessarily mean “evidence of lack”. Clusters originally thought to be homogeneous were lately shown to possess MPs, though with only a small fraction of SG stars or small spread in abundances (see e.g. the case of IC 4449, [Dalessandro et al. 2018b](#)). On the other hand, when the observed spread in abundance is small, MPs can be claimed where there may be not present. For instance, the original claim of MP in NGC 6791 ([Geisler et al. 2012](#)) has not been confirmed by later more extensive and accurate data sets ([Bragaglia et al. 2014](#); [Villanova et al. 2018](#)). With these caveats, a census of clusters for which MPs were observed has been presented in [Carretta et al. \(2010c\)](#); [Gratton et al. \(2012a\)](#), while [MacLean et al. \(2015\)](#) studied the possible presence of Na and O variations compiling data in 20 open clusters (finding none). The census has been updated in [Krause et al. \(2016\)](#) and in [Bragaglia et al. \(2017\)](#), where more extra-galactic clusters and open clusters were added and results from photometry were considered. Presently, we have information on more than half the known MW GCs. Fig. 8 shows the mass-age plot for GCs in the MW, Fornax, the MCs, and for some MW open clusters (masses are generally from [Baumgardt et al. 2019](#) for MW GCs, [Mackey and Gilmore 2003a,b](#) for the Magellanic Clouds (MCs) and Fornax, and [Piskunov et al. 2008](#) for open clusters (these last are highly uncertain see Tables 8, 9, and 10 for references. Had we used M_V as a proxy for mass, as done e.g. in [Bragaglia et al. \(2017](#), see their Fig. 9), we would have seen more low-mass clusters but without information on presence or absence of MPs. Furthermore, many new low-mass clusters are being found combining large scale photometric surveys and Gaia (see e.g. [Koposov et al. 2017](#); [Ryu and Lee 2018](#); [Torrealba et al. 2019](#)). They are not easy objects to study, either with photometry or spectroscopy, given their faintness and low number of stars but it would be interesting to observe them.

There are 5 MW GCs for which no MP has been detected to date (E 3, Pal 12, Ter 7, Pal 1, and Rup 106, see [Salinas and Strader 2015](#); [Cohen 2004](#); [Sbordone et al. 2005](#); [Sakari et al. 2011](#); [Villanova et al. 2013](#)) and they have generally a low mass, with the exception of the last one. There are lower-mass clusters showing MPs, but we show here the present-day mass, while as discussed previously the original one would be a better choice. However, we do not have the latter for the open clusters and the extra-galactic clusters. We are then forced to use the present-day mass if we want to compare the different cluster families, keeping in mind the strong and differential mass loss affecting clusters during their lifetimes. Anyway, we also note that [Carretta \(2019\)](#) shows that present-day masses of GCs essentially preserve the ranking provided by initial masses, apart from a few exceptions located near the central regions of the Galaxy. This conclusion is here implicitly supported by the two panels of Fig. 6.

The only two open clusters where a large number of stars were observed on purpose to detect variations in Na, O are Berkeley 39 ([Bragaglia et al. 2012](#)) and NGC 6791 ([Geisler et al. 2012](#); [Bragaglia et al. 2014](#); [Cunha et al. 2015](#); [Villanova et al. 2018](#)). No indication of spread in these elements was found (see e.g. the different conclusions in [Geisler et al. 2012](#) and [Villanova et al. 2018](#)). After the compilation in [MacLean et al. \(2015\)](#), data for significant samples of stars in many other clus-

ters are being acquired by studies or surveys such as the Gaia-ESO or APOGEE (see some examples and references in Table 10). Also for those clusters the variations in O and Na never exceed the errors. Furthermore, high-resolution spectroscopic studies consistently found that open clusters have very homogeneous abundances, once evolutionary effects are taken into account.

From Fig. 8, mass seems to be the fundamental player for the presence of MPs. In fact, even if MPs are present in MCs clusters of ages comparable to those of the old open clusters, they are more massive. The possible dependence on age will be discussed later in the paper (Sect. 3.6).

3.4 Type I and Type II clusters

To interpret the HST multi-colour photometry, Milone et al. (2017a) introduced the concept of the chromosome map. This is the distribution of points for individual stars in the $\Delta_{F275W,F336W,F438W}$ versus $\Delta_{F275W,F814W}$ pseudo-two-colour diagram within an individual GC (see Fig. 1). The vertical axis in this diagram is proportional to the spread in the N abundance (higher values of $\Delta_{F275W,F336W,F438W}$ corresponding to higher N abundance), while the horizontal one is proportional to the He content (lower values of $\Delta_{F275W,F814W}$ indicate stars with higher He abundances), though it is also sensitive to metallicity and differential reddening (see discussion in Marino et al. 2019). In the majority of clusters, stars distribute in two main groups, one characterized by low N and He (FG stars), and the other by higher values of the abundances of these elements (SG stars). Milone et al. (2017a) called these clusters of Type I. However, in a small number of clusters the situation is more complex, with at least a third group of stars occupying a region of high N but low He abundances. Milone et al. (2017a) classified them in a Type II class, and put in this class also ω Cen=NGC 5139 and M 54=NGC 6715. However, the chromosome maps for these two clusters are more complex than those of the remaining Type II ones, and they may well be a separate class of objects (see also Marino et al. 2019). A more extensive discussion of the properties of Type II clusters is given by Marino et al. (2018b), who proposed to distinguish these clusters according to the type of chemical anomalies they show (spread in CNO, Fe, or s-process elements). While this kind of separation is not novel (e.g. the Type II GCs are essentially the iron-complex GCs considered by Johnson et al. 2015), the application to a homogeneous set of GCs makes the use of Type I/II classification a useful working tool.

Since the chromosome map is likely reflecting the imprinting of the early evolution of a cluster, Type II clusters clearly had a more complex evolution than Type I clusters. They are usually massive clusters, but there is not a one-to-one correspondence between the cluster mass and their classification according to the chromosome map. However, a clue may be provided by Fig. 10, where we plot the run of the initial mass of GCs (Baumgardt et al. 2019) with the apocenter of their orbit R_{apo} (Baumgardt et al. 2019), with different symbols for clusters belonging to the different classes according to Milone et al. (2017a). Here, we assumed that NGC 7078=M 15 is a Type II cluster following Nardiello et al. (2018b). In this diagram, Type II clusters occupy the upper envelope of the distribution, that is, they are systematically among

the largest clusters for a given apocenter distance. Part of this segregation might be due to selection effects, because there are many GCs that are not plotted in this diagram because they were not included in the survey by [Milone et al. \(2017a\)](#), which is biased against outer halo GCs. Since they adopted the sample of GCs of the ACS Survey by [Sarajedini et al. \(2007\)](#), their selection include 25 bulge/disk GCs, 25 inner halo clusters and only 6 outer halo GCs, where the classification is the one defined in [Carretta et al. \(2010c\)](#). Also, there are massive GCs that are not of Type II, such as 47 Tuc=NGC 104, NGC 2808, or NGC 2419. The two last GCs have however a complex chromosome map, even if not clearly displaying the characteristic shape of Type II clusters⁷. We may consider R_{apo} as a proxy for the distance where clusters formed; actually it should be better considered as a lower limit for this quantity, because the orbit of a GC within a satellite of the galaxy should decay with the orbit of the host, likely dominated by dynamical friction, as e.g. it was likely the case for M 54=NGC 6715 in the Sagittarius galaxy. However, statistically we may consider that a large value of R_{apo} implies that the GC formed farther out in the meta-galaxy. We may then interpret the correlation between complexity of the chromosome map, M_{in} and R_{apo} as an indication that the environment actually played a role in the multiple population phenomenon, in the sense that very massive clusters that formed in the very outer regions of the meta-galaxy had the possibility of a more extended and complex evolution than clusters that formed closer to the center.

Finally, there are clusters missing a clear classification but suspected to display an Fe abundance spread, such as e.g. NGC 5824 ([Da Costa et al. 2014](#); [Roederer et al. 2016](#)); however this particular claim has been recently dismissed by [Mucciarelli et al. \(2018\)](#), who rather suggested that this object has a very extreme Mg-Al anti-correlation. Even more recently, [Yuan et al. \(2019\)](#) proposed that NGC 5824 is the nuclear star cluster of a galaxy that originates the Cetus stream.

Type II clusters have several other systematic differences with respect to Type I. They in fact show a split subgiant branch, that may be interpreted as due to a variation in the total CNO content ([Yong et al. 2009, 2014b](#); [Marino et al. 2011b, 2012, 2015](#); [Carretta et al. 2013a](#); [Villanova et al. 2014](#); [Yong et al. 2009](#); [Ventura et al. 2009](#); [Yong et al. 2015](#)), and indication of some definite spread in the abundances of s-process elements ([Marino et al. 2011b](#); [D’Orazi et al. 2011](#); [Carretta et al. 2013b](#); [Johnson et al. 2015](#); [Marino et al. 2015](#); [Yong et al. 2016](#); [Marino et al. 2018b](#)). The various features observed for these clusters likely require that in addition to H-burning at high temperatures (within supermassive stars, fast rotating massive stars or massive AGB stars) there should also be a contribution by triple- α reactions occurring during thermal pulses (in AGB stars), at least if the scenario of multiple generations is correct. The timescale required for the evolution of stars that produce this nucleosynthesis is $\gtrsim 0.2\text{--}0.5$ Gyr (see e.g. [Cristallo et al. 2015](#)) that is much longer than that required for those stars where H-burning at high temperature occurs. In this group of clusters there are typically at least four different populations (Na-poor, CNO-poor; Na-rich, CNO-poor; Na-poor, CNO-rich; Na-rich CNO rich: see e.g. the cases of M 22=NGC 6656,

⁷ NGC 2808 has at least five different populations ([Milone et al. 2015b](#); [Carretta et al. 2015](#)). NGC 2419, a very massive cluster with a very large apocenter distance, also shares many characteristics of the chromosome map with NGC 2808, as suggested by the very recent study by [Zennaro et al. \(2019\)](#). However, it is not plotted in Fig. 10 because it actually lacks an explicit classification in Type I/II classes.

Marino et al. 2012; NGC 1851, Gratton et al. 2012c; Lardo et al. 2012; NGC 5286, Marino et al. 2015), but there are clearly more complex cases, such as the seven populations of M 2=NGC 7089 (Yong et al. 2014b; Milone et al. 2015a). In addition, there is clear evidence for a significant spread in the Fe-peak elements, suggestive of a deep potential well able to keep at least a (very small, see Sect. 8.1.2) fraction of the supernova ejecta, for M 54=NGC 6715 (Carretta et al. 2010b,a), ω Cen=NGC 5139 (Norris and Da Costa 1995; Suntzeff and Kraft 1996; Stanford et al. 2006; Johnson and Pilachowski 2010; Marino et al. 2011a; D’Orazi et al. 2011; Gratton et al. 2011a; Villanova et al. 2014; Bellini et al. 2017), and NGC 6273 (Johnson et al. 2015, 2017a). More limited spread in Fe abundances (≤ 0.2 dex) have been claimed also for M 22=NGC 6656 (Marino et al. 2012), NGC 1851 (Carretta et al. 2011a; Gratton et al. 2012c), NGC 5286 (Marino et al. 2015), M 2=NGC 7089 (Yong et al. 2014b; Milone et al. 2015a), and NGC 6934 (Marino et al. 2018b), though some of these results are controversial (see e.g. Mucciarelli et al. 2015b; Lardo et al. 2016, for M 22=NGC 6656 and M 2=NGC 7089, respectively). Finally there is the case of M 15=NGC 7078, which, unique among Type II shows a spread in the content of the r -process elements (Sobeck et al. 2011; Worley et al. 2013), while its Fe content is uniform (Carretta et al. 2009c). No obvious Fe abundance variation was instead found in the Type II clusters NGC 362 and NGC 6388 (Carretta et al. 2009c,b, 2013b; Carretta and Bragaglia 2018), while there are not yet published high-resolution spectroscopic data for NGC 1261. As mentioned in Section 2.5, detection of star-to-star variations in the Fe and total CNO abundance is expected to be more difficult in a metal-rich cluster. This may be the case of NGC 6388 (but neither of NGC 362 nor M 15=NGC 7078), so that lack of detection of these variations might not mean that there is a systematic difference between this cluster and the remaining Type II clusters.

In addition, Type II clusters tend to have a larger initial mass than Type I with the same value of IQR[Na/O] and IQR[Al/Mg], or conversely tend to have a smaller value of IQR[Na/O] and IQR[Al/Mg] for the same mass (see Fig. 9). On the other hand, there is no clear offset for the N abundance indicators ($A_{F275W,F336W,F438W}$ or the fraction of first generation stars). This indicates that while the multiple population phenomenon is present as in Type I clusters, in Type II clusters the role played by H-burning at very high temperature is smaller, perhaps because its effect is diluted by other contributions to nucleosynthesis.

On the whole, the emerging pattern from chemistry is of significant age spreads and complex chemical evolution within individual Type II clusters. There is clear indication that they had a quite long history within isolated fragments before the internal evolution of the fragment itself or interaction with our own Galaxy caused the final dispersal of any residual gas. This is obviously the case of M 54=NGC 6715, that is the nucleus of the Sagittarius dwarf galaxy (Ibata et al. 1994; Bellazzini et al. 2008). It has long been suggested that ω Cen=NGC 5139 also is the stripped nucleus of a dispersed dwarf galaxy (see e.g. Bekki and Freeman 2003, though direct evidence is still elusive (see e.g. Navarrete et al. 2015; see however also Myeong et al. 2018b,a for possible hints that the ashes of this galaxy might actually be dispersed in the Galactic halo, and the very recent result by Ibata et al. 2019 that identifies a stellar stream found on Gaia DR2 data as the possible tidal tails). Searches for extended

halos of stars around other Type II clusters, possible remnants of the galaxies originally surrounding them and to be separated from narrow tidal tails along the orbit that may arise also for isolated clusters, have been performed by e.g. [Olszewski et al. \(2009\)](#); [Carballo-Bello et al. \(2014\)](#). The evidence is now established for NGC 1851 ([Olszewski et al. 2009](#); [Kuzma et al. 2018](#)), M 2=NGC 7089 ([Kuzma et al. 2016](#)), NGC 6779=M 56 ([Piatti and Carballo-Bello 2019](#)) while it is not clear and possibly absent for others (see e.g. NGC 1261: [Kuzma et al. 2018](#)). On the other hand, the chemical evolution of these objects is surely far from being well described by a closed box model, as already showed by [Suntzeff and Kraft \(1996\)](#) for the case of ω Cen=NGC 5139, where these authors estimated that some 90% of the original mass should have been lost. We will come back on this point in Sect. 8.1.2. More in general, we notice that the typical apocenter distance of these clusters ($\sim 5 - 50$ kpc) likely underestimates the distance at the epoch of formation because the orbit of a large mass satellite is expected to become closer to the Galactic center with time due to the effect of dynamical friction. It is then not unreasonable to think that the fragments where Type II clusters formed could have had a prolonged star formation phase before they interacted with the Galaxy and dispersed.

3.5 Metallicity dependence

While mass is the leading parameter determining the fraction of first/second generation stars, metallicity clearly plays an important role in the actual nucleosynthesis causing the pattern observed within GCs. This is shown by a comparison of Fig. 7 and Fig. 9. In the first one we plotted the run of the spread of UV colours along the RGB $\Delta_{F275W, F336W, F438W}$, a proxy for the spread in N abundances, with the initial cluster mass ([Baumgardt et al. 2019](#)). In the second one we plot the run of the interquartiles of the distribution of the [Na/O] (upper panel) and [Al/Mg] (lower panel) within a cluster with the initial mass of the clusters. These figures shows the expected correlation with cluster mass. The interquartiles are larger than the observational errors (here we assumed 0.2 dex, that is about three times the normal uncertainty in the relevant abundances) only for clusters with initial masses above $3 \times 10^5 M_{\odot}$ for the [Na/O] anti-correlation, and for even a larger mass for the [Al/Mg] one. In addition to this higher threshold with respect to what is observed for the N abundance variations, there is a clear trend for steeper relations for the metal-poor clusters than for the most metal-rich ones. This is very obvious for the [Al/Mg] anti-correlation: only extremely massive (initial mass above $3 \times 10^6 M_{\odot}$) metal-rich clusters show a (limited) spread in the Al abundances. This confirms what was originally found by [Carretta et al. \(2009b\)](#) and seen also in APOGEE and Gaia-ESO data (see [Mészáros et al. 2015](#); [Masseron et al. 2019](#); [Pancino et al. 2017](#)). An even more extreme effect is exhibited by the Ca-K anti-correlation, that has been actually found only in the very massive and metal-poor cluster NGC 2419 ([Mucciarelli et al. 2012a](#); [Carretta et al. 2013b](#)) and in NGC 2808 ([Mucciarelli et al. 2015a](#)).

In Section 2 we have seen that the various anti-correlations seen in GCs can be interpreted as due to H-burning occurring at different temperatures. The trends existing with mass and metallicity in Type I clusters can then be interpreted as due to pol-

lutters where this burning occurs at increasing temperature. This likely signals a drift toward more massive polluters with increasing cluster mass. In the scenario where the polluters are massive AGB stars, the trend with metallicity may be explained by the fact that the temperature of hot bottom burning is expected to be higher in lower metallicity stars (Lattanzio et al. 2000; Ventura et al. 2009).

In general, it is probable that even within a single GC we must consider different classes of polluters. This is quite obvious for Type II clusters, that cannot be described by a simple mono-parametric dilution distribution. However, there is evidence that a single dilution distribution cannot reproduce simultaneously the [Na/O] and [Al/Mg] anti-correlations even in Type I clusters such as NGC 6752 (Carretta et al. 2012) and NGC 2808 (Carretta 2014, 2015), or NGC 6402 (Johnson et al. 2019) for which no type is available. This suggests that often the GC formation cannot be described by a simple scenario with only two episodes of star formation and that the multiple population phenomenon is possibly more complex.

3.6 Is there an age dependence?

There have been several attempts to assess if mass is indeed the leading parameter determining the presence of multiple populations in massive clusters and to better understand the timescale of the multiple population process, that would be crucial to understand the nature of the polluters. The (possible) evidence for a dependence on age refers to studies of GC analogs both very young and more mature.

A potentially attractive road is in fact to look for multiple populations in young very populous clusters in nearby galaxies – there are not such clusters in the MW (Portegies Zwart et al. 2010). Of course, this faces with the difficulties of observing far and very dense clusters, but it can be attempted and a summary of results is given in the recent review by Bastian and Lardo (2018).

Among the important results of this line of investigation is the lack of evidence for interstellar matter in clusters older than a few Myr (Longmore 2015; Cabrera-Ziri et al. 2015; Bastian and Strader 2014; Hollyhead et al. 2015). If this result would also apply to young GCs, it would be a clear difficulty for scenarios where MPs are formed in various episodes of star formation, though this should be considered carefully for the different timescales involved. On the other hand, it is not obvious that the dynamical conditions of young populous clusters are actually the same met by objects that are now GCs. Alternatively, Lardo et al. (2017a) examined the case of three super-star clusters in the Antennae with ages 7–40 Myr and masses in the range 4×10^5 – $1.1 \times 10^6 M_{\odot}$. Given the large distance, they could only observe integrated spectra of the clusters and in order to enhance the contribution by red supergiants they considered near-IR spectra where they could only measure Al lines among the possible indices of multiple populations. They did not find evidence for Al enrichment and concluded against the presence of multiple populations in these clusters. However, this is likely not conclusive because within Galactic GCs, large Al spreads are generally limited to clusters with a metallicity below 1/10th of solar (see the lower panel of Fig. 9), while the clusters in the Antennae likely have near-solar metallicity (Lardo et al. 2015). No spread in the Al abundances is actually observed e.g. in

47 Tuc=NGC 104 or NGC 6528, that when young were likely much more massive than the clusters observed by [Lardo et al. \(2017a\)](#).

The second line of evidence of the influence of age concerns surveys of populous clusters in the MCs, that host a population of relatively massive clusters both as old as the MW GCs and young, accessible to more traditional spectroscopic and photometric studies. [Mucciarelli et al. \(2009\)](#) found evidence of multiple populations (based on Na, O anti-correlation) in three very old clusters (NGC 1786, NGC 2210, NGC 2257, see also Table 9), while no evidence was instead found in the younger clusters NGC 1866 ([Mucciarelli et al. 2011](#), about 100 Myr) and NGC 1806 ([Mucciarelli et al. 2014a](#), about 1.7 Gyr old). The only old cluster in the Small MC (SMC), NGC 121, was found to host multiple populations by [Dalessandro et al. \(2016\)](#) and [Niederhofer et al. \(2017a\)](#), based on HST photometry showing the effects of CN variations. The few stars for which high resolution spectra were obtained by the former work did not show spreads in Na or O. This agrees with the small fraction of second generation stars in the cluster, compared to MW analogs.

More recently, the Bologna and Liverpool groups joined forces to search for signatures of large star-to-star variation in the N abundances, based mostly on HST photometry (i.e. based on C, N, and possibly O variations without information on Na, Mg, and Al). No cluster younger than 2 Gyr showed sign of the presence of multiple populations (see Table 9). Interestingly, these studies resulted in the discovery of two cases of multiple population in clusters 2 Gyr old (NGC 1978: [Martocchia et al. 2018b](#); Hodge 6: [Hollyhead et al. 2019](#)). According to the first study, there is no evidence that the SG is much younger than the first one in those particular clusters, with an upper limit at about 20 Myr. Although the results for NGC 1978 and Hodge 6 should be considered with some caution because the SG in those clusters only constitutes $\leq 20\%$ of the total mass in the cluster, making them the clusters with the smallest fraction of SG stars known, these are important constraints for models of multiple populations. They possibly limit the temporal scale where the phenomenon can occur (at least in Type I clusters) and rule out the possibility that some cosmological effects makes the multiple population phenomenon possible only at high redshift. The absence of any clear evidence for multiple populations in clusters younger than about 2 Gyr prompted the authors to argue that there is an age dependence of this phenomenon, with a threshold between 1.7 and 2 Gyr (yet unexplained by stellar evolution). These data are included in Fig. 6. However, this same figure also indicates that the young clusters considered in the survey are barely massive enough to show the multiple population phenomenon and lie in a region of the initial cluster mass - fraction of FG stars diagram where there are large cluster-to-cluster variations in the fraction of FG stars within a limited mass range. This suggests that clusters in this range of masses might have different histories, and that there may not be a single mass threshold value but rather a range of masses where the transition between single and MP cluster occurs. This is further complicated by the fact that the original cluster masses are not accurately known. We think that disentangling the effect of individual histories from an age effect needs then a large sample of clusters; fortunately, more clusters are being added by different groups. The most massive young cluster not showing any significant spread in N abundances is NGC 419 ([Martocchia et al. 2017](#)), that likely had an original mass of $2 \times 10^5 M_{\odot}$. On the other hand, NGC 1978

([Martocchia et al. 2018b](#)) and Hodge 6 ([Hollyhead et al. 2019](#)) are only slightly older than NGC 419, and of similar mass ($\sim 1 - 2 \times 10^5 M_{\odot}$). We further notice that there are much older clusters of similar mass that also do not show evidence of multiple populations or have a very minor fraction of SG stars, such as Ruprecht 106 ([Villanova et al. 2013](#); [Dotter et al. 2018](#)) or Terzan 8 ([Carretta et al. 2014](#)). We conclude that the role played by cluster age is not yet soundly determined. At variance with [Bastian and Lardo \(2018\)](#), we then think it is premature to consider age as a basic parameter in the multiple population phenomenon and that more observations are required to settle this issue.

4 Impact of chemical anomalies on stellar evolution

The multiple population phenomenon impacts nearly all phases of stellar evolution, leading to significant deviations of the colour-magnitude diagrams of GCs with respect to simple stellar isochrones. Actually, the first clear evidence of the multiple populations can be traced back to the second half of the '60s, with the discovery of the so-called second parameter effect on the horizontal branch ([van den Bergh 1967](#)) and of the wide red giant branch of ω Cen=NGC 5139 ([Woolley 1966](#)). In this section, we will briefly review these points examining some of the main features.

4.1 The main sequence

Multiple populations impact the main sequences of GCs. Ultra-violet CMDs show effects related to the spread of He, light elements and n-capture elements. In the optical, the effect is detectable only for what concerns the spread in Helium and heavy element abundances. The latter is actually limited to those few clusters (such as ω Cen=NGC 5139; [Piotto et al. 2005](#); [Stanford et al. 2006](#); [Villanova et al. 2014](#); [Milone et al. 2017b](#)), where the different populations differ in the Fe content. The first realization that large variations in the He abundances can be responsible for a split of the main sequence of the mono-metallic cluster NGC 2808 came from the studies of [D'Antona et al. \(2005\)](#); [Piotto et al. \(2007\)](#). On the same timescale, a similar conclusion was reached for the multi-metallic cluster ω Cen=NGC 5139 by [Norris \(2004\)](#) from star counts, and by [Piotto et al. \(2005\)](#) from the determination of the metal abundance for stars of different colours. Splitting of sequences is however generally tiny and the high quality of HST photometry is usually needed to separate them: for instance, strict upper limits on He abundance variations were obtained from the very narrow MS of NGC 6397 by [di Criscienzo et al. \(2010\)](#), consistent with the very tiny difference of $\Delta Y=0.01$ later found by [Milone et al. \(2012b\)](#) for this cluster. In addition, He abundance variations should be separated from other effects, such as differential reddening, contamination by field stars, binarity, and variations in heavy element abundances (for this last point, see [Marino et al. 2019](#)). This is best achieved using multicolour photometry, as first demonstrated by [Milone et al. \(2012e\)](#) for the case of 47 Tuc=NGC 104. Milone and coworkers then applied this method to several other GCs: NGC 6397 ([Milone et al. 2012b](#)), NGC 6752 ([Milone et al. 2013](#)),

M 62=NGC 6266 (Milone et al. 2014a), M 2=NGC 7089 (Milone et al. 2015a), NGC 6352 Nardiello et al. (2015), and again NGC 2808 (Milone et al. 2015b). Finally, exploiting the extensive HST survey with the WFC3 by Piotto et al. (2015); Nardiello et al. (2018a), Milone et al. (2018c) determined He abundances for a wide sample of GCs (for a recent discussion of the aspects related to stellar models, see Cassisi et al. 2017). These are used in the discussion in Section 4.3.

A second important piece of information that can be obtained using the main sequence is the luminosity function of the different populations. This first shows that the spread in the proton-capture elements is not limited to the external layers of the stars, as suggested by the fact that the extension of the anti-correlations is similar in main sequence and red giant branch stars that have largely different depth of the outer convective envelope (Gratton et al. 2001; Cohen et al. 2002). The determination of the luminosity function is more complex, because dynamical effects might cause selective losses of the first/second generation stars, if they have a systematically different distribution within a cluster, as e.g. observed in the case of 47 Tuc=NGC 104 (Milone et al. 2018b) or ω Cen=NGC 5139 (Bellini et al. 2017). After consideration of these effects, it has been found that the fraction of stars in different generations in the lower main sequence are actually quite similar to those measured along the red giant branch, at least in the cases of M 4=NGC 6121 (Milone et al. 2014a) and NGC 6752 (Milone et al. 2019b), and possibly even NGC 2808 (Milone et al. 2012e). On the other hand, the only available determination of the mass function of different populations in NGC 2808 (Milone et al. 2012a) revealed significant differences. This represents an important constraint for models of the multiple populations (see Section 6).

4.2 RGB bump

Standard stellar evolutionary models (Iben et al. 1969) predict that the maximum penetration of the outer convective envelope at the base of the RGB (first dredge-up) leaves behind a discontinuity in the hydrogen content. When the star evolves along the RGB, the H-burning shell is moving outward in mass and when it reaches a region that has a higher H content (i.e. the inner edge of the previous first dredge-up) a hydrostatic readjustment occurs which causes the star to expand and move down the RGB temporarily, before it continues ascending the RGB. This causes a bump in the luminosity function: this is indeed found in the observational data (King et al. 1985). The luminosity of this bump depends on age, metallicity, and helium content (e.g. Sweigart and Mengel 1979; Cassisi and Salaris 1997). In particular, stars with higher He are expected to have a brighter RGB bump.⁸

After the pioneering work by Sollima et al. (2005) on ω Cen=NGC 5139, Bragaglia et al. (2010a) tried to see if stars of FG and SG, as defined by Na abundances, separated at the bump for 14 GCs in the Carretta et al. (2009c,b) sample. Indeed, a difference in the average position of the two populations showed up, implying a

⁸ It is worth noting that current models do not reproduce the correct zero-point Cassisi et al. (2011), however observational studies have been concentrating on differential effects, and we will limit our discussion to those in this text.

difference in He of about 0.05. However, due to the limited statistic, the result was obtained combining all GCs together⁹ and differences in RGB bump luminosity and the connected He difference were scarcely significant, even if in line with other tracers and expectations.

Later on, the luminosity of the bump of different populations has been traced using photometry, thus circumventing the scarcity of stars observed spectroscopically. [Nataf et al. \(2011\)](#) found a gradient in RGB bump properties in 47 Tuc=NGC 104, with the bump becoming less luminous and populated moving toward the external regions. They interpreted this as a variation in He abundance, under the idea that He-enriched SG stars are more centrally concentrated. [Milone et al. \(2015b\)](#) detected the RGB bump in four of the five populations they identified in NGC 2808 using a combination of optical and UV HST filters. By comparing the resulting differences in magnitudes with stellar models they were able to measure the implied differences in Y, which were in line with that found with other methods employing main sequence, HB and RGB stars. More recently, [Lee \(2017, 2018\)](#) employed wide field Strömgren photometry coupled with a narrow-band filter sensitive to CN variations to separate CN-strong (SG) and weak (FG) stars. They investigated the relative abundance in He using the bump magnitude and derived a difference of ΔY about 0.028 and 0.016 in M 5=NGC 5904 and NGC 6752, respectively, in agreement with other methods.

The most recent and exhaustive work is by [Lagioia et al. \(2018\)](#), who studied the RGB bump of the 56 GCs in the UV Legacy Survey ([Piotto et al. 2015](#)), excluding only ω Cen=NGC 5139 because of its complexity and including NGC 2808 which had already been published by [Milone et al. \(2015b\)](#). [Lagioia et al. \(2018\)](#) separated the different populations using the chromosome map and determined the RGB bump level for FG and SG stars in each of the bands. They retained for further consideration only those clusters with enough statistics (at least 15 stars in each RGB bump) and with a difference in magnitude between FG, SG significant at better than 90%. This means they were left with 26 GCs (plus NGC 2808). Considering only clusters for which they later derived also ΔY , the difference in magnitude is -0.033 ± 0.008 mag (for comparison, [Bragaglia et al. 2010b](#) found -0.045 ± 0.042). They then compared the differences in magnitude with the magnitude of synthetic RGB bump stars, derived from synthetic spectra with atmospheric parameters (in particular metallicity and temperature) and light-element abundances (C, N, O) appropriate for FG, SG stars and considering two He abundances (standard and enhanced). Difference in He mostly affect the optical bands and [Lagioia et al. \(2018\)](#) determined the ΔY implied by the Δmag using synthetic CMDs for the RGB based on the BaSTI tracks¹⁰; they were able to derive the information for 18 clusters, finding that $\Delta Y \leq 0.035$ for 14 of them, and about zero for 4 of them. For these GCs (not including NGC 2808), they found $\langle \Delta Y \rangle = 0.011 \pm 0.002$ between FG and SG stars, without correlation with [Fe/H] or M_V . A comparison with values derived from the main sequence ([Milone et al. 2018c](#)) is presented in Fig. 11, where we use the difference in Y between FG and SG. The two methods give a consistent ranking, even if the slope is not 1.

⁹ NGC 2808, the cluster showing the largest He differences, was not in the calculation, since no star below the RGB bump was observed for this cluster in that survey.

¹⁰ See <http://basti.oa-abruzzo.inaf.it/> ([Pietrinferni et al. 2006, 2004](#))

4.3 The horizontal branch

Variations in the He abundances have been called to explain the complex morphology of the horizontal branch since the '70s and early '80s (see e.g. [Norris et al. 1981](#)). The basic idea is that He-rich stars evolve faster than He-normal ones while on the main sequence. So He-rich horizontal branch stars are expected to be less massive than He-normal ones, and then to be bluer. After a couple of decades, this argument has been resurrected by [D'Antona et al. \(2002\)](#), who used it to explain the horizontal branches of M 13=NGC 6205 and NGC 6752. In [D'Antona and Caloi \(2004\)](#) a large variation of the He content was called for the case of NGC 2808, soon brilliantly confirmed by the discovery of the splitting of the main sequence ([D'Antona et al. 2005](#); [Piotto et al. 2007](#)). A direct link between the colours of stars along the horizontal branch and the multiple population phenomenon was obtained by in-situ observation of the expected abundance variations in NGC 6752 by [Villanova et al. \(2009\)](#), then confirmed by those in other clusters: M 4=NGC 6121 ([Marino et al. 2011c](#)), NGC 2808 ([Gratton et al. 2011b](#); [Marino et al. 2014](#)), NGC 1851 ([Gratton et al. 2012b](#)), 47 Tuc=NGC 104 and M 5=NGC 5904 ([Gratton et al. 2013](#)), M 22=NGC 6656 ([Gratton et al. 2014](#)), M 30=NGC 7099 and NGC 6397 ([Mucciarelli et al. 2014a](#)), and NGC 6723 ([Gratton et al. 2015](#)). A complication in these comparisons is that the atmospheres of the hottest stars along the horizontal branch (warmer/bluer than the so-called Grundahl jump: [Grundahl et al. 1999](#)) are in radiative equilibrium, leading to large effects related to diffusion and radiation pressure resulting in a very odd abundance pattern (see [Behr et al. 1999](#)). This makes it impossible to sample the whole horizontal branch in many clusters for the abundances of the elements that are diagnostics of the multiple populations.

Another possible approach is to reconstruct the He abundances from the location of the stars on the horizontal branch by comparisons with evolutionary models, as pioneered by [D'Antona et al. \(2002\)](#), and later applied by many others, e.g. [Dalesandro et al. \(2011, 2013\)](#) who used a combination of ground-based and UV HST bands, where different He translates (also) into different magnitudes; they derived the He content and dispersion of NGC 2808, where they recovered the distinct populations, and M 3=NGC 5272, M 13=NGC 6205, and M 79=NGC 1904. This is not an easy task, because the horizontal branch is also shaped by the metal abundance, the age, the total CNO content, and the mass-loss along the red giant branch. Luckily, metal abundances are well established (see [Carretta et al. 2009a](#)) and ages are also now quite well settled, thanks to the progress allowed by HST photometry (see e.g. [Marín-Franch et al. 2009](#); [Dotter et al. 2011](#); [VandenBerg et al. 2013](#)). The main issue concerns mass-loss, that depends on metal abundance and likely contains a small random term, variable from star-to-star; it is even possible that mass-loss is different for He-normal and He-rich stars, as discussed in [Salaris et al. \(2016\)](#) and very recently by [Tailo et al. \(2019\)](#). Since different assumptions are used by each author, comparison between results is not easy. We will then consider here only extensive data sets, such as those of [Dotter et al. \(2010\)](#); [Gratton et al. \(2010a\)](#), and [Milone et al. \(2014b\)](#). The upper panel of Fig. 12 compares the spread of the He abundances within individual GCs derived from an analysis of the distribution of stars along the horizontal branch ([Gratton et al. 2010a](#)) with those from the colours

of main sequence stars (Milone et al. 2018c). While there is some spread exceeding the error bars, there is an overall good correlation between the two estimates, with a linear correlation coefficient of $r=0.51$ over 51 clusters. The significance of this correlation is very high. Residuals around the identity lines are correlated with the metal abundance of the cluster; namely, the spread in He abundance derived from the main sequence is systematically larger than that derived from the horizontal branch for the most metal-rich clusters ($[\text{Fe}/\text{H}] > -0.8$), while typically the opposite holds for more metal-poor clusters. On the whole, the existence of such differences is not surprising, given the complexity of deriving He abundances in clusters. The most uncertain case is for the derivation of the He abundance from the horizontal branch of clusters with red horizontal branches because in this case a quite large variation in the mass (that is, on the He abundance) has only a very minor effect on the horizontal branch¹¹. A considerable reduction of the scatter between the two data sets is obtained if we correct the spread in He abundances determined from the HB using the empirical formula $\Delta Y_{\text{cor}} = \Delta Y_{\text{HB}} (0.58 + 0.36/[\text{Fe}/\text{H}]^2)$ (see lower panel of Fig. 12). The only discrepant case is NGC 2808; we notice that for this cluster the spread in mass along the HB (Gratton et al. 2010a), and then in helium abundance, is likely underestimated. Hereinafter, we will adopt the average of the helium spread from Milone et al. (2018c) and these corrected values for the HB as the best current estimate of the spread in He abundances within a cluster.

As discussed by Bragaglia et al. (2010a), if we may assume that the metal abundance is the same for all stars within a cluster, it is possible to derive the difference in He abundance between second and first generation stars also from the difference in the value of $[\text{Fe}/\text{H}]$, because a change in the He abundance is anti-correlated with the change in the H abundance, and it is then correlated with that in $[\text{Fe}/\text{H}]$. Since the expected variation in H abundances are small (at most, $\sim 20\%$), quite large samples of accurate and uniform $[\text{Fe}/\text{H}]$ values must be considered. Fig. 13 compares the spread in He abundances within a cluster with the offset in $[\text{Fe}/\text{H}]$ values obtained in Bragaglia et al. (2010a). The correlation is good, with a linear correlation coefficient of 0.65 that is highly significant.

If we combine the two sets of determinations of the He spread within a cluster, it is clear that these spreads are rather small for the majority of the GCs. Also, this quantity is very well correlated with the cluster mass, as derived by Baumgardt et al. (2019) (see Fig. 14). The most discrepant case is that of NGC 2419, that has a spread in He larger than expected for its mass. The very good correlation existing between the spread in the He abundance and the cluster mass is a clear indication that cluster mass is indeed the main parameter determining the spread in He abundances. In particular,

¹¹ An example of the difficulties in deriving He abundance variations from clusters with red horizontal branch is given by a comparison of the spread in He abundances for the SMCs clusters NGC 121, NGC 339, NGC 416, and Lindsay 1 as determined from the horizontal branch by Chantreau et al. (2019), and from a pseudo-chromosome map by Lagioia et al. (2018). While the first study found variations in the He abundances as large as $\Delta Y = 0.08$, the second one only found very tiny spreads, with the highest value being $\Delta Y = 0.010 \pm 0.003$. Chantreau et al. (2019) noticed this difference, and attributed it to the different meaning of ΔY in the two studies - maximum excursion with respect to mean difference between first and second generation stars, although it seems quite difficult to justify a factor of almost ten difference between the two results this way. We then think that the spread in He abundances derived for red horizontal branch clusters should be taken with caution.

we find that only clusters with a mass larger than $3 \times 10^5 M_{\odot}$ have a spread in He abundances larger than 0.01.

4.4 Asymptotic giant branch stars vs red giant stars

Table 1 Number of RGB and AGB stars belonging to first and second-generation stars in GCs. The corresponding fractions of SG stars are given in Cols. 6 and 7 for RGB and AGB stars, respectively. Data references are: [Campbell et al. 2013](#); [MacLean et al. 2016, 2018a](#), [Wang et al. 2016; 2017](#), [Lapenna et al. 2015](#), [Mucciarelli et al. 2019](#), and [Masseron et al. 2019](#).

| NGC | Other | RGB _{FG} | RGB _{SG} | AGB _{FG} | AGB _{SG} | f(RGB _{SG}) | f(AGB _{SG}) |
|----------------------------|--------|-------------------|-------------------|-------------------|-------------------|-----------------------|-----------------------|
| MacLean/Campbell et al. | | | | | | | |
| NGC 6121 | M 4 | 48 | 58 | 15 | 0 | 0.55±0.05 | < 0.06 |
| NGC 6397 | | 18 | 30 | 3 | 5 | 0.63±0.07 | 0.63±0.17 |
| NGC 6752 | | 7 | 17 | 20 | 0 | 0.71±0.09 | < 0.05 |
| Lapenna/Mucciarelli et al. | | | | | | | |
| NGC 6266 | M 62 | 7 | 6 | 5 | 0 | 0.46±0.14 | < 0.20 |
| NGC 6752 | | 6 | 8 | 11 | 8 | 0.57±0.13 | 0.42±0.11 |
| Wang et al. | | | | | | | |
| NGC 104 | 47 Tuc | 9 | 18 | 24 | 16 | 0.67±0.10 | 0.40±0.08 |
| NGC 2808 | | 23 | 24 | 14 | 17 | 0.51±0.07 | 0.55±0.09 |
| NGC 5904 | M5 | 11 | 24 | 5 | 10 | 0.69±0.08 | 0.67±0.12 |
| NGC 5986 | | 5 | 8 | 3 | 4 | 0.72±0.11 | 0.57±0.19 |
| NGC 6121 | M4 | 15 | 48 | 9 | 10 | 0.76±0.06 | 0.53±0.11 |
| NGC 6205 | M13 | 23 | 73 | 2 | 14 | 0.76±0.04 | 0.88±0.08 |
| NGC 6266 | M62 | 5 | 8 | 5 | 0 | 0.62±0.13 | < 0.20 |
| NGC 6752 | | 6 | 18 | 17 | 3 | 0.75±0.09 | 0.15±0.08 |
| NGC 6809 | M55 | 26 | 51 | 8 | 15 | 0.66±0.05 | 0.65±0.11 |
| Masseron et al. | | | | | | | |
| NGC 5024 | M 53 | 20 | 17 | 2 | 1 | 0.46±0.08 | 0.33±0.27 |
| NGC 5272 | M 3 | 66 | 40 | 21 | 7 | 0.38±0.05 | 0.25±0.08 |
| NGC 6205 | M 13 | 28 | 68 | 11 | 4 | 0.71±0.05 | 0.27±0.11 |
| NGC 6341 | M 92 | 11 | 38 | 7 | 9 | 0.78±0.06 | 0.56±0.12 |
| NGC 7078 | M 15 | 39 | 62 | 2 | 4 | 0.61±0.05 | 0.67±0.19 |

In 1981, [Norris et al.](#) found indication for a lack of CN-strong stars within their AGB sample in the cluster NGC 6752, as compared to stars on the first-ascent giant branch, where CN-strong stars are the dominant population. One of the possible explanations suggested by [Norris et al. \(1981\)](#) is that those we now recognize as SG stars and which are enriched in He and thus less massive relative to the FG stars, will fail in ascending the giant branch for a second time, evolving directly to white dwarfs from the HB phase (as AGB manqué stars, e.g., [Greggio and Renzini 1990](#)). This pioneering work brought to light the presence of what is currently called the “AGB problem”, which has received special attention in recent years. Despite considerable work, a clear picture and a comprehensive understanding is still not in hand.

[Snedden et al. \(2000\)](#) compared the CN distributions along the AGB and RGB in different clusters by considering extant literature studies of NGC 6752 ([Norris et al. 1981](#)), M 13=NGC 6205 ([Suntzeff 1981](#)), and M 4=NGC 6121 ([Norris et al. 1981](#); [Suntzeff and Smith 1991](#)). The conclusion of their study pointed to a general lack of

SG, CN-strong AGB stars, although to differing extents for each of the three clusters (with NGC 6752 the obvious case of a total dearth of CN-strong AGB stars).

Campbell et al. (2006) also reviewed the status of the field at that time, collecting literature data and stressing the need for further investigations based on larger samples of AGB stars in clusters. In their Table 1, the authors showed GCs classified according to the presence of CN weak and CN strong stars within the AGB population for M 3=NGC 5272, M 4=NGC 6121, M 5=NGC 5904, M 13=NGC 6205, M 15=NGC 7078, M 53=NGC 5024, NGC 6752 and 47 Tuc=NGC 104 (see that paper for details and references). Out of 8 GCs, only M 5=NGC 5904 and 47 Tuc=NGC 104 displayed a significant population of CN-strong AGB stars.

In qualitative agreement with theory (Greggio and Renzini 1990), these studies suggested that the stars with the smallest mass along the HB either cannot reach the AGB or they leave it earlier than more massive stars. This should appear as a correlation between HB morphology and counts of stars on the AGB. Gratton et al. (2010b) explored this relation and indeed found that there is a good correlation between the mass of the hottest 10% stars on the HB and the count ratio between AGB and RGB stars ($f_{AGB} = n(AGB)/n(RGB)$). On the other hand, these counts suggest that even in those clusters that have the smallest ratio between the number of AGB and RGB stars, still there are more AGB stars than expected in the case that all SG stars avoid the AGB. Actually, if we compare the counts of AGB stars by Gratton et al. (2010b) with the fraction of FG/SG stars determined by Milone et al. (2017a), we find that even in extreme cases at least half of the SG stars should reach the AGB, and in clusters that do not have an extended blue HB, virtually all of them should go through this phase. We should then expect that the fraction of SG stars along the AGB is never below ~50%, in many clusters should be of the order of two-thirds, and that this fraction should depend on the morphology of the HB.

In the last few years, various groups tried to determine the ratio between FG and SG stars along the AGB using spectroscopy, mainly exploiting the Na/O anticorrelation, but in some cases also the Al/Mg distribution. The main results are collected in Table 1. Taken at face value, the picture is complex and quite at odds with expectations, with sometimes conflicting results obtained for the same cluster. For instance, in the case of NGC 6752 (that has an extended blue HB), Campbell et al. (2013) found that all AGB stars belong to the FG of the cluster (see their Figure 2), corroborating previous evidence by Norris et al. (1981). A low fraction of SG stars of this GC along the AGB is also found by Wang et al. (2017); this contrasts with the theoretical expectation that 50% of the AGB stars are predicted to be SG (Cassisi et al. 2014). These results were questioned by Lapenna et al. (2016), who instead detected a significant population of moderately Na-enhanced AGB stars in NGC 6752, while confirming that no extreme Na-rich stars are present within their AGB sample, which is in line with Cassisi et al. (2014) [but see also Campbell et al. 2017]. An extreme case is that of M 4=NGC 6121: for this cluster, MacLean et al. (2016) found that, despite the lack of an extended blue HB, all the AGBs are found to be consistent with FG. This finding has been disputed by Wang et al. (2017), Lardo et al. (2017b) and Marino et al. (2017). A new discussion by MacLean et al. (2018b) concluded that a significant disagreement between theory and observations still remains for this cluster. MacLean et al. (2018a) investigated many possibilities for this hypothetical offset

between AGB and RGB stars. On the other hand, Wang et al. (2016) analysed a quite numerous sample of RGB and AGB stars in NGC 2808 and found almost identical distributions. This is quite unexpected given the extended blue HB of NGC 2808. Based on only 6 AGB stars, Marino et al. (2017) concluded that multiple populations are present both in the RGB and AGB of NGC 2808; however, as it appears from their Figure 3, the Na and O distributions for AGBs are skewed towards higher Oxygen and lower Sodium abundances relative to the RGBs by Carretta et al. (2009c), who found RGB stars in NGC 2808 exhibit extreme patterns in terms of [Na/Fe] and [O/Fe] ratios, up to +1 and -1 dex, respectively.

These studies mainly used optical spectra, from which Na and O abundances can be obtained. Near infrared spectra obtained with APOGEE have also been used. In this case, [Al/Fe] are generally used to assign stars to the different populations (García-Hernández et al. 2015; Majewski et al. 2017). Quite extensive samples of early AGB stars along with a control sample of RGB stars have been obtained by Masseron et al. (2019) for M 3=NGC 5272, M 13=NGC 6205, M 92=NGC 6341, M 53=NGC 5024, and M 15=NGC 7078. They have detected Al-rich AGB stars in all of them. A significant Mg-Al anticorrelation is emerging for cluster NGC 6341=M 92, and less evident for NGC 5272=M 3 and NGC 6205=M 13, while for NGC 7078=M 15 and NGC 5024=M 53 low statistics prevent from drawing any conclusion. In order to estimate if there is a lack of Al-rich stars (here defined as those with [Al/Fe] > 0.25 dex) on the AGB in these clusters, we may count the number of Al-rich and Al-poor stars along the RGB and the AGB (see Figure 15). In the RGB we obtain 164 Al-poor stars and 225 Al-rich ones; the same numbers in the AGB are 43 Al-poor and 25 Al-rich stars¹². This indicates a significant (at 4σ level) lack of Al-rich stars along the AGB: the latter have $\sim 40\%$ of Al-rich (i.e. SG) stars with respect to what is expected according to the population ratios observed on the RGB.

Overall, there is a general trend for a lack of SG AGB stars. If we sum up results obtained for the whole samples observed by individual groups, MacLean et al. (2016) found $57\pm 2\%$ of SG RGB stars and $32\pm 4\%$ of SG AGB stars. The difference is less pronounced, but still clear, if we consider the results obtained by Wang and coworkers: in this case, SG stars make up $69\pm 2\%$ of the RGB stars and $51\pm 4\%$ of the AGB stars. Considering the total sample analysed by Masseron et al. (2019), the fractions of SG stars along the RGB and the AGB are $58\pm 3\%$ and $37\pm 6\%$, respectively. On the other hand, the fraction of SG stars along the AGB is almost identical if we restrict to GCs with extreme HB morphology (i.e., M 13=NGC 6205, M 62=NGC 6266, M 2=NGC 7089, NGC 6752, NGC 2808, and M 15=NGC 7078); the same is true if we restrict the sample to those with red HBs. Thus the relationship with the HB morphology seems not so straightforward and other causes might be underneath. Moreover, in several cases there are no SG stars detected, and this happens also for GCs that do not have an extended blue HB.

A more careful inspection of this complex pattern shows that we are facing several issues:

¹² These calculations are restricted to those stars that have Al abundances, which comprises more than 90% of the total sample.

- often there is the suspicion that there are small but significant offsets between the abundance ratios determined from RGB and AGB stars. This is e.g. exemplified by the study of NGC 6121=M4 by [MacLean et al. \(2016\)](#), where the Na abundances determined for the AGB stars appear to be typically ~ 0.15 dex below those obtained for the RGB stars, or by the different results depending on the way abundances are obtained for the stars in NGC 2808 by [Wang et al. \(2016\)](#). The existence and possible origin of these offsets is debated ([Lardo et al. 2017b](#); [Marino et al. 2017](#); [Campbell et al. 2017](#); [MacLean et al. 2018b](#)), and the issue is not yet settled;
- stars are assigned to FG or SG by comparing their abundances with a given threshold. Often distributions are rather continuous, so that the value of the threshold is quite arbitrary and the exact choice has a large impact on the counts¹³. As an example of this kind of problem, we may consider the case of NGC 6752 ([Campbell et al. 2013](#); [Wang et al. 2016](#); [Lapenna et al. 2016](#)): the three distribution of Na abundances in the different studies all look quite similar with each other, but the conclusions on the counts are very discrepant (see [Campbell et al. 2017](#), where for NGC 6752 all the studies agree very precisely in $A(\text{Na})$ -their Fig 13).
- AGB is a rather fast evolutionary phase: as a consequence, samples of AGB stars are generally not numerous and random errors are large when compared with the expected variation on the frequency of FG/SG stars;
- finally, as we have seen in Section 3, the various anti-correlations might be telling somewhat different stories: for instance, the Mg-Al anticorrelation (considered by [Masseron et al. 2019](#)) is rarely present among metal-rich GCs, and there may be stars that are clearly classified as SG stars from the strength of N bands that may look quite similar to FG stars according to the Na-O or Mg-Al abundances or even the CN bands.

We may then re-examine the results collected in Table 1 taking into account these issues. We find that there are facts that look solidly established and others that are still open. In the first group we may place (i) the lower overall frequency of SG stars in the AGB, that is found in all studies though with significant cluster-to-cluster differences; and (ii) the virtual absence of AGB stars with extremely large Na/Al excesses in clusters with very extended horizontal branches (e.g. NGC 6752: [Campbell et al. 2013](#); [Lapenna et al. 2016](#); [Wang et al. 2016](#); M 13=NGC 6205: [Masseron et al. 2019](#); NGC6266: [Lapenna et al. 2015](#)), though there might be some stars with extreme composition in the AGB of NGC 2808 ([Wang et al. 2016](#); [Marino et al. 2017](#)). We note however that the most extremely O-poor stars in this cluster are not very Na-rich, as shown by [Carretta et al. \(2007\)](#), so it is not clear that they can be found using Na abundances alone. In general, the lack of stars with large Na/Al excess might contribute to explaining the apparent dearth of SG AGB stars in these GCs, even though there might also be a number of AGB SG stars with small or moderate excesses of these elements that are disguised in the FG group. On the other hand, the lack of SG stars in GCs that do not have a very extended HB (such as NGC 6121=M 4) is still to be established firmly.

¹³ Note that [MacLean et al. \(2016\)](#) rather use the observed minima in the $[\text{Na}/\text{H}]$ distribution to separate FG and SG stars along the AGB and the RGB comparison dataset

Future observations of some critical pairs such as e.g., NGC 288 and NGC 362 (one of the most famous second-parameter *pairs*) or the determination of the Al abundances along the AGB of NGC 2808 might help in shedding light on this still poorly understood field of research. In these kind of investigations a careful selection of genuine AGB stars, avoiding RGB contamination, along with reliable parameter determination (with possible offset and/or NLTE effects that have to be taken into account), and the use of RGB control sample is of vital importance.

5 Lithium

5.1 Lithium and mixing

The predicted difference in depth of the convective envelope between main sequence and lower red giants (Iben 1964) is confirmed by the dilution effect of lithium when stars evolve from the main sequence to the lower red giant branch (luminosity below the RGB bump, that we use here as a dividing line because Li is severely depleted after this evolutionary phase). The effect is similarly present in both field (Gratton et al. 2000) and GC stars (NGC 6397, Lind et al. 2009; NGC 6121=M 4; ω Cen=NGC 5139 Monaco et al. (2010); Mucciarelli et al. 2011; NGC 104=47 Tuc (Dobrovolskas et al. 2014), M 30=NGC 7099: Gruyters et al. 2016) (see Fig. 16).

The actual Li dilution depends on the ratio of the mass contained in the region where Li is not burnt during the main sequence and in the convective envelope at the base of the RGB; this quantity is (weakly) dependent on metallicity and age. Mucciarelli et al. (2012b) examined the run of the Li abundance in field low-luminosity giants and found a quite constant value of $\log n(\text{Li}) = 0.94$ over a wide range of Fe abundances ($-3.4 < [\text{Fe}/\text{H}] < -1.3$). Then, they considered the dependence expected from stellar evolutionary models. The quantity they considered is the expected depletion between the pre-main sequence and the RGB phases; they hence did not consider the possible surface depletion due to diffusion on the main-sequence. Even so, the result depends on the treatment of convection. Independently of this, the models show a weak dependence on metallicity, with values changing by some 0.11-0.16 dex when metallicity ranges from $[\text{Fe}/\text{H}]=-2.14$ to $[\text{Fe}/\text{H}]=-1.01$. The slope is a bit steeper when diffusion is taken into account, because diffusion is expected to have a larger impact in lower metallicity stars that have a thinner outer convective envelope.

On the whole, there is good agreement between observations and theoretical prediction. This strongly argues against the possibility that abnormal mixing (that would cause destruction of large amounts of Li) is the cause of the abundance anomalies related to multiple populations (Pancino 2018).

5.2 Lithium and multiple populations: observations

In the multiple population framework, a number of studies have been conducted in order to ascertain the run of lithium with proton-capture element abundances in GC

Table 2 Fraction of stars with extreme composition along the [Na/O] anticorrelation (E-stars: Carretta et al. 2009c) and of Li-poor stars in various clusters

| Cluster | [Fe/H] | $\log M_{rmin}$ | Type | E-Fraction | Ref | Li-poor | Ref |
|----------|--------|-----------------|------|-----------------|-----|-------------------|-----|
| NGC 362 | -1.26 | 6.06 | 2 | 0.03 ± 0.02 | 3 | 0.04 ± 0.03 | 7 |
| NGC 1904 | -1.60 | 6.08 | | 0.10 ± 0.04 | 1 | 0.14 ± 0.08 | 7 |
| NGC 2808 | -1.14 | 6.36 | 1 | 0.14 ± 0.03 | 9 | 0.14 ± 0.05 | 7 |
| NGC 5904 | -1.29 | 5.96 | 1 | 0.07 ± 0.02 | 1 | 0.074 ± 0.030 | 6 |
| NGC 6121 | -1.16 | 6.03 | 1 | 0.00 ± 0.01 | 1 | 0.00 ± 0.26 | 8 |
| NGC 6218 | -1.37 | 5.63 | 1 | 0.03 ± 0.02 | 1 | 0.00 ± 0.02 | 6 |
| NGC 6397 | -2.02 | 5.60 | 1 | 0.00 ± 0.01 | 1 | 0.020 ± 0.008 | 4 |
| NGC 6752 | -1.54 | 5.83 | 1 | 0.40 ± 0.06 | 2 | 0.30 ± 0.05 | 5 |
| NGC 7099 | -2.27 | 5.79 | 1 | 0.03 ± 0.02 | 2 | 0.11 ± 0.08 | 10 |

References: 1. Carretta et al. (2010c); 2. Carretta et al. (2012); 3. Carretta et al. (2013a); 4. Lind et al. (2009); 5. Shen et al. (2010); 6. D’Orazi et al. (2014); 7. D’Orazi et al. (2015); 8. D’Orazi and Marino (2010); 9. Carretta (2015); 10. Gruyters et al. (2016)

Table 3 Dilution as obtained from Na and O abundances published in Carretta et al’s papers (Col. 2) along with lithium differences between intermediate SG stars and primordial stars (Col. 3), the amount of Li produced with respect to the original value (Col. 4) and the difference in maximum Na and minimum O content (Col. 5).

| GC | I Dilution | Li(I-P) | Li(Prod-Original) | $[\text{Na/Fe}]_{\text{max}} - [\text{O/Fe}]_{\text{min}}$ |
|----------|------------|------------------|-------------------|--|
| NGC 362 | 0.53 | -0.03 ± 0.03 | -0.07 ± 0.08 | 0.90 |
| NGC 1904 | 0.47 | -0.14 ± 0.04 | -0.32 ± 0.19 | 1.32 |
| NGC 2808 | 0.50 | -0.05 ± 0.03 | -0.11 ± 0.09 | 1.56 |
| NGC 5904 | 0.54 | -0.02 ± 0.03 | -0.04 ± 0.08 | 1.30 |
| NGC 6121 | 0.62 | 0.04 ± 0.05 | 0.10 ± 0.11 | 0.94 |
| NGC 6218 | 0.51 | -0.02 ± 0.05 | -0.04 ± 0.12 | 0.96 |
| NGC 6397 | 0.73 | -0.02 ± 0.03 | -0.08 ± 0.17 | 0.71 |
| NGC 6752 | 0.40 | -0.13 ± 0.07 | -0.25 ± 0.21 | 1.05 |

stars¹⁴. Lithium offers critical diagnostics for the investigations of the internal pollution source. In fact, because of its very fragile nature (the Li burning temperature is $T \approx 2.5 \times 10^6 \text{K}$), it is expected that material processed at the much higher temperatures of the hot H-burning via CNO re-cycled in the formation of the subsequent generation(s) of stars within a GC, is free of Li. Thus, while FG stars should exhibit a Li abundance pattern compatible with their field counterparts ($A(\text{Li}) \sim 2.0 - 2.2$ dex), SG stars should be depleted in Li unless Li is produced in the polluters. This implies a positive correlation between Li and O (and/or C, Mg) and an anti-correlation between Li and Na (and/or N, Al).

Most interesting, while massive stars (supermassive stars, fast rotating and/or binaries) can only destroy Li, intermediate mass AGB stars may activate the *Cameron-Fowler* mechanism: the ${}^3\text{He}(\alpha, \gamma){}^7\text{Be}$ reaction takes place in the stellar interiors and then convective processes bring the material outwards, where the temperature is much lower. By capturing one electron, the reaction ${}^7\text{Be}(e^-, \nu){}^7\text{Li}$ could produce lithium, under the condition that it is not rapidly destroyed by thermonuclear reac-

¹⁴ The investigation of the Li discrepancy as measured in Pop II stars with respect to the standard Big Bang nucleosynthesis is not discussed in this review, since our main focus is the multiple population scenarios. We refer the reader to Sbordone et al. (2010), Mucciarelli et al. (2014b), Fu et al. (2015), and references therein for a specific discussion on this topic

tions (Cameron and Fowler 1971). As a consequence, any Li production would tend to erase the above-mentioned Li-Na-O (anti)correlations, by furnishing compelling evidence for intermediate mass AGBs as polluters in GCs.

With this background in mind, several GCs have been investigated with the simultaneous determination of Li/Na/O/Al for samples of dwarf and giant stars. We considered here only giants fainter than the RGB *bump*, because Li is completely destroyed after this evolutionary phase. In 2005, Pasquini et al. analysed 9 TO stars in NGC 6752 and found a statistically meaningful anti-correlation between Li and Na and a positive correlation Li-O; this result was later confirmed, upon a larger sample of 112 stars, by Shen et al. (2010). Crucially, both studies revealed that the slope in the Li-O plane is not 1, as expected in the simple pollution scenario of ejected material that is Li free. Conversely, SG stars (Na-rich, O-poor) still exhibit a significant amount of Li, which cannot be explained by invoking a dilution of processed material with pristine matter. The presence of a Li-Na anti-correlation is also evident from the main-sequence stars analysed by Gruyters et al. (2014).

A weak hint of Li-Na anti-correlation has been also detected by Lind et al. (2009) in the cluster NGC 6397 ($[Fe/H] \approx -2$), whereas D’Orazi et al. (2010b) found a very peculiar pattern for the metal-rich GC 47 Tuc=NGC 104 ($[Fe/H] \approx -0.7$ dex): the Li content does not show an anti-correlation with Na, and only a weak correlation appears with O, with a large scatter in the Li abundance distribution of FG stars. This suggests a primordial Li dispersion that is probably related to the high-metallicity nature of this GC (i.e., a Pop II analogue of M 67, see Pace et al. 2012 and references therein), and not connected to the MP scenario.

M 4=NGC 6121 is certainly the most thoroughly examined GC in terms of Li abundances. D’Orazi and Marino (2010) determined Li and p-capture elements for 109 RGB stars (below the bump) and found that FG and SG stars share the same Li content, with lack of any (anti)correlations. At present, the only explanation we have for such a trend is that Li has been produced within the polluters, suggesting that intermediate massive AGBs are at work, at least in this cluster. This result has been later corroborated by Mucciarelli et al. (2011) and Monaco et al. (2012), while a very weak trend has been found by Spite et al. (2016). Similarly to M 4=NGC 6121, M 12=NGC 6218 ($[Fe/H] \approx -1.3$) and NGC 362 ($[Fe/H] \approx -1.3$) have been found to host Li-rich SG stars, with no significant Li dispersion in contrast to the large variations in Al and Na abundances (D’Orazi et al. 2014, 2015). In both these GCs, FG and SG stars exhibit the same Li abundance, making Li production across the different stellar generations unavoidable to explain the observed pattern. It may appear quite implausible of obtaining a constant Li content when the initial and enriched materials are mixed in different amounts because it requires the enriched material to have a similar Li abundance as the original material. This clearly requires some more insight; we will come back on this point on the next subsection.

On the other hand, the more massive clusters M 5=NGC 5904, NGC 1904 and NGC 2808 behave differently: while they are still comprised of a dominant population of Li-rich SG stars, these GCs also host an extreme population that reveals large enhancement in Al/Na accompanied by a Li depletion (D’Orazi et al. 2014, 2015). In Fig. 17 we show the run of Al abundances in RGB stars (below the bump luminosity) for NGC 2808 (originally from D’Orazi et al. 2015): this GC hosts a large

fraction of SG stars (including extreme stars in terms of their Al abundances) that are Li normal, that is with a Li content in agreement with its original value. Most interesting, a handful of extreme stars exhibit a substantial Li depletion (red upside-down triangles in Fig. 17). The fraction of Li-poor stars in NGC 2808 (0.14 ± 0.08) is actually consistent with the fraction of E-stars found by Carretta (2015) and of stars belonging to E-population defined by Milone et al. (2015b). These are stars with extreme overabundance of He, Al and Si and underabundance of O and Mg. These are also likely the stars with anomalous K and Sc abundances (Carretta 2015; Mucciarelli et al. 2015a). Unluckily, a star-to-star correspondence between these abundance patterns cannot be obtained because the samples of stars analyzed do not overlap. For this group of stars, we are not able to discriminate whether polluters are either massive stars or a sub-class of intermediate mass AGB stars that are not able to produce Li (because for example of their mass, metallicity, or a combination of both). The observational evidence is that in this kind of GCs more than one polluter class has to be involved in order to reproduce the complex chemical pattern, as also recently found by Carretta and Bragaglia (2018) in NGC 2808 using O, Na, Al abundances in a large sample of brighter RGB stars and by Johnson et al. (2019) in NGC 6402.

Considering all the GCs for which Li and p-capture element abundances have been determined (Table 2)¹⁵, there is a significant correlation between the fraction of stars with extreme composition along the [Na/O] anticorrelation (E-stars, following the definition by Carretta et al. 2009c) and the fraction of Li-poor stars (see Fig. 18). The Pearson correlation coefficient is 0.94 over nine GCs, with an extremely low probability that this is a random result. The general picture emerging from the analysis of all the GCs for which Li has been determined in conjunction with p-capture elements suggests that *the more massive the cluster, the larger the Li variation*. In other words, the Li production across the different stellar generations is larger (more efficient) in relatively low-mass GCs. In this framework, the cluster metallicity does also play a role: NGC 362 is much less massive than NGC 2808 and has a metal content more than a factor of two higher than NGC 1904, which indicates that Li production is less efficient in more massive and more metal-poor systems. Moreover, the fraction of Li-poor stars in GCs is anticorrelated with the dilution of the stars with intermediate composition along the [Na/O] anti-correlation (I-stars, following the definition by Carretta et al. 2009c), with a Pearson correlation coefficient of $r = -0.74$. This means that the larger is the fraction of extreme Li-poor stars, the lower is the dilution for the I population. This suggests that extreme Li-poor and I populations are not independent, at least in some clusters. There is also a strong negative correlation ($r = -0.83$) between the fraction of Li-poor stars and the difference in Li abundance between SG and FG stars: the larger the Li content detected in SG stars, the lower the fraction of Li-poor stars in GC. Both these aspects might be simply reflecting the dependence on the GC (current) mass: however, there is no evidence for a direct correlation between the fraction of Li-poor star and the cluster mass.

A further complication to this composite mosaic is added by the recent analysis of Li, Na, and Al in 199 RGB stars in the peculiar GC ω Cen=NGC 5139 by Mucciarelli

¹⁵ Given the primordial Li scatter in NGC 104, which is unrelated to the multiple population scenarios, this GC was omitted from the present discussion.

et al. (2018). Here, only the most metal-poor component displays a clear Li-Na (and Al) anti-correlation, and from the point of view of Li, the cluster hosts at least 4 populations: FG stars coexist with Li-rich SG stars, with Li-poor SG stars, and with the anomalous (metal-rich) population that is only characterized by Li depletion.

5.3 Lithium and multiple population: some considerations

The argument related to the Li production within the polluters have been often overlooked in the literature, despite being a crucial diagnostic that should be considered to disentangle the stellar source of the polluters. At first glance, it might appear that there is a sort of “conspiracy” in that the Li production within the polluters has to be exactly at the same level of the original (primordial) Li content, i.e., $A(\text{Li}) \approx 2-2.2$ dex. How much is this exactly the case depends on the abundance of Lithium in the diluting material (see Section 8.1). Usually it is assumed that the diluting material has the original Li abundance; we should remark that this is not obvious, because this depends on its origin; for instance, in Sect. 8.1.1 we will consider the case of diluting material from interacting intermediate mass binaries (Vanbeveren et al. 2012) that should be Li-poor. Anyhow, in Fig. 19, we plot the difference in Li abundances for FG and SG (only intermediate) stars as a function of the dilution factors (where dilution 0 means pure ejecta and dilution 1 is for pristine material), as obtained from Na and O abundances and anti-correlations published by Carretta and collaborators. The orange curve represents the dilution under the assumption that there is no Li production within the polluters: as it can be seen from the plot, this curve does not reproduce the observed points, corroborating the indication that we must call for Li production in the polluters. In this context it is noteworthy that in case the diluting (pristine) material is Li-free, as it could be in the case of interacting binaries as source of diluters, the Li production would have been even more efficient.

If we now consider that the relationship between the observed Li abundance, the Li production and the dilution factor can be expressed as

$$Li_{prod} = \log [(10^{Li_{SG}} - dil \times 10^{Li_{FG}})/(1 - dil)]$$

and we can derive the amount of Li that has to be produced as a function of the dilution - in the hypothesis that the diluting material has the original Li abundance. This is the quantity that we have considered in Fig. 20, where we plot the difference in the Li production with respect to the original value as a function of the difference in ratios $[\text{Na}/\text{O}]_{\text{max}}$ and $[\text{Na}/\text{O}]_{\text{min}}$ from the Carretta’s papers (Carretta et al. 2009c, 2013a). There is a hint for an anti-correlation between the two quantities, although the scatter is quite large. The argument is not so much different - but the relation should be tighter - if we assume that the diluting material is Li-poor.

The only polluter proposed so far able to produce Lithium are AGB stars: on the whole there is a reasonable agreement of the required Li production and at least some of the AGB model predictions (red solid line in Fig. 20), that is, those by D’Antona et al. (2012). However, this agreement depends on details of the AGB models that suffer dramatic uncertainties, which include, but are not limited to: (i) the treatment of convection, (ii) the mass loss law, and (iii) the nuclear reaction rates. There are

numerous works in the literature where these topics have been extensively discussed (see e.g. [Ventura et al. 2009](#); [D’Orazi et al. 2013](#); [Doherty et al. 2014](#), and references therein). The relevant aspect in this context is that the Li production, as revealed in SG intermediate stars of GCs, seems to point towards AGB model details that are in agreement with the lesson learnt from Na, O, Mg and Al nucleosynthesis. Thus, we require an enhancement in the α_{MLT} parameter (defined as the ratio between the characteristic size of the convective elements and the pressure scale-height). Note that the standard values between 1.7 and 2.05 are calibrated on the Sun, whereas for instance observations suggest that values up to ~ 2.6 are needed to reproduce massive AGB stars in the MCs; ([McSaveney et al. 2007](#)). Moreover, in order to have significant Li production in intermediate-mass AGB stars the mass loss has to be fast (otherwise the Li is burned again within the stellar interiors), following the approach by [Bloeker \(1995\)](#). This mass loss is higher than the formula by [Vassiliadis and Wood \(1993\)](#), reducing the lifetime of the star, and consequently the number of the thermal pulses. This last choice is now further corroborated by recent investigations such as e.g., the counts of massive (above $3 M_{\odot}$) AGB stars in the SMC ([Pastorelli et al. 2019](#), and references therein). Other critical points are however still kept alive, such as for example the efficiency of the third dredge-up and the number of thermal pulses, which would cause significant CNO and s-process element variation even in stars with masses around $\sim 5 M_{\odot}$ ([Marigo et al.](#), in preparation).

6 Evidence from dynamics

Another important piece of evidence is provided by dynamical considerations coming from both the gas and the stars. Many complex processes are involved in the evolution of GCs, in particular in their turbulent early stages where the characteristics of multiple populations are set. In this Section we will analyse the main issues related to the dynamical properties of these two components with the aim of discussing the involved problematics and to identify possible signatures of the formation process of multiple populations imprinted in the kinematics of the stars observed today.

6.1 Gas dynamics

GCs are currently deprived of gas, so that all the available information on the properties of the gaseous component from which all the stellar populations originated must be deduced from the chemical composition of stars survived till the present day. Although a commonly accepted picture of the GC formation process is still missing, it is possible to define some general characteristics of the gas-rich cloud in which proto-GCs formed.

A working hypothesis is that GCs formed in conditions resembling those occurring today in starburst galaxies where several massive clusters are observed to form. In particular, observations in the most massive star forming regions in the Local Group (like e.g. NGC 346 in the SMC, and NGC 604 in M 33) show a stellar complex forming in a cavity surrounded by a large amount of gas. Hydrodynamical

simulations of turbulent molecular clouds suggest that the final star cluster form from the hierarchical merger of several sub-clumps, composed by both stars and residual gas (Zamora-Avilés and Vázquez-Semadeni 2014). In this scenario, a first question is whether multiple populations formed in independent clumps before their merging or this process formed a single homogeneous FG (Elmegreen 2017). Unfortunately, the hierarchical or monolithic origin of star clusters is still matter of debate (Bonnell et al. 2011; Banerjee and Kroupa 2015) and hydrodynamical simulations performed till now are far from providing detailed predictions for the chemical enrichment of the individual clumps.

An important constraint is set by the formation and evolution of the most massive FG stars. Indeed, massive O stars emit a large fraction of high-energy photons able to ionize the intra-cluster medium thus preventing star formation during their entire life (Bodenheimer et al. 1979). However, such massive stars often form in the dense centers of stars-forming region, possibly as a result of competitive accretion or primordial mass segregation (Bonnell et al. 2003; McMillan et al. 2007). Under this condition, most of the ionizing power of UV photons is absorbed by the gas flowing onto the star limiting the erosion of the neutral/molecular gas to a small region surrounding the source (Dale and Bonnell 2011). Magnetic fields could also act as a further feedback agent, reheating the gas at epochs of the order of a few Myr (Balsara et al. 2008). In this case, little is known about their impact on the evolution of the intra-cluster medium.

At the end of their evolution (after $3 \div 30$ Myr depending on their mass) massive ($8 < M/M_{\odot} < 25$) stars explode as SNe II whose feedback have enough energy ($\sim 10^{51}$ erg) to clean the intra-cluster medium from residual gas. An effect of the gas expulsion is that it acts as a net loss of potential energy occurring in a timescale much shorter than the dynamical time (the characteristic timescale over which stars react to potential changes). In this situation the cluster is off-virial equilibrium and reacts with a sudden expansion. The potential change exerts a mechanical work on stars pushing up their orbital energies. Those stars reaching the level of the inner Lagrangian point can evaporate from the system. A similar process has been advocated by D’Ercole et al. (2008b) to explain the puzzling predominance of SG stars (the so-called “mass-budget problem”). In this case, the loss of the ejecta of FG SNe II induce an early episode of loss of FG stars (characterized by higher energies and therefore more prone to evaporation) over a timescale long enough to allow the formation of the SG. The material expelled by massive stars in the SN II explosion is enriched in Fe and α -elements and may contaminate the composition of the surrounding gas. This poses a strong problem for many of the pollution/dilution models developed so far. Indeed, in all the models predicting a SG forming from the ejecta of massive ($8 < M/M_{\odot} < 20$) stars, the polluted gas is released in the same time interval of SNe II explosion. It is therefore necessary to recycle these ejecta into SG stars before the explosion of the first SN expels or contaminate the gas.

The same fate is expected for the pristine gas which has been hypothesized to be a source of the dilution necessary to explain the extent of the Na-O anticorrelation. Note that the SN feedbacks could be unable to unbind the primordial gas if the proto-cluster has a mass $> 10^7 M_{\odot}$ (Leigh et al. 2013). So, a way to retain the pristine gas while expelling the SNe II ejecta before these two chemically different gas mix is

needed. [D’Ercole et al. \(2016\)](#) proposed a scenario in which GCs form in the disc of dwarf galaxies at high-redshift ($z \sim 2$) which later merge with the MW. The wind powered by SNe II create a bubble which breaks out the disc, releasing most of the Fe-, α -rich material out of the galaxy. Only a negligible fraction of this gas mix with the gas in the disc which therefore maintains its primordial composition. When the bubble reaches a critical radius (~ 700 pc) the wind ram pressure is not able to balance the gravitational attraction of the cluster and the bubble contracts falling onto the potential well where the SG is forming. The entire process should last ~ 40 -50 Myr after the end of the SNe II explosion, but this timescale could be shortened assuming the cluster in motion with respect to the surrounding medium. In this case the boundaries of the gaseous bubble feel a different brake from the surrounding gas, creating a relative motion with the stellar component (which is instead not subject to any friction). Of course, most of these considerations rely on simplified simulations where spherical geometry is assumed to reduce the problem to a 1D treatment. The situation could be different in 3D simulations where the gas could find some escape route through the inhomogeneities of the surrounding medium altering both the duration of the gas removal and the mixing efficiency ([Calura et al. 2015](#)). Note that alternative sources of dilution have been proposed e.g. from outflows of non-conservative mass-transfer in binaries, which can occur after SNe II explosion and are therefore not affected by such an effect (see Section 8.1).

Another issue related to the gas dynamics is linked to the duration of the star formation burst forming the SG. A relatively extended period is needed to explain the spread observed in the anticorrelation plots (see Fig. 2), which cannot be explained only in terms of observational uncertainties. However, if SG forms in an extended interval of time, its massive stars would have enough time to explode leading to the same problem discussed above.

For this reason, most of the scenarios proposed so far require either a fast and inhomogeneous mixing of material expelled by massive stars ([Bastian et al. 2013](#); [Elmegreen 2017](#); [Gieles et al. 2018](#)) or an initial mass function for the SG characterized by a cutoff at high-mass preventing the explosion of SG SNe II ([D’Ercole et al. 2008b](#); [Charbonnel et al. 2014](#)). An alternative hypothesis is that SG massive stars are quickly ejected from the cluster before explosion as a result of their interactions in three- and four-body interactions. This effect could be accelerated by *i*) primordial mass segregation and *ii*) the fast segregation and decoupling of these massive stars from the rest of the cluster (the so-called “Spitzer instability”; [Spitzer 1969](#)).

In the above discussion the feedback provided by SNe Ia has been overlooked. These explosions are indeed twice more energetic than core-collapse SNe being more efficient in expelling the gas from the cluster polluting the intra-cluster medium of Fe and Fe-peak elements. SNe Ia can explode at any time provided that a sizeable population of binaries involving white dwarfs are available. Given the uncertainties on the progenitor of these explosions (both single-degenerate or double-degenerate models have pro and cons), a precise constraint on the SNe Ia timing is not available, but theoretical models predict a rise of the explosion rate between 70 and 400 Myr, depending on the adopted model, from the formation of the FG ([Wang and Han 2012](#)). This timescale constitutes a limit for those models involving a pollution from intermediate-mass stars.

6.2 Stellar dynamics

After the initial turbulent phase of their formation, FG and SG stars are expected to have different distribution in the phase-space determined by the corresponding properties of the gas from which they originate. Different scenarios predict different properties of multiple populations. In particular, in those scenarios predicting a SG formed by the gas collected in a cooling flow of low-velocity winds, SG stars are expected to be more centrally concentrated and with a lower mean kinetic energy (i.e. velocity dispersion at the same distance from the center) with respect to FG (D'Ercole et al. 2008b). Moreover, any pre-existing angular momentum possessed by the cooling gas is conserved during the collapse thus leading to an increase of the systemic rotation speed (Bekki 2010, 2011). A larger radial anisotropy is also expected for SG stars since, forming from a cloud off-virial equilibrium, should retain information on the radial motion in their final velocity (Lynden-Bell 1967). Because of the many uncertainties in the theory of star formation, little is known on the expected initial mass functions of the two populations, although the basic principle of competitive accretion predicts that concentrated populations (like the SG) are expected to have on average a bottom-heavy initial mass function (Bonnell et al. 2011). Scenarios predicting a SG formed from material ejected in-situ in the central cluster region (Decressin et al. 2007; Gieles et al. 2018) predict similar characteristics with the remarkable exception that the two generations should share the same rotation pattern. Finally, if the chemical peculiarities of SG stars comes from an accretion of gas onto their proto-stellar disks (Bastian et al. 2013), they are expected to be constituted by those low-mass stars spending most of their lives in the cluster core. So, while SG stars in this scenario should share some of the structural and dynamical properties predicted by other models (concentration and low velocity dispersion), they should be characterized by a high-mass cutoff in their mass function, radial anisotropy and low rotational velocity (at odds with what predicted by other scenarios; Hénault-Brunet et al. 2015).

Unfortunately, in the subsequent evolution (constituting more than 99% of the entire cluster life) stars of both populations interact between them and with the Galactic tidal field, moving across the phase-space. Differences between the structural and kinematic properties of FG and SG can be created or erased by the above effects.

Rotation is expected to be present since the formation of GCs because of the large-scale torques present in the original cloud (Mapelli 2017). Additionally, a small degree of rotation can emerge in the outermost regions because of the interaction with the tidal field. Indeed, the Coriolis force produced by the joint motion of the star and the cluster is directed inward/outward according to the retrograde/prograde motion of the star. So, stars on prograde orbits are more easily expelled leaving a retrograde rotation close to the tidal radius (Henon 1970; Keenan and Innanen 1975; Read et al. 2006; Tiongco et al. 2016a). FG stars, mainly located at large radii should be more prone to this effect than SG ones. In the same way, a certain degree of radial anisotropy can be primordial in all populations as a consequence of the violent relaxation occurring in the first stage of cluster formation (Lynden-Bell 1967). During the subsequent evolution, radial anisotropy can develop outside the core where a significant number of stars are ejected by close encounters occurring in the central

region (Lynden-Bell and Wood 1968). This effect is however reversed in the outermost regions where stars on tangential orbits are protected from evaporation by the angular momentum barrier (at the tidal radius, only stars with positive radial velocity $v_r = \sqrt{E - L^2/2r}$ can escape; Oh and Lin 1992; Tiongco et al. 2016b). So, SG stars spending most of their lives in the central region should develop radial anisotropy more efficiently than FG ones, while the opposite trend is expected in the outermost portion of the cluster. Another effect produced by dynamical evolution is on the mass function: stars with low masses indeed tend to acquire energy in collisions as a result of the tendency toward kinetic energy equipartition. They therefore are more prone to evaporate, leading to a flattening of the mass function as the mass-loss process proceeds. Numerical simulations show that in a tidally limited single population cluster the rate at which stars of different masses evaporate is a unique function of the fraction of lost mass, with larger mass-loss rate leading to flatter mass functions (Vesperini and Heggie 1997; Baumgardt and Makino 2003). On the other hand, clusters starting from a compact structure develop strong mass segregation before expanding up to the tidal boundary, and are characterized by a more efficient depletion of their mass function (Trenti et al. 2010). The SG should be less exposed to tidal stress during its entire evolution and started its evolution in an underfilling configuration. N-body simulations by Vesperini et al. (2018) have shown that the balance between the two above effects leads to only marginal differences in the present-day mass functions of FG and SG.

Among the dynamical processes that erase primordial kinematical differences the dominant one is two-body relaxation. In particular, long-range interactions lead stars to exchange kinetic energy so that after a timescale compared to the relaxation time stellar orbital energies are randomized. The effect of two-body relaxation is therefore to homogenize the kinematic properties of FG and SG stars erasing the signatures left by their different formation mechanism. As a rule of thumb, the timescale needed for a star to lose memory of its original motion is:

$$t_{rel} = \frac{v^2}{D[(\Delta v_{\parallel})^2]} \sim 0.063 \frac{\sigma^3}{G^2 m \rho \ln \Lambda}$$

where v is the initial velocity, $D[(v_{\parallel})^2]$ is the diffusion coefficient responsible for the spread in the velocity component parallel to the motion, G is the Newton gravitational constant, m is the mean mass of cluster stars, ρ is the density, $\sigma = \langle v^2 \rangle^{1/2}$ is the 3D velocity dispersion and $\ln \Lambda$ is the Coulomb logarithm (Spitzer 1969). From the above formula it is immediately apparent that this quantity varies within the cluster (since both ρ and σ are functions of the distance from the center). In any realistic model (e.g. King 1966) the relaxation time is shorter in the center and increases at large distances. This is a consequence of the largest number of interactions occurring in the dense central region accelerating the exchange of kinetic energy among stars. In a real cluster the situation is however more complex since stars vary their distance from the cluster center along their orbits passing through regions characterized by different efficiency of interaction. Usually, to have a gross estimate of the collisional status of an entire system as a function of its general parameters, the above timescale is integrated over the half-mass radius to obtain the so-called "half-mass relaxation

time”:

$$t_{rh} = \frac{0.138}{m \ln \Lambda} \sqrt{\frac{M r_h^3}{G}}$$

On average, in clusters with an age larger than their corresponding half-mass relaxation time, the process of two-body relaxation had enough time to randomize stellar orbits. At a first look, all the Galactic GCs lie in this regime with the only exceptions of ω Cen=NGC 5139, NGC 2419 and Pal 14. Note however that the above calculation consider the cluster as a whole while stars follow different kind of orbits. Thus, the distribution of individual orbit-averaged relaxation times, while peaked at short timescales have a long tail extending in the range exceeding the cluster age. This is shown in Fig. 21 where the distribution of orbit-averaged relaxation time for a sample of 10^6 synthetic particles in a King (1966) potential with a typical GC mass and size ($M = 5 \times 10^5 M_\odot$ $r_h = 4 pc$) is shown. While the half-mass relaxation time of this simulation is $t_{rh} = 2 Gyr$, $\sim 29\%$ of the particles have orbits characterized by an average relaxation time longer than 12 Gyr being therefore only marginally affected by two-body relaxation. As expected, these stars are those with orbits confined in the outermost region of the cluster and occupy a peculiar region of the energy-angular momentum plane characterized by large energies and modulus of the angular momentum. So, the differences between the primordial FG and SG distribution in this portion of the phase-space (determining the rotation and anisotropy at large radii) are expected to be preserved even after an Hubble time and visible today.

Beside two-body relaxation, the interaction with the tidal field, while possibly creating small differences between the two populations close to the tidal radius (see above), also contributes to erase primordial differences. Indeed, the presence of the tidal field accelerates the process of mass-loss both imposing an energy cut and through the energy perturbations produced by disk/bulge shocks (Hénon 1971; Ostriker et al. 1972; Aguilar et al. 1988). This process carries away angular momentum, so that the larger is the fraction of lost stars, the smaller is the residual rotation (Tiongco et al. 2017). In a similar way, clusters losing a significant fraction of stars shrink, thus decreasing their half-mass relaxation time and boosting the effect of two-body relaxation.

The effect of dynamical evolution on the kinematic and structural properties of multiple populations has been studied using detailed N-body simulations by Hénault-Brunet et al. (2015) (see also Tiongco et al. 2019) who found that, by assuming reasonable initial conditions for two formation scenarios, the final rotation pattern of FG and SG should show opposite trends similar to those set at the beginning of the simulation. A conservation of the segregation of SG in the innermost region has been also noticed by Vesperini et al. (2013) using a set of N-body simulations. They found that a complete dynamical mixing between the two populations occurs only in the most evolved GCs, while in many of them the SG should remain more concentrated than FG still today. A similar consideration holds for the velocity dispersion of the two populations. Indeed, in any system at equilibrium the density and the velocity dispersion of each population (n_{pop} and σ_{pop} , respectively) are univocally connected

by the Jeans equation:

$$\frac{dn_{pop}\sigma_{pop}^2}{dr} = -n_{pop}g$$

where $g = GM(< r)/r^2$ is the gravitational acceleration at the radius r , $M(< r)$ is the mass enclosed within r and an isotropic distribution is considered. So, the difference in the present-day radial distribution of the two populations naturally reflects into a difference in the corresponding velocity dispersions. Similar results have been obtained also by [Mastrobuono-Battisti and Perets \(2013\)](#) who analysed the evolution of an N-body simulation tailored to ω Cen=NGC 5139 and found that the initial concentration, flattening, small dispersion and rotation of the SG are preserved after 12 Gyr of evolution.

Summarizing, regardless of the adopted scenario for the formation of multiple populations, SG stars should appear more concentrated, with a smaller velocity dispersion (measured at the same distance from the cluster center), a smaller fraction of binaries and a significant radial anisotropy at intermediate radii. A larger rotation amplitude is also expected for this population if the scenarios involving an original cooling flow are correct.

From the observational side, the concentration of SG stars has been proved in almost all GCs (e.g. [Sollima et al. 2007](#); [Lardo et al. 2011](#), with only a few possible exceptions, NGC 6362, NGC 6093=M 80, NGC 7078=M 15, [Dalessandro et al. 2014, 2018a](#); [Larsen et al. 2015](#), respectively. For M 15 see however also [Nardiello et al. 2018b](#)). This difference does not seem to be associated with any velocity dispersion difference, although some tentative evidence has been proposed in some cluster ([Bellazzini et al. 2012](#); [Dalessandro et al. 2018c](#)). In this regard, note that velocity dispersion profiles suffer from uncertainties which are several times larger than those of projected density because of the limited sample of radial velocities available. The first evidence of differences in the anisotropy profile of FG/SG stars have been put forward thanks to the accurate proper motions obtained through HST in 47 Tuc ([Richer et al. 2013](#); [Bellini et al. 2015](#); [Milone et al. 2018c](#)) and NGC 362 ([Libralato et al. 2018](#)), with the SG displaying a larger degree of radial anisotropy with respect to the FG. The only available evidence to date of differences in the rotation pattern of different generations of stars is provided by [Pancino et al. \(2007\)](#) (in ω Cen=NGC 5139) and [Cordero et al. \(2017\)](#) (M 13=NGC 6205) who found opposite results: while SG stars in ω Cen=NGC 5139 share the same rotation pattern of FG ones, in M 13 they have an average rotation amplitude which is larger than the rest of the cluster stars. All this evidence agree with the expectations of the theoretical models exposed above. Another evidence related to structural differences between FG/SG is provided by [Milone et al. \(2012d\)](#) who found that SG stars in NGC 2808 have a flatter mass function with respect to FG ones. Consider however, that the mass function measured in a limited radial range is not representative of the global mass function, so that it is hard to interpret this evidence without a complete modelling of the dynamical evolution of this cluster accounting for this observational bias. Moreover, a consensus on the star formation theory determining the shape of the initial mass function is missing (see e.g. [Adams and Fatuzzo 1996](#); [Chabrier et al. 2014](#)) so that it is not clear if the turbulent environment where multiple populations formed could have lead to primordial

differences in their initial mass functions which left traces on their present-day mass functions.

Another aspect poorly investigated till now regards the fraction of massive remnants retained by GCs. In the commonly accepted scenario, black holes and neutron stars formed after SN II explosions should receive natal kicks resulting from the off-center onset of the deflagration process. Models of asymmetric SN II explosions predict kick velocity distributions characterized by dispersions of $\sigma_k = 80 - 100 \text{ km s}^{-1}$, i.e. larger than the cluster escape speed, so they are expected to be ejected outside the cluster after their formation (Drukier 1996; Moody and Sigurdsson 2009). Assuming a Plummer (1911) model and a Maxwellian distribution of velocities truncated at the cluster escape speed, the fraction of neutron stars/black holes which can be retained by a cluster with mass M and Plummer radius r_0 is:

$$f_{ret} = \left[\text{Erfi}f(x) - \frac{2}{\sqrt{\pi}} x \exp(-x^2) \right]$$

where:

$$x = \left(\frac{3\pi}{32} + \sqrt{2^{2/3} - 1} \frac{r_h \sigma_k^2}{G M} \right)^{-1/2}$$

The above formula indicates that the retention fraction is a rapidly increasing function of the ratio M/r_h . Assuming $r_h = 4 \text{ pc}$ and $M = 5 \times 10^5 M_\odot$, the above relation predicts a retention of less than 1% of massive remnants. On the other hand, this fraction increases to 18% if GCs were an order of magnitude more massive at their birth, as required by some of the formation scenarios of multiple populations. While the most massive remnants (e.g. black holes with a mass contrast >10 with respect to the mean cluster mass) are expected to quickly evaporate as a result of the Spitzer instability, the less massive neutron stars will be retained more efficiently than the other less massive stars till the present day. Unfortunately, assuming a standard initial mass function (IMF), the mass contained in neutron stars will never exceed a few percent of the total mass, so that a proof of this scenario cannot be obtained from dynamical considerations. However, an increased retention of neutron star could help to explain the high fraction of millisecond pulsars observed in GCs (exceeding by a factor 100-1000 over the field population, Verbunt et al. 1989) which would be otherwise difficult to be explained if all neutron stars were expelled by natal kicks.

7 Binaries

It is well established that a very large proportion, if not the majority, of stars in the field are in multiple systems, with the binary fraction increasing as a function of stellar mass (see e.g. Moe and Di Stefano 2017). Metallicity and environmental density seem to play a role in the incidence and orbital parameters of double systems. The binary fraction seems to increase with decreasing metallicity (Moe et al. 2018). On the other hand dense systems seem to disrupt these objects and thus decrease their incidence (see e.g. Duchêne et al. 2018).

Binaries play an important role in our understanding of GCs. They are a source of heating, and thus they are relevant to the study of GC dynamics. Many of the exotic

objects (e.g. Blue Straggler Stars - BSS, CH-stars, cataclysmic variables, milli-second pulsars, X-ray binaries, etc.) found in GCs are the result of the evolution of a binary system. Accurate accounting for binaries has bearings on the derivation of the cluster mass and luminosity function.

Photometric searches for binaries in GCs have been undertaken since the early '90s, looking either for eclipsing binaries (e.g. [Yan and Reid 1996](#)) or for stars on the so-called binary sequence (located on the red side of the MS – e.g. [Bolte 1992](#); [Rubenstein and Bailyn 1997](#); [Bellazzini et al. 2002](#); [Sollima et al. 2007b](#); [Milone et al. 2012c, 2016](#) just to name a few). The earlier method is limited to systems with large orbital inclination and tends to favour short orbital periods (which however are more common in clusters than in the field, see below for a discussion), but it provides information about the periods and can be applied to any evolutionary stage. The latter is more complete in terms of the binary census, but is limited to the MS stage and to binaries with high mass-ratios, and provides no information on the binary orbital parameters.

Radial velocity monitoring is another avenue to characterize the binary population. While the availability of spectrographs with high-multiplexing capabilities like e.g. FLAMES@VLT has made this kind of search reasonably efficient for GC giants, the statistics is based still on samples several orders of magnitude smaller than that of photometry. The use of MUSE has also shown promise in this field (see e.g. [Giesers et al. 2019](#)). The method is biased towards shorter periods and large orbital inclinations, but it can provide information on the orbital parameters and on the composition of the binary stars.

7.1 Overall frequency of binaries GCs

7.1.1 Observational evidence

Observations agree in finding binary fractions among GC stars generally lower than found in the field for stars of similar kind. This is consistent with the general expectation that a concentrated environment tends to disrupt binaries ([Heggie 1975](#)). The measured overall fractions show however considerable variations. [Milone et al. \(2016\)](#) investigated the monovariate relations of the MS binary fraction and various cluster parameters for 59 GCs, and found an anti-correlation with cluster luminosity and a correlation with BSS incidence, confirming earlier findings reported by [Sollima et al. \(2010\)](#) and [Sollima \(2008\)](#) on the basis of smaller samples, who suggested that cluster mass might be one of the driving parameters to the binary fraction.

Figure 22 shows the run of the binary fractions (we will be using the total binary fraction from the HST-WFC field listed in [Milone et al. 2012c, 2016](#)) and the initial and present time cluster masses ([Baumgardt et al. 2019](#)). The quantities are clearly anti-correlated, with an effect that is more pronounced when initial rather than final masses are used (Spearman correlation coefficients -0.81 and -0.77 respectively). On the other hand, [Milone et al.](#) found a moderate anti-correlation of the binary fraction with core relaxation time.

7.1.2 Evolution of binary systems in GCs

The estimate of the fraction of expected binaries in a GC and of their characteristics requires rather extensive and detailed N-body simulations. In particular, such a complexity is due to the fact that binary orbital periods (hours to few tens of years) are much smaller than the characteristic dynamical time of stars (10^5 to 10^{10} yr). This imposes an upper limit to the time-step of the simulation when a close encounter involving a binary star is going to occur. For these reasons, predictions on the dependence of the binary fraction on the various GC parameters were performed using Monte Carlo (Ivanova et al. 2005; Fregeau and Rasio 2007; Fregeau et al. 2009) and simplified analytical (Sollima 2008) calculations. Predictions from N-body simulations have been provided by Hurley et al. (2007) and Trenti et al. (2007). In all these last studies however, to reduce computation time, only those binaries with binding energy larger than the average kinetic energy of single stars are considered.

The basic idea is that the lower incidence of binaries found in clusters with respect to the field is due to their being high density environments, with high velocity dispersion and thus large typical relative velocities. Therefore, close encounters of the double system with a third stellar object are much more likely than in the field. In these events, the outcome depends on the relative energies of the involved parties. Encounters where the binding energy of the binary exceeds the kinetic energy of the third star will tend to make the system more bound, while in the opposite case the binary will become looser (or possibly be disrupted). This is the so-called Heggie's Law (Heggie 1975), which states that in an environment such as a GC the effect of three body encounters over time will make soft binaries become softer and hard binaries become harder (see also Heggie and Hut 2003, for a review).

Binary ionization can happen under two conditions: *i*) the relative velocity of the binary and the incoming star is rather large, exceeding the so-called critical velocity (Hut and Bahcall 1983), which depends on the binary binding energy and on the masses of the three stars involved. For stars of similar mass, this is very similar to the binary orbital velocity (save for a shape factor which accounts for details of the encounter, including inclination of the encounter and eccentricity of the orbit); *ii*) the ionizing star must get close enough for the collision to take place, a distance comparable to the separation of the double system.

7.2 Frequency of binaries in different stellar populations

A surprisingly small number of observational studies have attempted to study binaries in different GC stellar populations.

D'Orazi et al. (2010b) took an indirect approach, deriving the incidence of Ba stars (which are known to belong to binary systems of rather short period) among the FG and SG in 15 Galactic GC and finding that their fraction in FG stars is similar to the field, but much smaller in the SG. They also reported on the binary fraction based on long term radial velocity monitoring for the cluster NGC 6121, finding a binary fraction in FG stars over one order of magnitude larger than in SG stars.

Lucatello et al. (2015) used radial velocity monitoring to derive the binary fraction in FG and SG stars in 10 GCs. The reported binary incidences in the two population are $4.9 \pm 1.3\%$ among FG stars and $1.2 \pm 0.4\%$ among SG stars. They then report that the binary fraction in FG is four times larger than in SG, under the assumption that the period distributions in the two populations is the same. They conclude that such finding suggests that SG stars were born in a denser environment than FG stars. It is worth noticing, that, as discussed before, the denser an environment the more binaries are ionized but also the period distribution of the surviving ones is skewed toward shorter periods. Therefore, the binary fraction detection efficiency from searches of spectroscopic binaries is expected to be lower for FG than SG binaries, given that the latter likely have a period distribution more skewed toward shorter periods, and thus the ratio between the binary fraction in the two populations is expected to be even larger than the one detected.

Dalessandro et al. (2018b) monitored the radial velocity of over 500 members of the low mass cluster NGC 6362. They also found that the incidence of binaries was over an order of magnitude higher among FG stars than in SG stars.

These observational findings are a good match for theoretical predictions. Vesperini et al. (2011) used an hybrid analytical-numerical approach to follow the evolution of the binary population in the context of multiple populations. They found that one of the consequences of the SG forming in a more centrally concentrated environment than the FG was indeed a lower binary fraction in the former with respect to the latter. The reason behind this difference is the increased disruption rate that SG binaries experience as a consequence of a larger number of stellar encounters in the high density environment of their birth. The above finding has been confirmed by N-body simulations by Hong et al. (2015, 2016) who also found that such a difference is expected to be observable only for those binaries above a critical separation, while tight binaries (e.g. those producing X-ray binaries) should be less affected by such an effect.

As a caveat, we remind that Hong et al. (2019) find that the present time spatial distribution is affected by the differences in the binary fractions, and that the relative incidence of FG and SG binaries might very well show considerable radial dependence even after the spatial distribution of single stars from the two populations become identical.

Given the different incidence of binaries in FG and SG discussed above, one can wonder if the trend observed in Fig. 22 could be interpreted as a simple consequence of the decreasing fraction of FG stars with increasing mass (see Fig. 6.) High mass clusters are dominated by SG, where binaries are very rare, while low mass clusters are mostly FG, which has a much larger binary fraction. Fig. 26 shows the run of the binary fraction, of the frequency of BSS with respect to subgiant branch stars, and an averaged one as a function of the FG fraction. The upper panel, as discussed, shows that the fractions of binaries and of FG stars is correlated, however a simple calculation shows that such trend is not reproducible by just changing the FG fraction while keeping the fractions of binaries in FG and SG stars constant, but requires that each of these quantities themselves also varies with the FG fraction (and hence with the mass).

7.3 Toy model and the different populations

In order to interpret the implications of the binary fraction within GCs in the context of multiple populations, we may use a simple toy model. For the sake of simplicity we will assume that, at its formation, the distribution of FG and SG (ρ_{FG} and ρ_{SG} , respectively) can be represented by the superposition of two [Plummer \(1911\)](#) models as a function of radius (r) within the cluster, with different masses and characteristic radii. An initial fraction of 50% of binaries are distributed with the same radial distribution of their parent populations and with the period/semi-major axes distribution of field stars ($g(a)$ taken from [Raghavan et al. 2010](#)), where a is the semi-major axis. We consider equal-mass stars with mass of $m = 0.5 M_{\odot}$, no mass segregation between binaries and single stars and no dynamical evolution. These are no doubt incredibly simplistic approximations, however the underlying assumption is that the main driver of the evolution of the binary fractions in both populations is the process of ionization mainly occurring at early stages, while the subsequent evolution and its details act as second order effects.

The local ionization rate can be calculated from the relation ([Hut and Bahcall 1983](#)):

$$\Delta(a, r) = \frac{1}{N_b} \frac{dN_b}{dt} = \frac{3 \rho(r) \pi a^2 \sigma(r) R(a, r)}{\sqrt{2} m}$$

where:

$$R(a, r) = 1.64 / [(1 + 0.2/x)(1 + \exp(x))]$$

and $x = \frac{G m}{2 a \sigma^2}$ is the hardness parameter, G being the gravitational constant. Note that in the above formula $N_b(t)$ is the number of binaries at the time t , M is the cluster mass, $\rho = \rho_{FG} + \rho_{SG}$ is the overall mass density profile and σ is the velocity dispersion in any one direction which includes the contribution of both populations (calculated by solving the isotropic Jeans equation). For a given semi-major axis a , the average ionization rate k of FG/SG binaries can be calculated by integrating over the corresponding density profiles:

$$k_{FG}(a) = \frac{1}{(1 - f_M) M} \int_0^{+\infty} 4\pi r^2 \rho_{FG} \Delta(a, r) dr$$

$$k_{SG}(a) = \frac{1}{f_M M} \int_0^{+\infty} 4\pi r^2 \rho_{SG} \Delta(a, r) dr$$

while the fraction of surviving binaries at the time t is given by:

$$\eta(t) = \frac{N_b(t)}{N_b(0)} = \int g(a) \exp[-k t] da$$

The fraction of binaries of each generation is then calculated from the above quantity as:

$$f_b(t) = \frac{\eta(t) f_b(0)}{(1 - \eta(t) f_b(0) + 1)}$$

In the above calculation, there are four free parameters: the global mass and half-mass radius of the system, and the ratio between the masses (f_M) and characteristic

radii (f_R) of FG/SG. The evolution of the binary fraction of FG and SG assuming $f_M = 0.5$, $f_R = 0.1$, $r_h = 4 pc$ and $M = 10^6 M_\odot$ is shown in the top-right panel of Fig. 25. It is apparent that the fractions of binaries of both populations are mainly set in the first few 100 Myr with only a negligible evolution at later time. This is a consequence of the adopted period distribution which peaks at periods of ~ 300 yrs, so that most of the binaries in both populations are soft and are quickly destroyed, while the remaining hard binaries survive for a long time.

The above toy model does not account for the dynamical evolution of the system which certainly affects both populations. However, N-body simulations by D'Ercole et al. (2008b) show that in a realistic cluster the FG roughly maintains a constant size, while SG expands further reducing the ionization efficiency. So, the structural evolution occurring over a long timescale should play only a second-order role in decreasing the number of binaries. The consequence of the above consideration is that the binary fractions of FG/SG contain crucial information on the early stage of cluster evolution when the maximum efficiency of binary ionization determined these fractions (see also Fregeau et al. 2009).

We randomly extracted the four involved parameters over a wide range ($0 < f_M < 1$; $0 < f_R < 1$; $6 < \log M/M_\odot < 7.5$; $0 < \log r_h/pc < 1.5$) and calculated the corresponding fraction of FG/SG binaries after 12 Gyr of evolution. We found that the final ratio $f_{b,SG}/f_{b,FG}$ is a unique function of the f_R parameter, and it is almost insensitive to the other parameters. In particular, the values of $f_{b,SG}/f_{b,FG} < 0.2$ measured in real GCs can be obtained only assuming $f_R < 0.15$ i.e. a SG forming in a volume ~ 300 times smaller than that of FG (see the bottom panels of Fig. 25). Moreover, the general value $5\% < f_{b,FG} < 10\%$ can be obtained only assuming initial half-mass densities ($\rho_{hm} \equiv \frac{3M}{8\pi r_h^3}$) in the range $3.2 < \log \rho_{hm} < 5.2$.

In the top-left panel of Fig. 25 the distribution of semi-major axes of the surviving binaries in our toy model is also shown. Note that the cutoff occurs for both populations at rather small values. This could explain the correlation between the overall binary fraction and the BSS incidence, whose precursors must be systems with relatively small separations ($< 200 R_\odot$, that is $< 1 au$).

Of course, the above calculation is approximated and relies on the strong assumption that binaries in GCs form in the same fashion as in the field. Moreover, other complex processes (like binary-binary interactions, segregation of binaries, exchanges between binary components, hardening/softening, coalescence, tidal capture, stellar evolution and tidal field effects, etc.) could have non-negligible effects in shaping the long-term evolution of the binary fraction in both populations. However, the above exercise provides an example of the unique information on the original properties of GCs retrievable from the properties of FG/SG binaries.

7.4 Blue stragglers, CH/Ba stars, and the contribution of binaries to the fraction of stars with chemical anomalies

Internal mixing (related e.g. to rotation) or heavy mass-loss in binary systems may cause significant variations of the surface abundances, in particular for Carbon and Nitrogen. This is indeed expected (Sarna and De Greve 1996) and observed in the

case of a fraction of the BSS (Sandage 1953; Ferraro et al. 2006b)¹⁶ and Ba-CH stars (D’Orazi et al. 2010a). While we expect that only a minority of stars in a cluster are BSS or Ba-CH stars - or the result of their evolution - caution should be exerted when considering cases where the fraction of N-enriched stars is very low as evidence for multiple populations. In the following we will try to have a first rough estimate of the incidence of such objects on number counts of stars along the RGB.

Those binaries with separation of the order of or smaller than 1 au are expected to interact during the evolution along the red giant branch producing mass-transfer BSS (McCrea 1964) or along the asymptotic giant branch producing Ba-stars or CH stars (McClure et al. 1980). This separation should roughly corresponds to initial periods of the order of 1 year. If we then consider the period distribution for field binaries by Raghavan et al. (2010), we end up with a fraction of interacting binaries that is about 14% of the total. Since binaries make up some 46% of the F-G spectral type stars in the solar neighbourhood, we expect that about 6% of the stars may show some abundance anomalies related to being binaries. This is similar to the fraction of BSS per main sequence star in open clusters, that is between 7 and 10% for clusters older than 1 Gyr (de Marchi et al. 2006; Ahumada and Lapasset 2007, with the caveat that an improved demographics of BSS in open clusters should be derived using the Gaia data on membership in clusters) while the fraction of Ba-stars is of the order of 2% (Luck and Bond 1991).

On the other hand, the fraction of BSS declines with cluster mass/luminosity down to a fraction more than an order of magnitude smaller in massive GCs (Piotto et al. 2004; de Marchi et al. 2006; Moretti et al. 2008). As shown in Fig. 23 there is indeed a good correlation between the incidence of BSS and the fraction of binaries in a cluster, that may be interpreted in terms of the evolution of primordial binaries, which is affected by the stellar encounters (see e.g. Davies et al. 2004). This decline parallels that in the binary fraction of binaries in FG/SG stars (see previous subsection). This good agreement can be used to reduce the scatter in the relation between the fraction of first generation stars and of binaries, as shown in Fig. 26, where we compare results obtained using only the binary fraction determined from main sequence stars, the incidence of BSS, and averaging the two.

Once H at center is exhausted, BSS in old clusters are expected to evolve along the RGB, where they may then mix with single stars in the colour-magnitude diagram. Since they are more massive, they should be slightly bluer and evolve somewhat faster, and then they should be under-represented along the RGB. To evaluate this last term, we may use evolutionary tracks (e.g. the BASTI ones, Pietrinfermi et al. 2006). While a complete analysis is beyond the purposes of this review, we found that e.g. for α -enhanced tracks with $Z=0.004$, a star with $1.3 M_{\odot}$ employs 60% of the time of a star with $0.9 M_{\odot}$ to evolve from an absolute $M_V = 2$ to the tip of the RGB. We then expect that the post-BSS may be of the order of 6% of the RGB stars in an old open cluster, and likely an order of magnitude less in a typical GC; Ba/CH-stars are expected to be about a factor of five less frequent. This fraction should then be multiplied by the fraction of those BSS that are C-poor and N-rich, that is about 15%

¹⁶ BSS may also be produced by collision in the dense core of GCs. In that case, there should not be large chemical anomalies (Lombardi et al. 1995). However, the majority of BSS in both globular and open clusters are likely the aftermath of the evolution of primordial binaries (see e.g. Piotto et al. 2004).

(Ferraro et al. 2006b). Evolved BSS may then generate a small ($\sim 1\%$) population of chemical anomalous stars in old open clusters that should be taken into account when searching for evidence of multiple populations within them. On the other hand, we expect that the impact of these objects within most GCs is negligible.

8 GCs and the halo

8.1 Mass budget

The peculiar nucleosynthesis observed in GCs, so much different from that typically observed in the field of galaxies, suggests that the material from which SG stars form is processed in the interior of only a fraction of the original stars present in a cluster. Since the SG stars typically makes up the majority of cluster stars (at least in massive clusters), this suggests that the original mass of the FG stars should be much larger than currently observed. This became known as the mass budget issue (e.g. Prantzos and Charbonnel 2006; Decressin et al. 2007; Carretta et al. 2010c; Renzini et al. 2015; Larsen et al. 2014; Bastian and Lardo 2018). Data presented earlier in this review are actually a bit different from those used in previous discussions, so it might be worth to revisit this item. In the following, we will examine the mass budget issue separately for Type I and Type II GCs, following the scheme adopted in previous sections.

8.1.1 The case of Type I GCs

In a simple schematic view, SG stars are made of a mix of the ejecta from a fraction of the FG stars (M_{ej}) and of pristine material. We call dilution (d) the fraction of pristine material in the material used to form SG stars. The total mass available M_A to form SG stars is $M_{ej}/(1-d)$. We call mass budget factor $b = M_{SG}/M_A$ the ratio between the observed mass in the SG stars and the available mass. If $b > 1$, then the fraction of FG stars lost from the cluster since its origin should be larger than the average fraction of stars lost from the cluster, that is, FG stars should have been lost from the cluster more efficiently than SG stars. This likely occurred very early in the history of the clusters.

In order to quantify b we need to know the fraction of FG and SG (as represented e.g. by the fraction of FG stars (f_{FG}) in a cluster, the average dilution factor, make some assumption about the initial mass function, and estimate how much mass is locked into remnants of the FG stars, and is then not available to form the SG stars.

Hereinafter, we will consider that the IMF is represented by a power law between 0.25 and $60 M_{\odot}$, with exponent α between -1.7 and -2.3 (see Beuther et al. 2007; and Hosek et al. 2019 and references therein); here $\alpha = -2.3$ represents the Salpeter mass function and note that with this assumption, the lower extreme of integration provides a result very similar to the Kroupa (2002) mass function. Once subtracted the mass locked in remnants, the mass given back to the interstellar medium by a FG star may be represented by:

$$M_{back} = 0.894 M_* - 0.434 M_{\odot} \quad (1)$$

for $0.9 < M_* < 9 M_\odot$, and:

$$M_{back} = 0.9 M_* - 0.5 M_\odot \quad (2)$$

for $M_* > 9 M_\odot$ (see e.g. [Cummings et al. 2018](#)).

With these assumptions, the fraction of mass given back to the interstellar medium by intermediate mass stars ($3 < M_* < 9 M_\odot$) in units of the initial mass of first generation stars is 0.155 for $\alpha = -1.7$, 0.153 for $\alpha = -2.0$, and 0.120 if $\alpha = -2.3$. The same values for massive stars ($9 < M_* < 60 M_\odot$) are 0.463 for $\alpha = -1.7$, 0.290 for $\alpha = -2.0$, and 0.142 if $\alpha = -2.3$. In this schematic view, the FG stars that pollute the ISM from which SG stars form cover a relatively large range of masses, that are likely characterized by different yields. We do not discuss this point in detail here because we are only interested in the mass budget issue. Here, we simply assume that once properly weighted, the material given back to the interstellar material has the appropriate composition to generate SG stars, after an appropriate dilution with pristine material; see however Section 5.3 for a case where the variation of the yield as a function of mass was considered in more detail.

Using the work by [Milone et al. \(2017a\)](#) and [Baumgardt et al. \(2019\)](#), we find that the fraction of FG stars depend on the initial mass of the cluster, being about $f_{FG} = 0.6$ for clusters with an initial mass of about $2 \times 10^5 M_\odot$, $f_{FG} = 0.36$ for clusters with an initial mass of about $10^6 M_\odot$, and $f_{FG} = 0.2$ for clusters with an initial mass of about $3 \times 10^6 M_\odot$.

We will then consider separately two different groups of SG stars, one characterized by a value of the dilution factor of about 0.5, and a second one characterized by a much smaller dilution factor, say about 0.05. The first group corresponds to the I population, and the second one to the E population (see Section 5, where we considered the E population defined by [Carretta et al. 2009c](#) in the context of the Li abundances). As we have seen in Sect. 5, the I population has a Li abundance not too different from that of the FG stars. This requires production of Li in the polluter. Since the only polluter known able to produce Li on a relatively short timescale is the intermediate mass AGB stars, in our estimates of the mass budget we will assume that the I population is produced by diluting the ejecta of these stars. On the other hand, there is no similar constraint for the E population or at least, for the fraction of the E stars that do not have Li. Besides, the high He abundances related to this population are more easily produced by supermassive stars or fast rotating massive stars (even if the latter cannot produce material depleted in Mg, one of the signatures of the E population). We will then assume that the E population is produced by these stars. We notice that the fraction of E stars f_E over the total is null for small GCs ($2 \times 10^5 M_\odot$), about 0.05 in clusters with $10^6 M_\odot$, and about 0.2 for clusters with an initial mass of about $3 \times 10^6 M_\odot$. We also notice that the fraction of I stars in a cluster is then $f_I = 1 - f_{FG} - f_E$. Finally, in this approach we should have two separate mass budget factors, one for the I stars (b_I) and the other for the E stars (b_E).

We may then combine these different assumptions to derive the values for the mass budget factor. We will consider clusters in three bins of mass, because they have different fractions of FG, I and E stars. Results are given in Table 4. Inspection of this table shows that the mass budget factor actually has quite small values (between 2 and 3) for low mass clusters and raises to large values (around 10) for massive

Table 4 Mass budget factors for clusters of different mass

| M_{in} (M_{\odot}) | α | 2.0×10^5 | 1.0×10^6 | 3.0×10^6 |
|-----------------------------|----------|--------------------|--------------------|--------------------|
| f_{FG} | | 0.60 | 0.36 | 0.20 |
| f_E | | 0.00 | 0.05 | 0.20 |
| M_{FG} (M_{\odot}) | | 1.2×10^5 | 3.6×10^5 | 0.6×10^6 |
| M_I (M_{\odot}) | | 0.8×10^5 | 5.9×10^5 | 1.8×10^6 |
| M_E (M_{\odot}) | | 0 | 0.5×10^5 | 0.6×10^6 |
| b_I | -1.7 | 2.0 | 5.0 | 9.1 |
| b_I | -2.0 | 2.1 | 5.0 | 9.2 |
| b_I | -2.3 | 2.6 | 6.4 | 11.8 |
| b_E | -1.7 | 0.0 | 0.3 | 2.1 |
| b_E | -2.0 | 0.0 | 0.5 | 3.3 |
| b_E | -2.3 | 0.0 | 0.9 | 6.5 |
| M_{start} (M_{\odot}) | -1.7 | 2.42×10^5 | 1.79×10^6 | 5.45×10^6 |
| M_{start} (M_{\odot}) | -2.0 | 2.46×10^5 | 1.81×10^6 | 5.54×10^6 |
| M_{start} (M_{\odot}) | -2.3 | 3.14×10^5 | 2.31×10^6 | 7.06×10^6 |
| $M_{gas,I}$ (M_{\odot}) | | 4.24×10^4 | 3.13×10^5 | 9.54×10^5 |
| $M_{gas,E}$ (M_{\odot}) | | 0.0 | 2.50×10^3 | 3.00×10^4 |

clusters. Also, the mass budget factor is larger for the I population than for the E one. This implies that in the scenario considered here, where I stars are polluted by the ejecta of massive AGB stars and E stars by those of fast rotating massive stars (though a contribution by supermassive stars could not be excluded), we found that no more than half of the ejecta of this second group of stars are enough to provide the mass locked into E stars. Hence, the constraint for the initial mass in the FG required to produce the SG stars ($M_{start} = b_I \times M_{FG}$) is determined by the I stars. These values are listed in the bottom part of Table 4. It might appear a bit surprising at first look, but these values are within a factor of 1.5 to 3.5 the values of M_{in} , mainly depending on the cluster mass. This is due to the combination of the rather large value of dilution appropriate to I stars and of the small fraction of FG stars in massive clusters. Anyhow, these values indicate that in the scenario here considered, very early Type I GCs should not need to be enormously more massive than at the end of the formation of the SG. We should emphasize that this result is obtained because in this scenario we separate the production of I stars (from the ejecta of AGB stars) from the production of E stars (from more massive stars).

Another interesting point concerns the total mass of diluting material required. Expressed in units of the original mass M_{start} , this quantity is about 15% for the formation of I stars and it ranges from 0 up to 0.5% for the formation of the E stars (this second value is actually so low that does not provide any strong requirement). The first one is more challenging. Where does this diluting mass come from? As first possibility, it may be a simple consequence of stellar evolution; dilution would then be a natural process, likely governed by simple statistical laws, with no need of any specific hydrodynamical model.

We consider here the possibility that dilution is provided by mass loss from single stars and/or interacting binaries. The first case has been examined by Gratton and Carretta (2010), who concluded that the wind from young main sequence stars may provide at most some 1-1.5% (that is, a tenth of what is needed) of the original mass as diluting material on a timescale of a few $10^7 - 10^8$ yr. More promising is the case of close binaries that have a Roche lobe overflow or develop a common envelope, as proposed by Vanbeveren et al. (2012): they might have non-conservative evolution and lose a substantial fraction of their mass before material in the envelope is nuclearly processed. The material lost in this phase is possibly available as diluting material. As noticed by Vanbeveren et al. (2012) and considered previously by de Mink et al. (2009), actually part of this material is enriched in helium and nitrogen and possibly depleted in carbon and oxygen¹⁷ and may be considered as polluting rather than diluting material. Population synthesis models based on detailed computations of binary evolution over a range of parameters (mass, separation, mass ratios) are required; Vanbeveren et al. (2012) provided a first exploration. One of the assumptions made by them is that 50% of the stars in the mass range 3 to 9 M_{\odot} are in binaries with period less than 10 years and with a mass fraction $q > 0.1$. This is very similar to what found by Moe and Di Stefano (2017), who reviewed the incidence of binaries among field stars and concluded that 50% of those in the mass range 3–9 M_{\odot} and virtually all the O-stars have a companion with a mass ratio larger than 0.1 and period less than 5000 days, so that they should evolve through a phase of mass transfer through Roche lobe overflow. The timescale of mass loss from O-type binaries (that is the original proposal of de Mink et al. 2009 for the polluting material) is very similar to that of core-collapse SNe: since there is very little trace of contamination by the ejecta of these SNe, it is very difficult that mass loss from massive binaries contribute here. But Vanbeveren et al. (2012) computations suggest that in the case of intermediate mass stars, binaries might indeed provide the required dilution, at least so far as the O-Na and Mg-Al anti-correlations are considered¹⁸. Part of this diluting material is slightly enriched in He, but this might perhaps not be a serious concern because the final effect on the He abundances is limited. The computations by Vanbeveren et al. (2012) should be repeated with updated stellar evolutionary code. Moreover, binary distributions more appropriate for the case of GCs must be considered, taking into account both “ionization” as well as hardening processes (Heggie and Hut 2003). Since binaries properties are found to depend on the cluster mass (see Sect. 7) this parameter might influence the dilution if this is the way it is generated. An important aspect not considered by Vanbeveren et al. (2012) is how much Lithium is preserved in the matter lost by these binaries. Actually Li is preserved only in the outer 0.03 M_{\odot} of a 5 M_{\odot} star (D’Antona and Cassisi, private communications), so that we may consider the ejecta of intermediate mass binaries to be almost Li-free. This possibly calls for a dilution parameter for Li different from that needed for O, though not in the way required to explain observations of e.g. NGC 6752 (Pasquini et al. 2005).

¹⁷ There is evidence that Algol systems - that are interacting intermediate mass binaries - are depleted in C (Tomkin et al. 1993; Sarna and De Greve 1996).

¹⁸ Note that the mass budget values discussed above should be revised in this scenario because only a fraction of the massive AGB stars should contribute to nucleosynthesis. On the other hand, in this scenario the diluting material was already present in the GC since its birth.

We conclude that at present the origin of the diluting material for Type I GCs is not yet well understood, and it is still possible that we need a substantial reservoir of pristine gas that is later accreted on the cluster (D’Ercole et al. 2011, 2016; Calura et al. 2019), though these last scenarios might have difficulty to produce the right amount of gas at the right moment (see e.g. Renzini et al. 2015). However, this concern is not applicable for individual cases, such as e.g. NGC 2808, the archetypical GC considered in D’Ercole et al. (2016), that may well have its own peculiar history.

8.1.2 The case of Type II GCs

Table 5 Number of Type II SNe compatible with Fe abundance spread in Type II clusters

| NGC | [Fe/H] | $\log M_{\text{in}}$ | f(typeII) | M(typeII) | d[Fe/H] | ref | dM(Fe) | nSN | f(SN) |
|------|--------|----------------------|-----------|-----------|---------|-----|--------|------|---------|
| 362 | -1.26 | 6.06 | 0.075 | 8.6E+04 | <0.050 | 1 | <0.7 | <10 | <4.2E-4 |
| 1261 | -1.27 | 5.86 | 0.038 | 2.8E+04 | | | | | |
| 1851 | -1.18 | 6.11 | 0.300 | 3.9E+05 | 0.065 | 2 | 5.2 | 74 | 2.7E-3 |
| 5139 | -1.53 | 6.86 | 0.640 | 4.6E+05 | 0.300 | 3 | 172.3 | 2461 | 1.6E-2 |
| 5286 | -1.69 | 6.11 | 0.167 | 2.2E+06 | 0.140 | 4 | 2.1 | 30 | 1.1E-3 |
| 6388 | -0.55 | 6.42 | 0.299 | 7.9E+05 | <0.050 | 5 | <34.2 | <489 | <8.7E-3 |
| 6656 | -1.70 | 6.01 | 0.403 | 4.1E+05 | 0.150 | 6 | 4.3 | 61 | 2.8E-3 |
| 6715 | -1.49 | 6.51 | 0.460 | 1.5E+06 | 0.150 | 7 | 25.1 | 359 | 5.2E-3 |
| 6934 | -1.47 | 5.74 | 0.067 | 3.7E+04 | 0.200 | 8 | 0.9 | 13 | 1.1E-3 |
| 7078 | -2.37 | 6.08 | 0.050 | 6.0E+04 | <0.050 | 9 | <0.1 | <1 | <2.2E-5 |
| 7089 | -1.65 | 6.38 | 0.043 | 1.0E+05 | 0.170 | 10 | 1.4 | 20 | 3.9E-4 |

References: 1. Carretta et al. (2013a); 2. Gratton et al. (2012b); 3. Johnson et al. (2015); 4. Marino et al. (2015); 5. Carretta and Bragaglia (2018); 6. Marino et al. (2011a); 7. Carretta et al. (2010a); 8. Marino et al. (2018b); 9. Carretta et al. (2009a); 10. Yong et al. (2014a).

Note: f(typeII) is the fraction of stars belonging to the population of stars occupying a region of high N but low He abundances in the chromosome diagram (Milone et al. 2017a). The values of f(typeII) for NGC 1851 and NGC 6715 have been corrected for misprints in the original paper

In order to better understand the origin of the abundance anomalies observed in Type II clusters, we may try to set some quantities. We will first focus on the variation of the abundance of Fe that likely implies the capability of these clusters to retain a (small) fraction of the ejecta of supernovae (SNe); the same argument can also be used to quantify the inability of Type I clusters to do the same. We first notice that in those clusters where there is variation of Fe abundances, very similar results are also obtained for the α -elements Si and Ca: this includes NGC 5286 (Marino et al. 2015), NGC 6273 (Johnson et al. 2015), NGC 6656=M 22 (Marino et al. 2011a), NGC 7089 (Yong et al. 2014a), NGC 6715=M 54 (Carretta et al. 2010a), NGC 5139= ω Cen (Johnson and Pilachowski 2010; Johnson et al. 2015; Marino et al. 2011b). This is not what is expected if the observed Fe is produced in thermonuclear SNe, and rather argues for core collapse SNe.

Second, the fraction of the SNe ejecta that is retained by a Type II cluster is observed to be a function of the cluster mass. To show this, we collected relevant data in Table 8.1.2. They include the metallicity (Harris 1996), the initial mass of the clusters (Baumgardt et al. 2019), the fraction of Type II stars (Milone et al. 2017a), and the offset in [Fe/H] between the normal (metal-poor) stars and those that are

metal-enriched from a number of literature references. Combined with the solar Fe content (Asplund et al. 2009), these quantities allow to estimate how much additional Fe is needed to reproduce the observed abundance spread. If we now assume that each core collapse SN produces a given amount of Fe (we assumed $0.07 M_{\odot}$: Umeda and Yoshida 2017), we may estimate the number of SNe whose ejecta may reproduce the observed abundance spread. Finally, this number can be compared to the total number of SNe that are expected to explode in a young GC. This last value actually depends on the adopted mass function. If we consider a Kroupa (2002) IMF, the rule of thumb is a SN every $100 M_{\odot}$. We may then estimate the fraction of the SN ejecta that is incorporated in the Type II stars. These values are indeed very small, the largest one being less than 2% for ω Cen=NGC 5139 (very similar values are actually cited by Renzini et al. 2015 and are given by Marino et al. 2019). There is a roughly linear correlation between this quantity and the mass of the cluster (see Fig. 27). This agrees with the naive idea that the deepest is the potential well of a GC, the highest should be its ability to retain SN ejecta. The very small fraction of SN ejecta that can be kept within a GC may obviously be related to their very large kinetic energy: the ejecta of a single SN have in fact a kinetic energy comparable to the whole potential energy of the residual gas within a GC. Since the production of Fe in SNe is primary, stringent constraints are obtained for the most metal-poor clusters, such as NGC 7078=M 15, for which a single core collapse SN should produce a detectable star-to-star variation in the Fe abundances.

We may repeat similar arguments for the production of CNO and s -process elements. Data for CNO are scarce, because derivation of the total abundance from spectroscopy is difficult. This is exemplified by the case of NGC 1851, for which Yong et al. (2015) obtained a large difference of 0.6 dex between the two populations using spectroscopy, while smaller offsets of ~ 0.15 dex have been considered to justify the distributions of colour and magnitudes of subgiant and horizontal branch stars (Gratton et al. 2012b). There is better agreement at a value of ~ 0.3 dex between the various determinations for NGC 6656=M 22 (Marino et al. 2011b; Alves-Brito et al. 2012; Gratton et al. 2014). On the whole, this data might perhaps be compatible with the production by core collapse SNe, being not too far from the spread seen for Fe. On the other hand, the variation in the abundances of the second peak s -process elements (Ba, La, etc.) between FG and Type II one is well established at a value in the range 0.4–0.7 dex in most Type II GCs (Marino et al. 2011b; D’Orazi et al. 2011; Carretta et al. 2013b; Johnson et al. 2015; Marino et al. 2015; Yong et al. 2016; Marino et al. 2018b). An even larger spread is observed in the most metal-rich population of ω Cen=NGC 5139 (Smith et al. 2000; D’Orazi et al. 2011), where a quite large enhancement of the third-peak element Pb is also observed (D’Orazi et al. 2011). The production of the heavy s -process elements calls for a significant contribution by the thermal pulse phase in moderate mass ($\gtrsim 2$ – $4 M_{\odot}$) AGB stars (see Section 2.4). However, in order to reproduce the observed pattern, we should consider in addition to these stars, also the contribution to O by the core collapse SNe and moreover a substantial dilution by unprocessed material, that reduces the abundance offset between FG and Type II stars by an order of magnitude. This large dilution implies a conspicuous reservoir of gas with pristine composition available. The mass of this reservoir is of the order of the initial mass for those clusters where the fraction of

Type II stars is < 0.1 , that is roughly half of the Type II clusters, but it is as much as 5 times larger in clusters such as NGC 1851 and NGC 6656=M 22, that have a large fraction of Type II stars. We notice that this large dilution implies that the first Type II stars should have a composition similar to that of the FG stars in the cluster. On the other hand, while such a large reservoir of gas may well be present in GC forming in dwarf galaxies, their intervention just at the right moment is a clear difficulty for the scenarios of formation of Type II GCs.

If is interesting to note that none of the clusters studied so far shows Fe spread without *s*-process spread. This might be surprising given that the *s*-process and Fe variation come from independent nucleosynthetic sites which have different timescales ($\sim 200 - 500$ Myr vs a few Myr respectively) and hence if re-accretion would occur on a timescale shorter than a few hundreds Myr, it would produce Fe abundance variations with not a significant variation in the *s*-process elements. The number of clusters with known Fe spread and well studied *s*-process abundances is rather small, and this could then be an artifact of small number statistics; however, it is intriguing to think that this could be hinting at some mechanism that led to the formation of the Fe enriched populations only with a considerable time lag with respect to the original population. This looks easier to explain within the context of a dwarf satellite (see e.g. [D'Antona et al. 2016](#); [D'Ercole et al. 2016](#); [Bekki and Tsujimoto 2016](#))

8.1.3 Conclusions about mass budget

In order to explain the chemical composition of GCs, we should assume that the original mass involved in the star formation episodes that finally led to the formation of present-day GCs was significantly larger than their final mass and that the ejecta from the polluters were diluted by a large amount of gas with primordial composition, especially in Type II clusters. Since the presence of diluting material seems a general feature, scenarios for the formation of GCs should explain its origin in a simple way. As considered in Section 8.1, the mass loss from chemically unevolved binary stars might possibly explain the less demanding case of Type I clusters. On the other hand, Type II GCs might have formed far from the center of the MW (see Fig. 10 and discussion in Sect. 3.4) within satellites that had a chemical evolution independent of the main stream of the Galaxy for quite a long time, possibly helping in providing the required reservoir of diluting gas to be used for further generations. In a more limited way, something similar might have occurred also for Type I GCs too, or at least for a fraction of them (see e.g. [Bekki et al. 2007](#)). In this framework, we might think of a “normal” mass-dependent evolutionary sequence for isolated structures (that observed in Type II GCs) that was interrupted quite early by interactions with the MW in Type I GCs. However, the reproduction of the right time scales at which the dilution and star formation episodes occurs needs much more elaboration, so that we are still far from a satisfactory model.

We finally notice here that Type II clusters must possibly be thought as an extension to low masses of the generic existence of a central massive object that contains a mean fraction $\sim 0.2\%$ of the total mass of a galaxy ([Ferrarese et al. 2006](#)). This underlines that GCs might possibly be a heterogeneous class of transition objects between normal stellar clusters and the very compact objects at the center of galaxies.

8.2 GC stars in the field

Globular clusters were disrupted in the Galactic halo and even more in the bulge: [Baumgardt and Hilker \(2018\)](#) estimated that at least 80% of the original population of GCs is now dissolved, and that the remaining GCs have lost a significant fraction of their stars. There is observable evidence of the loss of these stars. [Grillmair and Dionatos \(2006\)](#) discovered a long stream in the halo, named GD-1 stream, which is found to be narrow, cold and metal-poor ([Huang et al. 2018](#)). These features strongly point towards an origin from a stripped or disrupted GC ([Koposov et al. 2010](#)), even if the progenitor is no longer detectable. The same tale is told by other very narrow stellar streams ([Grillmair 2009](#)). Very small dispersions in the estimated metallicity (e.g. $\sigma_{[\text{Fe}/\text{H}]} < 0.1$ dex) are usually taken as evidence that the stream resulted from the disruption of a globular cluster, rather than a dwarf galaxy. Although among the iron complex GCs currently known (e.g., ω Cen=NGC 5139, M 54=NGC 6715, M 22=NGC 6656) the spread in $[\text{Fe}/\text{H}]$ can reach 0.3 dex, the narrow nature of several identified streams strongly indicates that probably they originated from lower mass, mono-metallic GCs (see also [Veljanoski and Helmi 2018](#)).

Thus, GCs were disrupted. But GCs also are currently in disruption, as clearly shown by the famous tidal tails associated to the globular cluster Pal 5 ([Odenkirchen et al. 2001, 2003](#)). GCs are mostly found in the halo, so they obviously contribute to the Galactic halo, but the actual contribution is not limited to the current $\sim 2\%$ of the total mass enclosed in GCs. Depending on the formation environment, the dynamical evolution of GCs is subject to a number of external processes, apart from the internal mechanism of evolution. Critical to cluster disruption are shocks due to the interaction with any irregularity in the gravitational potential (see the introduction in [Webb et al. 2018](#) and references therein). As a consequence, how actually GCs contributed to the formation of the halo by releasing stars that become unbound over almost a full Hubble time is a difficult question, because we have very limited knowledge of the environment where GCs started their evolution about 0.5-1 Gyr after the Big Bang. The consequence is that we are limited by a number of assumptions and we have to rely on indirect probes to evaluate the contribution of GCs to the halo formation.

It is likely that at the early phases of Galaxy formation the impact of collision with giant molecular clouds was more relevant than today, and this is a chief mechanism to generate GC shredding and disruption ([Webb et al. 2018](#)). However, an estimate of the GMC distribution in the proto-MW is an educated guess, at best. The same gravitational potential of the early Galaxy is not known and its temporal evolution could have had important impact in the tidal stress exerted on proto-GCs ([Li and Gnedin 2019](#)). Many related questions remains unanswered, such as: was the thickening of an early disk simultaneous to the formation of halo and bulge? Was the influence of the mass distribution in central Galactic regions enough to affect orbits of the just formed GCs? Were the major merger(s) occurring about 10 Gyr ago accompanied by the formation and/or disruption of GCs or did the falling satellites of the Galaxy simply release their population of associated GCs into the halo of the main Galaxy?

An attempt to include the GC formation in a cosmological context has been made in the past using sub-grid resolution post processing of cosmological simulations (e.g. [Beasley et al. 2002](#); [Prieto and Gnedin 2008](#); [Griffen et al. 2010](#)). In particular, [Reina-](#)

Campos et al. (2018), adopting a simplified recipe for the formation of GCs from molecular cores, suggests that a relatively small mass-loss occurs over the subsequent evolution. On the other hand, their simplified treatment of dynamical evolution as well as the unknown initial structure of proto-GCs make this conclusion weak.

Despite these issues being largely without a firm answer, we expect a contribution from GCs simply because they lose mass. Mass loss is expected in particular at early phases (Lynden-Bell 1967; Baumgardt et al. 2008; Vesperini et al. 2010), but GCs are in general dynamically evolved systems, so that mass loss is predicted to occur over their whole lifetime (e.g. McLaughlin and Fall 2008; Webb et al. 2018; Baumgardt et al. 2019), so it is possible that many clusters dissolved, as corroborated by the lack of GCs with large ratios of halo-mass to Jacobi radius in the near dissolution region (see Baumgardt et al. 2010).

Early and even recent studies on the contribution of GCs to the halo focussed on dwarf galaxies or the entire systems of GCs captured from dwarfs (e.g. Lin and Richer 1992; Fusi Pecci et al. 1995; Forbes and Bridges 2010), rather than on the contribution to halo stars from GCs. The main reason is that it is relatively simple to distinguish between the chemical pattern of GCs and dwarf galaxies when the tagging is made using abundances of α -elements, as usually occurred in these works. However, on the high- α plateau, GC stars are often superimposed to other Galactic components, such as stars formed in-situ, accreted or even kicked out (see Sheffield et al. 2012). α -elements may be able to resolve GC stars from dSph stars, to some extent, but not so from field halo MW stars. Fortunately, one can use another diagnostic provided by the chemical pattern of SG stars in GCs, since this signature is unambiguously unique among old stellar systems.

A first attempt was made in Carretta et al. (2010c) by comparing Na abundances in field stars with SG stars in GCs. They found a small fraction of stars with SG signature, 6 Na-rich stars out of 144 examined. After excluding 4 objects (likely binary stars) a fraction of 1.4% resulted. This number was doubled to 2.8% by considering the typical ratio of FG to SG stars in present-day GCs.

More systematic studies later found similar fractions of SG stars by looking for large N excesses in metal-poor halo stars with low resolution spectra acquired in the Sloan survey. Martell and Grebel (2010) selected from the SEGUE survey 49 relatively CN-strong, CH-weak stars out of an initial sample of 1958 giant (likely halo) stars, corresponding to a fraction 2.5%. Similar results were obtained in Martell et al. (2011) by selecting from SEGUE-2 spectra of more distant RGB stars and retrieving a fraction of 3% of stars with SG composition, in good agreement with more serendipitous discoveries based on the O abundances, like in the study by Ramírez et al. (2012). Out of a sample of 67 halo stars, the latter authors found 2 O-poor stars for which Nissen and Schuster (2010) obtained very high Na abundances. This being exactly the pattern along the Na-O anti-correlation in GCs, Ramírez et al. (2012) estimated a fraction of $3 \pm 2\%$ unless one of the two O-poor stars is revealed to be polluted by a mass transfer events, as hinted by its large abundance of Barium and Yttrium.

Also higher temperature ranges of the burning regions, sampled by the Mg-Al anti-correlation, have been used to trace the possible origin of some field stars back to GCs. Using abundances from the Gaia-ESO survey, Lind et al. (2015) found one

halo star with high Aluminum and large Mg depletion out of few hundreds of examined field stars. They considered this finding not inconsistent with the estimates by [Martell and Grebel \(2010\)](#); [Martell et al. \(2011\)](#), especially because the Mg-Al anti-correlation is not found in all GCs, in contrast to the C-N and Na-O anti-correlations, but only in the most massive and/or metal-poor ones ([Carretta et al. 2009b](#); [Mészáros et al. 2015](#)). This occurrence led [Fernández-Trincado et al. \(2017\)](#) to conclude that the finding from APOGEE survey of Mg-poor, Al-rich stars mostly in the metal-rich regime was inconsistent with an origin from GCs. Note that by itself the deficiency in Mg can be also viewed as the distinctive signature of stars shredded from accreted dwarf galaxy. However, no large enhancement in Al is expected in dSph's stars (e.g. [Shetrone et al. 2001](#)).

In view of these uncertainties, currently one of the most used approaches for tracking SG stars in the halo remains the selection according to N enhancement. [Martell et al. \(2016\)](#) used APOGEE spectra to find 5 stars with N and Al enhancements out of 253 halo giants, after discarding stars with high C abundances and evidence of binarity. The resulting fraction of 2% of stars with SG pattern agrees with previous results. Two important caveats have to be considered. First, the normal evolution of low-mass stars naturally distribute them along a C-N anti-correlation as surface abundances are changed by the dredge-up and the extra-mixing episode on the RGB ([Gratton et al. 2000](#); [Martell et al. 2008](#)). Care must be then exercised to pick up stars that are real outliers at any evolutionary phase. Second, as pointed out by [Smith \(2015\)](#), the comparison of the C, N, O, and Na pattern observed in GCs reveal an apparent decoupling between the C-N and Na-O anti-correlation, which in turn is related to processing at different temperatures and may occur in different stars altogether.

To these, we add another caveat based on the kinematic signatures of these stars that can now be provided using Gaia astrometric information. We note that almost all the candidate SG stars in the field found in previously mentioned and other recent studies ([Fernández-Trincado et al. 2016](#); [Tang et al. 2019](#)) show orbits characterised by high eccentricities. Peculiar chemical abundances, especially concerning α -elements such as Mg, and a dominance of high eccentricity orbits have been recently found as the distinctive chemo-dynamical signature of the massive accretion event that about 8-10 Gyr ago brought the so called Gaia-Enceladus dwarf ([Helmi et al. 2018](#)) into the MW ([Haywood et al. 2018](#); [Simion et al. 2019](#); [Iorio and Belokurov 2019](#); [Mackereth et al. 2019](#)). While in a couple of cases preliminary orbit comparison allows to claim that candidate stars lost by GCs were compatible with an origin from the massive GC ω Cen=NGC 5139 ([Lind et al. 2015](#); [Fernández-Trincado et al. 2016](#)) we caution that a full chemical characterization with all the species involved in multiple population in GCs would provide a more clear cut clue to the origin of these stars, since GCs and remnants of past accretion events cleanly separate in the abundance space.

Taking these caveats into account, various indicators concur to assess the estimates of the fraction of SG in the field in a range from 2 to 4–5%. Considering the typical ratios of FG to SG stars observed in present-day GCs, the total contribution of GCs to the mass budget of the Galactic halo critically depends on the assumptions made for the mass loss at early phases. Strong mass loss, namely if GCs were initially

> 10 times more massive (the value proposed for massive GCs in Sect. 8) and were able to lose about 90% of their mass at early times, would inflate the observed estimates to fractions from 13-17% up to 40-50% of stars in the halo originally formed in GCs (Vesperini et al. 2010; Schaerer and Charbonnel 2011; Martell et al. 2011, 2016; Gratton et al. 2012a). Without this strong mass loss, a limited fraction of about 4-5% of the halo in mass would be originated in GCs (Martell et al. 2011). A simple formalism was recently presented by Koch et al. (2019) to estimate the fraction of the Galactic halo in stars originally born in GCs, as inferred by the observed fraction of 2.6% of field stars with CN-strong (SG) signature from SDSS-IV DR14. Their derived value of 11% stems from a number of different assumptions clearly discussed in their work, with the early mass loss rate from GCs and the number of completely dissolved GCs being the major still unknown relevant factors, poorly constrained by observations.

9 Conclusions and open issues

We reviewed current knowledge about the chemical composition of GCs. They show a quite high level of complexity that may be understood by considering that they are transition objects between single stellar population clusters (the open clusters) and fully developed cases of chemical evolution (galaxies). From a structural point of view, GCs clearly differentiate from most dwarf galaxies (see Fig. 28), being much more compact and lacking dark matter. However, as shown e.g. by Dabringhausen et al. (2008), they merge into the sequence of compact galaxies.

The complexity of GC chemistry has so far defied attempts to explain all observed features in a single scenario (e.g. Renzini et al. 2015; Bastian and Lardo 2018). This might be perhaps attributed to the coexistence of different polluters and different diluters. While there is a vast literature concerning possible polluters (see e.g. the review by Bastian and Lardo 2018), less attention has been paid to the diluters. We suggest that there might actually be two different diluting mechanisms active in GCs. A first one may be considered as “intrinsic” to GCs, that is a mechanism that is present in all GCs with more or less similar trend, likely modulated by the mass or initial density. This mechanism might be related to the usual anti-correlations found in GCs. While mass-loss by single stars might play some role (Gratton and Carretta 2010), the most likely candidate for this dilution are interacting binaries (Vanbeveren et al. 2012). This mechanism acts on the same timescale of the polluter and the mass is lost through winds at similar speed, and it does not then need any special history: it should repeat self-similarly from cluster-to-cluster and be essentially universal to GCs. The second mechanism is “extrinsic” and it is only relevant for massive GCs, being in particular related to Type II GCs. This extrinsic mechanism shows a wide range of variation from cluster-to-cluster both on the amount of involved mass and in the timescale where it occurs, that is however typically longer than that of the first mechanism. This second dilution mechanism is responsible for the variety of the characteristics of massive clusters, as can be obtained from the chromosome map (Milone et al. 2017a; Marino et al. 2018b). On the whole, the best candidate for this second mechanism is some variety of the mass re-accretion considered by D’Ercole et al.

(2011, 2016), and most likely related to the formation within a satellite (Bekki and Freeman 2003; Bekki et al. 2007; Bekki and Tsujimoto 2016; D’Ercole et al. 2016). We suggest that massive clusters may represent a continuum from cases where there was no re-accretion at all (e.g. 47 Tuc=NGC 104), others where the re-accretion (if any) occurred on a quite short time-scale (e.g. NGC 2808 or NGC 2419), to others where the time-scale was longer but with very different amounts of mass re-accreted (see e.g. the comparison between NGC 362 and NGC 1851 or NGC 6656=M 22), to finally complex cases with several re-accretion episodes (such as ω Cen=NGC 5139). This last clearly recall the case of nuclear star clusters (Bekki and Freeman 2003). Note that when we compare NGC 2808 and NGC 2419 with the other type I GCs, a number of peculiarities makes them unique: e.g. variations of the abundances of K and Sc and a large spread in He abundance. These facts suggest the contribution by a class of polluters not relevant for other GCs of this class. A full analysis of the chemical composition of the K- and Sc-rich stars might reveal if they coincide with the super He-rich stars and what is their Li-content. This last point is crucial to establish the nature of the polluter. Though there is no evidence of variation of Fe and total CNO content, the chromosome diagrams of NGC 2808 and NGC 2419 are complex and different from those of typical type I clusters, indicating the presence of several different populations, perhaps each one associated to different polluters and diluters. Their mass and position in the Galaxy is more similar to type II rather than type I clusters. These peculiarities suggest that they may be considered as a special class of GCs and that they may be discussed in the context of Type II GCs.

Summarizing, the interplay between the two different diluting mechanisms, coupled with the possibility of different polluters (supermassive stars: Gieles et al. 2018; fast rotating massive stars: Decressin et al. 2007; massive AGB stars: Ventura et al. 2001) might help to understand the variety of chemical evolution observed in GCs.

Besides complexity, there are a number of problematic points still open and we name here the most relevant in our opinion. First, while nucleosynthesis in massive AGB stars has some of the properties useful to describe many (but likely not all) of the chemical peculiarities observed in GCs, theoretical models are still not robust enough to unequivocally predict the relevant yields. These crucially depend on details that are poorly understood, including convection, mass loss, and the same nuclear cross sections. A suitable combination of these parameters and of their dependence on stellar mass is indeed able to produce the right nucleosynthesis (see e.g. Ventura et al. 2001; D’Antona et al. 2016); however, it is not at all obvious that this combination is really the correct one to be considered (see e.g. Karakas and Lattanzio 2014). While some recent progress has been made in the positive direction (see e.g. the case of the mass loss rate: Pastorelli et al. 2019), it is still too early for a definite conclusion. Second, while there is clear indication that Lithium should be produced in the polluters at least for the case of the widespread intermediate population (and this argues for the important role played by massive AGB stars), this production should mimic the original abundance, strongly constraining models. Again, this production requires that particular recipes are adopted for the evolution of these stars. Third, the timescale involved in the re-accretion events needed to explain Type II clusters is quite constrained by the fact that variation in the abundances of *s*-process elements seems very common, while this is not the case e.g. for the variation of Fe, and there is no known case

where there is variation of Fe abundances but not of the s -process elements. While this might be simply the consequence of a limited statistics, there may be something more basic behind this fact.

Finally, we wish to stress the importance of the implications related to the binary frequencies in the different populations of globular clusters. GCs are usually thought as very high density environments where a number of exotic objects may form. The difference in binary frequency between first and second generation stars indicate that the very dense environment is actually the one at the origin of the second generation; there the density is two order of magnitudes larger than for the first generation. In addition, in both cases there is a strong (roughly linear) dependence on the initial mass. This suggests that the extremely high densities that may be at the origin of the exotic objects are likely related to the second generations in very massive clusters or even in their big brothers, the nuclear star clusters and the compact galaxies. This is the most favourable ambient for the runaway growth of massive or even super-massive compact objects (Ferrarese et al. 2006; Gieles et al. 2018). This underlines the general importance of a better understanding of the formation of GCs.

Acknowledgements This work has made use of BaSTI web tools and of TOPCAT (Taylor 2017). We thank Alessio Mucciarelli for having provided us with unpublished results, and Leo Girardi and Emanuele Dalessandro. We also wish to thank Nate Bastian, Simon Campbell, Santi Cassisi, Franca D'Antona, Enrico Vesperini, and an anonymous referee for having read a draft version of the review and having provided very useful comments. Finally, we wish to thank Frank Schulz that made the many editing steps required to have this review publishable.

References

- Adams FC, Fatuzzo M (1996) A Theory of the Initial Mass Function for Star Formation in Molecular Clouds. *ApJ* 464:256, DOI 10.1086/177318, [astro-ph/9601139](#)
- Aguilar L, Hut P, Ostriker JP (1988) On the evolution of globular cluster systems. I - Present characteristics and rate of destruction in our Galaxy. *ApJ* 335:720–747, DOI 10.1086/166961
- Ahumada JA, Lapasset E (2007) New catalogue of blue stragglers in open clusters. *A&A* 463:789–797, DOI 10.1051/0004-6361/20054590
- Alves-Brito A, Yong D, Meléndez J, Vásquez S, Karakas AI (2012) CNO and F abundances in the globular cluster M 22 (NGC 6656). *A&A* 540:A3, DOI 10.1051/0004-6361/201118623, [1202.0797](#)
- Anthony-Twarog BJ, Laird JB, Payne D, Twarog BA (1991) Ca II H and K filter photometry on the UVBY system. I - The standard system. *AJ* 101:1902–1914, DOI 10.1086/115815
- Armandroff TE, Da Costa GS (1991) Metallicities for old stellar systems from Ca II triplet strengths in member giants. *AJ* 101:1329–1337, DOI 10.1086/115769
- Armosky BJ, Sneden C, Langer GE, Kraft RP (1994) Abundance trends among neutron capture elements in giants of globular clusters M5, M3, M13, M92, and M15. *AJ* 108:1364–1374, DOI 10.1086/117158
- Asplund M, Grevesse N, Sauval AJ, Scott P (2009) The Chemical Composition of the Sun. *ARA&A* 47:481–522, DOI 10.1146/annurev.astro.46.060407.145222, [0909.0948](#)
- Bagdonas V, Drazdauskas A, Tautvaisiene G, Smiljanic R, Chorniy Y (2018) Chemical composition of giant stars in the open cluster IC 4756. *A&A* 615:A165, DOI 10.1051/0004-6361/201832695, [1804.01975](#)
- Balsara DS, Bendinelli AJ, Tilley DA, Massari AR, Howk JC (2008) Simulating anisotropic thermal conduction in supernova remnants - II. Implications for the interstellar medium. *MNRAS* 386:642–656, DOI 10.1111/j.1365-2966.2008.13121.x, [0711.2295](#)
- Banerjee S, Kroupa P (2015) The formation of NGC 3603 young starburst cluster: ‘prompt’ hierarchical assembly or monolithic starburst? *MNRAS* 447:728–746, DOI 10.1093/mnras/stu2445, [1412.1473](#)

- Bastian N, de Mink SE (2009) The effect of stellar rotation on colour-magnitude diagrams: on the apparent presence of multiple populations in intermediate age stellar clusters. *MNRAS* 398(1):L11–L15, DOI 10.1111/j.1745-3933.2009.00696.x, [0906.1590](#)
- Bastian N, Lardo C (2015) Globular cluster mass-loss in the context of multiple populations. *MNRAS* 453:357–364, DOI 10.1093/mnras/stv1661, [1507.05634](#)
- Bastian N, Lardo C (2018) Multiple Stellar Populations in Globular Clusters. *ARA&A* 56:83–136, DOI 10.1146/annurev-astro-081817-051839, [1712.01286](#)
- Bastian N, Strader J (2014) Constraining globular cluster formation through studies of young massive clusters - III. A lack of gas and dust in massive stellar clusters in the LMC and SMC. *MNRAS* 443:3594–3600, DOI 10.1093/mnras/stu1407, [1407.2726](#)
- Bastian N, Lamers HJGLM, de Mink SE, Longmore SN, Goodwin SP, Gieles M (2013) Early disc accretion as the origin of abundance anomalies in globular clusters. *MNRAS* 436:2398–2411, DOI 10.1093/mnras/stt1745, [1309.3566](#)
- Bastian N, Cabrera-Ziri I, Salaris M (2015a) A general abundance problem for all self-enrichment scenarios for the origin of multiple populations in globular clusters. *MNRAS* 449:3333–3346, DOI 10.1093/mnras/stv543, [1503.03071](#)
- Bastian N, Cabrera-Ziri I, Salaris M (2015b) A general abundance problem for all self-enrichment scenarios for the origin of multiple populations in globular clusters. *MNRAS* 449:3333–3346, DOI 10.1093/mnras/stv543, [1503.03071](#)
- Bastian N, Kamann S, Cabrera-Ziri I, Georgy C, Ekström S, Charbonnel C, de Juan Ovelar M, Usher C (2018) Extended main sequence turnoffs in open clusters as seen by Gaia - I. NGC 2818 and the role of stellar rotation. *MNRAS* 480:3739–3746, DOI 10.1093/mnras/sty2100, [1807.10779](#)
- Baumgardt H, Hilker M (2018) A catalogue of masses, structural parameters, and velocity dispersion profiles of 112 Milky Way globular clusters. *MNRAS* 478:1520–1557, DOI 10.1093/mnras/sty1057, [1804.08359](#)
- Baumgardt H, Makino J (2003) Dynamical evolution of star clusters in tidal fields. *MNRAS* 340:227–246, DOI 10.1046/j.1365-8711.2003.06286.x, [astro-ph/0211471](#)
- Baumgardt H, Kroupa P, Parmentier G (2008) The influence of residual gas expulsion on the evolution of the Galactic globular cluster system and the origin of the Population II halo. *MNRAS* 384:1231–1241, DOI 10.1111/j.1365-2966.2007.12811.x, [0712.1591](#)
- Baumgardt H, Parmentier G, Gieles M, Vesperini E (2010) Evidence for two populations of Galactic globular clusters from the ratio of their half-mass to Jacobi radii. *MNRAS* 401:1832–1838, DOI 10.1111/j.1365-2966.2009.15758.x, [0909.5696](#)
- Baumgardt H, Parmentier G, Anders P, Grebel EK (2013) The star cluster formation history of the LMC. *MNRAS* 430:676–685, DOI 10.1093/mnras/sts667, [1207.5576](#)
- Baumgardt H, Hilker M, Sollima A, Bellini A (2019) Mean proper motions, space orbits, and velocity dispersion profiles of Galactic globular clusters derived from Gaia DR2 data. *MNRAS* 482:5138–5155, DOI 10.1093/mnras/sty2997, [1811.01507](#)
- Beasley MA, Baugh CM, Forbes DA, Sharples RM, Frenk CS (2002) On the formation of globular cluster systems in a hierarchical Universe. *MNRAS* 333(2):383–399, DOI 10.1046/j.1365-8711.2002.05402.x, [astro-ph/0202191](#)
- Bedin LR, Piotto G, Anderson J, Cassisi S, King IR, Momany Y, Carraro G (2004) ω Centauri: The Population Puzzle Goes Deeper. *ApJL* 605:L125–L128, DOI 10.1086/420847, [astro-ph/0403112](#)
- Behr BB (2003) Chemical Abundances and Rotation Velocities of Blue Horizontal-Branch Stars in Six Globular Clusters. *ApJS* 149:67–99, DOI 10.1086/377509, [astro-ph/0307178](#)
- Behr BB, Cohen JG, McCarthy JK, Djorgovski SG (1999) Striking Photospheric Abundance Anomalies in Blue Horizontal-Branch Stars in Globular Cluster M13. *ApJL* 517:L135–L138, DOI 10.1086/312052, [astro-ph/9903437](#)
- Behr BB, Cohen JG, McCarthy JK (2000) Rotations and Abundances of Blue Horizontal-Branch Stars in Globular Cluster M15. *ApJL* 531:L37–L40, DOI 10.1086/312524, [astro-ph/0002119](#)
- Bekki K (2010) Rotation and Multiple Stellar Population in Globular Clusters. *ApJL* 724:L99–L103, DOI 10.1088/2041-8205/724/1/L99, [1010.3841](#)
- Bekki K (2011) Secondary star formation within massive star clusters: origin of multiple stellar populations in globular clusters. *MNRAS* 412:2241–2259, DOI 10.1111/j.1365-2966.2010.18047.x, [1011.5956](#)
- Bekki K, Freeman KC (2003) Formation of ω Centauri from an ancient nucleated dwarf galaxy in the young Galactic disc. *MNRAS* 346:L11–L15, DOI 10.1046/j.1365-2966.2003.07275.x, [astro-ph/0310348](#)
- Bekki K, Tsujimoto T (2016) Formation of Anomalous Globular Clusters with Metallicity Spreads: A

- Unified Picture. *ApJ* 831:70, DOI 10.3847/0004-637X/831/1/70
- Bekki K, Campbell SW, Lattanzio JC, Norris JE (2007) Origin of abundance inhomogeneity in globular clusters. *MNRAS* 377:335–351, DOI 10.1111/j.1365-2966.2007.11606.x, [astro-ph/0702289](#)
- Bellazzini M, Fusi Pecci F, Messineo M, Monaco L, Rood RT (2002) Deep Hubble Space Telescope WFC2 Photometry of NGC 288. I. Binary Systems and Blue Stragglers. *AJ* 123:1509–1527, DOI 10.1086/339222, [astro-ph/0112343](#)
- Bellazzini M, Ibata RA, Chapman SC, Mackey AD, Monaco L, Irwin MJ, Martin NF, Lewis GF, Dalessandro E (2008) The Nucleus of the Sagittarius Dwarf Galaxy and M54: a Window on the Process of Galaxy Nucleation. *AJ* 136:1147–1170, DOI 10.1088/0004-6256/136/3/1147, [0807.0105](#)
- Bellazzini M, Bragaglia A, Carretta E, Gratton RG, Lucatello S, Catanzaro G, Leone F (2012) Na-O anticorrelation and HB. IX. Kinematics of the program clusters A link between systemic rotation and HB morphology? *A&A* 538:A18, DOI 10.1051/0004-6361/201118056, [1111.2688](#)
- Bellini A, Vesperini E, Piotto G, Milone AP, Hong J, Anderson J, van der Marel RP, Bedin LR, Cassisi S, D'Antona F, Marino AF, Renzini A (2015) The Hubble Space Telescope UV Legacy Survey of Galactic Globular Clusters: The Internal Kinematics of the Multiple Stellar Populations in NGC 2808. *ApJL* 810:L13, DOI 10.1088/2041-8205/810/1/L13, [1508.01804](#)
- Bellini A, Milone AP, Anderson J, Marino AF, Piotto G, van der Marel RP, Bedin LR, King IR (2017) The State-of-the-art HST Astro-photometric Analysis of the Core of ω Centauri. III. The Main Sequence's Multiple Populations Galore. *ApJ* 844:164, DOI 10.3847/1538-4357/aa7b7e, [1706.07063](#)
- Benitez N, Dupke R, Moles M, Sodre L, Cenarro J, Marin-Franch A, Taylor K, Cristobal D, Fernandez-Soto A, Mendes de Oliveira C, Cepa-Nogue J, Abramo LR, Alcaniz JS, Overzier R, Hernandez-Monteagudo C, Alfaro EJ, Kanaan A, Carvano JM, Reis RRR, Martinez Gonzalez E, Ascaso B, Ballesteros F, Xavier HS, Varela J, Ederocliste A, Vazquez Ramio H, Broadhurst T, Cypriano E, Angulo R, Diego JM, Zandivarez A, Diaz E, Melchior P, Umetsu K, Spinelli PF, Zittrin A, Coe D, Yepes G, Vielva P, Sahni V, Marcos-Caballero A, Shu Kitaura F, Maroto AL, Masip M, Tsujikawa S, Carneiro S, Gonzalez Nuevo J, Carvalho GC, Reboucas MJ, Carvalho JC, Abdalla E, Bernui A, Pigozzo C, Ferreira EGM, Chandrachani Devi N, Bengaly CAP Jr, Campista M, Amorim A, Asari NV, Bongiovanni A, Bonoli S, Bruzual G, Cardiel N, Cava A, Cid Fernandes R, Coelho P, Cortesi A, Delgado RG, Diaz Garcia L, Espinosa JMR, Galliano E, Gonzalez-Serrano JI, Falcon-Barroso J, Fritz J, Fernandes C, Gorgas J, Hoyos C, Jimenez-Teja Y, Lopez-Aguerre JA, Lopez-San Juan C, Mateus A, Molino A, Novais P, OMill A, Oteo I, Perez-Gonzalez PG, Poggianti B, Proctor R, Ricciardelli E, Sanchez-Blazquez P, Storch-Bergmann T, Telles E, Schoennell W, Trujillo N, Vazdekis A, Viironen K, Daflon S, Aparicio-Villegas T, Rocha D, Ribeiro T, Borges M, Martins SL, Marcolino W, Martinez-Delgado D, Perez-Torres MA, Sifert BB, Calvao MO, Sako M, Kessler R, Alvarez-Candal A, De Pra M, Roig F, Lazzaro D, Gorosabel J, Lopes de Oliveira R, Lima-Neto GB, Irwin J, Liu JF, Alvarez E, Balmes I, Chueca S, Costa-Duarte MV, da Costa AA, Dantas MLL, Diaz AY, Fabregat J, Ferrari F, Gavela B, Gracia SG, Gruel N, Gutierrez JLL, Guzman R, Hernandez-Fernandez JD, Herranz D, Hurtado-Gil L, Jablonsky F, Laporte R, Le Tiran LL, Licandro J, Lima M, Martin E, Martinez V, Montero JJC, Penteado P, Pereira CB, Peris V, Quilis V, Sanchez-Portal M, Soja AC, Solano E, Torra J, Valdivielso L (2014) J-PAS: The Javalambre-Physics of the Accelerated Universe Astrophysical Survey. *arXiv e-prints* [1403.5237](#)
- Bertelli G, Nasi E, Girardi L, Chiosi C, Zoccali M, Gallart C (2003) Testing Intermediate-Age Stellar Evolution Models with VLT Photometry of Large Magellanic Cloud Clusters. III. Padova Results. *AJ* 125:770–784, DOI 10.1086/345961, [astro-ph/0211169](#)
- Beuther H, Churchwell EB, McKee CF, Tan JC (2007) The Formation of Massive Stars. Protostars and Planets V pp 165–180, [astro-ph/0602012](#)
- Bloecker T (1995) Stellar evolution of low and intermediate-mass stars. I. Mass loss on the AGB and its consequences for stellar evolution. *A&A* 297:727
- Boberg OM, Friel ED, Vesperini E (2015) Chemical Abundances in NGC 5053: A Very Metal-poor and Dynamically Complex Globular Cluster. *ApJ* 804:109, DOI 10.1088/0004-637X/804/2/109, [1504.01791](#)
- Boberg OM, Friel ED, Vesperini E (2016) Chemical Abundances in NGC 5024 (M53): A Mostly First Generation Globular Cluster. *ApJ* 824:5, DOI 10.3847/0004-637X/824/1/5
- Böcek Topcu G, Afşar M, Sneden C (2016) The chemical compositions and evolutionary status of red giants in the open cluster NGC 6940. *MNRAS* 463:580–597, DOI 10.1093/mnras/stw1974
- Bodenheimer P, Tenorio-Tagle G, Yorke HW (1979) The gas dynamics of H II regions. II - Two-dimensional axisymmetric calculations. *ApJ* 233:85–96, DOI 10.1086/157368
- Bolte M (1992) CCD Photometry in the Globular Cluster NGC 288. I. Blue Stragglers and Main-Sequence

- Binary Stars. *ApJS* 82:145, DOI 10.1086/191712
- Bonatto C, Chies-Santos AL, Coelho PRT, Varela J, Larsen SS, Javier Cenarro A, San Roman I, Marín-Franch A, Mendes de Oliveira C, Molino A, Ederoclite A, Cortesi A, López-Sanjuan C, Cristóbal-Hornillos D, Vázquez Ramió H, Sodr  L, Sampedro L, Costa-Duarte MV, Novais PM, Dupke R, Overzier RA, Ribeiro T, Santos WA, Schoennell W (2019) J-PLUS: A wide-field multi-band study of the M 15 globular cluster. Evidence of multiple stellar populations in the RGB. *A&A* 622:A179, DOI 10.1051/0004-6361/201732441, [1804.03966](#)
- Bonnell IA, Bate MR, Vine SG (2003) The hierarchical formation of a stellar cluster. *MNRAS* 343:413–418, DOI 10.1046/j.1365-8711.2003.06687.x, [astro-ph/0305082](#)
- Bonnell IA, Smith RJ, Clark PC, Bate MR (2011) The efficiency of star formation in clustered and distributed regions. *MNRAS* 410:2339–2346, DOI 10.1111/j.1365-2966.2010.17603.x, [1009.1152](#)
- Bragaglia A, Carretta E, Gratton R, D’Orazi V, Cassisi S, Lucatello S (2010a) Helium in first and second-generation stars in globular clusters from spectroscopy of red giants. *A&A* 519:A60, DOI 10.1051/0004-6361/201014702, [1005.2659](#)
- Bragaglia A, Carretta E, Gratton RG, Lucatello S, Milone A, Piotto G, D’Orazi V, Cassisi S, Sneden C, Bedin LR (2010b) X-shooter Observations of Main-sequence Stars in the Globular Cluster NGC 2808: First Chemical Tagging of a He-normal and a He-rich Dwarf. *ApJL* 720:L41–L45, DOI 10.1088/2041-8205/720/1/L41, [1007.5299](#)
- Bragaglia A, Gratton RG, Carretta E, D’Orazi V, Sneden C, Lucatello S (2012) Searching for multiple stellar populations in the massive, old open cluster Berkeley 39. *A&A* 548:A122, DOI 10.1051/0004-6361/201220366, [1211.1142](#)
- Bragaglia A, Sneden C, Carretta E, Gratton RG, Lucatello S, Bernath PF, Brooke JSA, Ram RS (2014) Searching for Chemical Signatures of Multiple Stellar Populations in the Old, Massive Open Cluster NGC 6791. *ApJ* 796:68, DOI 10.1088/0004-637X/796/1/68, [1409.8283](#)
- Bragaglia A, Carretta E, Sollima A, Donati P, D’Orazi V, Gratton RG, Lucatello S, Sneden C (2015) NGC 6139: a normal massive globular cluster, or a first-generation dominated cluster? Clues from the light elements. *A&A* 583:A69, DOI 10.1051/0004-6361/201526592, [1507.07562](#)
- Bragaglia A, Carretta E, D’Orazi V, Sollima A, Donati P, Gratton RG, Lucatello S (2017) NGC 6535: the lowest mass Milky Way globular cluster with a Na-O anti-correlation? Cluster mass and age in the multiple population context. *A&A* 607:A44, DOI 10.1051/0004-6361/201731526, [1708.07705](#)
- Bragaglia A, Fu X, Mucciarelli A, Andreuzzi G, Donati P (2018) The chemical composition of the oldest nearby open cluster Ruprecht 147. *A&A* 619:A176, DOI 10.1051/0004-6361/201833888, [1809.06868](#)
- Briley MM, Cohen JG (2001) Calibration of the CH and CN Variations Among Main-Sequence Stars in M71 and in M13. *AJ* 122:242–247, DOI 10.1086/321115, [astro-ph/0104099](#)
- Briley MM, Cohen JG, Stetson PB (2004) The Chemical Inhomogeneity of Faint M13 Stars: Carbon and Nitrogen Abundances. *AJ* 127:1579–1587, DOI 10.1086/382100, [astro-ph/0312315](#)
- Brodie JP, Strader J (2006) Extragalactic Globular Clusters and Galaxy Formation. *ARA&A* 44:193–267, DOI 10.1146/annurev.astro.44.051905.092441, [astro-ph/0602601](#)
- Çalışkan Ş, Christlieb N, Grebel EK (2012) Abundance analysis of the outer halo globular cluster Palomar 14. *A&A* 537:A83, DOI 10.1051/0004-6361/201016355, [1110.5151](#)
- Cabrera-Ziri I, Bastian N, Longmore SN, Brogan C, Hollyhead K, Larsen SS, Whitmore B, Johnson K, Chandar R, Henshaw JD, Davies B, Hibbard JE (2015) Constraining globular cluster formation through studies of young massive clusters - V. ALMA observations of clusters in the Antennae. *MNRAS* 448:2224–2231, DOI 10.1093/mnras/stv163, [1501.05657](#)
- Cabrera-Ziri I, Lardo C, Mucciarelli A (2019) Constant light element abundances suggest that the extended P1 in NGC 2808 is not a consequence of CNO-cycle nucleosynthesis. *MNRAS* DOI 10.1093/mnras/stz707, [1903.03621](#)
- Calura F, Few CG, Romano D, D’Ercole A (2015) Feedback from Massive Stars and Gas Expulsion from Proto-Globular Clusters. *ApJL* 814:L14, DOI 10.1088/2041-8205/814/1/L14, [1511.03277](#)
- Calura F, D’Ercole A, Vesperini E, Vanzella E, Sollima A (2019) Formation of Second Generation Stars in Globular Clusters. *MNRAS* p 1995, DOI 10.1093/mnras/stz2055, [1906.09137](#)
- Cameron AGW, Fowler WA (1971) Lithium and the s-PROCESS in Red-Giant Stars. *ApJ* 164:111, DOI 10.1086/150821
- Campbell SW, Lattanzio JC, Elliott LM (2006) Are There Radical Cyanogen Abundance Differences Between Galactic Globular Cluster RGB and AGB Stars? arXiv e-prints [astro-ph/0603779](#)
- Campbell SW, D’Orazi V, Yong D, Constantino TN, Lattanzio JC, Stancliffe RJ, Angelou GC, Wylie-de Boer EC, Grundahl F (2013) Sodium content as a predictor of the advanced evolution of globular

- cluster stars. *Nature* 498:198–200, DOI 10.1038/nature12191, [1305.7090](#)
- Campbell SW, MacLean BT, D’Orazi V, Casagrande L, de Silva GM, Yong D, Cottrell PL, Lattanzio JC (2017) NGC 6752 AGB stars revisited. I. Improved AGB temperatures remove apparent overionisation of Fe I. *A&A* 605:A98, DOI 10.1051/0004-6361/201731101, [1707.02840](#)
- Cantat-Gaudin T, Vallenari A, Zaggia S, Bragaglia A, Sordo R, Drew JE, Eisloffel J, Farnhill HJ, Gonzalez-Solares E, Greimel R, Irwin MJ, Kupcu-Yoldas A, Jordi C, Blomme R, Sampedro L, Costado MT, Alfaro E, Smiljanic R, Magrini L, Donati P, Friel ED, Jacobson H, Abbas U, Hatzidimitriou D, Spagna A, Vecchiato A, Balaguer-Nunez L, Lardo C, Tosi M, Pancino E, Klutsch A, Tautvaisiene G, Drazdauskas A, Puzeras E, Jiménez-Esteban F, Maiorca E, Geisler D, San Roman I, Villanova S, Gilmore G, Randich S, Bensby T, Flaccomio E, Lanzafame A, Recio-Blanco A, Damiani F, Hourihane A, Jofré P, de Laverny P, Masseron T, Morbidelli L, Prisinzano L, Sacco GG, Sbordone L, Worley CC (2014) The Gaia-ESO Survey: Stellar content and elemental abundances in the massive cluster NGC 6705. *A&A* 569:A17, DOI 10.1051/0004-6361/201423851, [1407.1510](#)
- Carballo-Bello JA, Sollima A, Martínez-Delgado D, Pila-Díez B, Leaman R, Fliri J, Muñoz RR, Corral-Santana JM (2014) A search for stellar tidal debris of defunct dwarf galaxies around globular clusters in the inner Galactic halo. *MNRAS* 445:2971–2993, DOI 10.1093/mnras/stu1949, [1409.7390](#)
- Carretta E (2006) Abundances in Red Giant Stars of NGC 2808 and Correlations between Chemical Anomalies and Global Parameters in Globular Clusters. *AJ* 131:1766–1783, DOI 10.1086/499565, [astro-ph/0511144](#)
- Carretta E (2014) Three Discrete Groups with Homogeneous Chemistry along the Red Giant Branch in the Globular Cluster NGC 2808. *ApJL* 795:L28, DOI 10.1088/2041-8205/795/2/L28, [1410.3476](#)
- Carretta E (2015) Five Groups of Red Giants with Distinct Chemical Composition in the Globular Cluster NGC 2808. *ApJ* 810:148, DOI 10.1088/0004-637X/810/2/148, [1507.07553](#)
- Carretta E (2016) Spectroscopic evidence of Multiple Stellar Populations in Globular Clusters. arXiv e-prints [1611.04728](#)
- Carretta E (2019) Empirical estimates of the Na-O anti-correlation in 95 Galactic globular clusters. *A&A* 624:A24, DOI 10.1051/0004-6361/201935110, [1903.04494](#)
- Carretta E, Bragaglia A (2018) Observing multiple populations in globular clusters with the ESO archive: NGC 6388 reloaded. *A&A* 614:A109, DOI 10.1051/0004-6361/201832660, [1802.06787](#)
- Carretta E, Bragaglia A, Cacciari C, Rossetti E (2003) Proton capture elements in the globular cluster NGC 2808. I. First detection of large variations in sodium abundances along the Red Giant Branch. *A&A* 410:143–154, DOI 10.1051/0004-6361:20031315, [astro-ph/0309021](#)
- Carretta E, Bragaglia A, Cacciari C (2004) Star-to-Star Na and O Abundance Variations along the Red Giant Branch in NGC 2808. *ApJL* 610:L25–L28, DOI 10.1086/423034, [astro-ph/0406119](#)
- Carretta E, Gratton RG, Lucatello S, Bragaglia A, Bonifacio P (2005) Abundances of C, N, O in slightly evolved stars in the globular clusters NGC 6397, NGC 6752 and 47 Tuc. *A&A* 433:597–611, DOI 10.1051/0004-6361:20041892, [astro-ph/0411241](#)
- Carretta E, Bragaglia A, Gratton RG, Leone F, Recio-Blanco A, Lucatello S (2006) Na-O anticorrelation and HB. I. The Na-O anticorrelation in NGC 2808. *A&A* 450:523–533, DOI 10.1051/0004-6361:20054369, [astro-ph/0511833](#)
- Carretta E, Bragaglia A, Gratton RG, Lucatello S, Momany Y (2007) Na-O anticorrelation and horizontal branches. II. The Na-O anticorrelation in the globular cluster NGC 6752. *A&A* 464:927–937, DOI 10.1051/0004-6361:20065208, [astro-ph/0701174](#)
- Carretta E, Bragaglia A, Gratton R, D’Orazi V, Lucatello S (2009a) Intrinsic iron spread and a new metallicity scale for globular clusters. *A&A* 508:695–706, DOI 10.1051/0004-6361/200913003, [0910.0675](#)
- Carretta E, Bragaglia A, Gratton R, Lucatello S (2009b) Na-O anticorrelation and HB. VIII. Proton-capture elements and metallicities in 17 globular clusters from UVES spectra. *A&A* 505:139–155, DOI 10.1051/0004-6361/200912097, [0909.2941](#)
- Carretta E, Bragaglia A, Gratton RG, Lucatello S, Catanzaro G, Leone F, Bellazzini M, Claudi R, D’Orazi V, Momany Y, Ortolani S, Pancino E, Piotto G, Recio-Blanco A, Sabbi E (2009c) Na-O anticorrelation and HB. VII. The chemical composition of first and second-generation stars in 15 globular clusters from GIRAFFE spectra. *A&A* 505:117–138, DOI 10.1051/0004-6361/200912096, [0909.2938](#)
- Carretta E, Bragaglia A, Gratton RG, Lucatello S, Bellazzini M, Catanzaro G, Leone F, Momany Y, Piotto G, D’Orazi V (2010a) Detailed abundances of a large sample of giant stars in M 54 and in the Sagittarius nucleus. *A&A* 520:A95, DOI 10.1051/0004-6361/201014924, [1006.5866](#)
- Carretta E, Bragaglia A, Gratton RG, Lucatello S, Bellazzini M, Catanzaro G, Leone F, Momany Y, Piotto G, D’Orazi V (2010b) M54 + Sagittarius = ω Centauri. *ApJL* 714:L7–L11, DOI 10.1088/2041-8205/

- 714/1/L7, [1002.1963](#)
- Carretta E, Bragaglia A, Gratton RG, Recio-Blanco A, Lucatello S, D’Orazi V, Cassisi S (2010c) Properties of stellar generations in globular clusters and relations with global parameters. *A&A* 516:A55, DOI 10.1051/0004-6361/200913451, [1003.1723](#)
- Carretta E, Bragaglia A, Gratton R, D’Orazi V, Lucatello S (2011a) A Strömgren view of the multiple populations in globular clusters. *A&A* 535:A121, DOI 10.1051/0004-6361/201117180, [1109.3199](#)
- Carretta E, Lucatello S, Gratton RG, Bragaglia A, D’Orazi V (2011b) Multiple stellar populations in the globular cluster NGC 1851. *A&A* 533:A69, DOI 10.1051/0004-6361/201117269, [1106.3174](#)
- Carretta E, Bragaglia A, Gratton RG, Lucatello S, D’Orazi V (2012) Chemical Tagging of Three Distinct Populations of Red Giants in the Globular Cluster NGC 6752. *ApJL* 750:L14, DOI 10.1088/2041-8205/750/1/L14, [1204.0259](#)
- Carretta E, Bragaglia A, Gratton RG, Lucatello S, D’Orazi V, Bellazzini M, Catanzaro G, Leone F, Momany Y, Sollima A (2013a) NGC 362: another globular cluster with a split red giant branch. *A&A* 557:A138, DOI 10.1051/0004-6361/201321905, [1307.4085](#)
- Carretta E, Gratton RG, Bragaglia A, D’Orazi V, Lucatello S, Sollima A, Sneden C (2013b) Potassium in Globular Cluster Stars: Comparing Normal Clusters to the Peculiar Cluster NGC 2419. *ApJ* 769:40, DOI 10.1088/0004-637X/769/1/40, [1303.4740](#)
- Carretta E, Bragaglia A, Gratton RG, D’Orazi V, Lucatello S, Sollima A (2014) Terzan 8: a Sagittarius-flavoured globular cluster. *A&A* 561:A87, DOI 10.1051/0004-6361/201322676, [1311.2589](#)
- Carretta E, Bragaglia A, Gratton RG, D’Orazi V, Lucatello S, Sollima A, Momany Y, Catanzaro G, Leone F (2015) The normal chemistry of multiple stellar populations in the dense globular cluster NGC 6093 (M 80). *A&A* 578:A116, DOI 10.1051/0004-6361/201525951, [1503.03074](#)
- Carretta E, Bragaglia A, Lucatello S, D’Orazi V, Gratton RG, Donati P, Sollima A, Sneden C (2017) Chemical characterisation of the globular cluster NGC 5634 associated to the Sagittarius dwarf spheroidal galaxy. *A&A* 600:A118, DOI 10.1051/0004-6361/201630004, [1701.03116](#)
- Carretta E, Bragaglia A, Lucatello S, Gratton RG, D’Orazi V, Sollima A (2018) Aluminium abundances in five discrete stellar populations of the globular cluster NGC 2808. *A&A* 615:A17, DOI 10.1051/0004-6361/201732324, [1801.09689](#)
- Cassisi S, Salaris M (1997) A critical investigation on the discrepancy between the observational and the theoretical red giant luminosity function ‘bump’. *Monthly Notices of the Royal Astronomical Society* 285(3):593–603, DOI 10.1093/mnras/285.3.593, [astro-ph/9702029](#)
- Cassisi S, Marín-Franch A, Salaris M, Aparicio A, Monelli M, Pietrinferni A (2011) The magnitude difference between the main sequence turn off and the red giant branch bump in Galactic globular clusters. *A&A* 527:A59, DOI 10.1051/0004-6361/201016066, [1012.0419](#)
- Cassisi S, Salaris M, Pietrinferni A, Vink JS, Monelli M (2014) On the missing second generation AGB stars in NGC 6752. *A&A* 571:A81, DOI 10.1051/0004-6361/201424540, [1410.3599](#)
- Cassisi S, Salaris M, Pietrinferni A, Hyder D (2017) On the determination of the He abundance distribution in globular clusters from the width of the main sequence. *MNRAS* 464:2341–2348, DOI 10.1093/mnras/stw2579, [1610.01755](#)
- Catelan M (2009) Horizontal branch stars: the interplay between observations and theory, and insights into the formation of the Galaxy. *ApSS* 320:261–309, DOI 10.1007/s10509-009-9987-8, [astro-ph/0507464](#)
- Chabrier G, Hennebelle P, Charlot S (2014) Variations of the Stellar Initial Mass Function in the Progenitors of Massive Early-type Galaxies and in Extreme Starburst Environments. *ApJ* 796:75, DOI 10.1088/0004-637X/796/2/75, [1409.8466](#)
- Chantereau W, Salaris M, Bastian N, Martocchia S (2019) Helium enrichment in intermediate-age Magellanic Clouds clusters: towards an ubiquity of multiple stellar populations? arXiv e-prints [1902.01806](#)
- Charbonnel C, Chantereau W, Krause M, Primas F, Wang Y (2014) Are there any first-generation stars in globular clusters today? *A&A* 569:L6, DOI 10.1051/0004-6361/201424804, [1410.3967](#)
- Cohen JG (2004) Palomar 12 as a Part of the Sagittarius Stream: The Evidence from Abundance Ratios. *AJ* 127:1545–1554, DOI 10.1086/382104, [astro-ph/0311187](#)
- Cohen JG, Briley MM, Stetson PB (2002) Carbon and Nitrogen Abundances in Stars at the Base of the Red Giant Branch in M5. *AJ* 123:2525–2540, DOI 10.1086/340179, [astro-ph/0112199](#)
- Cordero MJ, Pilachowski CA, Johnson CI, McDonald I, Zijlstra AA, Simmerer J (2014) Detailed Abundances for a Large Sample of Giant Stars in the Globular Cluster 47 Tucanae (NGC 104). *ApJ* 780:94, DOI 10.1088/0004-637X/780/1/94, [1311.1541](#)
- Cordero MJ, Hénault-Brunet V, Pilachowski CA, Balbinot E, Johnson CI, Varri AL (2017) Differences in the rotational properties of multiple stellar populations in M13: a faster rotation for the ‘extreme’

- chemical subpopulation. *MNRAS* 465:3515–3535, DOI 10.1093/mnras/stw2812, [1610.09374](#)
- Cowan JJ, Sneden C, Lawler JE, Arahamian A, Wiescher M, Langanke K, Martínez-Pinedo G, Thielemann FK (2019) Making the Heaviest Elements in the Universe: A Review of the Rapid Neutron Capture Process. arXiv e-prints [1901.01410](#)
- Cristallo S, Straniero O, Gallino R, Piersanti L, Domínguez I, Lederer MT (2009) Evolution, Nucleosynthesis, and Yields of Low-Mass Asymptotic Giant Branch Stars at Different Metallicities. *ApJ* 696:797–820, DOI 10.1088/0004-637X/696/1/797, [0902.0243](#)
- Cristallo S, Straniero O, Piersanti L, Gobrecht D (2015) Evolution, Nucleosynthesis, and Yields of AGB Stars at Different Metallicities. III. Intermediate-mass Models, Revised Low-mass Models, and the ph-FRUIITY Interface. *The Astrophysical Journal Supplement Series* 219(2):40, DOI 10.1088/0067-0049/219/2/40, [1507.07338](#)
- Cummings JD, Kalirai JS, Tremblay PE, Ramirez-Ruiz E, Choi J (2018) The White Dwarf Initial-Final Mass Relation for Progenitor Stars from 0.85 to 7.5 M_{\odot} . *ApJ* 866:21, DOI 10.3847/1538-4357/aadfd6, [1809.01673](#)
- Cunha K, Smith VV, Johnson JA, Bergemann M, Mészáros S, Shetrone MD, Souto D, Allende Prieto C, Schiavon RP, Frinchaboy P, Zasowski G, Bizyaev D, Holtzman J, García Pérez AE, Majewski SR, Nidever D, Beers T, Carrera R, Geisler D, Gunn J, Hearty F, Ivans I, Martell S, Pinsonneault M, Schneider DP, Sobek J, Stello D, Stassun KG, Skrutskie M, Wilson JC (2015) Sodium and Oxygen Abundances in the Open Cluster NGC 6791 from APOGEE H-band Spectroscopy. *ApJL* 798:L41, DOI 10.1088/2041-8205/798/2/L41, [1411.2034](#)
- Da Costa GS (2016) The Ca II triplet in red giant spectra: [Fe/H] determinations and the role of [Ca/Fe]. *MNRAS* 455:199–206, DOI 10.1093/mnras/stv2315, [1510.00766](#)
- Da Costa GS, Held EV, Saviane I (2014) NGC 5824: a luminous outer halo globular cluster with an intrinsic abundance spread. *MNRAS* 438:3507–3520, DOI 10.1093/mnras/stt2467, [1312.5796](#)
- Dabringhausen J, Hilker M, Kroupa P (2008) From star clusters to dwarf galaxies: the properties of dynamically hot stellar systems. *MNRAS* 386:864–886, DOI 10.1111/j.1365-2966.2008.13065.x, [0802.0703](#)
- Dale JE, Bonnell I (2011) Ionizing feedback from massive stars in massive clusters: fake bubbles and untriggered star formation. *MNRAS* 414:321–328, DOI 10.1111/j.1365-2966.2011.18392.x, [1103.1532](#)
- Dalessandro E, Salaris M, Ferraro FR, Cassisi S, Lanzoni B, Rood RT, Fusi Pecci F, Sabbi E (2011) The peculiar horizontal branch of NGC 2808. *MNRAS* 410:694–704, DOI 10.1111/j.1365-2966.2010.17479.x, [1008.4478](#)
- Dalessandro E, Salaris M, Ferraro FR, Mucciarelli A, Cassisi S (2013) The horizontal branch in the UV colour-magnitude diagrams - II. The case of M3, M13 and M79. *MNRAS* 430:459–471, DOI 10.1093/mnras/sts644, [1212.4419](#)
- Dalessandro E, Massari D, Bellazzini M, Miocchi P, Mucciarelli A, Salaris M, Cassisi S, Ferraro FR, Lanzoni B (2014) First Evidence of Fully Spatially Mixed First and Second Generations in Globular Clusters: The Case of NGC 6362. *ApJL* 791:L4, DOI 10.1088/2041-8205/791/1/L4, [1407.0484](#)
- Dalessandro E, Lapenna E, Mucciarelli A, Origlia L, Ferraro FR, Lanzoni B (2016) Multiple Populations in the Old and Massive Small Magellanic Cloud Globular Cluster NGC 121. *ApJ* 829:77, DOI 10.3847/0004-637X/829/2/77, [1607.05736](#)
- Dalessandro E, Cadelano M, Vesperini E, Salaris M, Ferraro FR, Lanzoni B, Raso S, Hong J, Webb JJ, Zocchi A (2018a) The Peculiar Radial Distribution of Multiple Populations in the Massive Globular Cluster M80. *ApJ* 859:15, DOI 10.3847/1538-4357/aabb56, [1804.03222](#)
- Dalessandro E, Lardo C, Cadelano M, Saracino S, Bastian N, Mucciarelli A, Salaris M, Stetson P, Pancino E (2018b) IC 4499 revised: Spectro-photometric evidence of small light-element variations. *A&A* 618:A131, DOI 10.1051/0004-6361/201833650, [1807.07618](#)
- Dalessandro E, Mucciarelli A, Bellazzini M, Sollima A, Vesperini E, Hong J, Hénault-Brunet V, Ferraro FR, Ibata R, Lanzoni B, Massari D, Salaris M (2018c) The Unexpected Kinematics of Multiple Populations in NGC 6362: Do Binaries Play a Role? *ApJ* 864:33, DOI 10.3847/1538-4357/aad4b3, [1807.07918](#)
- D’Antona F, Caloi V (2004) The Early Evolution of Globular Clusters: The Case of NGC 2808. *ApJ* 611:871–880, DOI 10.1086/422334, [astro-ph/0405016](#)
- D’Antona F, Caloi V, Montalbán J, Ventura P, Gratton R (2002) Helium variation due to self-pollution among Globular Cluster stars. Consequences on the horizontal branch morphology. *A&A* 395:69–75, DOI 10.1051/0004-6361:20021220, [astro-ph/0209331](#)
- D’Antona F, Bellazzini M, Caloi V, Pecci FF, Galletti S, Rood RT (2005) A Helium Spread among the

- Main-Sequence Stars in NGC 2808. *ApJ* 631:868–878, DOI 10.1086/431968, [astro-ph/0505347](#)
- D’Antona F, D’Ercole A, Carini R, Vesperini E, Ventura P (2012) Models for the lithium abundances of multiple populations in globular clusters and the possible role of the big bang lithium. *MNRAS* 426:1710–1719, DOI 10.1111/j.1365-2966.2012.21663.x, [1207.1544](#)
- D’Antona F, Vesperini E, D’Ercole A, Ventura P, Milone AP, Marino AF, Tailo M (2016) A single model for the variety of multiple-population formation(s) in globular clusters: a temporal sequence. *MNRAS* 458:2122–2139, DOI 10.1093/mnras/stw387, [1602.05412](#)
- D’Antona F, Milone AP, Tailo M, Ventura P, Vesperini E, di Criscienzo M (2017) Stars caught in the braking stage in young Magellanic Cloud clusters. *Nature Astronomy* 1:0186, DOI 10.1038/s41550-017-0186, [1707.07711](#)
- Davies MB, Piotto G, de Angeli F (2004) Blue straggler production in globular clusters. *MNRAS* 349:129–134, DOI 10.1111/j.1365-2966.2004.07474.x, [astro-ph/0401502](#)
- de Marchi F, de Angeli F, Piotto G, Carraro G, Davies MB (2006) Search and analysis of blue straggler stars in open clusters. *A&A* 459:489–497, DOI 10.1051/0004-6361/20064898, [astro-ph/0608464](#)
- de Mink SE, Pols OR, Langer N, Izzard RG (2009) Massive binaries as the source of abundance anomalies in globular clusters. *A&A* 507:L1–L4, DOI 10.1051/0004-6361/200913205, [0910.1086](#)
- de Silva GM, Gibson BK, Lattanzio J, Asplund M (2009) On and Na abundance patterns in open clusters of the Galactic disk. *A&A* 500:L25–L28, DOI 10.1051/0004-6361/200912279, [0905.4354](#)
- Decressin T, Meynet G, Charbonnel C, Prantzos N, Ekström S (2007) Fast rotating massive stars and the origin of the abundance patterns in galactic globular clusters. *A&A* 464:1029–1044, DOI 10.1051/0004-6361:20066013, [astro-ph/0611379](#)
- Denisenkov PA, Denisenkova SN (1989) Possible Explanation of the Correlation Between Nitrogen and Sodium Over Abundances for Red Giants in Globular Clusters. *Astronomicheskij Tsirkulyar* 1538:11
- D’Ercole A, Vesperini E, D’Antona F, McMillan SLW, Recchi S (2008a) Formation and dynamical evolution of multiple stellar generations in globular clusters. *Monthly Notices of the Royal Astronomical Society* 391(2):825–843, DOI 10.1111/j.1365-2966.2008.13915.x, [0809.1438](#)
- D’Ercole A, Vesperini E, D’Antona F, McMillan SLW, Recchi S (2008b) Formation and dynamical evolution of multiple stellar generations in globular clusters. *MNRAS* 391:825–843, DOI 10.1111/j.1365-2966.2008.13915.x, [0809.1438](#)
- D’Ercole A, D’Antona F, Ventura P, Vesperini E, McMillan SLW (2010) Abundance patterns of multiple populations in globular clusters: a chemical evolution model based on yields from AGB ejecta. *MNRAS* 407(2):854–869, DOI 10.1111/j.1365-2966.2010.16996.x, [1005.1892](#)
- D’Ercole A, D’Antona F, Vesperini E (2011) Formation of multiple populations in globular clusters: constraints on the dilution by pristine gas. *MNRAS* 415:1304–1309, DOI 10.1111/j.1365-2966.2011.18776.x, [1103.4715](#)
- D’Ercole A, D’Antona F, Carini R, Vesperini E, Ventura P (2012) The role of super-asymptotic giant branch ejecta in the abundance patterns of multiple populations in globular clusters. *MNRAS* 423(2):1521–1533, DOI 10.1111/j.1365-2966.2012.20974.x, [1203.4992](#)
- D’Ercole A, D’Antona F, Vesperini E (2016) Accretion of pristine gas and dilution during the formation of multiple-population globular clusters. *MNRAS* 461:4088–4098, DOI 10.1093/mnras/stw1583, [1607.00951](#)
- di Criscienzo M, D’Antona F, Ventura P (2010) A detailed study of the main sequence of the globular cluster NGC 6397: can we derive constraints on the existence of multiple populations? *A&A* 511:A70, DOI 10.1051/0004-6361/200912516, [0912.3150](#)
- Dias B, Barbuy B, Saviane I, Held EV, Da Costa GS, Ortolani S, Gullieuszik M, Vásquez S (2016) FORS2/VLT survey of Milky Way globular clusters. II. Fe and Mg abundances of 51 Milky Way globular clusters on a homogeneous scale. *A&A* 590:A9, DOI 10.1051/0004-6361/201526765, [1603.02672](#)
- Dobrovolskas V, Kučinskas A, Bonifacio P, Korotin SA, Steffen M, Sbordone L, Caffau E, Ludwig HG, Royer F, Prakapavičius D (2014) Abundances of lithium, oxygen, and sodium in the turn-off stars of Galactic globular cluster 47 Tucanae. *A&A* 565:A121, DOI 10.1051/0004-6361/201322868, [1311.1072](#)
- Doherty CL, Gil-Pons P, Lau HHB, Lattanzio JC, Siess L, Campbell SW (2014) Super and massive AGB stars - III. Nucleosynthesis in metal-poor and very metal-poor stars - $Z = 0.001$ and 0.0001 . *MNRAS* 441:582–598, DOI 10.1093/mnras/stu571, [1403.5054](#)
- Donati P, Cantat Gaudin T, Bragaglia A, Friel E, Magrini L, Smiljanic R, Vallenari A, Tosi M, Sordo R, Tautvaisiene G, Blanco-Cuaresma S, Costado MT, Geisler D, Klutsch A, Mowlavi N, Muñoz C, San Roman I, Zaggia S, Gilmore G, Randich S, Bensby T, Flaccomio E, Koposov SE, Korn AJ, Pancino E,

- Recio-Blanco A, Franciosini E, de Laverny P, Lewis J, Morbidelli L, Prisinzano L, Sacco G, Worley CC, Hourihane A, Jofré P, Lardo C, Maiorca E (2014) The Gaia-ESO Survey: Reevaluation of the parameters of the open cluster Trumpler 20 using photometry and spectroscopy. *A&A* 561:A94, DOI 10.1051/0004-6361/201322911, [1312.3925](#)
- D'Orazi V, Marino AF (2010) Lithium Abundances in Red Giants of M4: Evidence for Asymptotic Giant Branch Star Pollution in Globular Clusters? *ApJL* 716:L166–L169, DOI 10.1088/2041-8205/716/2/L166, [1005.3376](#)
- D'Orazi V, Gratton R, Lucatello S, Carretta E, Bragaglia A, Marino AF (2010a) Ba Stars and Other Binaries in First and Second Generation Stars in Globular Clusters. *ApJL* 719:L213–L217, DOI 10.1088/2041-8205/719/2/L213, [1007.2164](#)
- D'Orazi V, Lucatello S, Gratton R, Bragaglia A, Carretta E, Shen Z, Zaggia S (2010b) Lithium and Proton-capture Elements in Globular Cluster Dwarfs: The Case of 47 Tuc. *ApJL* 713:L1–L5, DOI 10.1088/2041-8205/713/1/L1, [1003.0013](#)
- D'Orazi V, Gratton RG, Pancino E, Bragaglia A, Carretta E, Lucatello S, Sneden C (2011) Chemical enrichment mechanisms in ω Centauri: clues from neutron-capture elements. *A&A* 534:A29, DOI 10.1051/0004-6361/201117630, [1108.5216](#)
- D'Orazi V, Campbell SW, Lugaro M, Lattanzio JC, Pignatari M, Carretta E (2013) On the internal pollution mechanisms in the globular cluster NGC 6121 (M4): heavy-element abundances and AGB models. *MNRAS* 433:366–381, DOI 10.1093/mnras/stt728, [1304.7009](#)
- D'Orazi V, Angelou GC, Gratton RG, Lattanzio JC, Bragaglia A, Carretta E, Lucatello S, Momany Y (2014) Lithium Abundances in Globular Cluster Giants: NGC 6218 (M12) and NGC 5904 (M5). *ApJ* 791:39, DOI 10.1088/0004-637X/791/1/39, [1406.5513](#)
- D'Orazi V, Gratton RG, Angelou GC, Bragaglia A, Carretta E, Lattanzio JC, Lucatello S, Momany Y, Sollima A, Beccari G (2015) Lithium abundances in globular cluster giants: NGC 1904, NGC 2808, and NGC 362. *MNRAS* 449:4038–4047, DOI 10.1093/mnras/stv612, [1503.05925](#)
- Dotter A, Sarajedini A, Anderson J, Aparicio A, Bedin LR, Chaboyer B, Majewski S, Marín-Franch A, Milone A, Paust N, Piotto G, Reid IN, Rosenberg A, Siegel M (2010) The ACS Survey of Galactic Globular Clusters. IX. Horizontal Branch Morphology and the Second Parameter Phenomenon. *ApJ* 708:698–716, DOI 10.1088/0004-637X/708/1/698, [0911.2469](#)
- Dotter A, Sarajedini A, Anderson J (2011) Globular Clusters in the Outer Galactic Halo: New Hubble Space Telescope/Advanced Camera for Surveys Imaging of Six Globular Clusters and the Galactic Globular Cluster Age-metallicity Relation. *ApJ* 738:74, DOI 10.1088/0004-637X/738/1/74, [1106.4307](#)
- Dotter A, Milone AP, Conroy C, Marino AF, Sarajedini A (2018) Ruprecht 106: A Riddle, Wrapped in a Mystery, inside an Enigma. *ApJL* 865:L10, DOI 10.3847/2041-8213/aae08f, [1808.05582](#)
- Drukier GA (1996) Retention fractions for globular cluster neutron stars. *MNRAS* 280:498–514, DOI 10.1093/mnras/280.2.498, [astro-ph/9512163](#)
- Duchêne G, Lacour S, Moraux E, Goodwin S, Bouvier J (2018) Is stellar multiplicity universal? Tight stellar binaries in the Orion nebula Cluster. *MNRAS* 478:1825–1836, DOI 10.1093/mnras/sty1180, [1805.00965](#)
- Dupree AK, Avrett EH (2013) Direct Evaluation of the Helium Abundances in Omega Centauri. *ApJL* 773:L28, DOI 10.1088/2041-8205/773/2/L28, [1307.5860](#)
- Dupree AK, Dotter A, Johnson CI, Marino AF, Milone AP, Bailey JI III, Crane JD, Mateo M, Olszewski EW (2017) NGC 1866: First Spectroscopic Detection of Fast-rotating Stars in a Young LMC Cluster. *ApJL* 846:L1, DOI 10.3847/2041-8213/aa85dd, [1708.03386](#)
- Elmegreen BG (2017) Globular Cluster Formation at High Density: A Model for Elemental Enrichment with Fast Recycling of Massive-star Debris. *ApJ* 836:80, DOI 10.3847/1538-4357/836/1/80, [1701.01034](#)
- Feltzing S, Primas F, Johnson RA (2009) Stellar abundances and ages for metal-rich Milky Way globular clusters. Stellar parameters and elemental abundances for 9 HB stars in NGC 6352. *A&A* 493:913–930, DOI 10.1051/0004-6361:200810137, [0810.4832](#)
- Fernández-Trincado JG, Robin AC, Moreno E, Schiavon RP, García Pérez AE, Vieira K, Cunha K, Zamora O, Sneden C, Souto D, Carrera R, Johnson JA, Shetrone M, Zasowski G, García-Hernández DA, Majewski SR, Reylé C, Blanco-Cuaresma S, Martínez-Medina LA, Pérez-Villegas A, Valenzuela O, Pichardo B, Meza A, Mészáros S, Sobek J, Geisler D, Anders F, Schultheis M, Tang B, Roman-Lopes A, Mennickent RE, Pan K, Nitschelm C, Allard F (2016) Discovery of a Metal-poor Field Giant with a Globular Cluster Second-generation Abundance Pattern. *ApJ* 833:132, DOI 10.3847/1538-4357/833/2/132, [1604.01279](#)

- Fernández-Trincado JG, Zamora O, García-Hernández DA, Souto D, Dell’Agli F, Schiavon RP, Geisler D, Tang B, Villanova S, Hasselquist S, Mennickent RE, Cunha K, Shetrone M, Allende Prieto C, Vieira K, Zasowski G, Sobek J, Hayes CR, Majewski SR, Placco VM, Beers TC, Schleicher DRG, Robin AC, Mészáros S, Masseron T, García Pérez AE, Anders F, Meza A, Alves-Brito A, Carrera R, Minniti D, Lane RR, Fernández-Alvar E, Moreno E, Pichardo B, Pérez-Villegas A, Schultheis M, Roman-Lopes A, Fuentes CE, Nitschelm C, Harding P, Bizyaev D, Pan K, Oravetz D, Simmons A, Ivans II, Blanco-Cuaresma S, Hernández J, Alonso-García J, Valenzuela O, Chanamé J (2017) Atypical Mg-poor Milky Way Field Stars with Globular Cluster Second-generation-like Chemical Patterns. *ApJL* 846:L2, DOI 10.3847/2041-8213/aa8032, [1707.03108](#)
- Ferrarese L, Côté P, Dalla Bontà E, Peng EW, Merritt D, Jordán A, Blakeslee JP, Hasegan M, Mei S, Piatek S, Tonry JL, West MJ (2006) A Fundamental Relation between Compact Stellar Nuclei, Supermassive Black Holes, and Their Host Galaxies. *ApJL* 644:L21–L24, DOI 10.1086/505388, [astro-ph/0603840](#)
- Ferraro FR, Mucciarelli A, Carretta E, Origlia L (2006a) On the Iron Content of NGC 1978 in the LMC: A Metal-rich, Chemically Homogeneous Cluster. *ApJL* 645:L33–L36, DOI 10.1086/506178, [astro-ph/0605646](#)
- Ferraro FR, Sabbi E, Gratton R, Piotto G, Lanzoni B, Carretta E, Rood RT, Sills A, Fusi Pecci F, Moehler S, Beccari G, Lucatello S, Compagni N (2006b) Discovery of Carbon/Oxygen-depleted Blue Straggler Stars in 47 Tucanae: The Chemical Signature of a Mass Transfer Formation Process. *ApJL* 647:L53–L56, DOI 10.1086/507327, [astro-ph/0610081](#)
- Forbes DA, Bridges T (2010) Accreted versus in situ Milky Way globular clusters. *MNRAS* 404:1203–1214, DOI 10.1111/j.1365-2966.2010.16373.x, [1001.4289](#)
- Forbes DA, Lasky P, Graham AW, Spitler L (2008) Uniting old stellar systems: from globular clusters to giant ellipticals. *MNRAS* 389:1924–1936, DOI 10.1111/j.1365-2966.2008.13739.x, [0806.1090](#)
- Fregeau JM, Rasio FA (2007) Monte Carlo Simulations of Globular Cluster Evolution. IV. Direct Integration of Strong Interactions. *ApJ* 658:1047–1061, DOI 10.1086/511809, [astro-ph/0608261](#)
- Fregeau JM, Ivanova N, Rasio FA (2009) Evolution of the Binary Fraction in Dense Stellar Systems. *ApJ* 707:1533–1540, DOI 10.1088/0004-637X/707/2/1533, [0907.4196](#)
- Freiburghaus C, Rosswog S, Thielemann FK (1999) R-Process in Neutron Star Mergers. *ApJL* 525:L121–L124, DOI 10.1086/312343
- Fu X, Bressan A, Molaro P, Marigo P (2015) Lithium evolution in metal-poor stars: from pre-main sequence to the Spite plateau. *MNRAS* 452:3256–3265, DOI 10.1093/mnras/stv1384, [1506.05993](#)
- Fusi Pecci F, Bellazzini M, Cacciari C, Ferraro FR (1995) The Young Globular Clusters of the Milky Way and the Local Group Galaxies: Playing with Great Circles. *AJ* 110:1664, DOI 10.1086/117639, [astro-ph/9507065](#)
- Gaia Collaboration, Helmi A, van Leeuwen F, McMillan PJ, Massari D, Antoja T, Robin AC, Lindegren L, Bastian U, Arenou F, et al (2018) Gaia Data Release 2. Kinematics of globular clusters and dwarf galaxies around the Milky Way. *A&A* 616:A12, DOI 10.1051/0004-6361/201832698, [1804.09381](#)
- García-Hernández DA, Mészáros S, Monelli M, Cassisi S, Stetson PB, Zamora O, Shetrone M, Lucatello S (2015) Clear Evidence for the Presence of Second-generation Asymptotic Giant Branch Stars in Metal-poor Galactic Globular Clusters. *ApJL* 815:L4, DOI 10.1088/2041-8205/815/1/L4, [1511.05714](#)
- Geisler D, Villanova S, Carraro G, Pilachowski C, Cummings J, Johnson CI, Bresolin F (2012) The Unique Na:O Abundance Distribution in NGC 6791: The First Open(?) Cluster with Multiple Populations. *ApJL* 756:L40, DOI 10.1088/2041-8205/756/2/L40, [1207.3328](#)
- Georgiev IY, Hilker M, Puzia TH, Goudfrooij P, Baumgardt H (2009) Globular cluster systems in nearby dwarf galaxies - II. Nuclear star clusters and their relation to massive Galactic globular clusters. *MNRAS* 396:1075–1085, DOI 10.1111/j.1365-2966.2009.14776.x, [0903.2857](#)
- Gieles M, Charbonnel C, Krause MGH, Hénault-Brunet V, Agertz O, Lamers HJGLM, Bastian N, Guilandris A, Zocchi A, Petts JA (2018) Concurrent formation of supermassive stars and globular clusters: implications for early self-enrichment. *MNRAS* 478:2461–2479, DOI 10.1093/mnras/sty1059, [1804.04682](#)
- Giersz M, Askar A, Wang L, Hypki A, Leveque A, Spurzem R (2019) MOCCA survey data base- I. Dissolution of tidally filling star clusters harbouring black hole subsystems. *MNRAS* 487(2):2412–2423, DOI 10.1093/mnras/stz1460, [1904.01227](#)
- Giesers B, Kamann S, Dreizler S, Husser TO, Askar A, Göttgens F, Brinchmann J, Latour M, Weibacher PM, Wendt M, Roth MM (2019) A stellar census in globular clusters with MUSE: Binaries in NGC 3201. arXiv e-prints arXiv:1909.04050, [1909.04050](#)

- Glatt K, Grebel EK, Sabbi E, Gallagher JS III, Nota A, Sirianni M, Clementini G, Tosi M, Harbeck D, Koch A, Kayser A, Da Costa G (2008) Age Determination of Six Intermediate-Age Small Magellanic Cloud Star Clusters with HST/ACS. *AJ* 136:1703–1727, DOI 10.1088/0004-6256/136/4/1703, [0807.3744](#)
- Glatt K, Grebel EK, Jordi K, Gallagher JS III, Da Costa G, Clementini G, Tosi M, Harbeck D, Nota A, Sabbi E, Sirianni M (2011) Present-day Mass Function of Six Small Magellanic Cloud Intermediate-age and Old Star Clusters. *AJ* 142:36, DOI 10.1088/0004-6256/142/2/36
- Goudfrooij P, Girardi L, Kozhurina-Platais V, Kalirai JS, Platais I, Puzia TH, Correnti M, Bressan A, Chandar R, Kerber L, Marigo P, Rubele S (2014) Extended Main Sequence Turnoffs in Intermediate-age Star Clusters: A Correlation between Turnoff Width and Early Escape Velocity. *ApJ* 797:35, DOI 10.1088/0004-637X/797/1/35, [1410.3840](#)
- Gratton R, Sneden C, Carretta E (2004) Abundance Variations Within Globular Clusters. *ARA&A* 42:385–440, DOI 10.1146/annurev.astro.42.053102.133945
- Gratton RG, Carretta E (2010) Diluting the material forming the second generation stars in globular clusters: the contribution by unevolved stars. *A&A* 521:A54, DOI 10.1051/0004-6361/201014997, [1007.4894](#)
- Gratton RG, Sneden C, Carretta E, Bragaglia A (2000) Mixing along the red giant branch in metal-poor field stars. *A&A* 354:169–187
- Gratton RG, Bonifacio P, Bragaglia A, Carretta E, Castellani V, Centurion M, Chieffi A, Claudi R, Clementini G, D’Antona F, Desidera S, François P, Grundahl F, Lucatello S, Molaro P, Pasquini L, Sneden C, Spite F, Straniero O (2001) The O-Na and Mg-Al anticorrelations in turn-off and early subgiants in globular clusters. *A&A* 369:87–98, DOI 10.1051/0004-6361:20010144, [astro-ph/0012457](#)
- Gratton RG, Lucatello S, Bragaglia A, Carretta E, Momany Y, Pancino E, Valenti E (2006) Na-O anticorrelation and HB. III. The abundances of NGC 6441 from FLAMES-UVES spectra. *A&A* 455:271–281, DOI 10.1051/0004-6361:20064957, [astro-ph/0603858](#)
- Gratton RG, Lucatello S, Bragaglia A, Carretta E, Cassisi S, Momany Y, Pancino E, Valenti E, Caloi V, Claudi R, D’Antona F, Desidera S, François P, James G, Moehler S, Ortolani S, Pasquini L, Piotto G, Recio-Blanco A (2007) Na-O anticorrelation and horizontal branches. V. The Na-O anticorrelation in NGC 6441 from Giraffe spectra. *A&A* 464:953–965, DOI 10.1051/0004-6361:20066061, [astro-ph/0701179](#)
- Gratton RG, Carretta E, Bragaglia A, Lucatello S, D’Orazi V (2010a) The second and third parameters of the horizontal branch in globular clusters. *A&A* 517:A81, DOI 10.1051/0004-6361/200912572, [1004.3862](#)
- Gratton RG, D’Orazi V, Bragaglia A, Carretta E, Lucatello S (2010b) The connection between missing AGB stars and extended horizontal branches. *A&A* 522:A77, DOI 10.1051/0004-6361/201015405, [1010.5913](#)
- Gratton RG, Johnson CI, Lucatello S, D’Orazi V, Pilachowski C (2011a) Multiple populations in ω Centauri: a cluster analysis of spectroscopic data. *A&A* 534:A72, DOI 10.1051/0004-6361/201117093, [1105.5544](#)
- Gratton RG, Lucatello S, Carretta E, Bragaglia A, D’Orazi V, Momany YA (2011b) The Na-O anticorrelation in horizontal branch stars. I. NGC 2808. *A&A* 534:A123, DOI 10.1051/0004-6361/201117690, [1109.4013](#)
- Gratton RG, Carretta E, Bragaglia A (2012a) Multiple populations in globular clusters. Lessons learned from the Milky Way globular clusters. *A&AR* 20:50, DOI 10.1007/s00159-012-0050-3, [1201.6526](#)
- Gratton RG, Lucatello S, Carretta E, Bragaglia A, D’Orazi V, Al Momany Y, Sollima A, Salaris M, Cassisi S (2012b) The Na-O anticorrelation in horizontal branch stars. II. NGC 1851. *A&A* 539:A19, DOI 10.1051/0004-6361/201118491, [1201.1772](#)
- Gratton RG, Villanova S, Lucatello S, Sollima A, Geisler D, Carretta E, Cassisi S, Bragaglia A (2012c) Spectroscopic analysis of the two subgiant branches of the globular cluster NGC 1851. *A&A* 544:A12, DOI 10.1051/0004-6361/201219276, [1205.5719](#)
- Gratton RG, Lucatello S, Sollima A, Carretta E, Bragaglia A, Momany Y, D’Orazi V, Cassisi S, Pietrinferri A, Salaris M (2013) The Na-O anticorrelation in horizontal branch stars. III. 47 Tucanae and M 5. *A&A* 549:A41, DOI 10.1051/0004-6361/201219976, [1210.4069](#)
- Gratton RG, Lucatello S, Sollima A, Carretta E, Bragaglia A, Momany Y, D’Orazi V, Cassisi S, Salaris M (2014) The Na-O anticorrelation in horizontal branch stars. IV. M 22. *A&A* 563:A13, DOI 10.1051/0004-6361/201323101, [1401.7109](#)
- Gratton RG, Lucatello S, Sollima A, Carretta E, Bragaglia A, Momany Y, D’Orazi V, Salaris M, Cassisi S, Stetson PB (2015) The Na-O anticorrelation in horizontal branch stars. V. NGC 6723. *A&A* 573:A92, DOI 10.1051/0004-6361/201424393, [1410.8378](#)

- Grabel EK (2016) Globular Clusters in the Local Group. In: Meiron Y, Li S, Liu FK, Spurzem R (eds) *Star Clusters and Black Holes in Galaxies across Cosmic Time*, IAU Symposium, vol 312, pp 157–170, DOI 10.1017/S1743921315008078
- Greggio L, Renzini A (1990) Clues on the hot star content and the ultraviolet output of elliptical galaxies. *ApJ* 364:35–64, DOI 10.1086/169384
- Griffen BF, Drinkwater MJ, Thomas PA, Helly JC, Pimblet KA (2010) Globular cluster formation within the Aquarius simulation. *MNRAS* 405(1):375–386, DOI 10.1111/j.1365-2966.2010.16458.x, [0910.0310](#)
- Grillmair CJ (2009) Four New Stellar Debris Streams in the Galactic Halo. *ApJ* 693:1118–1127, DOI 10.1088/0004-637X/693/2/1118, [0811.3965](#)
- Grillmair CJ, Dionatos O (2006) Detection of a 63 deg Cold Stellar Stream in the Sloan Digital Sky Survey. *ApJL* 643:L17–L20, DOI 10.1086/505111, [astro-ph/0604332](#)
- Grundahl F, VandenBerg DA, Andersen MI (1998) Strömgren Photometry of Globular Clusters: The Distance and Age of M13, Evidence for Two Populations of Horizontal-Branch Stars. *ApJL* 500:L179–L182, DOI 10.1086/311419, [astro-ph/9806081](#)
- Grundahl F, Catelan M, Landsman WB, Stetson PB, Andersen MI (1999) Hot Horizontal-Branch Stars: The Ubiquitous Nature of the “Jump” in Strömgren u, Low Gravities, and the Role of Radiative Levitation of Metals. *ApJ* 524:242–261, DOI 10.1086/307807, [astro-ph/9903120](#)
- Gruyters P, Nordlander T, Korn AJ (2014) Atomic diffusion and mixing in old stars. V. A deeper look into the globular cluster NGC 6752. *A&A* 567:A72, DOI 10.1051/0004-6361/201423590, [1405.6543](#)
- Gruyters P, Lind K, Richard O, Grundahl F, Asplund M, Casagrande L, Charbonnel C, Milone A, Primas F, Korn AJ (2016) Atomic diffusion and mixing in old stars. VI. The lithium content of M30. *A&A* 589:A61, DOI 10.1051/0004-6361/201527948, [1603.01565](#)
- Harbeck D, Smith GH, Grabel EK (2003) CN Abundance Variations on the Main Sequence of 47 Tucanae. *AJ* 125:197–207, DOI 10.1086/345570, [astro-ph/0210364](#)
- Harris WE (1996) A Catalog of Parameters for Globular Clusters in the Milky Way. *AJ* 112:1487, DOI 10.1086/118116
- Hatzidimitriou D, Held EV, Tognelli E, Bragaglia A, Magrini L, Bravi L, Gazeas K, Dapergolas A, Drazdauskas A, Delgado-Mena E, Friel ED, Minkeviciute R, Sordo R, Tautvaisiene G, Gilmore G, Randich S, Feltzing S, Vallenari A, Alfaro EJ, Flaccomio E, Lanzafame AC, Pancino E, Smiljanic R, Bayo A, Bergemann M, Carraro G, Casey AR, Costado MT, Damiani F, Franciosini E, Gonneau A, Jofré P, Lewis J, Monaco L, Morbidelli L, Worley CC, Zaggia S (2019) The Gaia-ESO Survey: The inner disc, intermediate-age open cluster Pismis 18. *A&A* 626:A90, DOI 10.1051/0004-6361/201834636, [1906.09828](#)
- Haywood M, Di Matteo P, Lehnert MD, Snaith O, Khoperskov S, Gómez A (2018) In Disguise or Out of Reach: First Clues about In Situ and Accreted Stars in the Stellar Halo of the Milky Way from Gaia DR2. *ApJ* 863:113, DOI 10.3847/1538-4357/aad235, [1805.02617](#)
- Heggie D, Hut P (2003) *The Gravitational Million-Body Problem: A Multidisciplinary Approach to Star Cluster Dynamics*. Cambridge University Press, Cambridge, UK
- Heggie DC (1975) Binary evolution in stellar dynamics. *MNRAS* 173:729–787, DOI 10.1093/mnras/173.3.729
- Helmi A, Babusiaux C, Koppelman HH, Massari D, Veljanoski J, Brown AGA (2018) The merger that led to the formation of the Milky Way’s inner stellar halo and thick disk. *Nature* 563:85–88, DOI 10.1038/s41586-018-0625-x, [1806.06038](#)
- Hénault-Brunet V, Gieles M, Agertz O, Read JI (2015) Multiple populations in globular clusters: the distinct kinematic imprints of different formation scenarios. *MNRAS* 450:1164–1198, DOI 10.1093/mnras/stv675, [1503.07532](#)
- Henon M (1970) Numerical exploration of the restricted problem. VI. Hill’s case: Non-periodic orbits. *A&A* 9:24–36
- Hénon MH (1971) *The Monte Carlo Method* (Papers appear in the Proceedings of IAU Colloquium No. 10 Gravitational N-Body Problem (ed. by Myron Lecar), R. Reidel Publ. Co., Dordrecht-Holland.). *ApSS* 14:151–167, DOI 10.1007/BF00649201
- Herschel W (1814) *Astronomical Observations Relating to the Sidereal Part of the Heavens, and Its Connection with the Nebulous Part; Arranged for the Purpose of a Critical Examination*. Philosophical Transactions of the Royal Society of London Series I 104:248–284
- Hollyhead K, Bastian N, Adamo A, Silva-Villa E, Dale J, Ryon JE, Gazak Z (2015) Studying the YMC population of M83: how long clusters remain embedded, their interaction with the ISM and implications for GC formation theories. *MNRAS* 449:1106–1117, DOI 10.1093/mnras/stv331, [1502.03823](#)

- Hollyhead K, Kacharov N, Lardo C, Bastian N, Hilker M, Rejkuba M, Koch A, Grebel EK, Georgiev I (2017) Evidence for multiple populations in the intermediate-age cluster Lindsay 1 in the SMC. *MNRAS* 465:L39–L43, DOI 10.1093/mnras/slw179, [1609.01302](#)
- Hollyhead K, Lardo C, Kacharov N, Bastian N, Hilker M, Rejkuba M, Koch A, Grebel EK, Georgiev I (2018) Kron 3: a fourth intermediate age cluster in the SMC with evidence of multiple populations. *MNRAS* 476:114–121, DOI 10.1093/mnras/sty230, [1801.09670](#)
- Hollyhead K, Martocchia S, Lardo C, Bastian N, Kacharov N, Niederhofer F, Cabrera-Ziri I, Dalessandro E, Mucciarelli A, Salaris M, Usher C (2019) Spectroscopic detection of multiple populations in the ~2 Gyr old cluster Hodge 6 in the LMC. *arXiv e-prints* [1902.02297](#)
- Hong J, Vesperini E, Sollima A, McMillan SLW, D’Antona F, D’Ercole A (2015) Evolution of binary stars in multiple-population globular clusters. *MNRAS* 449:629–638, DOI 10.1093/mnras/stv306, [1503.02087](#)
- Hong J, Vesperini E, Sollima A, McMillan SLW, D’Antona F, D’Ercole A (2016) Evolution of binary stars in multiple-population globular clusters - II. Compact binaries. *MNRAS* 457:4507–4514, DOI 10.1093/mnras/stw262, [1604.01045](#)
- Hong J, Patel S, Vesperini E, Webb JJ, Dalessandro E (2019) Spatial mixing of binary stars in multiple-population globular clusters. *MNRAS* 483:2592–2599, DOI 10.1093/mnras/sty3308, [1812.01229](#)
- Hosek MW Jr, Lu JR, Anderson J, Najarro F, Ghez AM, Morris MR, Clarkson WI, Albers SM (2019) The Unusual Initial Mass Function of the Arches Cluster. *ApJ* 870:44, DOI 10.3847/1538-4357/aef90, [1808.02577](#)
- Huang Y, Liu X, Chen B, Zhang H, Yuan H, Xiang M, Wang C, Tian Z (2018) Member stars of the GD1 tidal stream from the SDSS, LAMOST and Gaia surveys. *arXiv e-prints* [1806.03748](#)
- Hurley JR, Aarseth SJ, Shara MM (2007) The Core Binary Fractions of Star Clusters from Realistic Simulations. *ApJ* 665:707–718, DOI 10.1086/517879, [0704.0290](#)
- Hut P, Bahcall JN (1983) Binary-single star scattering. I - Numerical experiments for equal masses. *ApJ* 268:319–341, DOI 10.1086/160956
- Ibata R, Bellazzini M, Malhan K, Martin N, Bianchini P (2019) Identification of the Long Stellar Stream of the Prototypical Massive Globular Cluster ω Centauri. *arXiv e-prints* [1902.09544](#)
- Ibata RA, Gilmore G, Irwin MJ (1994) A dwarf satellite galaxy in Sagittarius. *Nature* 370:194–196, DOI 10.1038/370194a0
- Iben I, Rood RT, Strom KM, Strom SE (1969) Ratio of Horizontal Branch Stars to Red Giant Stars in Globular Clusters. *Nature* 224(5223):1006–1008, DOI 10.1038/2241006a0
- Iben I Jr (1964) Evolution through Alpha-Burning ($M = 3 \rightarrow 15M_{\odot}$). *AJ* 69:545, DOI 10.1086/109317
- Iorio G, Belokurov V (2019) The shape of the Galactic halo with Gaia DR2 RR Lyrae. Anatomy of an ancient major merger. *MNRAS* 482:3868–3879, DOI 10.1093/mnras/sty2806, [1808.04370](#)
- Ivanova N, Belczynski K, Fregeau JM, Rasio FA (2005) The evolution of binary fractions in globular clusters. *MNRAS* 358:572–584, DOI 10.1111/j.1365-2966.2005.08804.x, [astro-ph/0501131](#)
- Ivans II, Sneden C, Kraft RP, Suntzeff NB, Smith VV, Langer GE, Fulbright JP (1999) Star-to-Star Abundance Variations among Bright Giants in the Mildly Metal-poor Globular Cluster M4. *AJ* 118:1273–1300, DOI 10.1086/301017, [astro-ph/9905370](#)
- James G, François P, Bonifacio P, Carretta E, Gratton RG, Spite F (2004) Heavy elements and chemical enrichment in globular clusters. *A&A* 427:825–838, DOI 10.1051/0004-6361:20041512, [astro-ph/0408330](#)
- Jang S, Lee YW, Joo SJ, Na C (2014) Multiple populations in globular clusters and the origin of the Oosterhoff period groups. *MNRAS* 443:L15–L19, DOI 10.1093/mnras/slu064, [1404.7508](#)
- Johnson CI, Pilachowski CA (2010) Chemical Abundances for 855 Giants in the Globular Cluster Omega Centauri (NGC 5139). *ApJ* 722:1373–1410, DOI 10.1088/0004-637X/722/2/1373, [1008.2232](#)
- Johnson CI, Rich RM, Pilachowski CA, Caldwell N, Mateo M, Bailey JI III, Crane JD (2015) A Spectroscopic Analysis of the Galactic Globular Cluster NGC 6273 (M19). *AJ* 150:63, DOI 10.1088/0004-6256/150/2/63, [1507.00756](#)
- Johnson CI, Caldwell N, Rich RM, Pilachowski CA, Hsyu T (2016) The Chemical Composition of Red Giant Branch Stars in the Galactic Globular Clusters NGC 6342 and NGC 6366. *AJ* 152:21, DOI 10.3847/0004-6256/152/1/21, [1606.08491](#)
- Johnson CI, Caldwell N, Rich RM, Mateo M, Bailey JI III, Clarkson WI, Olszewski EW, Walker MG (2017a) A Chemical Composition Survey of the Iron-complex Globular Cluster NGC 6273 (M19). *ApJ* 836:168, DOI 10.3847/1538-4357/836/2/168, [1611.05830](#)
- Johnson CI, Caldwell N, Rich RM, Mateo M, Bailey JI III, Olszewski EW, Walker MG (2017b) Chemical Complexity in the Eu-enhanced Monometallic Globular NGC 5986. *ApJ* 842:24, DOI

- 10.3847/1538-4357/aa7414, [1705.10840](#)
- Johnson CI, Rich RM, Caldwell N, Mateo M, Bailey JI III, Olszewski EW, Walker MG (2018) Exploring the Chemical Composition and Double Horizontal Branch of the Bulge Globular Cluster NGC 6569. *AJ* 155:71, DOI 10.3847/1538-3881/aaa294, [1801.10475](#)
- Johnson CI, Caldwell N, Rich RM, Mateo M, Bailey JI (2019) Light Element Discontinuities Suggest an Early Termination of Star Formation in the Globular Cluster NGC 6402 (M14). *MNRAS* DOI 10.1093/mnras/stz587, [1903.01951](#)
- Johnson JA, Ivans II, Stetson PB (2006) Chemical Compositions of Red Giant Stars in Old Large Magellanic Cloud Globular Clusters. *ApJ* 640:801–822, DOI 10.1086/498882, [astro-ph/0512132](#)
- Kacharov N, Koch A, McWilliam A (2013) A comprehensive chemical abundance study of the outer halo globular cluster M 75. *A&A* 554:A81, DOI 10.1051/0004-6361/201321392, [1304.4247](#)
- Käppeler F (1999) The origin of the heavy elements: the s process. *Prog Part Nucl Phys* (UK), Vol 43, p 419 - 483 43:419–483
- Karakas AI, Lattanzio JC (2003) Production of Aluminium and the Heavy Magnesium Isotopes in Asymptotic Giant Branch Stars. *PASA* 20:279–293, DOI 10.1071/AS03010
- Karakas AI, Lattanzio JC (2014) The Dawes Review 2: Nucleosynthesis and Stellar Yields of Low- and Intermediate-Mass Single Stars. *PASA* 31:e030, DOI 10.1017/pasa.2014.21, [1405.0062](#)
- Keenan DW, Innanen KA (1975) Numerical investigation of galactic tidal effects on spherical stellar systems. *AJ* 80:290–302, DOI 10.1086/111744
- Kim HS, Cho J, Sharples RM, Vazdekis A, Beasley MA, Yoon SJ (2016) A New Catalog of Homogenized Absorption Line Indices for Milky Way Globular Clusters from High-resolution Integrated Spectroscopy. *ApJS* 227:24, DOI 10.3847/1538-4365/227/2/24, [1610.08061](#)
- King CR, Da Costa GS, Demarque P (1985) The luminosity function on the subgiant branch of 47 Tucanae. A comparison of observation and theory. *ApJ* 299:674–682, DOI 10.1086/163733
- King IR (1966) The structure of star clusters. III. Some simple dynamical models. *AJ* 71:64, DOI 10.1086/109857
- Koch A, McWilliam A (2014) The chemical composition of a regular halo globular cluster: NGC 5897. *A&A* 565:A23, DOI 10.1051/0004-6361/201323119, [1403.1262](#)
- Koch A, Grebel EK, Martell SL (2019) Purveyors of fine halos: Re-assessing globular cluster contributions to the Milky Way halo buildup with SDSS-IV. *A&A* 625:A75, DOI 10.1051/0004-6361/201834825, [1904.02146](#)
- Koposov SE, Rix HW, Hogg DW (2010) Constraining the Milky Way Potential with a Six-Dimensional Phase-Space Map of the GD-1 Stellar Stream. *ApJ* 712:260–273, DOI 10.1088/0004-637X/712/1/260, [0907.1085](#)
- Koposov SE, Belokurov V, Torrealba G (2017) Gaia 1 and 2. A pair of new Galactic star clusters. *MNRAS* 470:2702–2709, DOI 10.1093/mnras/stx1182, [1702.01122](#)
- Kraft RP (1979) On the nonhomogeneity of metal abundances in stars of globular clusters and satellite subsystems of the Galaxy. *ARA&A* 17:309–343, DOI 10.1146/annurev.aa.17.090179.001521
- Kraft RP (1994) Abundance differences among globular-cluster giants: Primordial versus evolutionary scenarios. *PASP* 106:553–565, DOI 10.1086/133416
- Kraft RP, Sneden C, Langer GE, Prosser CF (1992) Oxygen abundances in halo giants. II - Giants in the globular clusters M13 and M3 and the intermediately metal-poor halo field. *AJ* 104:645–668, DOI 10.1086/116261
- Kraft RP, Sneden C, Smith GH, Shetrone MD, Fulbright J (1998) Proton Capture Chains in Globular Cluster Stars. III. Abundances of Giants in the Second-Parameter Globular Cluster NGC 7006. *AJ* 115:1500–1515, DOI 10.1086/300279
- Krause M, Charbonnel C, Decressin T, Meynet G, Prantzos N (2013) Superbubble dynamics in globular cluster infancy. II. Consequences for secondary star formation in the context of self-enrichment via fast-rotating massive stars. *A&A* 552:A121, DOI 10.1051/0004-6361/201220694, [1302.2494](#)
- Krause MGH, Charbonnel C, Bastian N, Diehl R (2016) Gas expulsion in massive star clusters?. Constraints from observations of young and gas-free objects. *A&A* 587:A53, DOI 10.1051/0004-6361/201526685, [1512.04256](#)
- Kroupa P (2002) The Initial Mass Function of Stars: Evidence for Uniformity in Variable Systems. *Science* 295:82–91, DOI 10.1126/science.1067524, [astro-ph/0201098](#)
- Kruijssen JMD (2014) Globular cluster formation in the context of galaxy formation and evolution. *Classical and Quantum Gravity* 31(24):244006, DOI 10.1088/0264-9381/31/24/244006, [1407.2953](#)
- Kruijssen JMD (2015) Globular clusters as the relics of regular star formation in ‘normal’ high-redshift galaxies. *MNRAS* 454:1658–1686, DOI 10.1093/mnras/stv2026, [1509.02163](#)

- Kuzma PB, Da Costa GS, Mackey AD, Roderick TA (2016) The outer envelopes of globular clusters - I. NGC 7089 (M2). *MNRAS* 461:3639–3652, DOI 10.1093/mnras/stw1561, [1606.05949](#)
- Kuzma PB, Da Costa GS, Mackey AD (2018) The outer envelopes of globular clusters. II. NGC 1851, NGC 5824 and NGC 1261. *MNRAS* 473:2881–2898, DOI 10.1093/mnras/stx2353, [1709.02915](#)
- Lada CJ, Lada EA (2003) Embedded Clusters in Molecular Clouds. *ARA&A* 41:57–115, DOI 10.1146/annurev.astro.41.011802.094844, [astro-ph/0301540](#)
- Lagioia EP, Milone AP, Marino AF, Cassisi S, Aparicio AJ, Piotto G, Anderson J, Barbuy B, Bedin LR, Bellini A, Brown T, D’Antona F, Nardiello D, Ortolani S, Pietrinferni A, Renzini A, Salaris M, Sarajedini A, van der Marel R, Vesperini E (2018) The Hubble Space Telescope UV Legacy Survey of Galactic Globular Clusters - XII. The RGB bumps of multiple stellar populations. *MNRAS* 475:4088–4103, DOI 10.1093/mnras/sty083, [1801.03395](#)
- Lamers HJGLM, Baumgardt H, Gieles M (2010) Mass-loss rates and the mass evolution of star clusters. *MNRAS* 409:305–328, DOI 10.1111/j.1365-2966.2010.17309.x, [1007.1078](#)
- Langer GE, Hoffman R, Sneden C (1993) Sodium-oxygen abundance anticorrelations and deep-mixing scenarios for globular-cluster giants. *PASP* 105:301–307, DOI 10.1086/133147
- Lapenna E, Mucciarelli A, Ferraro FR, Origlia L, Lanzoni B, Massari D, Dalessandro E (2015) Chemical Analysis of Asymptotic Giant Branch Stars in M62. *ApJ* 813:97, DOI 10.1088/0004-637X/813/2/97, [1509.08917](#)
- Lapenna E, Lardo C, Mucciarelli A, Salaris M, Ferraro FR, Lanzoni B, Massari D, Stetson PB, Cassisi S, Savino A (2016) Lost and Found: Evidence of Second-generation Stars Along the Asymptotic Giant Branch of the Globular Cluster NGC 6752. *ApJL* 826:L1, DOI 10.3847/2041-8205/826/1/L1, [1606.09256](#)
- Lardo C, Bellazzini M, Pancino E, Carretta E, Bragaglia A, Dalessandro E (2011) Mining SDSS in search of multiple populations in globular clusters. *A&A* 525:A114, DOI 10.1051/0004-6361/201015662, [1010.4697](#)
- Lardo C, Milone AP, Marino AF, Mucciarelli A, Pancino E, Zoccali M, Rejkuba M, Carrera R, Gonzalez O (2012) C and N abundances of main sequence and subgiant branch stars in NGC 1851. *A&A* 541:A141, DOI 10.1051/0004-6361/201118763, [1202.6176](#)
- Lardo C, Davies B, Kudritzki RP, Gazak JZ, Evans CJ, Patrick LR, Bergemann M, Plez B (2015) Red Supergiants as Cosmic Abundance Probes: The First Direct Metallicity Determination of NGC 4038 in the Antennae. *ApJ* 812:160, DOI 10.1088/0004-637X/812/2/160, [1509.04937](#)
- Lardo C, Mucciarelli A, Bastian N (2016) The iron dispersion of the globular cluster M2, revised. *MNRAS* 457:51–63, DOI 10.1093/mnras/stv2802, [1512.00691](#)
- Lardo C, Cabrera-Ziri I, Davies B, Bastian N (2017a) Searching for globular cluster-like abundance patterns in young massive clusters - II. Results from the Antennae galaxies. *MNRAS* 468:2482–2488, DOI 10.1093/mnras/stx628, [1703.04591](#)
- Lardo C, Salaris M, Savino A, Donati P, Stetson PB, Cassisi S (2017b) Multiple populations along the asymptotic giant branch of the globular cluster M4. *MNRAS* 466:3507–3512, DOI 10.1093/mnras/stw3374, [1612.08929](#)
- Larsen SS, Brodie JP, Grundahl F, Strader J (2014) Nitrogen Abundances and Multiple Stellar Populations in the Globular Clusters of the Fornax dSph. *ApJ* 797:15, DOI 10.1088/0004-637X/797/1/15, [1409.0541](#)
- Larsen SS, Baumgardt H, Bastian N, Brodie JP, Grundahl F, Strader J (2015) Radial Distributions of Sub-Populations in the Globular Cluster M15: A More Centrally Concentrated Primordial Population. *ApJ* 804:71, DOI 10.1088/0004-637X/804/1/71, [1503.00726](#)
- Larsen SS, Baumgardt H, Bastian N, Hernandez S, Brodie JP (2019) Hubble Space Telescope photometry of multiple stellar populations in the inner parts of NGC 2419. *arXiv e-prints* [1902.01416](#)
- Lattanzio J, Forestini M, Charbonnel C (2000) Nucleosynthesis in intermediate mass AGB stars. *MSAIt* 71:737–744, [astro-ph/9912298](#)
- Lee JW (2015) Multiple Stellar Populations of Globular Clusters from Homogeneous Ca by Photometry. I. M22 (NGC 6656). *ApJS* 219:7, DOI 10.1088/0067-0049/219/1/7, [1506.00116](#)
- Lee JW (2017) Multiple Stellar Populations of Globular Clusters from Homogeneous Ca-CN Photometry. II. M5 (NGC 5904) and a New Filter System. *ApJ* 844:77, DOI 10.3847/1538-4357/aa7b8c, [1706.07969](#)
- Lee JW (2018) Multiple Stellar Populations of Globular Clusters from Homogeneous Ca-CN Photometry. III. NGC 6752. *ApJS* 238:24, DOI 10.3847/1538-4365/aadcad, [1901.10107](#)
- Lee JW (2019) Multiple stellar populations of globular clusters from homogeneous Ca-CN photometry. IV. Toward precision populational tagging. *arXiv e-prints* [1901.09584](#)

- Lee JW, Kang YW, Lee J, Lee YW (2009a) Enrichment by supernovae in globular clusters with multiple populations. *Nature* 462:480–482, DOI 10.1038/nature08565, [0911.4798](#)
- Lee JW, Lee J, Kang YW, Lee YW, Han SI, Joo SJ, Rey SC, Yong D (2009b) Chemical Inhomogeneity in Red Giant Branch Stars and RR Lyrae variables in NGC 1851: Two Subpopulations in Red Giant Branch. *ApJL* 695:L78–L82, DOI 10.1088/0004-637X/695/1/L78
- Leigh N, Giersz M, Webb JJ, Hypki A, De Marchi G, Kroupa P, Sills A (2013) The state of globular clusters at birth: emergence from the gas-embedded phase. *MNRAS* 436:3399–3412, DOI 10.1093/mnras/stt1825, [1309.7054](#)
- Letarte B, Hill V, Jablonka P, Tolstoy E, François P, Meylan G (2006) VLT/UVES spectroscopy of individual stars in three globular clusters in the Fornax dwarf spheroidal galaxy. *A&A* 453:547–554, DOI 10.1051/0004-6361:20054439, [astro-ph/0603315](#)
- Li H, Gnedin OY (2019) Star cluster formation in cosmological simulations - III. Dynamical and chemical evolution. *MNRAS* 486(3):4030–4043, DOI 10.1093/mnras/stz1114, [1810.11036](#)
- Libralato M, Bellini A, van der Marel RP, Anderson J, Watkins LL, Piotto G, Ferraro FR, Nardiello D, Vesperini E (2018) Hubble Space Telescope Proper Motion (HSTPROMO) Catalogs of Galactic Globular Cluster. VI. Improved Data Reduction and Internal-kinematic Analysis of NGC 362. *ApJ* 861:99, DOI 10.3847/1538-4357/aac6c0, [1805.05332](#)
- Lim B, Rauw G, Nazé Y, Sung H, Hwang N, Park BG (2019) Extended main sequence turn-off originating from a broad range of stellar rotational velocities. *Nature Astronomy* 3:76–81, DOI 10.1038/s41550-018-0619-5, [1811.01593](#)
- Lim D, Han SI, Lee YW, Roh DG, Sohn YJ, Chun SH, Lee JW, Johnson CI (2015) Low-resolution Spectroscopy for the Globular Clusters with Signs of Supernova Enrichment: M22, NGC 1851, and NGC 288. *ApJS* 216:19, DOI 10.1088/0067-0049/216/1/19, [1412.1832](#)
- Lin DNC, Richer HB (1992) Young globular clusters in the Milky Way Galaxy. *ApJL* 388:L57–L60, DOI 10.1086/186329
- Lind K, Primas F, Charbonnel C, Grundahl F, Asplund M (2009) Signatures of intrinsic Li depletion and Li-Na anti-correlation in the metal-poor globular cluster NGC 6397. *A&A* 503:545–557, DOI 10.1051/0004-6361/200912524, [0906.2876](#)
- Lind K, Koposov SE, Battistini C, Marino AF, Ruchti G, Serenelli A, Worley CC, Alves-Brito A, Asplund M, Barklem PS, Bensby T, Bergemann M, Blanco-Cuaresma S, Bragaglia A, Edvardsson B, Feltzing S, Gruyters P, Heiter U, Jofre P, Korn AJ, Nordlander T, Ryde N, Soubiran C, Gilmore G, Randich S, Ferguson AMN, Jeffries RD, Vallenari A, Allende Prieto C, Pancino E, Recio-Blanco A, Romano D, Smiljanic R, Bellazzini M, Damiani F, Hill V, de Laverny P, Jackson RJ, Lardo C, Zaggia S (2015) The Gaia-ESO Survey: A globular cluster escapee in the Galactic halo. *A&A* 575:L12, DOI 10.1051/0004-6361/201425554, [1502.03934](#)
- Lindblad B (1922) Spectrophotometric methods for determining stellar luminosity. *ApJ* 55, DOI 10.1086/142660
- Lombardi JC Jr, Rasio FA, Shapiro SL (1995) On blue straggler formation by direct collisions of main sequence stars. *ApJL* 445:L117–L120, DOI 10.1086/187903, [astro-ph/9502106](#)
- Longmore SN (2015) Heart of darkness: dust obscuration of the central stellar component in globular clusters younger than ~100 Myr in multiple stellar population models. *MNRAS* 448:L62–L66, DOI 10.1093/mnras/slu203, [1501.01216](#)
- Lucatello S, Sollima A, Gratton R, Vesperini E, D’Orazi V, Carretta E, Bragaglia A (2015) The incidence of binaries in globular cluster stellar populations. *A&A* 584:A52, DOI 10.1051/0004-6361/201526957, [1509.05014](#)
- Luck RE, Bond HE (1991) Subgiant CH stars. II - Chemical compositions and the evolutionary connection with barium stars. *ApJS* 77:515–540, DOI 10.1086/191615
- Lynden-Bell D (1967) Statistical mechanics of violent relaxation in stellar systems. *MNRAS* 136:101, DOI 10.1093/mnras/136.1.101
- Lynden-Bell D, Wood R (1968) The gravo-thermal catastrophe in isothermal spheres and the onset of red-giant structure for stellar systems. *MNRAS* 138:495, DOI 10.1093/mnras/138.4.495
- Mackereth JT, Schiavon RP, Pfeffer J, Hayes CR, Bovy J, Anguiano B, Allende Prieto C, Hesselquist S, Holtzman J, Johnson JA, Majewski SR, O’Connell R, Shetrone M, Tissera PB, Fernández-Trincado JG (2019) The origin of accreted stellar halo populations in the Milky Way using APOGEE, Gaia, and the EAGLE simulations. *MNRAS* 482:3426–3442, DOI 10.1093/mnras/sty2955, [1808.00968](#)
- Mackey AD, Gilmore GF (2003a) Surface brightness profiles and structural parameters for 53 rich stellar clusters in the Large Magellanic Cloud. *MNRAS* 338:85–119, DOI 10.1046/j.1365-8711.2003.06021.x, [astro-ph/0209031](#)

- Mackey AD, Gilmore GF (2003b) Surface brightness profiles and structural parameters for globular clusters in the Fornax and Sagittarius dwarf spheroidal galaxies. *MNRAS* 340:175–190, DOI 10.1046/j.1365-8711.2003.06275.x, [astro-ph/0211396](#)
- MacLean BT, De Silva GM, Lattanzio J (2015) O, Na, Ba and Eu abundance patterns in open clusters. *MNRAS* 446:3556–3561, DOI 10.1093/mnras/stu2348, [1411.1185](#)
- MacLean BT, Campbell SW, De Silva GM, Lattanzio J, D’Orazi V, Simpson JD, Momany Y (2016) An extreme paucity of second population AGB stars in the ‘normal’ globular cluster M4. *MNRAS* 460(1):L69–L73, DOI 10.1093/mnras/slw073, [1604.05040](#)
- MacLean BT, Campbell SW, Amarsi AM, Nordlander T, Cottrell PL, De Silva GM, Lattanzio J, Constantino T, D’Orazi V, Casagrande L (2018a) On the AGB stars of M 4: a robust disagreement between spectroscopic observations and theory. *MNRAS* 481:373–395, DOI 10.1093/mnras/sty2297, [1808.06735](#)
- MacLean BT, Campbell SW, De Silva GM, Lattanzio J, D’Orazi V, Cottrell PL, Momany Y, Casagrande L (2018b) AGB subpopulations in the nearby globular cluster NGC 6397. *MNRAS* 475:257–265, DOI 10.1093/mnras/stx3217, [1712.03340](#)
- Magrini L, Randich S, Donati P, Bragaglia A, Adibekyan V, Romano D, Smiljanic R, Blanco-Cualesma S, Tautvaisiene G, Friel E, Overbeek J, Jacobson H, Cantat-Gaudin T, Vallenari A, Sordo R, Pancino E, Geisler D, San Roman I, Villanova S, Casey A, Hourihane A, Worley CC, Francois P, Gilmore G, Bensby T, Flaccomio E, Korn AJ, Recio-Blanco A, Carraro G, Costado MT, Franciosini E, Heiter U, Jofré P, Lardo C, de Laverny P, Monaco L, Morbidelli L, Sacco G, Sousa SG, Zaggia S (2015) The Gaia-ESO Survey: Insights into the inner-disc evolution from open clusters. *A&A* 580:A85, DOI 10.1051/0004-6361/201526305, [1505.04039](#)
- Majewski SR, Schiavon RP, Frinchaboy PM, Allende Prieto C, Barkhouser R, Bizyaev D, Blank B, Brunner S, Burton A, Carrera R, Chojnowski SD, Cunha K, Epstein C, Fitzgerald G, García Pérez AE, Hearty FR, Henderson C, Holtzman JA, Johnson JA, Lam CR, Lawler JE, Maseman P, Mészáros S, Nelson M, Nguyen DC, Nidever DL, Pinsonneault M, Shetrone M, Smee S, Smith VV, Stolberg T, Skrutskie MF, Walker E, Wilson JC, Zasowski G, Anders F, Basu S, Beland S, Blanton MR, Bovy J, Brownstein JR, Carlberg J, Chaplin W, Chiappini C, Eisenstein DJ, Elsworth Y, Feuillet D, Fleming SW, Galbraith-Frew J, García RA, García-Hernández DA, Gillespie BA, Girardi L, Gunn JE, Hasselquist S, Hayden MR, Hekker S, Ivans I, Kinemuchi K, Klaene M, Mahadevan S, Mathur S, Mosser B, Muna D, Munn JA, Nichol RC, O’Connell RW, Parejko JK, Robin AC, Rocha-Pinto H, Schultheis M, Serenelli AM, Shane N, Silva Aguirre V, Sobeck JS, Thompson B, Troup NW, Weinberg DH, Zamora O (2017) The Apache Point Observatory Galactic Evolution Experiment (APOGEE). *AJ* 154:94, DOI 10.3847/1538-3881/aa784d, [1509.05420](#)
- Mapelli M (2017) Rotation in young massive star clusters. *MNRAS* 467:3255–3267, DOI 10.1093/mnras/stx304, [1702.00415](#)
- Marín-Franch A, Aparicio A, Piotto G, Rosenberg A, Chaboyer B, Sarajedini A, Siegel M, Anderson J, Bedin LR, Dotter A, Hempel M, King I, Majewski S, Milone AP, Paust N, Reid IN (2009) The ACS Survey of Galactic Globular Clusters. VII. Relative Ages. *ApJ* 694:1498–1516, DOI 10.1088/0004-637X/694/2/1498, [0812.4541](#)
- Marino AF, Milone AP, Piotto G, Villanova S, Bedin LR, Bellini A, Renzini A (2009) A double stellar generation in the globular cluster NGC 6656 (M 22). Two stellar groups with different iron and s-process element abundances. *A&A* 505:1099–1113, DOI 10.1051/0004-6361/200911827, [0905.4058](#)
- Marino AF, Milone AP, Piotto G, Villanova S, Gratton R, D’Antona F, Anderson J, Bedin LR, Bellini A, Cassisi S, Geisler D, Renzini A, Zoccali M (2011a) Sodium-Oxygen Anticorrelation and Neutron-capture Elements in Omega Centauri Stellar Populations. *ApJ* 731:64, DOI 10.1088/0004-637X/731/1/64, [1102.1653](#)
- Marino AF, Sneden C, Kraft RP, Wallerstein G, Norris JE, Da Costa G, Milone AP, Ivans II, Gonzalez G, Fulbright JP, Hilker M, Piotto G, Zoccali M, Stetson PB (2011b) The two metallicity groups of the globular cluster M 22: a chemical perspective. *A&A* 532:A8, DOI 10.1051/0004-6361/201116546, [1105.1523](#)
- Marino AF, Villanova S, Milone AP, Piotto G, Lind K, Geisler D, Stetson PB (2011c) Sodium-Oxygen Anticorrelation Among Horizontal Branch Stars in the Globular Cluster M4. *ApJL* 730:L16, DOI 10.1088/2041-8205/730/2/L16, [1012.4931](#)
- Marino AF, Milone AP, Sneden C, Bergemann M, Kraft RP, Wallerstein G, Cassisi S, Aparicio A, Asplund M, Bedin RL, Hilker M, Lind K, Momany Y, Piotto G, Roederer IU, Stetson PB, Zoccali M (2012) The double sub-giant branch of NGC 6656 (M 22): a chemical characterization. *A&A* 541:A15, DOI 10.1051/0004-6361/201118381, [1202.2825](#)

- Marino AF, Milone AP, Przybilla N, Bergemann M, Lind K, Asplund M, Cassisi S, Catelan M, Casagrande L, Valcarce AAR, Bedin LR, Cortés C, D'Antona F, Jerjen H, Piotto G, Schlesinger K, Zoccali M, Angeloni R (2014) Helium enhanced stars and multiple populations along the horizontal branch of NGC 2808: direct spectroscopic measurements. *MNRAS* 437:1609–1627, DOI 10.1093/mnras/stt1993, [1310.4527](#)
- Marino AF, Milone AP, Karakas AI, Casagrande L, Yong D, Shingles L, Da Costa G, Norris JE, Stetson PB, Lind K, Asplund M, Collet R, Jerjen H, Sbordone L, Aparicio A, Cassisi S (2015) Iron and s-elements abundance variations in NGC 5286: comparison with ‘anomalous’ globular clusters and Milky Way satellites. *MNRAS* 450:815–845, DOI 10.1093/mnras/stv420, [1502.07438](#)
- Marino AF, Milone AP, Yong D, Da Costa G, Asplund M, Bedin LR, Jerjen H, Nardiello D, Piotto G, Renzini A, Shetrone M (2017) Spectroscopy and Photometry of Multiple Populations along the Asymptotic Giant Branch of NGC 2808 and NGC 6121 (M4). *ApJ* 843:66, DOI 10.3847/1538-4357/aa7852
- Marino AF, Milone AP, Casagrande L, Przybilla N, Balaguer-Núñez L, Di Criscienzo M, Serenelli A, Vilardeell F (2018a) Discovery of Extended Main Sequence Turnoffs in Galactic Open Clusters. *ApJL* 863:L33, DOI 10.3847/2041-8213/aad868, [1807.05888](#)
- Marino AF, Yong D, Milone AP, Piotto G, Lundquist M, Bedin LR, Chené AN, Da Costa G, Asplund M, Jerjen H (2018b) Metallicity Variations in the Type II Globular Cluster NGC 6934. *ApJ* 859:81, DOI 10.3847/1538-4357/aabdea, [1804.04158](#)
- Marino AF, Milone AP, Renzini A, D'Antona F, Anderson J, Bedin LR, Bellini A, Cordoni G, Lagioia EP, Piotto G, Tailo M (2019) The Hubble Space Telescope UV Legacy Survey of Galactic Globular Clusters. XIX. A Chemical Tagging of the Multiple Stellar Populations Over the Chromosome Maps. arXiv e-prints [1904.05180](#)
- Martell SL, Grebel EK (2010) Light-element abundance variations in the Milky Way halo. *A&A* 519:A14, DOI 10.1051/0004-6361/201014135, [1005.4070](#)
- Martell SL, Smith GH, Briley MM (2008) Deep Mixing and Metallicity: Carbon Depletion in Globular Cluster Giants. *AJ* 136:2522–2532, DOI 10.1088/0004-6256/136/6/2522, [0809.4470](#)
- Martell SL, Smolinski JP, Beers TC, Grebel EK (2011) Building the Galactic halo from globular clusters: evidence from chemically unusual red giants. *A&A* 534:A136, DOI 10.1051/0004-6361/201117644, [1109.3916](#)
- Martell SL, Shetrone MD, Lucatello S, Schiavon RP, Mészáros S, Allende Prieto C, García-Hernández DA, Beers TC, Nidever DL (2016) Chemical Tagging in the SDSS-III/APOGEE Survey: New Identifications of Halo Stars with Globular Cluster Origins. *ApJ* 825:146, DOI 10.3847/0004-637X/825/2/146, [1605.05792](#)
- Martocchia S, Bastian N, Usher C, Kozhurina-Platais V, Niederhofer F, Cabrera-Ziri I, Dalessandro E, Hollyhead K, Kacharov N, Lardo C, Larsen S, Mucciarelli A, Platais I, Salaris M, Cordero M, Geisler D, Hilker M, Li C, Mackey D (2017) The search for multiple populations in Magellanic Cloud Clusters - III. No evidence for multiple populations in the SMC cluster NGC 419. *MNRAS* 468:3150–3158, DOI 10.1093/mnras/stx660, [1703.04631](#)
- Martocchia S, Cabrera-Ziri I, Lardo C, Dalessandro E, Bastian N, Kozhurina-Platais V, Usher C, Niederhofer F, Cordero M, Geisler D, Hollyhead K, Kacharov N, Larsen S, Li C, Mackey D, Hilker M, Mucciarelli A, Platais I, Salaris M (2018a) Age as a major factor in the onset of multiple populations in stellar clusters. *MNRAS* 473:2688–2700, DOI 10.1093/mnras/stx2556, [1710.00831](#)
- Martocchia S, Niederhofer F, Dalessandro E, Bastian N, Kacharov N, Usher C, Cabrera-Ziri I, Lardo C, Cassisi S, Geisler D, Hilker M, Hollyhead K, Kozhurina-Platais V, Larsen S, Mackey D, Mucciarelli A, Platais I, Salaris M (2018b) The search for multiple populations in Magellanic Cloud clusters - IV. Coeval multiple stellar populations in the young star cluster NGC 1978. *MNRAS* 477:4696–4705, DOI 10.1093/mnras/sty916, [1804.04141](#)
- Massari D, Mucciarelli A, Dalessandro E, Bellazzini M, Cassisi S, Fiorentino G, Ibata RA, Lardo C, Salaris M (2017) The chemical composition of the low-mass Galactic globular cluster NGC 6362. *MNRAS* 468:1249–1258, DOI 10.1093/mnras/stx549, [1703.00385](#)
- Masseron T, García-Hernández DA, Mészáros S, Zamora O, Dell’Aglì F, Allende Prieto C, Edvardsson B, Shetrone M, Plez B, Fernández-Trincado JG, Cunha K, Jönsson H, Geisler D, Beers TC, Cohen RE (2019) Homogeneous analysis of globular clusters from the APOGEE survey with the BACCHUS code. I. The northern clusters. *A&A* 622:A191, DOI 10.1051/0004-6361/201834550, [1812.08817](#)
- Mastrobuono-Battisti A, Perets HB (2013) Evolution of Second-generation Stars in Stellar Disks of Globular and Nuclear Clusters: ω Centauri as a Test Case. *ApJ* 779:85, DOI 10.1088/0004-637X/779/1/85, [1304.6086](#)
- Mateluna R, Geisler D, Villanova S, Carraro G, Grocholski A, Sarajedini A, Cole A, Smith V (2012)

- Chemical abundances in the old LMC globular cluster Hodge 11. *A&A* 548:A82, DOI 10.1051/0004-6361/201219750
- McClure RD, Fletcher JM, Nemeč JM (1980) The binary nature of the barium stars. *ApJL* 238:L35–L38, DOI 10.1086/183252
- McConnachie AW (2012) The Observed Properties of Dwarf Galaxies in and around the Local Group. *AJ* 144:4, DOI 10.1088/0004-6256/144/1/4, [1204.1562](#)
- McCrea WH (1964) Extended main-sequence of some stellar clusters. *MNRAS* 128:147, DOI 10.1093/mnras/128.2.147
- McLaughlin DE, Fall SM (2008) Shaping the Globular Cluster Mass Function by Stellar-Dynamical Evaporation. *ApJ* 679:1272–1287, DOI 10.1086/533485, [0704.0080](#)
- McLaughlin DE, van der Marel RP (2005) Resolved Massive Star Clusters in the Milky Way and Its Satellites: Brightness Profiles and a Catalog of Fundamental Parameters. *ApJS* 161:304–360, DOI 10.1086/497429, [astro-ph/0605132](#)
- McMillan SLW, Vesperini E, Portegies Zwart SF (2007) A Dynamical Origin for Early Mass Segregation in Young Star Clusters. *ApJL* 655:L45–L49, DOI 10.1086/511763, [astro-ph/0609515](#)
- McSaveney JA, Wood PR, Scholz M, Lattanzio JC, Hinkle KH (2007) Abundances in intermediate-mass AGB stars undergoing third dredge-up and hot-bottom burning. *MNRAS* 378:1089–1100, DOI 10.1111/j.1365-2966.2007.11845.x, [0704.1907](#)
- Meléndez J, Asplund M, Gustafsson B, Yong D (2009) The Peculiar Solar Composition and Its Possible Relation to Planet Formation. *ApJL* 704(1):L66–L70, DOI 10.1088/0004-637X/704/1/L66, [0909.2299](#)
- Mészáros S, Martell SL, Shetrone M, Lucatello S, Troup NW, Bovy J, Cunha K, García-Hernández DA, Overbeek JC, Allende Prieto C, Beers TC, Frinchaboy PM, García Pérez AE, Hearty FR, Holtzman J, Majewski SR, Nidever DL, Schiavon RP, Schneider DP, Sobek JS, Smith VV, Zamora O, Zasowski G (2015) Exploring Anticorrelations and Light Element Variations in Northern Globular Clusters Observed by the APOGEE Survey. *AJ* 149:153, DOI 10.1088/0004-6256/149/5/153, [1501.05127](#)
- Mikolaitis Š, Tautvaišienė G, Gratton R, Bragaglia A, Carretta E (2010) Chemical composition of clump stars in the open cluster NGC 6134. *MNRAS* 407:1866–1874, DOI 10.1111/j.1365-2966.2010.17030.x, [1005.3944](#)
- Milone AP, Bedin LR, Piotto G, Anderson J (2009) Multiple stellar populations in Magellanic Cloud clusters. I. An ordinary feature for intermediate age globulars in the LMC? *A&A* 497:755–771, DOI 10.1051/0004-6361/200810870, [0810.2558](#)
- Milone AP, Marino AF, Cassisi S, Piotto G, Bedin LR, Anderson J, Allard F, Aparicio A, Bellini A, Buonanno R, Monelli M, Pietrinferni A (2012a) The Infrared Eye of the Wide-Field Camera 3 on the Hubble Space Telescope Reveals Multiple Main Sequences of Very Low Mass Stars in NGC 2808. *ApJL* 754:L34, DOI 10.1088/2041-8205/754/2/L34, [1206.5529](#)
- Milone AP, Marino AF, Piotto G, Bedin LR, Anderson J, Aparicio A, Cassisi S, Rich RM (2012b) A Double Main Sequence in the Globular Cluster NGC 6397. *ApJ* 745:27, DOI 10.1088/0004-637X/745/1/27, [1110.1077](#)
- Milone AP, Piotto G, Bedin LR, Aparicio A, Anderson J, Sarajedini A, Marino AF, Moretti A, Davies MB, Chaboyer B, Dotter A, Hempel M, Marín-Franch A, Majewski S, Paust NEQ, Reid IN, Rosenberg A, Siegel M (2012c) The ACS survey of Galactic globular clusters. XII. Photometric binaries along the main sequence. *A&A* 540:A16, DOI 10.1051/0004-6361/201016384, [1111.0552](#)
- Milone AP, Piotto G, Bedin LR, Cassisi S, Anderson J, Marino AF, Pietrinferni A, Aparicio A (2012d) Luminosity and mass functions of the three main sequences of the globular cluster NGC 2808. *A&A* 537:A77, DOI 10.1051/0004-6361/201116539, [1108.2391](#)
- Milone AP, Piotto G, Bedin LR, King IR, Anderson J, Marino AF, Bellini A, Gratton R, Renzini A, Stetson PB, Cassisi S, Aparicio A, Bragaglia A, Carretta E, D’Antona F, Di Criscienzo M, Lucatello S, Monelli M, Pietrinferni A (2012e) Multiple Stellar Populations in 47 Tucanae. *ApJ* 744:58, DOI 10.1088/0004-637X/744/1/58, [1109.0900](#)
- Milone AP, Marino AF, Piotto G, Bedin LR, Anderson J, Aparicio A, Bellini A, Cassisi S, D’Antona F, Grundahl F, Monelli M, Yong D (2013) A WFC3/HST View of the Three Stellar Populations in the Globular Cluster NGC 6752. *ApJ* 767:120, DOI 10.1088/0004-637X/767/2/120, [1301.7044](#)
- Milone AP, Marino AF, Bedin LR, Piotto G, Cassisi S, Dieball A, Anderson J, Jerjen H, Asplund M, Bellini A, Brogaard K, Dotter A, Giersz M, Heggie DC, Knigge C, Rich RM, van den Berg M, Buonanno R (2014a) The M 4 Core Project with HST - II. Multiple stellar populations at the bottom of the main sequence. *MNRAS* 439:1588–1595, DOI 10.1093/mnras/stu030, [1401.1091](#)
- Milone AP, Marino AF, Dotter A, Norris JE, Jerjen H, Piotto G, Cassisi S, Bedin LR, Recio Blanco

- A, Sarajedini A, Asplund M, Monelli M, Aparicio A (2014b) Global and Nonglobal Parameters of Horizontal-branch Morphology of Globular Clusters. *ApJ* 785:21, DOI 10.1088/0004-637X/785/1/21, [1312.4169](#)
- Milone AP, Marino AF, Piotto G, Bedin LR, Anderson J, Renzini A, King IR, Bellini A, Brown TM, Cassisi S, D'Antona F, Jerjen H, Nardiello D, Salaris M, Marel RPvd, Vesperini E, Yong D, Aparicio A, Sarajedini A, Zoccali M (2015a) The Hubble Space Telescope UV Legacy Survey of galactic globular clusters - II. The seven stellar populations of NGC 7089 (M2). *MNRAS* 447:927–938, DOI 10.1093/mnras/stu2446, [1411.5043](#)
- Milone AP, Marino AF, Piotto G, Renzini A, Bedin LR, Anderson J, Cassisi S, D'Antona F, Bellini A, Jerjen H, Pietrinferni A, Ventura P (2015b) The Hubble Space Telescope UV Legacy Survey of Galactic Globular Clusters. III. A Quintuple Stellar Population in NGC 2808. *ApJ* 808:51, DOI 10.1088/0004-637X/808/1/51, [1505.05934](#)
- Milone AP, Marino AF, Bedin LR, Dotter A, Jerjen H, Kim D, Nardiello D, Piotto G, Cong J (2016) The binary populations of eight globular clusters in the outer halo of the Milky Way. *MNRAS* 455:3009–3019, DOI 10.1093/mnras/stv2415, [1510.05086](#)
- Milone AP, Marino AF, Bedin LR, Anderson J, Apai D, Bellini A, Bergeron P, Burgasser AJ, Dotter A, Rees JM (2017a) The HST large programme on ω Centauri - I. Multiple stellar populations at the bottom of the main sequence probed in NIR-Optical. *MNRAS* 469:800–812, DOI 10.1093/mnras/stx836, [1704.00418](#)
- Milone AP, Marino AF, Bedin LR, Anderson J, Apai D, Bellini A, Bergeron P, Burgasser AJ, Dotter A, Rees JM (2017b) The HST large programme on ω Centauri - I. Multiple stellar populations at the bottom of the main sequence probed in NIR-Optical. *MNRAS* 469:800–812, DOI 10.1093/mnras/stx836, [1704.00418](#)
- Milone AP, Marino AF, Di Criscienzo M, D'Antona F, Bedin LR, Da Costa G, Piotto G, Tailo M, Dotter A, Angeloni R, Anderson J, Jerjen H, Li C, Dupree A, Granata V, Lagioia EP, Mackey AD, Nardiello D, Vesperini E (2018a) Multiple stellar populations in Magellanic Cloud clusters - VI. A survey of multiple sequences and Be stars in young clusters. *MNRAS* 477:2640–2663, DOI 10.1093/mnras/sty661, [1802.10538](#)
- Milone AP, Marino AF, Mastrobuono-Battisti A, Lagioia EP (2018b) Gaia unveils the kinematics of multiple stellar populations in 47 Tucanae. *MNRAS* 479:5005–5011, DOI 10.1093/mnras/sty1873, [1807.03511](#)
- Milone AP, Marino AF, Renzini A, D'Antona F, Anderson J, Barbuy B, Bedin LR, Bellini A, Brown TM, Cassisi S, Cordoni G, Lagioia EP, Nardiello D, Ortolani S, Piotto G, Sarajedini A, Tailo M, van der Marel RP, Vesperini E (2018c) The Hubble Space Telescope UV legacy survey of galactic globular clusters - XVI. The helium abundance of multiple populations. *MNRAS* 481:5098–5122, DOI 10.1093/mnras/sty2573, [1809.05006](#)
- Milone AP, Marino AF, Bedin LR, Anderson J, Apai D, Bellini A, Dieball A, Salaris M, Libralato M, Nardiello D, Bergeron P, Burgasser AJ, Rees JM, Rich RM, Richer HB (2019a) The HST Large Programme on NGC 6752 - II. Multiple populations at the bottom of the main sequence probed in NIR. *Monthly Notices of the Royal Astronomical Society* 484(3):4046–4053, DOI 10.1093/mnras/stz277, [1901.07230](#)
- Milone AP, Marino AF, Bedin LR, Anderson J, Apai D, Bellini A, Dieball A, Salaris M, Libralato M, Nardiello D, Bergeron P, Burgasser AJ, Rees JM, Rich RM, Richer HB (2019b) The HST Large Programme on NGC 6752. II. Multiple populations at the bottom of the main sequence probed in NIR. *MNRAS* DOI 10.1093/mnras/stz277, [1901.07230](#)
- Moe M, Di Stefano R (2017) Mind Your Ps and Qs: The Interrelation between Period (P) and Mass-ratio (Q) Distributions of Binary Stars. *ApJS* 230:15, DOI 10.3847/1538-4365/aa6fb6, [1606.05347](#)
- Moe M, Kratter KM, Badenes C (2018) The Close Binary Fraction of Solar-type Stars is Strongly Anti-correlated with Metallicity. *arXiv e-prints* [1808.02116](#)
- Moehler S, Sweigart AV, Landsman WB, Hammer NJ, Dreizler S (2004) Spectroscopic analyses of the blue hook stars in NGC 2808: A more stringent test of the late hot flasher scenario. *A&A* 415:313–323, DOI 10.1051/0004-6361:20034505, [astro-ph/0311215](#)
- Monaco L, Bonifacio P, Sbordone L, Villanova S, Pancino E (2010) The lithium content of ω Centauri. New clues to the cosmological Li problem from old stars in external galaxies. *A&A* 519:L3, DOI 10.1051/0004-6361/201015162, [1008.1817](#)
- Monaco L, Villanova S, Bonifacio P, Caffau E, Geisler D, Marconi G, Momany Y, Ludwig HG (2012) Lithium and sodium in the globular cluster. Detection of a Li-rich dwarf star: preservation or pollution? *A&A* 539:A157, DOI 10.1051/0004-6361/201117709, [1108.0138](#)

- Monelli M, Milone AP, Stetson PB, Marino AF, Cassisi S, del Pino Molina A, Salaris M, Aparicio A, Asplund M, Grundahl F, Piotto G, Weiss A, Carrera R, Cebrián M, Murabito S, Pietrinferni A, Sbordone L (2013) The SUMO project I. A survey of multiple populations in globular clusters. *MNRAS* 431:2126–2149, DOI 10.1093/mnras/stt273, [1303.5187](#)
- Moody K, Sigurdsson S (2009) Modeling the Retention Probability of Black Holes in Globular Clusters: Kicks and Rates. *ApJ* 690:1370–1377, DOI 10.1088/0004-637X/690/2/1370, [0809.1617](#)
- Moretti A, de Angeli F, Piotto G (2008) Environmental effects on the globular cluster blue straggler population: a statistical approach. *A&A* 483:183–197, DOI 10.1051/0004-6361/20078416
- Muñoz C, Villanova S, Geisler D, Saviane I, Dias B, Cohen RE, Mauro F (2017) The peculiar Na-O anticorrelation of the bulge globular cluster NGC 6440. *A&A* 605:A12, DOI 10.1051/0004-6361/201730468, [1705.02684](#)
- Muñoz C, Geisler D, Villanova S, Saviane I, Cortés CC, Dias B, Cohen RE, Mauro F, Moni Bidin C (2018) Chemical analysis of NGC 6528: one of the most metal-rich bulge globular clusters. *A&A* 620:A96, DOI 10.1051/0004-6361/201833373, [1809.04164](#)
- Mucciarelli A, Origlia L, Ferraro FR, Pancino E (2009) Looking Outside the Galaxy: The Discovery of Chemical Anomalies in Three Old Large Magellanic Cloud Clusters. *ApJL* 695:L134–L139, DOI 10.1088/0004-637X/695/2/L134, [0902.4778](#)
- Mucciarelli A, Salaris M, Lovisi L, Ferraro FR, Lanzoni B, Lucatello S, Gratton RG (2011) Lithium abundance in the globular cluster M4: from the turn-off to the red giant branch bump. *MNRAS* 412:81–94, DOI 10.1111/j.1365-2966.2010.17884.x, [1010.3879](#)
- Mucciarelli A, Bellazzini M, Ibata R, Merle T, Chapman SC, Dalessandro E, Sollima A (2012a) News from the Galactic suburbia: the chemical composition of the remote globular cluster NGC 2419. *MNRAS* 426:2889–2900, DOI 10.1111/j.1365-2966.2012.21847.x, [1208.0195](#)
- Mucciarelli A, Salaris M, Bonifacio P (2012b) Giants reveal what dwarfs conceal: Li abundance in lower red giant branch stars as diagnostic of the primordial Li. *MNRAS* 419:2195–2205, DOI 10.1111/j.1365-2966.2011.19870.x, [1109.4589](#)
- Mucciarelli A, Bellazzini M, Catelan M, Dalessandro E, Amigo P, Correnti M, Cortés C, D’Orazi V (2013) NGC 5694: another foster son of the Galactic halo. *MNRAS* 435:3667–3680, DOI 10.1093/mnras/stt1558, [1308.6653](#)
- Mucciarelli A, Dalessandro E, Ferraro FR, Origlia L, Lanzoni B (2014a) No Evidence of Chemical Anomalies in the Bimodal Turnoff Cluster NGC 1806 in the Large Magellanic Cloud. *ApJL* 793:L6, DOI 10.1088/2041-8205/793/1/L6, [1409.0259](#)
- Mucciarelli A, Salaris M, Bonifacio P, Monaco L, Villanova S (2014b) The cosmological lithium problem outside the Galaxy: the Sagittarius globular cluster M54. *MNRAS* 444:1812–1820, DOI 10.1093/mnras/stu1522, [1407.7596](#)
- Mucciarelli A, Bellazzini M, Merle T, Plez B, Dalessandro E, Ibata R (2015a) Potassium: A New Actor on the Globular Cluster Chemical Evolution Stage. The Case of NGC 2808. *ApJ* 801:68, DOI 10.1088/0004-637X/801/1/68, [1501.03161](#)
- Mucciarelli A, Lapenna E, Massari D, Pancino E, Stetson PB, Ferraro FR, Lanzoni B, Lardo C (2015b) A Chemical Trompe-l’œil: No Iron Spread in the Globular Cluster M22. *ApJ* 809:128, DOI 10.1088/0004-637X/809/2/128, [1507.01596](#)
- Mucciarelli A, Dalessandro E, Massari D, Bellazzini M, Ferraro FR, Lanzoni B, Lardo C, Salaris M, Cassisi S (2016) NGC 6362: The Least Massive Globular Cluster with Chemically Distinct Multiple Populations. *ApJ* 824:73, DOI 10.3847/0004-637X/824/2/73, [1604.04151](#)
- Mucciarelli A, Lapenna E, Ferraro FR, Lanzoni B (2018) The Chemical Composition of NGC 5824, a Globular Cluster without Iron Spread but with an Extreme Mg-Al Anticorrelation. *ApJ* 859:75, DOI 10.3847/1538-4357/aaba80, [1803.09759](#)
- Mucciarelli A, Lapenna E, Lardo C, Bonifacio P, Ferraro FR, Lanzoni B (2019) Confirming the Presence of Second-population Stars and the Iron Discrepancy along the AGB of the Globular Cluster NGC 6752. *ApJ* 870:124, DOI 10.3847/1538-4357/aaf3a4, [1811.10626](#)
- Myeong GC, Evans NW, Belokurov V, Sanders JL, Koposov SE (2018a) Discovery of new retrograde substructures: the shards of ω Centauri? *MNRAS* 478:5449–5459, DOI 10.1093/mnras/sty1403
- Myeong GC, Evans NW, Belokurov V, Sanders JL, Koposov SE (2018b) The Milky Way Halo in Action Space. *ApJL* 856:L26, DOI 10.3847/2041-8213/aab613, [1802.03351](#)
- Myeong GC, Evans NW, Belokurov V, Sanders JL, Koposov SE (2018c) The Sausage Globular Clusters. *ApJL* 863:L28, DOI 10.3847/2041-8213/aad7f7, [1805.00453](#)
- Nardiello D, Piotto G, Milone AP, Marino AF, Bedin LR, Anderson J, Aparicio A, Bellini A, Cassisi S, D’Antona F, Hidalgo S, Ortolani S, Pietrinferni A, Renzini A, Salaris M, Marel RPvd, Vesperini E

- (2015) The Hubble Space Telescope UV Legacy Survey of Galactic Globular Clusters - IV. Helium content and relative age of multiple stellar populations within NGC 6352. *MNRAS* 451:312–322, DOI 10.1093/mnras/stv971, [1504.07876](#)
- Nardiello D, Libralato M, Piotto G, Anderson J, Bellini A, Aparicio A, Bedin LR, Cassisi S, Granata V, King IR, Lucertini F, Marino AF, Milone AP, Ortolani S, Platais I, van der Marel RP (2018a) The Hubble Space Telescope UV Legacy Survey of Galactic Globular Clusters - XVII. Public Catalogue Release. *MNRAS* 481:3382–3393, DOI 10.1093/mnras/sty2515, [1809.04300](#)
- Nardiello D, Milone AP, Piotto G, Anderson J, Bedin LR, Bellini A, Cassisi S, Libralato M, Marino AF (2018b) The Hubble Space Telescope UV Legacy Survey of Galactic globular clusters - XIV. Multiple stellar populations within M 15 and their radial distribution. *MNRAS* 477:2004–2019, DOI 10.1093/mnras/sty719, [1803.05979](#)
- Nataf DM, Gould A, Pinsonneault MH, Stetson PB (2011) The Gradients in the 47 Tuc Red Giant Branch Bump and Horizontal Branch are Consistent with a Centrally Concentrated, Helium-enriched Second Stellar Generation. *ApJ* 736:94, DOI 10.1088/0004-637X/736/2/94, [1102.3916](#)
- Nataf DM, Wyse R, Schiavon RP, Ting YS, Minniti D, Cohen RE, Fernández-Trincado JG, Geisler D, Nitschelm C, Frinchaboy PM (2019) The Relationship Between Globular Cluster Mass, Metallicity, and Light Element Abundance Variations. arXiv e-prints [1904.07884](#)
- Navarrete C, Chanamé J, Ramírez I, Meza A, Anglada-Escudé G, Shkolnik E (2015) The Kapteyn Moving Group Is Not Tidal Debris From ω Centauri. *ApJ* 808:103, DOI 10.1088/0004-637X/808/1/103, [1506.02041](#)
- Niederhofer F, Bastian N, Kozhurina-Platais V, Hilker M, de Mink SE, Cabrera-Ziri I, Li C, Ercolano B (2016) Controversial age spreads from the main sequence turn-off and red clump in intermediate-age clusters in the LMC. *A&A* 586:A148, DOI 10.1051/0004-6361/201526484, [1510.08476](#)
- Niederhofer F, Bastian N, Kozhurina-Platais V, Larsen S, Hollyhead K, Lardo C, Cabrera-Ziri I, Kacharov N, Platais I, Salaris M, Cordero M, Dalessandro E, Geisler D, Hilker M, Li C, Mackey D, Mucciarelli A (2017a) The search for multiple populations in Magellanic Cloud clusters - II. The detection of multiple populations in three intermediate-age SMC clusters. *MNRAS* 465:4159–4165, DOI 10.1093/mnras/stw3084, [1612.00400](#)
- Niederhofer F, Bastian N, Kozhurina-Platais V, Larsen S, Salaris M, Dalessandro E, Mucciarelli A, Cabrera-Ziri I, Cordero M, Geisler D, Hilker M, Hollyhead K, Kacharov N, Lardo C, Li C, Mackey D, Platais I (2017b) The search for multiple populations in Magellanic Cloud clusters - I. Two stellar populations in the Small Magellanic Cloud globular cluster NGC 121. *MNRAS* 464:94–103, DOI 10.1093/mnras/stw2269, [1609.01595](#)
- Nissen PE, Schuster WJ (2010) Two distinct halo populations in the solar neighborhood. Evidence from stellar abundance ratios and kinematics. *A&A* 511:L10, DOI 10.1051/0004-6361/200913877, [1002.4514](#)
- Norris J, Smith GH (1983) The cyanogen distribution of the giants in NGC 2808. *ApJ* 275:120–124, DOI 10.1086/161517
- Norris J, Cottrell PL, Freeman KC, Da Costa GS (1981) The abundance spread in the giants of NGC 6752. *ApJ* 244:205–220, DOI 10.1086/158698
- Norris JE (2004) The Helium Abundances of ω Centauri. *ApJL* 612:L25–L28, DOI 10.1086/423986
- Norris JE, Da Costa GS (1995) The Giant Branch of omega Centauri. IV. Abundance Patterns Based on Echelle Spectra of 40 Red Giants. *ApJ* 447:680, DOI 10.1086/175909
- Odenkirchen M, Grebel EK, Rockosi CM, Dehnen W, Ibata R, Rix HW, Stolte A, Wolf C, Anderson JE Jr, Bahcall NA, Brinkmann J, Csabai I, Hennessy G, Hindsley RB, Ivezić Ž, Lupton RH, Munn JA, Pier JR, Stoughton C, York DG (2001) Detection of Massive Tidal Tails around the Globular Cluster Palomar 5 with Sloan Digital Sky Survey Commissioning Data. *ApJL* 548:L165–L169, DOI 10.1086/319095, [astro-ph/0012311](#)
- Odenkirchen M, Grebel EK, Dehnen W, Rix HW, Yanny B, Newberg HJ, Rockosi CM, Martínez-Delgado D, Brinkmann J, Pier JR (2003) The Extended Tails of Palomar 5: A 10 deg Arc of Globular Cluster Tidal Debris. *AJ* 126:2385–2407, DOI 10.1086/378601, [astro-ph/0307446](#)
- Oh KS, Lin DNC (1992) Tidal evolution of globular clusters. II - The effects of Galactic tidal field and diffusion. *ApJ* 386:519–538, DOI 10.1086/171037
- Olszewski EW, Schommer RA, Suntzeff NB, Harris HC (1991) Spectroscopy of giants in LMC clusters. I - Velocities, abundances, and the age-metallicity relation. *AJ* 101:515–537, DOI 10.1086/115701
- Olszewski EW, Saha A, Knezek P, Subramaniam A, de Boer T, Seitzer P (2009) A 500 Parsec Halo Surrounding the Galactic Globular NGC 1851. *AJ* 138:1570–1576, DOI 10.1088/0004-6256/138/6/1570, [0909.1755](#)

- O'Malley EM, Knaizev A, McWilliam A, Chaboyer B (2017) High-resolution Spectroscopic Abundances of Red Giant Branch Stars in NGC 6681. *ApJ* 846:23, DOI 10.3847/1538-4357/aa7b72, [1706.06962](#)
- Ostriker JP, Spitzer L Jr, Chevalier RA (1972) On the Evolution of Globular Clusters. *ApJL* 176:L51, DOI 10.1086/181018
- Otsuki K, Honda S, Aoki W, Kajino T, Mathews GJ (2006) Neutron-Capture Elements in the Metal-poor Globular Cluster M15. *ApJL* 641:L117–L120, DOI 10.1086/504106, [astro-ph/0603328](#)
- Overbeek JC, Friel ED, Donati P, Smiljanic R, Jacobson HR, Hatzidimitriou D, Held EV, Magrini L, Bragaglia A, Randich S, Vallenari A, Cantat-Gaudin T, Tautvaisiene G, Jiménez-Esteban F, Frasca A, Geisler D, Villanova S, Tang B, Muñoz C, Marconi G, Carraro G, San Roman I, Drazdauskas A, Ženoviene R, Gilmore G, Jeffries RD, Flaccomio E, Pancino E, Bayo A, Costado MT, Damiani F, Jofré P, Monaco L, Prisinzano L, Sousa SG, Zaggia S (2017) The Gaia-ESO Survey: the inner disk, intermediate-age open cluster Trumpler 23. *A&A* 598:A68, DOI 10.1051/0004-6361/201629345, [1611.00859](#)
- Pace G, Recio-Blanco A, Piotto G, Momany Y (2006) Abundance anomalies in hot horizontal branch stars of the Galactic globular cluster NGC 2808. *A&A* 452:493–501, DOI 10.1051/0004-6361:20054593
- Pace G, Castro M, Meléndez J, Théado S, do Nascimento JD Jr (2012) Lithium in M 67: From the main sequence to the red giant branch. *A&A* 541:A150, DOI 10.1051/0004-6361/201117704, [1203.4440](#)
- Pancino E (2018) Globular cluster chemistry in fast-rotating dwarf stars belonging to intermediate-age open clusters. *A&A* 614:A80, DOI 10.1051/0004-6361/201732351, [1802.06654](#)
- Pancino E, Galfo A, Ferraro FR, Bellazzini M (2007) The Rotation of Subpopulations in ω Centauri. *ApJL* 661:L155–L158, DOI 10.1086/518959, [0704.2962](#)
- Pancino E, Rejkuba M, Zoccali M, Carrera R (2010) Low-resolution spectroscopy of main sequence stars belonging to 12 Galactic globular clusters. I. CH and CN band strength variations. *A&A* 524:A44, DOI 10.1051/0004-6361/201014383, [1009.1589](#)
- Pancino E, Romano D, Tang B, Tautvaisiene G, Casey AR, Gruyters P, Geisler D, San Roman I, Randich S, Alfaro EJ, Bragaglia A, Flaccomio E, Korn AJ, Recio-Blanco A, Smiljanic R, Carraro G, Bayo A, Costado MT, Damiani F, Jofré P, Lardo C, de Laverny P, Monaco L, Morbidelli L, Sbordone L, Sousa SG, Villanova S (2017) The Gaia-ESO Survey. Mg-Al anti-correlation in iDR4 globular clusters. *A&A* 601:A112, DOI 10.1051/0004-6361/201730474, [1702.06083](#)
- Pasquini L, Bonifacio P, Molaro P, Francois P, Spite F, Gratton RG, Carretta E, Wolff B (2005) Li in NGC 6752 and the formation of globular clusters. *A&A* 441:549–553, DOI 10.1051/0004-6361:20053607, [astro-ph/0506651](#)
- Pasquini L, Mauas P, Käuffl HU, Cacciari C (2011) Measuring helium abundance difference in giants of NGC 2808. *A&A* 531:A35, DOI 10.1051/0004-6361/201116592, [1105.0346](#)
- Pastorelli G, Marigo P, Girardi L, Chen Y, Rubele S, Trabucchi M, Aringer B, Bladh S, Bressan A, Montalbán J, Boyer ML, Dalcanton JJ, Eriksson K, Groenewegen MAT, Höfner S, Lebzelter T, Nanni A, Rosenfield P, Wood PR, Cioni MRL (2019) Constraining the thermally-pulsing asymptotic giant branch phase with resolved stellar populations in the Small Magellanic Cloud. *arXiv e-prints* [1903.04499](#)
- Peña Suárez VJ, Sales Silva JV, Katime Santrich OJ, Drake NA, Pereira CB (2018) High-resolution Spectroscopic Observations of Single Red Giants in Three Open Clusters: NGC 2360, NGC 3680, and NGC 5822. *ApJ* 854:184, DOI 10.3847/1538-4357/aaa017
- Piatti AE, Carballo-Bello JA (2019) Extra-tidal structures around the Gaia Sausage candidate globular cluster NGC 6779 (M56). *MNRAS* 485:1029–1035, DOI 10.1093/mnras/stz500, [1902.05824](#)
- Piatti AE, Mackey AD (2018) Evidence of differential tidal effects in the old globular cluster population of the Large Magellanic Cloud. *MNRAS* 478:2164–2176, DOI 10.1093/mnras/sty1048, [1804.09549](#)
- Pietrinferni A, Cassisi S, Salaris M, Castelli F (2004) A Large Stellar Evolution Database for Population Synthesis Studies. I. Scaled Solar Models and Isochrones. *The Astrophysical Journal* 612(1):168–190, DOI 10.1086/422498, [astro-ph/0405193](#)
- Pietrinferni A, Cassisi S, Salaris M, Castelli F (2006) A Large Stellar Evolution Database for Population Synthesis Studies. II. Stellar Models and Isochrones for an α -enhanced Metal Distribution. *The Astrophysical Journal* 642(2):797–812, DOI 10.1086/501344, [astro-ph/0603721](#)
- Pignatari M, Gallino R, Heil M, Wiescher M, Käppeler F, Herwig F, Bisterzo S (2010) The Weak s-Process in Massive Stars and its Dependence on the Neutron Capture Cross Sections. *ApJ* 710:1557–1577, DOI 10.1088/0004-637X/710/2/1557
- Piotto G (2010) Observational Evidence of Multiple Stellar Populations in Star Clusters. *Publication of Korean Astronomical Society* 25:91–99, DOI 10.5303/PKAS.2010.25.3.091, [0902.1422](#)
- Piotto G, De Angeli F, King IR, Djorgovski SG, Bono G, Cassisi S, Meylan G, Recio-Blanco A, Rich RM,

- Davies MB (2004) Relative Frequencies of Blue Stragglers in Galactic Globular Clusters: Constraints for the Formation Mechanisms. *ApJL* 604:L109–L112, DOI 10.1086/383617, [astro-ph/0402592](#)
- Piotto G, Villanova S, Bedin LR, Gratton R, Cassisi S, Momany Y, Recio-Blanco A, Lucatello S, Anderson J, King IR, Pietrinferni A, Carraro G (2005) Metallicities on the Double Main Sequence of ω Centauri Imply Large Helium Enhancement. *ApJ* 621:777–784, DOI 10.1086/427796, [astro-ph/0412016](#)
- Piotto G, Bedin LR, Anderson J, King IR, Cassisi S, Milone AP, Villanova S, Pietrinferni A, Renzini A (2007) A Triple Main Sequence in the Globular Cluster NGC 2808. *ApJL* 661:L53–L56, DOI 10.1086/518503, [astro-ph/0703767](#)
- Piotto G, Milone AP, Bedin LR, Anderson J, King IR, Marino AF, Nardiello D, Aparicio A, Barbuy B, Bellini A, Brown TM, Cassisi S, Cool AM, Cunial A, Dalessandro E, D’Antona F, Ferraro FR, Hidalgo S, Lanzoni B, Monelli M, Ortolani S, Renzini A, Salaris M, Sarajedini A, van der Marel RP, Vesperini E, Zoccali M (2015) The Hubble Space Telescope UV Legacy Survey of Galactic Globular Clusters. I. Overview of the Project and Detection of Multiple Stellar Populations. *AJ* 149:91, DOI 10.1088/0004-6256/149/3/91, [1410.4564](#)
- Piskunov AE, Schilbach E, Kharchenko NV, Röser S, Scholz RD (2008) Tidal radii and masses of open clusters. *A&A* 477:165–172, DOI 10.1051/0004-6361/20078525
- Platais I, Cudworth KM, Kozhurina-Platais V, McLaughlin DE, Meibom S, Veillet C (2011) A New Look at the Old Star Cluster NGC 6791. *ApJL* 733:L1, DOI 10.1088/2041-8205/733/1/L1, [1104.5473](#)
- Plummer HC (1911) On the problem of distribution in globular star clusters. *MNRAS* 71:460–470, DOI 10.1093/mnras/71.5.460
- Portegies Zwart SF, McMillan SLW, Gieles M (2010) Young Massive Star Clusters. *ARA&A* 48:431–493, DOI 10.1146/annurev-astro-081309-130834, [1002.1961](#)
- Prantzos N, Charbonnel C (2006) On the self-enrichment scenario of galactic globular clusters: constraints on the IMF. *A&A* 458:135–149, DOI 10.1051/0004-6361/20065374, [astro-ph/0606112](#)
- Prantzos N, Hashimoto M, Nomoto K (1990) The s-process in massive stars - Yields as a function of stellar mass and metallicity. *A&A* 234:211–229
- Prantzos N, Charbonnel C, Iliadis C (2007) Light nuclei in galactic globular clusters: constraints on the self-enrichment scenario from nucleosynthesis. *A&A* 470:179–190, DOI 10.1051/0004-6361:20077205, [0704.3331](#)
- Prantzos N, Charbonnel C, Iliadis C (2017) Revisiting nucleosynthesis in globular clusters. The case of NGC 2808 and the role of He and K. *A&A* 608:A28, DOI 10.1051/0004-6361/201731528, [1709.05819](#)
- Prieto JL, Gnedin OY (2008) Dynamical Evolution of Globular Clusters in Hierarchical Cosmology. *ApJ* 689(2):919–935, DOI 10.1086/591777, [astro-ph/0608069](#)
- Qian YZ, Woosley SE (1996) Nucleosynthesis in Neutrino-driven Winds. I. The Physical Conditions. *ApJ* 471:331, DOI 10.1086/177973, [astro-ph/9611094](#)
- Raghavan D, McAlister HA, Henry TJ, Latham DW, Marcy GW, Mason BD, Gies DR, White RJ, ten Brummelaar TA (2010) A Survey of Stellar Families: Multiplicity of Solar-type Stars. *ApJS* 190:1–42, DOI 10.1088/0067-0049/190/1/1, [1007.0414](#)
- Raiteri CM, Busso M, Gallino R, Picchio G, Pulone L (1991) S-process nucleosynthesis in massive stars and the weak component. I - Evolution and neutron captures in a 25 solar mass star. *ApJ* 367:228–238, DOI 10.1086/169622
- Ramírez I, Meléndez J, Chanamé J (2012) Oxygen Abundances in Low- and High- α Field Halo Stars and the Discovery of Two Field Stars Born in Globular Clusters. *ApJ* 757:164, DOI 10.1088/0004-637X/757/2/164, [1208.3675](#)
- Read JI, Wilkinson MI, Evans NW, Gilmore G, Kleyna JT (2006) The tidal stripping of satellites. *MNRAS* 366:429–437, DOI 10.1111/j.1365-2966.2005.09861.x, [astro-ph/0506687](#)
- Reina-Campos M, Kruijssen JMD, Pfeffer J, Bastian N, Crain RA (2018) Dynamical cluster disruption and its implications for multiple population models in the E-MOSAICS simulations. *MNRAS* 481(3):2851–2857, DOI 10.1093/mnras/sty2451, [1809.03499](#)
- Renzini A (2008) Origin of multiple stellar populations in globular clusters and their helium enrichment. *MNRAS* 391:354–362, DOI 10.1111/j.1365-2966.2008.13892.x, [0808.4095](#)
- Renzini A (2017) Finding forming globular clusters at high redshifts. *MNRAS* 469:L63–L67, DOI 10.1093/mnras/lsx057, [1704.04883](#)
- Renzini A, D’Antona F, Cassisi S, King IR, Milone AP, Ventura P, Anderson J, Bedin LR, Bellini A, Brown TM, Piotto G, van der Marel RP, Barbuy B, Dalessandro E, Hidalgo S, Marino AF, Ortolani S, Salaris M, Sarajedini A (2015) The Hubble Space Telescope UV Legacy Survey of Galactic Globular Clusters - V. Constraints on formation scenarios. *MNRAS* 454:4197–4207, DOI 10.1093/mnras/stv2268,

- [1510.01468](#)
- Richer HB, Heyl J, Anderson J, Kalirai JS, Shara MM, Dotter A, Fahlman GG, Rich RM (2013) A Dynamical Signature of Multiple Stellar Populations in 47 Tucanae. *ApJL* 771:L15, DOI 10.1088/2041-8205/771/1/L15, [1306.1226](#)
- Roedderer IU, Mateo M, Bailey JJ, Spencer M, Crane JD, Shtetman SA (2016) Detailed chemical abundances in NGC 5824: another metal-poor globular cluster with internal heavy element abundance variations. *MNRAS* 455:2417–2439, DOI 10.1093/mnras/stv2462, [1510.06414](#)
- Rubenstein EP, Bailyn CD (1997) Hubble Space Telescope Observations of the Post-Core-Collapse Globular Cluster NGC 6752. II. A Large Main-Sequence Binary Population. *ApJ* 474:701–709, DOI 10.1086/303498
- Rutledge GA, Hesser JE, Stetson PB (1997) Galactic Globular Cluster Metallicity Scale from the Ca II Triplet II. Rankings, Comparisons, and Puzzles. *PASP* 109:907–919, DOI 10.1086/133959, [astro-ph/9707068](#)
- Ryu J, Lee MG (2018) Discovery of Two New Globular Clusters in the Milky Way. *ApJL* 863:L38, DOI 10.3847/2041-8213/aad8b7, [1808.03455](#)
- Sakari CM, Venn KA, Aoki W, Arimoto N, Dotter A (2011) Detailed Chemical Abundances of Four Stars in the Unusual Globular Cluster Palomar 1. *ApJ* 740:106, DOI 10.1088/0004-637X/740/2/106, [1107.5315](#)
- Salaris M, Cassisi S, Weiss A (2002) Red Giant Branch Stars: The Theoretical Framework. *PASP* 114(794):375–402, DOI 10.1086/342498, [astro-ph/0201387](#)
- Salaris M, Weiss A, Ferguson JW, Fusilier DJ (2006) On the Primordial Scenario for Abundance Variations within Globular Clusters: The Isochrone Test. *ApJ* 645:1131–1137, DOI 10.1086/504520, [astro-ph/0604137](#)
- Salaris M, Cassisi S, Pietrinferni A (2016) On the red giant branch mass loss in 47 Tucanae: Constraints from the horizontal branch morphology. *Astronomy and Astrophysics* 590:A64, DOI 10.1051/0004-6361/201628181, [1604.02874](#)
- Salinas R, Strader J (2015) No Evidence for Multiple Stellar Populations in the Low-mass Galactic Globular Cluster E 3. *ApJ* 809:169, DOI 10.1088/0004-637X/809/2/169, [1506.00637](#)
- San Roman I, Muñoz C, Geisler D, Villanova S, Kacharov N, Koch A, Carraro G, Tautvaisiene G, Vallenari A, Alfaro EJ, Bensby T, Flacco E, Francois P, Korn AJ, Pancino E, Recio-Blanco A, Smiljanic R, Bergemann M, Costado MT, Damiani F, Heiter U, Hourihane A, Jofré P, Lardo C, de Laverny P, Masseron T, Morbidelli L, Sbordone L, Sousa SG, Worley CC, Zaggia S (2015) The Gaia-ESO Survey: Detailed abundances in the metal-poor globular cluster NGC 4372. *A&A* 579:A6, DOI 10.1051/0004-6361/201525722, [1504.03497](#)
- Sandage AR (1953) The color-magnitude diagram for the globular cluster M 3. *AJ* 58:61–75, DOI 10.1086/106822
- Santrich OJK, Pereira CB, Drake NA (2013) Chemical analysis of giant stars in the young open cluster NGC 3114. *A&A* 554:A2, DOI 10.1051/0004-6361/201220252, [1304.1004](#)
- Sarajedini A, Bedin LR, Chaboyer B, Dotter A, Siegel M, Anderson J, Aparicio A, King I, Majewski S, Marín-Franch A, Piotto G, Reid IN, Rosenberg A (2007) The ACS Survey of Galactic Globular Clusters. I. Overview and Clusters without Previous Hubble Space Telescope Photometry. *AJ* 133:1658–1672, DOI 10.1086/511979, [astro-ph/0612598](#)
- Sarna MJ, De Greve JP (1996) Chemical Evolution of Algols. *QJRAS* 37:11
- Savino A, Massari D, Bragaglia A, Dalessandro E, Tolstoy E (2018) M13 multiple stellar populations seen with the eyes of Strömgren photometry. *MNRAS* 474:4438–4446, DOI 10.1093/mnras/stx3093, [1712.01284](#)
- Sbordone L, Bonifacio P, Marconi G, Buonanno R, Zaggia S (2005) Family ties: Abundances in Terzan 7, a Sgr dSph globular cluster. *A&A* 437:905–910, DOI 10.1051/0004-6361:20042315, [astro-ph/0505307](#)
- Sbordone L, Bonifacio P, Buonanno R, Marconi G, Monaco L, Zaggia S (2007) The exotic chemical composition of the Sagittarius dwarf spheroidal galaxy. *A&A* 465:815–824, DOI 10.1051/0004-6361:20066385, [astro-ph/0612125](#)
- Sbordone L, Bonifacio P, Caffau E, Ludwig HG, Behara NT, González Hernández JI, Steffen M, Cayrel R, Freytag B, van't Veer C, Molaro P, Plez B, Sivarani T, Spite M, Spite F, Beers TC, Christlieb N, François P, Hill V (2010) The metal-poor end of the Spite plateau. I. Stellar parameters, metallicities, and lithium abundances. *A&A* 522:A26, DOI 10.1051/0004-6361/200913282, [1003.4510](#)
- Schaerer D, Charbonnel C (2011) A new perspective on globular clusters, their initial mass function and their contribution to the stellar halo and the cosmic reionization. *MNRAS* 413:2297–2304, DOI

- 10.1111/j.1365-2966.2011.18304.x, [1101.1073](#)
- Searle L, Zinn R (1978) Compositions of halo clusters and the formation of the galactic halo. *ApJ* 225:357–379, DOI 10.1086/156499
- Sheffield AA, Majewski SR, Johnston KV, Cunha K, Smith VV, Cheung AM, Hampton CM, David TJ, Wagner-Kaiser R, Johnson MC, Kaplan E, Miller J, Patterson RJ (2012) Identifying Contributions to the Stellar Halo from Accreted, Kicked-out, and In Situ Populations. *ApJ* 761:161, DOI 10.1088/0004-637X/761/2/161, [1202.5310](#)
- Shen ZX, Bonifacio P, Pasquini L, Zaggia S (2010) Li - O anti-correlation in NGC 6752: evidence for Li-enriched polluting gas. *A&A* 524:L2, DOI 10.1051/0004-6361/201015738, [1011.1718](#)
- Shetrone MD, Côté P, Sargent WLW (2001) Abundance Patterns in the Draco, Sextans, and Ursa Minor Dwarf Spheroidal Galaxies. *ApJ* 548:592–608, DOI 10.1086/319022, [astro-ph/0009505](#)
- Simion IT, Belokurov V, Koposov SE (2019) Common origin for Hercules-Aquila and Virgo Clouds in Gaia DR2. *MNRAS* 482:921–928, DOI 10.1093/mnras/sty2744, [1807.01335](#)
- Smith GH (1987) The chemical inhomogeneity of globular clusters. *PASP* 99:67–90, DOI 10.1086/131958
- Smith GH (2015) A Comparison Between the Patterns of CN, O, and Na Inhomogeneities on the Red Giant Branch of Messier 71 Using Data from the Literature. *PASP* 127:1204, DOI 10.1086/684099
- Smith GH, Briley MM (2006) CN Abundance Inhomogeneities in the Globular Cluster Messier 13 (NGC 6205): Results Based on Merged Data Sets from the Literature. *PASP* 118:740–753, DOI 10.1086/503610
- Smith GH, Martell SL (2003) Comparing Deep Mixing in Globular Cluster and Halo Field Giants: Carbon Abundance Data from the Literature. *PASP* 115:1211–1219, DOI 10.1086/378078
- Smith GH, Sneden C, Kraft RP (2002) A Study of Abundances of Four Giants in the Low-Mass Globular Cluster Palomar 5. *AJ* 123:1502–1508, DOI 10.1086/338855
- Smith VV, Suntzeff NB, Cunha K, Gallino R, Busso M, Lambert DL, Straniero O (2000) The Chemical Evolution of the Globular Cluster ω Centauri (NGC 5139). *AJ* 119:1239–1258, DOI 10.1086/301276
- Smith VV, Cunha K, Ivans II, Lattanzio JC, Campbell S, Hinkle KH (2005) Fluorine Abundance Variations in Red Giants of the Globular Cluster M4 and Early-Cluster Chemical Pollution. *ApJ* 633:392–397, DOI 10.1086/444615, [astro-ph/0506763](#)
- Sneden C, Kraft RP, Shetrone MD, Smith GH, Langer GE, Prosser CF (1997) Star-To-Star Abundance Variations Among Bright Giants in the Metal-Poor Globular Cluster M15. *AJ* 114:1964, DOI 10.1086/118618
- Sneden C, Ivans II, Kraft RP (2000) Do AGB stars differ chemically from RGB stars in globular clusters? *MSAIt* 71:657–665, [astro-ph/0001018](#)
- Sobeck JS, Kraft RP, Sneden C, Preston GW, Cowan JJ, Smith GH, Thompson IB, Sheckman SA, Burley GS (2011) The Abundances of Neutron-capture Species in the Very Metal-poor Globular Cluster M15: A Uniform Analysis of Red Giant Branch and Red Horizontal Branch Stars. *AJ* 141:175, DOI 10.1088/0004-6256/141/6/175, [1103.1008](#)
- Sollima A (2008) The evolution of the binary population in globular clusters: a full analytical computation. *MNRAS* 388:307–322, DOI 10.1111/j.1365-2966.2008.13387.x, [0804.4107](#)
- Sollima A, Pancino E, Ferraro FR, Bellazzini M, Straniero O, Pasquini L (2005) Metallicities, Relative Ages, and Kinematics of Stellar Populations in ω Centauri. *ApJ* 634:332–343, DOI 10.1086/496945, [astro-ph/0509087](#)
- Sollima A, Ferraro FR, Bellazzini M, Origlia L, Straniero O, Pancino E (2007) Deep FORS1 Observations of the Double Main Sequence of ω Centauri. *ApJ* 654:915–922, DOI 10.1086/509711, [astro-ph/0609650](#)
- Sollima A, Beccari G, Ferraro FR, Fusi Pecci F, Sarajedini A (2007b) The fraction of binary systems in the core of 13 low-density Galactic globular clusters. *MNRAS* 380:781–791, DOI 10.1111/j.1365-2966.2007.12116.x, [0706.2288](#)
- Sollima A, Carballo-Bello JA, Beccari G, Ferraro FR, Pecci FF, Lanzoni B (2010) The fraction of binary systems in the core of five Galactic open clusters. *MNRAS* 401:577–585, DOI 10.1111/j.1365-2966.2009.15676.x, [0909.1277](#)
- Souto D, Cunha K, Smith V, Allende Prieto C, Pinsonneault M, Zamora O, García-Hernández DA, Mészáros S, Bovy J, García Pérez AE, Anders F, Bizyaev D, Carrera R, Frinchaboy PM, Holtzman J, Ivans I, Majewski SR, Shetrone M, Sobeck J, Pan K, Tang B, Villanova S, Geisler D (2016) Chemical Abundances in a Sample of Red Giants in the Open Cluster NGC 2420 from APOGEE. *ApJ* 830:35, DOI 10.3847/0004-637X/830/1/35, [1607.06102](#)
- Spite M, Spite F, Gallagher AJ, Monaco L, Bonifacio P, Caffau E, Villanova S (2016) Abundances in a sample of turnoff and subgiant stars in NGC 6121 (M 4). *A&A* 594:A79, DOI 10.1051/0004-6361/

- 201628759, [1608.03541](#)
- Spitzer L Jr (1969) Equipartition and the Formation of Compact Nuclei in Spherical Stellar Systems. *ApJL* 158:L139, DOI 10.1086/180451
- Stanford LM, Da Costa GS, Norris JE, Cannon RD (2006) The Age and Metallicity Relation of ω Centauri. *ApJ* 647:1075–1092, DOI 10.1086/505571, [astro-ph/0605612](#)
- Suntzeff NB (1981) Carbon and nitrogen abundances in the giant stars of the globular clusters M3 and M13. *ApJS* 47:1–32, DOI 10.1086/190750
- Suntzeff NB, Kraft RP (1996) The Abundance Spread Among Giants and Subgiants in the Globular Cluster Omega Centauri. *AJ* 111:1913, DOI 10.1086/117930, [astro-ph/9601013](#)
- Suntzeff NB, Smith VV (1991) Carbon isotopic abundances in giant stars in the CN-bimodal globular clusters NGC 6752 and M4. *ApJ* 381:160–172, DOI 10.1086/170638
- Sweigart AV, Mengel JG (1979) Meridional circulation and CNO anomalies in red giant stars. *ApJ* 229:624–641, DOI 10.1086/156996
- Tailo M, Milone AP, Marino AF, D’Antona F, Lagioia E, Cordoni G (2019) Mass loss of different stellar populations in Globular Clusters: the case of M4. *arXiv e-prints* [1902.03803](#)
- Tang B, Geisler D, Friel E, Villanova S, Smiljanic R, Casey AR, Randich S, Magrini L, San Roman I, Muñoz C, Cohen RE, Mauro F, Bragaglia A, Donati P, Tautvaisiene G, Drazdauskas A, Ženoviene R, Snaith O, Sousa S, Adibekyan V, Costado MT, Blanco-Cuaresma S, Jiménez-Esteban F, Carraro G, Zwitter T, François P, Jofrè P, Sordo R, Gilmore G, Flaccomio E, Koposov S, Korn AJ, Lanzafame AC, Pancino E, Bayo A, Damiani F, Franciosini E, Hourihane A, Lardo C, Lewis J, Monaco L, Morbidelli L, Prisinzano L, Sacco G, Worley CC, Zaggia S (2017) The Gaia-ESO survey: the inner disk intermediate-age open cluster NGC 6802. *A&A* 601:A56, DOI 10.1051/0004-6361/201629883, [1702.01109](#)
- Tang B, Liu C, Fernández-Trincado JG, Geisler D, Shi J, Zamora O, Worthey G, Moreno E (2019) Chemical and Kinematic Analysis of CN-strong Metal-poor Field Stars in LAMOST DR3. *ApJ* 871:58, DOI 10.3847/1538-4357/aaf6b1, [1812.01656](#)
- Taylor M (2017) TOPCAT: Desktop Exploration of Tabular Data for Astronomy and Beyond. *ArXiv e-prints* [1707.02160](#)
- Tiongco MA, Vesperini E, Varri AL (2016a) Kinematical evolution of tidally limited star clusters: the role of retrograde stellar orbits. *MNRAS* 461(1):402–411, DOI 10.1093/mnras/stw1341, [1606.06743](#)
- Tiongco MA, Vesperini E, Varri AL (2016b) Velocity anisotropy in tidally limited star clusters. *MNRAS* 455:3693–3701, DOI 10.1093/mnras/stv2574, [1511.02236](#)
- Tiongco MA, Vesperini E, Varri AL (2017) Kinematical evolution of tidally limited star clusters: rotational properties. *MNRAS* 469:683–692, DOI 10.1093/mnras/stx853, [1704.05918](#)
- Tiongco MA, Vesperini E, Varri AL (2019) Kinematical evolution of multiple stellar populations in star clusters. *MNRAS* 455:3693–3701, DOI 10.1093/mnras/stv2574, [1511.02236](#)
- Tomkin J, Lambert DL, Lemke M (1993) The Chemical Composition of Algol Systems - Part Five - Confirmation of Carbon Deficiencies in the Primaries of Eight Systems. *MNRAS* 265:581, DOI 10.1093/mnras/265.3.581
- Torrealba G, Belokurov V, Koposov SE (2019) Nine tiny star clusters in Gaia DR1, PS1, and DES. *MNRAS* 484:2181–2197, DOI 10.1093/mnras/stz071, [1805.06473](#)
- Trenti M, Heggie DC, Hut P (2007) Star clusters with primordial binaries - II. Dynamical evolution of models in a tidal field. *MNRAS* 374:344–356, DOI 10.1111/j.1365-2966.2006.11166.x, [astro-ph/0602409](#)
- Trenti M, Vesperini E, Pasquato M (2010) Tidal Disruption, Global Mass Function, and Structural Parameter Evolution in Star Clusters. *ApJ* 708(2):1598–1610, DOI 10.1088/0004-637X/708/2/1598, [0911.3394](#)
- Umeda H, Yoshida T (2017) Nucleosynthesis in Spherical Explosion Models of Core-Collapse Supernovae. In: Alsabti AW, Murdin P (eds) *Handbook of Supernovae*, Springer, Cham, p 1753, DOI 10.1007/978-3-319-21846-5_76
- van den Bergh S (1967) On the Helium Abundance in the Proto-Galaxy. *PASP* 79:460, DOI 10.1086/128531
- Vanbeveren D, Mennekens N, De Greve JP (2012) The effect of intermediate-mass close binaries on the chemical evolution of globular clusters. *A&A* 543:A4, DOI 10.1051/0004-6361/201118081, [1109.2713](#)
- VandenBerg DA, Brogaard K, Leaman R, Casagrande L (2013) The Ages of 55 Globular Clusters as Determined Using an Improved $\Delta V_{HB,TO}$ Method along with Color-Magnitude Diagram Constraints, and Their Implications for Broader Issues. *ApJ* 775:134, DOI 10.1088/0004-637X/775/2/

- 134, [1308.2257](#)
- Vassiliadis E, Wood PR (1993) Evolution of low- and intermediate-mass stars to the end of the asymptotic giant branch with mass loss. *ApJ* 413:641–657, DOI 10.1086/173033
- Veljanoski J, Helmi A (2018) Flavours in the box of chocolates: chemical abundances of kinematic sub-structures in the nearby stellar halo. arXiv e-prints [1804.06365](#)
- Ventura P, D’Antona F, Mazzitelli I, Gratton R (2001) Predictions for Self-Pollution in Globular Cluster Stars. *ApJL* 550:L65–L69, DOI 10.1086/319496, [astro-ph/0103337](#)
- Ventura P, Caloi V, D’Antona F, Ferguson J, Milone A, Piotto GP (2009) The C+N+O abundances and the splitting of the subgiant branch in the globular cluster NGC 1851. *MNRAS* 399:934–943, DOI 10.1111/j.1365-2966.2009.15335.x, [0907.1765](#)
- Ventura P, D’Antona F, Di Criscienzo M, Carini R, D’Ercole A, vesperini E (2012) Super-AGB-AGB Evolution and the Chemical Inventory in NGC 2419. *ApJL* 761:L30, DOI 10.1088/2041-8205/761/2/L30, [1211.3857](#)
- Verbunt F, Lewin WHG, van Paradijs J (1989) Millisecond radio pulsars in globular clusters. *MNRAS* 241:51–57, DOI 10.1093/mnras/241.1.51
- Vesperini E, Heggie DC (1997) On the effects of dynamical evolution on the initial mass function of globular clusters. *MNRAS* 289(4):898–920, DOI 10.1093/mnras/289.4.898, [astro-ph/9705073](#)
- Vesperini E, McMillan SLW, D’Antona F, D’Ercole A (2010) The Fraction of Globular Cluster Second-generation Stars in the Galactic Halo. *ApJL* 718:L112–L116, DOI 10.1088/2041-8205/718/2/L112, [1007.1668](#)
- Vesperini E, McMillan SLW, D’Antona F, D’Ercole A (2011) Binary star disruption in globular clusters with multiple stellar populations. *MNRAS* 416:355–360, DOI 10.1111/j.1365-2966.2011.19046.x, [1106.0756](#)
- Vesperini E, McMillan SLW, D’Antona F, D’Ercole A (2013) Dynamical evolution and spatial mixing of multiple population globular clusters. *MNRAS* 429:1913–1921, DOI 10.1093/mnras/sts434, [1212.2651](#)
- Vesperini E, Hong J, Webb JJ, D’Antona F, D’Ercole A (2018) Evolution of the stellar mass function in multiple-population globular clusters. *MNRAS* 476(2):2731–2742, DOI 10.1093/mnras/sty407, [1803.02381](#)
- Villanova S, Piotto G, Gratton RG (2009) The helium content of globular clusters: light element abundance correlations and HB morphology. I. NGC 6752. *A&A* 499:755–763, DOI 10.1051/0004-6361/200811493, [0903.3924](#)
- Villanova S, Geisler D, Carraro G, Moni Bidin C, Muñoz C (2013) Ruprecht 106: The First Single Population Globular Cluster? *ApJ* 778:186, DOI 10.1088/0004-637X/778/2/186, [1310.5900](#)
- Villanova S, Geisler D, Gratton RG, Cassisi S (2014) The Metallicity Spread and the Age-Metallicity Relation of ω Centauri. *ApJ* 791:107, DOI 10.1088/0004-637X/791/2/107, [1406.5069](#)
- Villanova S, Monaco L, Moni Bidin C, Assmann P (2016) A spectroscopic study of the globular Cluster NGC 4147. *MNRAS* 460:2351–2359, DOI 10.1093/mnras/stw1146, [1605.03408](#)
- Villanova S, Moni Bidin C, Mauro F, Muñoz C, Monaco L (2017) A spectroscopic study of the globular cluster M28 (NGC 6626). *MNRAS* 464:2730–2740, DOI 10.1093/mnras/stw2509, [1610.01834](#)
- Villanova S, Carraro G, Geisler D, Monaco L, Assmann P (2018) NGC 6791: A Probable Bulge Cluster without Multiple Populations. *ApJ* 867:34, DOI 10.3847/1538-4357/aae4e5, [1809.09661](#)
- Wang B, Han Z (2012) Progenitors of type Ia supernovae. *New Astron Rev* 56:122–141, DOI 10.1016/j.newar.2012.04.001, [1204.1155](#)
- Wang Y, Primas F, Charbonnel C, Van der Swaelmen M, Bono G, Chantereau W, Zhao G (2016) Sodium abundances of AGB and RGB stars in Galactic globular clusters. I. Analysis and results of NGC 2808. *A&A* 592:A66, DOI 10.1051/0004-6361/201628502, [1606.00973](#)
- Wang Y, Primas F, Charbonnel C, Van der Swaelmen M, Bono G, Chantereau W, Zhao G (2017) Sodium abundances of AGB and RGB stars in Galactic globular clusters. II. Analysis and results of NGC 104, NGC 6121, and NGC 6809. *A&A* 607:A135, DOI 10.1051/0004-6361/201730976, [1708.07634](#)
- Webb JJ, Reina-Campos M, Kruijssen JMD (2018) A systematic analysis of star cluster disruption by tidal shocks – I. Controlled N-body simulations and a new theoretical model. arXiv e-prints [1812.00014](#)
- Wilson OC, Aly MK (1956) The Possible Occurrence of λ 5876 of He I in Absorption in the Spectra of Certain Late-Type Stars. *PASP* 68:149, DOI 10.1086/126901
- Woolley RVDR (1966) Studies of the globular cluster [omega] Centauri I. *R Obs Ann* 2
- Worley CC, Hill V, Sobek J, Carretta E (2013) Ba and Eu abundances in M 15 giant stars. *A&A* 553:A47, DOI 10.1051/0004-6361/201321097, [1302.6122](#)
- Yan L, Reid IN (1996) Discovery of six short-period eclipsing binaries in the globular cluster M5. *MNRAS*

- 279:751–766, DOI 10.1093/mnras/279.3.751
- Yong D, Grundahl F (2008) An Abundance Analysis of Bright Giants in the Globular Cluster NGC 1851. *ApJL* 672:L29, DOI 10.1086/525850, [0711.1394](#)
- Yong D, Grundahl F, Johnson JA, Asplund M (2008a) Nitrogen Abundances in Giant Stars of the Globular Cluster NGC 6752. *ApJ* 684:1159–1169, DOI 10.1086/590658, [0806.0187](#)
- Yong D, Meléndez J, Cunha K, Karakas AI, Norris JE, Smith VV (2008b) Chemical Abundances in Giant Stars of the Tidally Disrupted Globular Cluster NGC 6712 from High-Resolution Infrared Spectroscopy. *ApJ* 689:1020–1030, DOI 10.1086/592229, [0807.4558](#)
- Yong D, Grundahl F, D’Antona F, Karakas AI, Lattanzio JC, Norris JE (2009) A Large C+N+O Abundance Spread in Giant Stars of the Globular Cluster NGC 1851. *ApJL* 695:L62–L66, DOI 10.1088/0004-637X/695/1/L62, [0902.1773](#)
- Yong D, Alves Brito A, Da Costa GS, Alonso-García J, Karakas AI, Pignatari M, Roederer IU, Aoki W, Fishlock CK, Grundahl F, Norris JE (2014a) Chemical abundances in bright giants of the globular cluster M62 (NGC 6266). *MNRAS* 439:2638–2650, DOI 10.1093/mnras/stu118, [1401.3784](#)
- Yong D, Roederer IU, Grundahl F, Da Costa GS, Karakas AI, Norris JE, Aoki W, Fishlock CK, Marino AF, Milone AP, Shingles LJ (2014b) Iron and neutron-capture element abundance variations in the globular cluster M2 (NGC 7089). *MNRAS* 441:3396–3416, DOI 10.1093/mnras/stu806, [1404.6873](#)
- Yong D, Grundahl F, Norris JE (2015) CNO abundances in the globular clusters NGC 1851 and NGC 6752. *MNRAS* 446:3319–3329, DOI 10.1093/mnras/stu2334, [1411.1474](#)
- Yong D, Da Costa GS, Norris JE (2016) Confirming the intrinsic abundance spread in the globular cluster NGC 6273 (M19) with calcium triplet spectroscopy. *MNRAS* 460:1846–1853, DOI 10.1093/mnras/stw1091, [1603.08606](#)
- Yuan Z, Smith MC, Xue XX, Li J, Liu C, Wang Y, Li L, Chang J (2019) Revealing the Complicated Story of the Cetus Stream with StarGO. *ApJ* 881(2):164, DOI 10.3847/1538-4357/ab2e09, [1902.05248](#)
- Zamora-Avilés M, Vázquez-Semadeni E (2014) An Evolutionary Model for Collapsing Molecular Clouds and their Star Formation Activity. II. Mass Dependence of the Star Formation Rate. *ApJ* 793:84, DOI 10.1088/0004-637X/793/2/84, [1308.4918](#)
- Zennaro M, Milone AP, Marino AF, Cordoni G, Lagioia EP, Tailo M (2019) Four stellar populations and extreme helium variation in the massive outer-halo globular cluster NGC 2419. *arXiv e-prints* [1902.02178](#)
- Zhang H, de Grijs R, Li C, Wu X (2018) No Evidence of Chemical Abundance Variations in the Intermediate-age Cluster NGC 1783. *ApJ* 853:186, DOI 10.3847/1538-4357/aaa428, [1712.08161](#)

10 Appendix 1: Summary of data for Milky Way GCs

This Appendix collects data for galactic GCs used in this review. We give information on the references used for the columns in Table 6, 7, and 8 in the following.

For Table 6:

- Col 1: Designation
- Col 2-3: R_{per} and R_{apo} in kpc from [Baumgardt et al. \(2019\)](#)
- Col 4-5-6-7-8-9: dMY, Ymed, Ymax, Ymax-Ymed, delta(B-V), delta(V-I) from [Gratton et al. \(2010a\)](#)

For Table 7:

- Col 1: Designation
- Col 2-3-4-5: dY2g1G, err, dYmax, err from [Milone et al. \(2018c\)](#) and [Zennaro et al. \(2019\)](#)
- Col 6: [Fe/H] from [Carretta \(2019\)](#)
- Col 7-8: d[Fe/H], err from [Bragaglia et al. \(2010a\)](#) (NGC 6402 from [Johnson et al. 2019](#))
- Col 9-10: $\log M_{\text{fin}}$, $\log M_{\text{in}}$ from [Baumgardt et al. \(2019\)](#)

For Table 8:

- Col 1: Designation
- Col 2-3: IQR(Na/O), Source: (1) Gratton et al. (2006, 2007); Carretta et al. (2007, 2009c,b, 2010b, 2011b, 2013a, 2014, 2015, 2017); Bragaglia et al. (2015, 2017); Carretta et al. (2018) (2) Villanova et al. (2016); (3) San Roman et al. (2015); (4) Boberg et al. (2015, 2016); (5) Marino et al. (2011a); (6) Kraft et al. (1992); (7) Marino et al. (2015); (8) Smith et al. (2002); (9) Mucciarelli et al. (2013); (10) Pancino et al. (2017); (11) Koch and McWilliam (2014); (12) Johnson et al. (2016); (13) Johnson et al. (2017a); (14) Johnson et al. (2017b); (15) Johnson et al. (2015); (16) Yong et al. (2014a); (17) Feltzing et al. (2009); (18) Mucciarelli et al. (2016); Massari et al. (2017); (19) Muñoz et al. (2017); (20) Villanova et al. (2017); (21) Marino et al. (2009); (22) O’Malley et al. (2017); (23) Kacharov et al. (2013); (24) Kraft et al. (1998); (25) Yong et al. (2014b); (26) Çalışkan et al. (2012); (27) Cohen (2004); (28) Villanova et al. (2013); (29) Muñoz et al. (2018); (30) Mucciarelli et al. (2018); (31) Johnson et al. (2018); (32) Sbordone et al. (2007); (33) Johnson et al. (2019)
- Col 4: IQR(Al/Mg) from Carretta et al. (2010b) and others determination from this group; only 1 digit: Mészáros et al. (2015)
- Col 5-6-7-8-9: dRGB, err, f(FG), err, GC type from Milone et al. (2017a) and Zennaro et al. (2019)
- Col 10: spectroscopic d[Al/Mg] from Milone et al. (2018c)

11 Appendix 2: Summary of data for MC clusters

This Appendix collects data for extra-galactic massive clusters used in this review. References for individual columns are as follows:

- Age: SMC: Glatt et al. (2008); Martocchia et al. (2017)
- LMC: Age/[Fe/H]/Mass: Mackey and Gilmore (2003a); Ferraro et al. (2006a); Niederhofer et al. (2016); Martocchia et al. (2018a)
- Fornax: Age/[Fe/H]/Mass: Mackey and Gilmore (2003b)
- Mass and Metallicity: Glatt et al. (2011)
- dCUnBI: Martocchia et al. (2017)
- Hodge 11: [Fe/H]: Mateluna et al. (2012)

Table 6 Main parameters for selected GCs

| Name | R_{per} (kpc) | R_{apo} (kpc) | dMY | Y^{med} | Y^{max} | $Y^{max} - Y^{med}$ | Δ ($B - V$) | Δ ($V - I$) |
|----------|--------------------|--------------------|-------|-----------|-----------|---------------------|-------------------------|-------------------------|
| NGC 104 | 5.46 | 7.44 | 0.0 | 0.234 | 0.234 | 0.0 | 0.0 | 0.0 |
| NGC 288 | 3.33 | 13.01 | 0.016 | 0.280 | 0.292 | 0.012 | 0.005 | 0.007 |
| NGC 362 | 1.05 | 12.48 | 0.059 | 0.243 | 0.289 | 0.046 | 0.018 | 0.025 |
| NGC 1261 | 1.41 | 19.93 | 0.068 | 0.244 | 0.297 | 0.053 | 0.021 | 0.029 |
| Eridanus | 33.56 | 134.93 | | | | | | |
| Pal 2 | 2.49 | 39.41 | | | | | | |
| NGC 1851 | 0.83 | 19.13 | 0.063 | 0.247 | 0.295 | 0.048 | 0.019 | 0.027 |
| NGC 1904 | 0.82 | 19.49 | 0.055 | 0.274 | 0.317 | 0.043 | 0.018 | 0.022 |
| NGC 2298 | 1.86 | 17.74 | 0.0 | 0.249 | 0.249 | 0.000 | 0.0 | 0.0 |
| NGC 2419 | 16.52 | 90.96 | | | | | | |
| NGC 2808 | 0.97 | 14.72 | 0.08 | 0.273 | 0.334 | 0.061 | 0.024 | 0.034 |
| Pal 3 | 65.31 | 124.42 | | | | | | |
| NGC 3201 | 8.15 | 23.54 | 0.032 | 0.253 | 0.278 | 0.025 | 0.010 | 0.013 |
| Pal 4 | 23.66 | 111.35 | | | | | | |
| NGC 4147 | 1.92 | 24.57 | 0.014 | 0.247 | 0.258 | 0.011 | 0.005 | 0.006 |
| NGC 4372 | 2.94 | 7.20 | 0.026 | 0.254 | 0.275 | 0.021 | 0.009 | 0.010 |
| Rup 106 | 4.71 | 35.18 | | | | | | |
| NGC 4590 | 8.86 | 29.20 | 0.036 | 0.228 | 0.257 | 0.029 | 0.012 | 0.013 |
| NGC 4833 | 0.79 | 7.39 | 0.078 | 0.246 | 0.308 | 0.062 | 0.026 | 0.030 |
| NGC 5024 | 9.09 | 21.96 | 0.0 | 0.241 | 0.241 | 0.0 | 0.0 | 0.0 |
| NGC 5053 | 10.28 | 17.69 | 0.017 | 0.234 | 0.248 | 0.014 | 0.006 | 0.006 |
| NGC 5139 | 1.35 | 7.00 | | | | | | |
| NGC 5272 | 5.44 | 15.14 | 0.030 | 0.249 | 0.272 | 0.023 | 0.009 | 0.012 |
| NGC 5286 | 1.16 | 13.27 | | | | | | |
| NGC 5466 | 7.95 | 65.53 | 0.0 | 0.223 | 0.223 | 0.000 | 0.0 | 0.0 |
| NGC 5634 | 4.27 | 23.91 | | | | | | |
| NGC 5694 | 3.98 | 66.04 | 0.028 | 0.246 | 0.268 | 0.022 | 0.009 | 0.010 |
| IC 4499 | 6.38 | 27.67 | | | | | | |
| NGC 5824 | 15.17 | 38.26 | 0.066 | 0.246 | 0.299 | 0.053 | 0.022 | 0.025 |
| Pal 5 | 17.40 | 24.30 | | | | | | |
| NGC 5897 | 2.86 | 9.31 | 0.0 | 0.253 | 0.253 | 0.000 | 0.0 | 0.0 |
| NGC 5904 | 2.90 | 24.20 | 0.040 | 0.262 | 0.293 | 0.031 | 0.012 | 0.017 |
| NGC 5927 | 3.99 | 5.42 | 0.011 | 0.250 | 0.256 | 0.006 | 0.002 | 0.004 |
| NGC 5946 | 0.83 | 5.82 | 0.054 | 0.258 | 0.300 | 0.042 | 0.017 | 0.023 |
| NGC 5986 | 0.67 | 5.05 | 0.085 | 0.261 | 0.328 | 0.067 | 0.027 | 0.034 |
| Lynga 7 | 1.91 | 4.56 | | | | | | |
| Pal 14 | 3.90 | 94.81 | | | | | | |
| NGC 6093 | 0.35 | 3.52 | 0.087 | 0.252 | 0.321 | 0.069 | 0.028 | 0.034 |
| NGC 6101 | 11.37 | 46.89 | 0.0 | 0.250 | 0.250 | 0.000 | 0.0 | 0.0 |
| NGC 6121 | 0.55 | 6.16 | 0.030 | 0.238 | 0.261 | 0.023 | 0.009 | 0.013 |
| NGC 6139 | 1.34 | 3.52 | | | | | | |
| NGC 6144 | 2.27 | 3.36 | | | | | | |

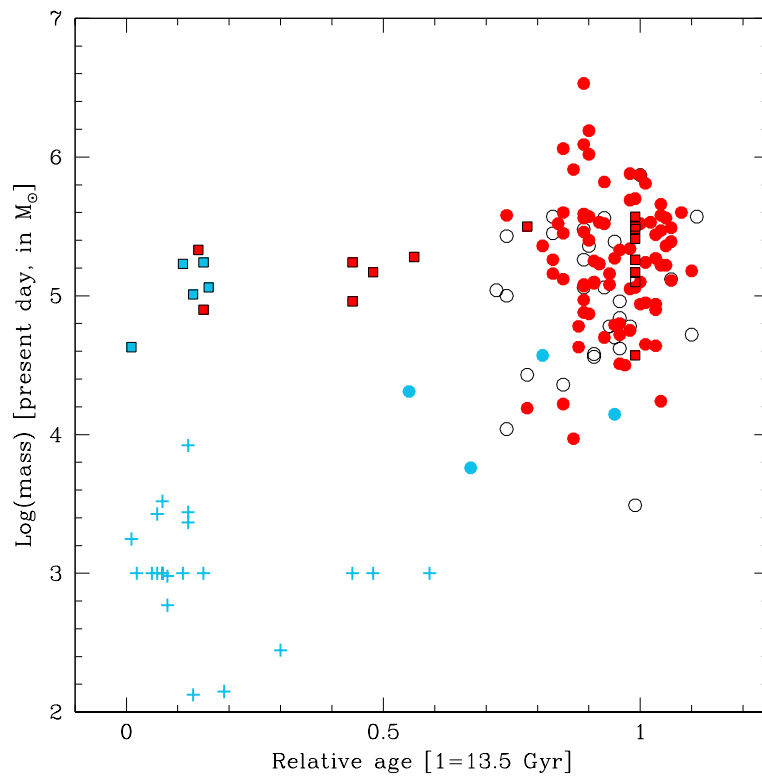


Fig. 8 Relative age (where 1=13.5 Gyr) versus the logarithm of the present-day cluster mass for MW GCs (open and filled circles), MW satellites GCs (SMC, LMC, Fornax; filled squares), and open clusters (plus signs; whenever the mass was not available from Piskunov et al. 2008, we adopted $\text{Log}(\text{mass})=3$). Open symbols indicate no information on MP, red and light blue colour indicates the presence or absence of MPs, respectively. All open clusters are single populations, while GCs in the MCs may show multiple populations even at comparable ages.

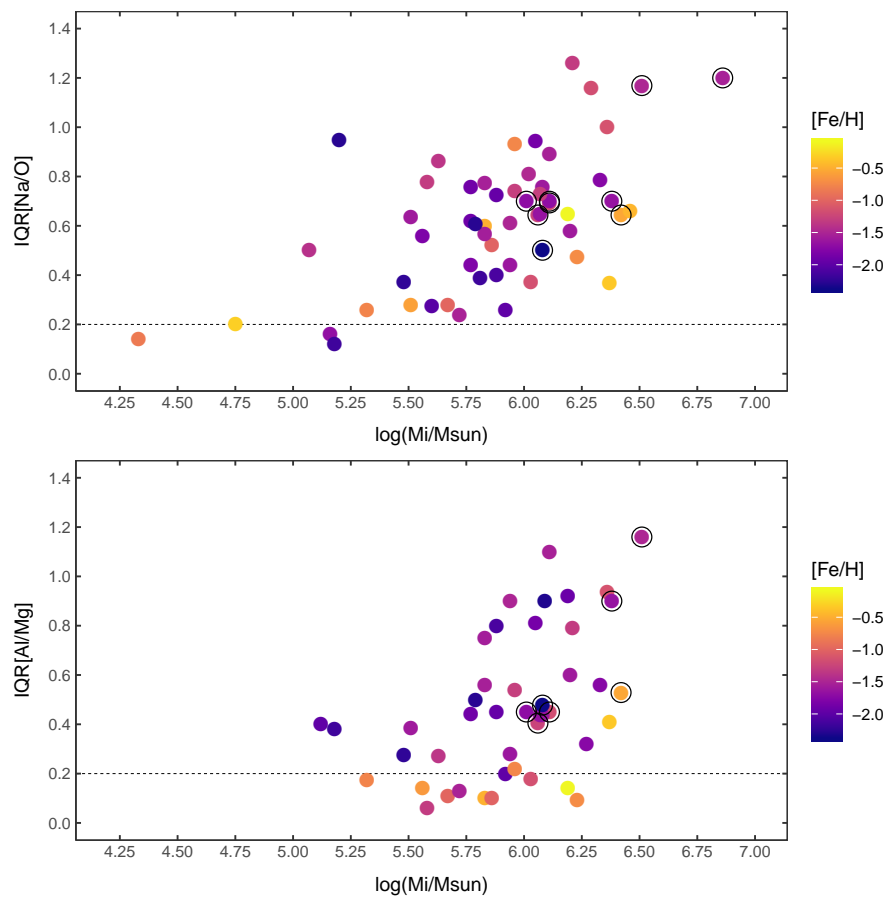


Fig. 9 Upper panel: run of the interquartile $\text{IQR}[\text{Na}/\text{O}]$ of the distribution of $[\text{Na}/\text{O}]$ abundance ratios within a cluster (see compilation in the Appendix) and the initial cluster mass from [Baumgardt et al. \(2019\)](#). Lower panel: the same, but for the interquartile $\text{IQR}[\text{Al}/\text{Mg}]$ of $[\text{Al}/\text{Mg}]$ abundance ratios. Circled symbols are for Type II clusters according to the classification by [Milone et al. \(2017a\)](#). Colours code metallicity (see scale on the right of the plot). Points below the dashed lines are actually consistent with no spread at all.

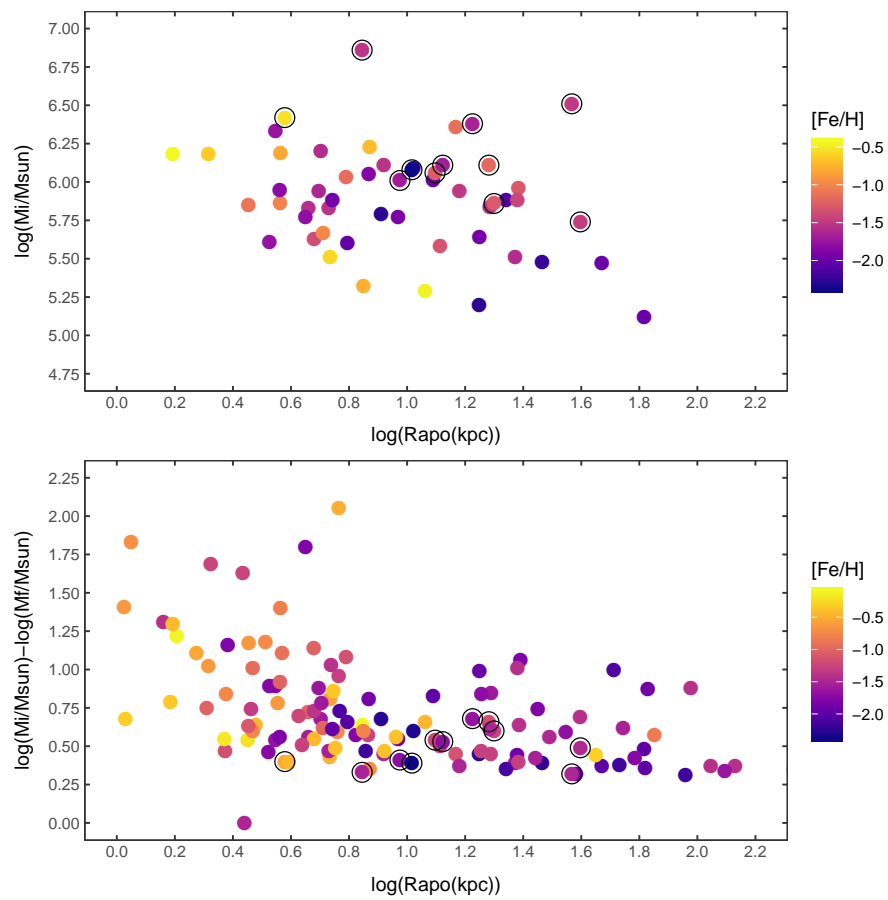


Fig. 10 Upper panel: run of the initial mass of GCs (Baumgardt et al. 2019) with the apocenter of their orbit (Baumgardt et al. 2019); lower panel: same for the mass lost by the GCs. Circled symbols are for Type II clusters according to the classification by Milone et al. (2017a). Colours code metallicity (see scale on the right of the plot)

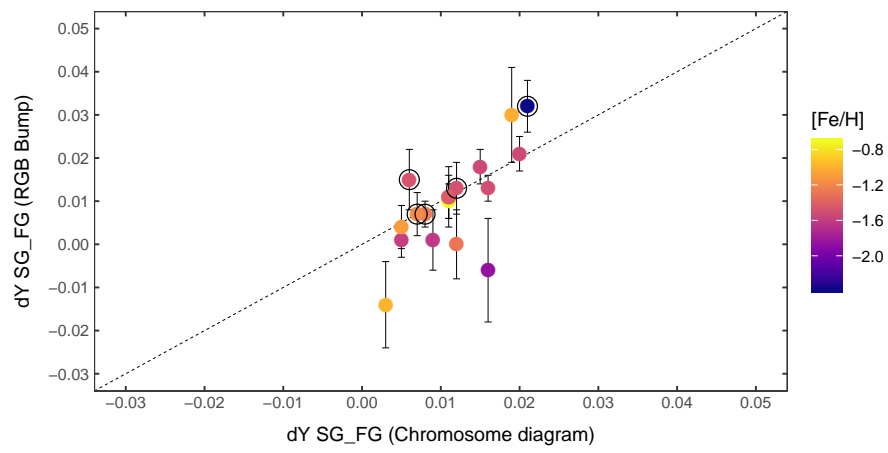


Fig. 11 Comparison between the difference in He abundances between second and first generation stars obtained from the chromosome map (Milone et al. 2018c) and from the luminosity of the RGB bump (Lagioia et al. 2018). Circled symbols are for Type II clusters. Colours code metallicity (see scale on the right of the plot). The overlaid dashed line represents equality.

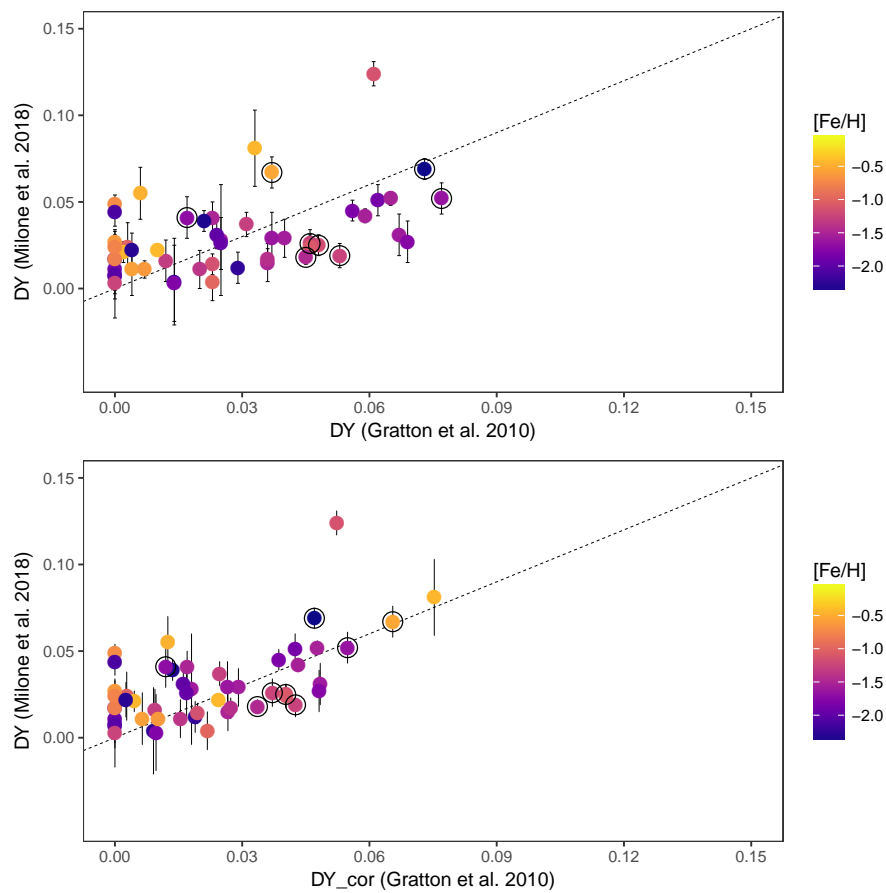


Fig. 12 Upper panel: comparison between the spread in He abundances within a cluster as obtained from the analysis of the horizontal branch (Gratton et al. 2010a) and from the main sequence stars (Milone et al. 2018c). Circled symbols are for Type II clusters according to the classification by Milone et al. (2017a). Colours code metallicity (see scale on the right of the plot). Lower panel: the same, after the systematic correction to the He abundance spread suggested in the text.

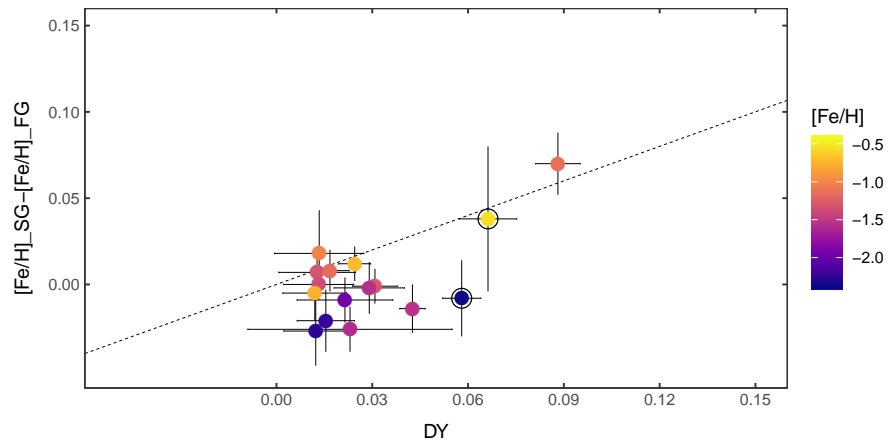


Fig. 13 Comparison between the spread in He abundances within a cluster (see text) and difference in [Fe/H] values between First and Second generation stars determined by [Bragaglia et al. \(2010a\)](#). Colours code metallicity (see scale on the right of the plot). The line is the expected correlation between these two quantities.

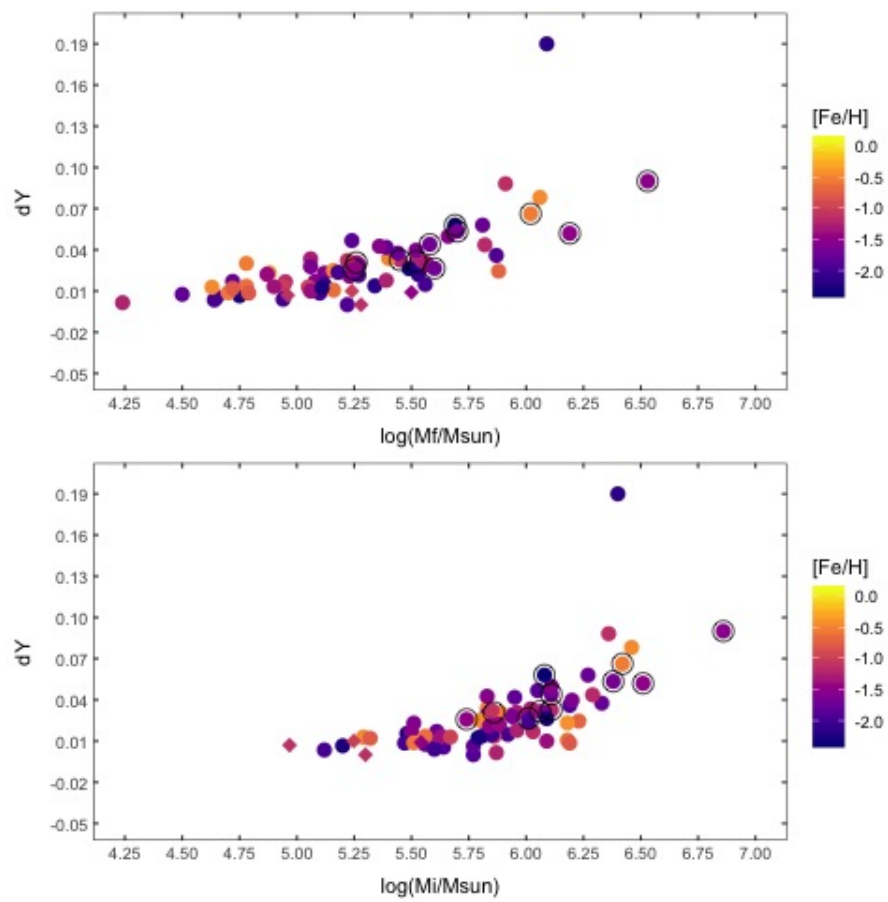


Fig. 14 Upper panel: run of the spread in He abundances within a cluster ΔY and the cluster mass from Baumgardt et al. (2019). Lower panel: the same, but using the initial mass from Baumgardt et al. (2019). The most discrepant case is NGC 2419. Diamonds and circled symbols indicate respectively MC clusters and Type II clusters. Colours code metallicity (see scale on the right of the plot)

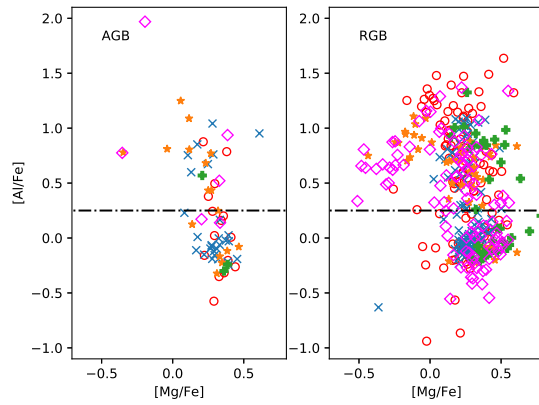


Fig. 15 $[Al/Fe]$ vs $[Mg/Fe]$ for early AGB (left-hand panel) and RGB stars (right-hand panel) by [Masseron et al. \(2019\)](#). Symbols are as follows: empty circles (M 13=NGC 6205), crosses (M 3=NGC 5272), starred symbols (M 92=NGC 6341), plus (M 53=NGC 5024) and diamonds (M 15=NGC 7078). The horizontal, dot-dashed line marks our definition of Al-rich/Al-poor population at $[Al/Fe]=+0.25$ dex.

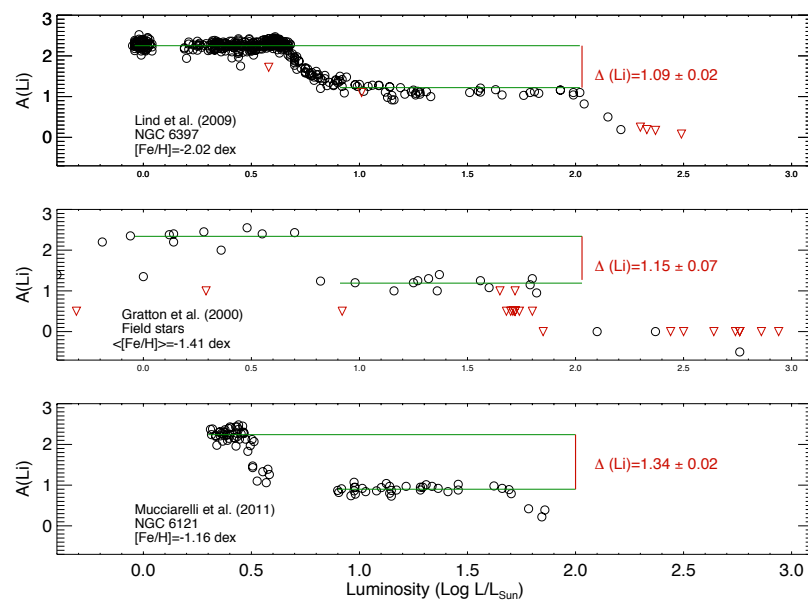


Fig. 16 Lithium evolution for field stars (middle panel) analysed by Gratton et al. (2000), NGC 6397 (upper panel) by Lind et al. (2009), and NGC 6121 (lower panel) by Mucciarelli et al. (2011). The $\Delta(\text{Li})$ represents the difference in abundances between main-sequence stars and sub giants because of the *first dredge-up*: this values depends on metallicity, being $[\text{Fe}/\text{H}] = -1.41$ dex the average for the field stars, $[\text{Fe}/\text{H}] = -2.02$ dex and $[\text{Fe}/\text{H}] = -1.16$ for NGC 6397 and NGC 6121, respectively.

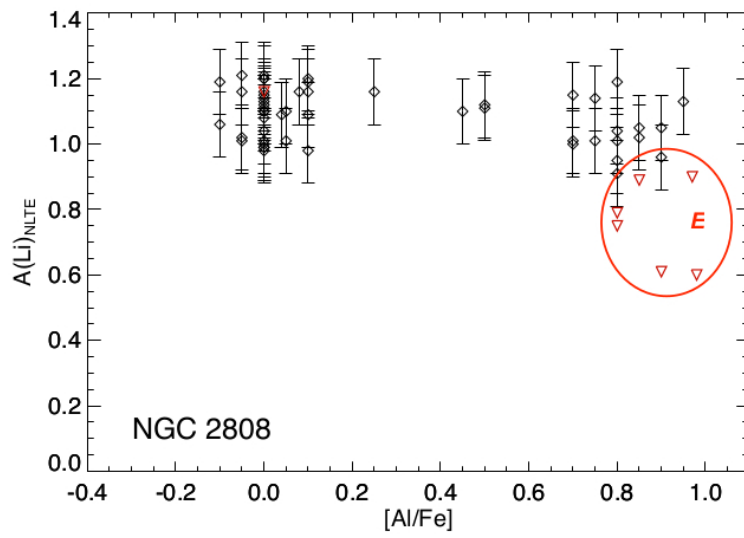


Fig. 17 Lithium as a function of aluminum abundances in RGB stars (below the bump) in NGC 2808 (re-adapted from [D’Orazi et al. 2015](#)). Upper limits in Li abundances are marked as upside-down triangles. The orange circle marks some stars belonging to the E-group, that is, have extreme composition along the $[\text{Na}/\text{O}]$ anticorrelation (for an exact definition see [Carretta et al. 2009c](#)) that are Li-poor.

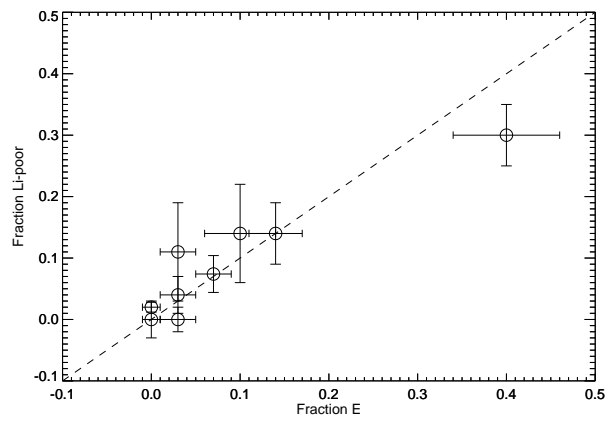


Fig. 18 Run of the fraction of Li-poor stars with the fraction of E-stars. Dashed line represents equality

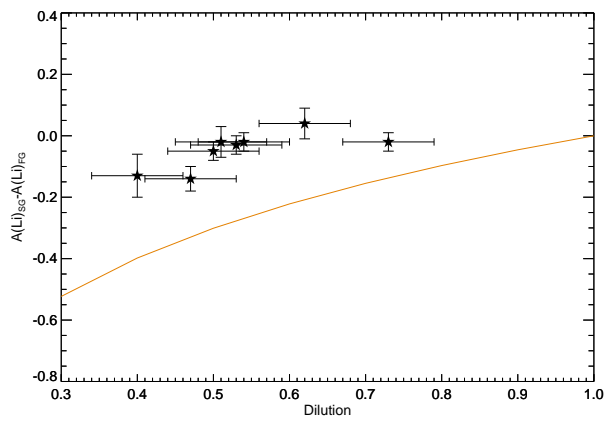


Fig. 19 Differences in Li abundances between first and intermediate second-generation stars as a function of dilution factors. Data are for clusters: NGC 362, NGC 1904, NGC 2808, NGC 5904, NGC 6121, NGC 6218, NGC 6397, NGC 6752 (see Table 2 for the corresponding references). The orange continuous line is the dilution process calculated under the assumption that there is no Li production within the polluters.

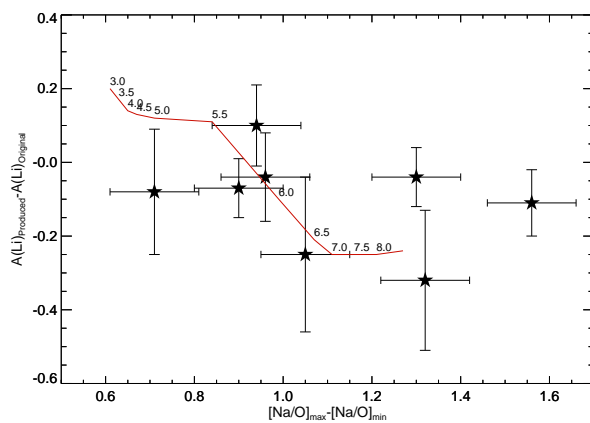


Fig. 20 Difference between Li abundances in the ejecta of the polluters and original Li abundances as a function of difference between the $[\text{Na}/\text{O}]$ ratio in the polluter and in the original material from which GC formed in a number of GCs. Red lines are predictions from models by [D'Antona et al. \(2012\)](#). These authors give Li production for stars of different masses. Since stars over a range of mass are likely to be involved in any pollution mechanism, we produced average values from these predictions weighting results for different masses using a [Kroupa \(2002\)](#) mass function; the average was done over a mass range of $[-2, 2] M_{\odot}$ around each value of the mass. The labels written over the line indicates the mean values considered.

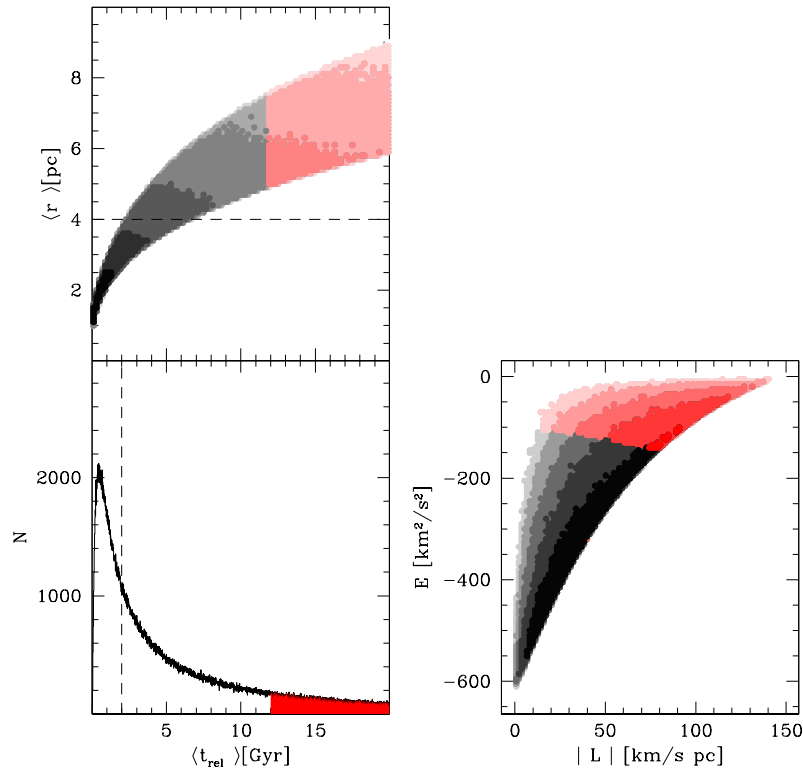


Fig. 21 Bottom left: Distribution of orbit-averaged relaxation times in a simulated cluster with $M = 5 \times 10^5 M_{\odot}$, $m = 0.5 M_{\odot}$, $r_h = 4$ pc and a King (1966) model profile with $W_0 = 5$. The half-mass relaxation time is indicated by the dashed line. Top left: distribution of orbit-averaged relaxation times as a function of the mean distance from the cluster center. Right: Distribution of particles in the E-L plane. The red area mark the region occupied by particles with $t > 12$ Gyr. Darker contours indicate regions with increasing density in logarithmic steps.

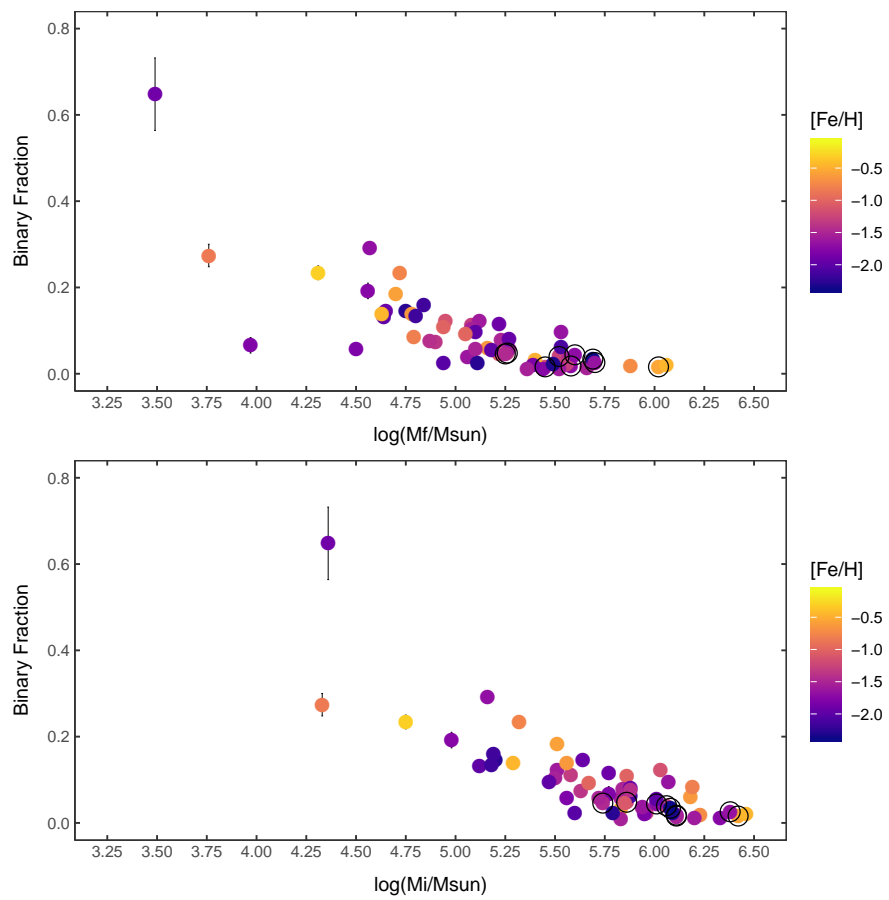


Fig. 22 Upper panel: run of binaries within a cluster (Milone et al. 2012c, 2016) and the cluster mass from Baumgardt et al. (2019). Lower panel: the same, but using the initial mass from Baumgardt et al. (2019). Circled symbols are for Type II clusters defined as in Milone et al. (2017a). Colours code metallicity (see scale on the right of the plot)

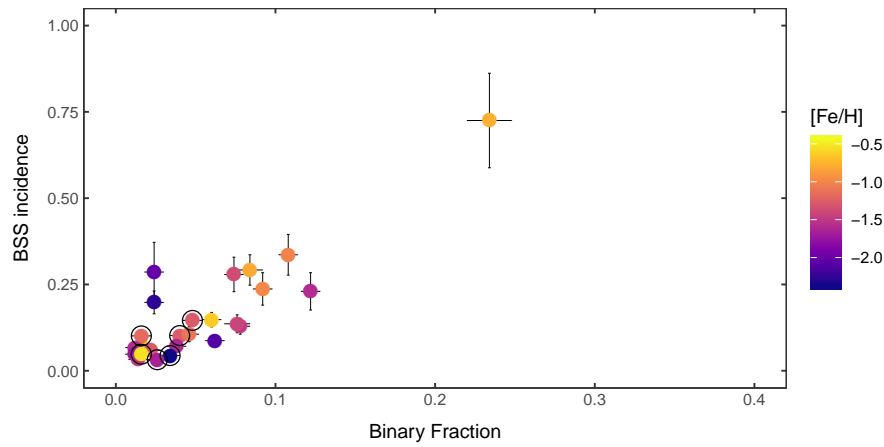


Fig. 23 Correlation between the fraction of binaries (Milone et al. 2012c, 2016) and the incidence of BSS (number of blue stragglers per 100 L_{\odot} in the same area: Moretti et al. 2008). Circled symbols are Type II clusters defined as in Milone et al. (2017a). Colours code metallicity (see scale on the right of the plot)

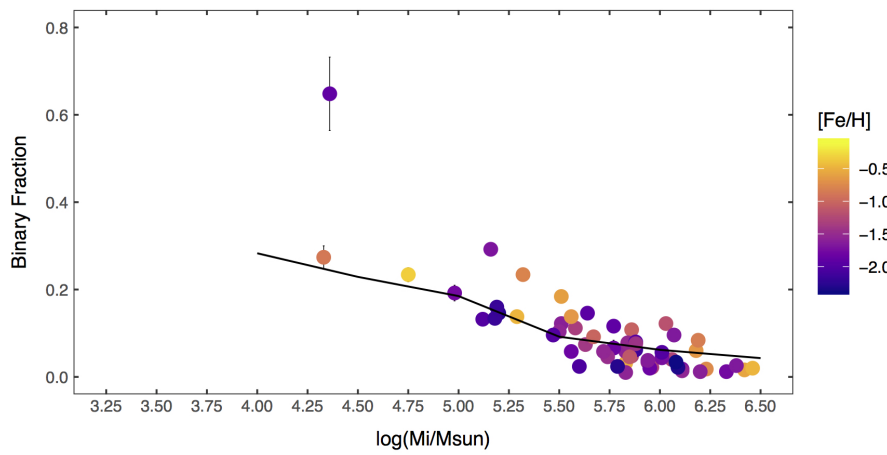


Fig. 24 Run of the fraction of binaries within a cluster (Milone et al. 2012c, 2016) with the cluster initial mass from Baumgardt et al. (2019). Circled symbols are for Type II clusters defined as in Milone et al. (2017a). Colours code metallicity (see scale on the right of the plot). The black line is the prediction with obtained with a simple model for binary destruction - see Section 7.3.

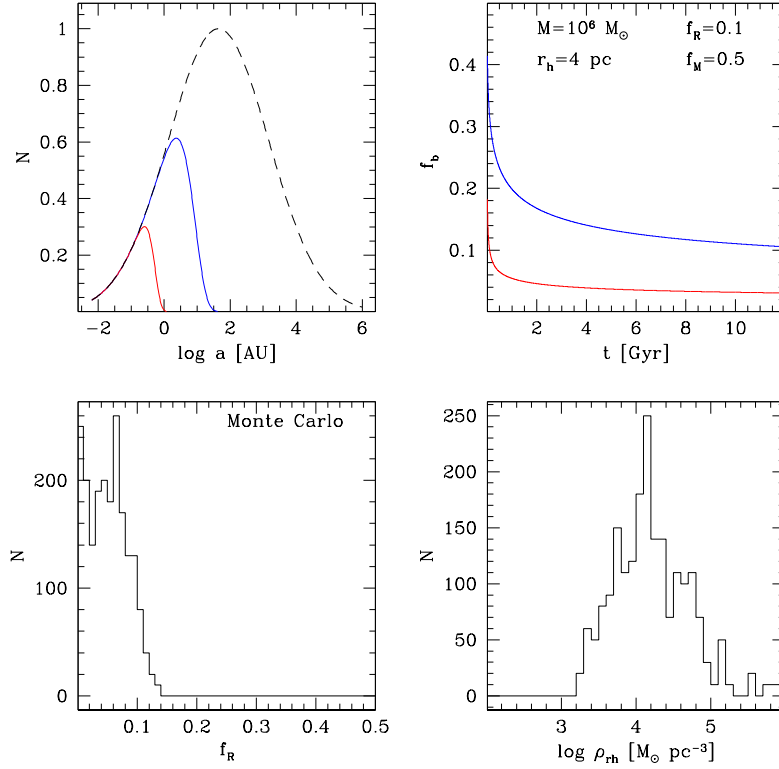


Fig. 25 Top panels: semi-major axes distribution (top-left) and binary fraction as a function of time (top-right) for the toy model simulation with $M = 10^6 M_\odot$, $r_h = 4$ pc, $f_M = 0.5$ and $f_R = 0.1$. Blue and red lines indicate predictions for the FG and SG, respectively, while the black dashed line indicates the original distribution at birth. Bottom panels: distribution of f_R (bottom-left) and $\log \rho_{th}$ for the Monte Carlo toy model simulations corresponding to final FG binary fractions $5\% < f_{b,FG} < 10\%$ and ratio $f_{b,SG}/f_{b,FG} < 0.2$.

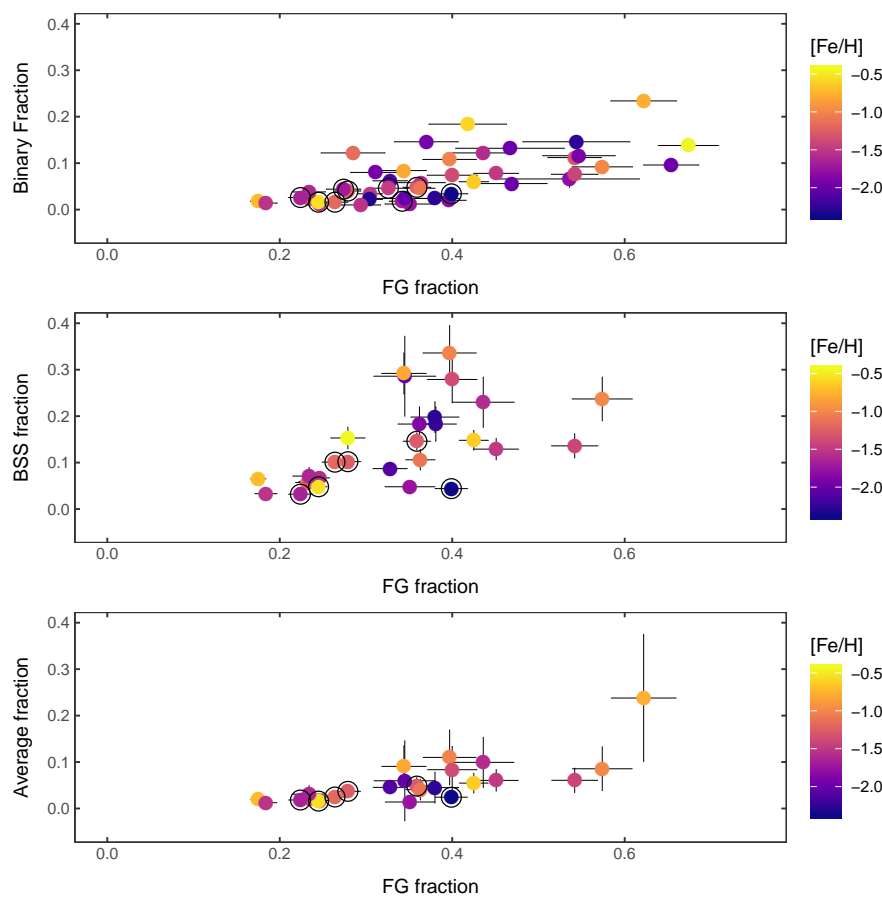


Fig. 26 Upper: run of the fraction of binaries within a cluster (Milone et al. 2012c, 2016) and the fraction of First Generation stars from Milone et al. (2017a). Circled symbols are for Type II clusters according to the classification by Milone et al. (2017a). Colours code metallicity (see scale on the right of the plot). Middle panel: the same, but with the incidence of BSS (Moretti et al. 2008). Lower panel: the same, but with the average of the fraction of binaries and of the incidence of BSS for individual clusters. This last was divided by 3 before making the average to scale it similarly to the binary fraction.

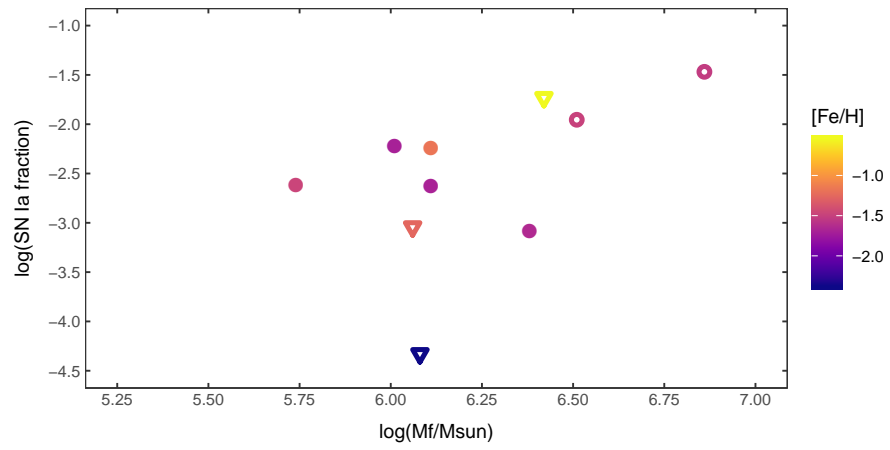


Fig. 27 Fraction of the ejecta of core collapse SNe retained by Type II GCs. Open circles (for NGC 5139 and NGC 6715) indicate uncertain quantities, inverted triangles indicate upper limits. Colours code metallicity (see scale on the right of the plot)

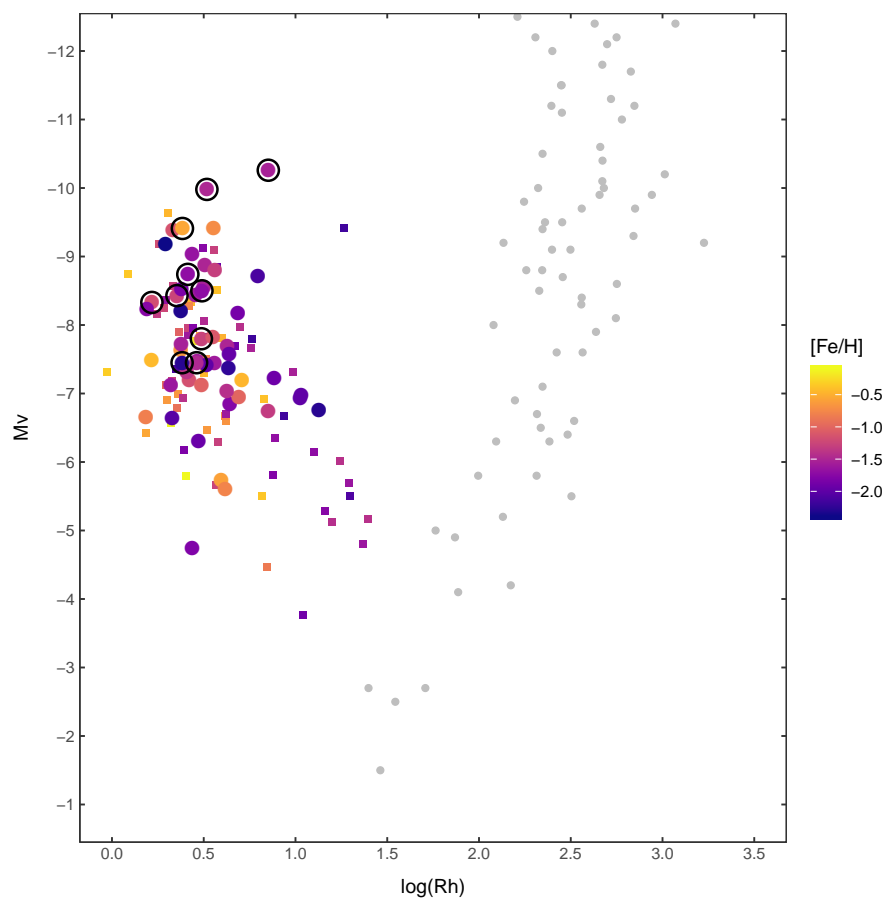


Fig. 28 Relation between M_V and half-mass radius for dwarf galaxies (grey circles) and GCs. Filled circles indicate Type I and Type II (circled symbols) clusters, while squares indicate clusters for which the type has not been determined. Colours code metallicity (see scale on the right of the plot). Data are taken by [McConnachie \(2012\)](#) for dwarfs, [Harris \(1996\)](#) and [Baumgardt and Hilker \(2018\)](#) for GCs.

Table 6 Cont...

| Name | R_{per} (kpc) | R_{apo} (kpc) | dMY | Υ^{med} | Υ^{max} | $\Upsilon^{max} - \Upsilon^{med}$ | Δ ($B - V$) | Δ ($V - I$) |
|----------|--------------------|--------------------|-------|------------------|------------------|-----------------------------------|-------------------------|-------------------------|
| Ter 3 | 2.26 | 3.25 | | | | | | |
| NGC 6171 | 1.02 | 3.65 | 0.005 | 0.232 | 0.235 | 0.003 | 0.001 | 0.002 |
| 1636-283 | 0.48 | 2.75 | | | | | | |
| NGC 6205 | 1.55 | 8.32 | 0.082 | 0.260 | 0.325 | 0.065 | 0.026 | 0.033 |
| NGC 6218 | 2.35 | 4.79 | 0.026 | 0.270 | 0.290 | 0.020 | 0.008 | 0.011 |
| NGC 6229 | 1.94 | 30.94 | | | | | | |
| NGC 6235 | 1.53 | 19.42 | | | | | | |
| NGC 6254 | 1.97 | 4.58 | 0.051 | 0.287 | 0.327 | 0.040 | 0.016 | 0.021 |
| Pal 15 | 1.68 | 51.54 | | | | | | |
| NGC 6266 | 0.83 | 2.36 | 0.068 | 0.262 | 0.314 | 0.052 | 0.020 | 0.029 |
| NGC 6273 | 1.22 | 3.33 | 0.104 | 0.261 | 0.344 | 0.083 | 0.034 | 0.041 |
| NGC 6284 | 1.28 | 7.35 | 0.028 | 0.278 | 0.300 | 0.022 | 0.009 | 0.012 |
| NGC 6287 | 1.25 | 5.86 | 0.027 | 0.230 | 0.252 | 0.022 | 0.009 | 0.010 |
| NGC 6304 | 1.77 | 3.01 | | | | | | |
| NGC 6316 | 1.45 | 4.79 | | | | | | |
| NGC 6333 | 1.16 | 6.65 | | | | | | |
| NGC 6341 | 1.00 | 10.53 | 0.027 | 0.239 | 0.260 | 0.021 | 0.009 | 0.009 |
| NGC 6342 | 1.12 | 1.88 | 0.027 | 0.250 | 0.267 | 0.017 | 0.006 | 0.011 |
| NGC 6352 | 2.98 | 3.59 | 0.0 | 0.258 | 0.258 | 0.000 | 0.0 | 0.0 |
| NGC 6356 | 3.17 | 8.35 | | | | | | |
| IC 1257 | 2.01 | 18.05 | | | | | | |
| NGC 6362 | 2.52 | 5.14 | 0.030 | 0.237 | 0.260 | 0.023 | 0.009 | 0.013 |
| NGC 6366 | 2.04 | 5.43 | 0.007 | 0.248 | 0.252 | 0.004 | 0.002 | 0.003 |
| Ter 4 | 0.41 | 1.45 | | | | | | |
| Liller 1 | 0.14 | 1.07 | | | | | | |
| NGC 6380 | 0.33 | 2.38 | | | | | | |
| Ter 2 | 0.18 | 1.12 | | | | | | |
| NGC 6388 | 1.11 | 3.79 | 0.060 | 0.250 | 0.287 | 0.037 | 0.014 | 0.023 |
| NGC 6397 | 2.63 | 6.23 | 0.0 | 0.262 | 0.262 | 0.000 | 0.0 | 0.0 |
| NGC 6401 | 0.60 | 2.04 | | | | | | |
| NGC 6402 | 0.65 | 4.35 | | | | | | |
| Pal 6 | 0.40 | 3.71 | | | | | | |
| NGC 6426 | 26.84 | 215.31 | | | | | | |
| Ter 5 | 0.82 | 2.83 | | | | | | |
| NGC 6440 | 0.30 | 1.53 | | | | | | |
| NGC 6441 | 1.00 | 3.91 | 0.053 | 0.250 | 0.283 | 0.033 | 0.012 | 0.021 |
| UKS 1 | 0.25 | 1.06 | | | | | | |
| NGC 6496 | 4.02 | 11.54 | 0.003 | 0.250 | 0.252 | 0.002 | 0.001 | 0.001 |
| Djorg 2 | 0.82 | 2.85 | | | | | | |
| NGC 6517 | 0.50 | 4.24 | | | | | | |
| Ter 10 | 0.94 | 2.41 | | | | | | |
| NGC 6528 | 0.41 | 1.61 | | | | | | |

Table 6 Cont...

| Name | R_{per} (kpc) | R_{apo} (kpc) | dMY | Y^{med} | Y^{max} | $Y^{max} - Y^{med}$ | Δ ($B - V$) | Δ ($V - I$) |
|----------|--------------------|--------------------|-------|-----------|-----------|---------------------|-------------------------|-------------------------|
| NGC 6535 | 1.01 | 4.47 | 0.018 | 0.272 | 0.286 | 0.014 | 0.006 | 0.007 |
| NGC 6541 | 1.76 | 3.64 | 0.071 | 0.252 | 0.308 | 0.056 | 0.023 | 0.028 |
| NGC 6544 | 0.62 | 5.48 | 0.017 | 0.273 | 0.286 | 0.013 | 0.005 | 0.007 |
| NGC 6553 | 1.29 | 2.35 | | | | | | |
| IC 1276 | 3.47 | 5.76 | | | | | | |
| Ter 12 | 2.99 | 5.82 | | | | | | |
| NGC 6569 | 1.84 | 2.94 | | | | | | |
| NGC 6584 | 2.10 | 19.25 | 0.046 | 0.235 | 0.271 | 0.036 | 0.014 | 0.019 |
| NGC 6624 | 0.46 | 1.56 | 0.017 | 0.250 | 0.260 | 0.010 | 0.004 | 0.006 |
| NGC 6626 | 0.57 | 2.90 | | | | | | |
| NGC 6637 | 0.73 | 2.07 | 0.010 | 0.247 | 0.254 | 0.007 | 0.003 | 0.004 |
| NGC 6638 | 0.40 | 2.94 | | | | | | |
| NGC 6642 | 0.37 | 2.11 | | | | | | |
| NGC 6652 | 0.65 | 3.66 | 0.0 | 0.242 | 0.242 | 0.000 | 0.0 | 0.0 |
| NGC 6656 | 2.96 | 9.45 | 0.021 | 0.252 | 0.269 | 0.017 | 0.007 | 0.008 |
| Pal 8 | 2.29 | 5.58 | | | | | | |
| NGC 6681 | 0.84 | 4.97 | 0.048 | 0.262 | 0.299 | 0.037 | 0.015 | 0.019 |
| NGC 6712 | 0.45 | 4.77 | | | | | | |
| NGC 6715 | 12.58 | 36.93 | | | | | | |
| NGC 6717 | 0.89 | 2.72 | 0.0 | 0.261 | 0.261 | 0.000 | 0.0 | 0.0 |
| NGC 6723 | 2.08 | 2.84 | 0.062 | 0.241 | 0.287 | 0.046 | 0.018 | 0.026 |
| NGC 6749 | 1.60 | 5.07 | | | | | | |
| NGC 6752 | 3.23 | 5.37 | 0.076 | 0.268 | 0.327 | 0.059 | 0.024 | 0.031 |
| NGC 6760 | 1.90 | 5.67 | | | | | | |
| NGC 6779 | 0.97 | 12.30 | 0.031 | 0.247 | 0.271 | 0.024 | 0.010 | 0.012 |
| Ter 7 | 13.14 | 44.72 | | | | | | |
| Pal 10 | 4.01 | 7.02 | | | | | | |
| Arp 2 | 18.46 | 60.87 | | | | | | |
| NGC 6809 | 1.59 | 5.54 | 0.032 | 0.250 | 0.275 | 0.025 | 0.011 | 0.012 |
| Ter 8 | 16.23 | 53.86 | | | | | | |
| Pal 11 | 5.43 | 9.16 | | | | | | |
| NGC 6838 | 4.77 | 7.08 | 0.0 | 0.227 | 0.227 | 0.000 | 0.0 | 0.0 |
| NGC 6864 | 2.06 | 17.98 | | | | | | |
| NGC 6934 | 2.60 | 39.52 | 0.058 | 0.238 | 0.283 | 0.045 | 0.018 | 0.023 |
| NGC 6981 | 1.29 | 24.01 | 0.047 | 0.238 | 0.274 | 0.036 | 0.015 | 0.019 |
| NGC 7006 | 2.07 | 55.50 | | | | | | |
| NGC 7078 | 3.57 | 10.39 | 0.091 | 0.232 | 0.305 | 0.073 | 0.031 | 0.032 |
| NGC 7089 | 0.56 | 16.80 | 0.097 | 0.253 | 0.330 | 0.077 | 0.031 | 0.039 |
| NGC 7099 | 1.49 | 8.15 | 0.005 | 0.245 | 0.249 | 0.004 | 0.002 | 0.002 |
| Pal 12 | 15.75 | 71.17 | | | | | | |
| Pal 13 | 9.04 | 67.47 | | | | | | |
| NGC 7492 | 4.27 | 28.23 | | | | | | |

Table 7 Additional parameters for selected GCs

| Name | dY_{2g1G} | err | dY_{max} | err | [Fe/H] | $d[Fe/H]$ | err | Log (M_{fin}) | Log (M_{in}) |
|----------|-------------|-------|------------|-------|--------|-----------|-------|----------------------|---------------------|
| NGC 104 | 0.011 | 0.005 | 0.049 | 0.005 | -0.72 | 0.012 | 0.010 | 5.88 | 6.23 |
| NGC 288 | 0.015 | 0.010 | 0.016 | 0.012 | -1.32 | 0.007 | 0.013 | 5.08 | 5.58 |
| NGC 362 | 0.008 | 0.006 | 0.026 | 0.008 | -1.26 | | | 5.52 | 6.06 |
| NGC 1261 | 0.004 | 0.004 | 0.019 | 0.007 | -1.27 | | | 5.26 | 5.86 |
| Eridanus | | | | | -1.43 | | | 4.04 | 4.41 |
| Pal 2 | | | | | -1.42 | | | 5.36 | 6.05 |
| NGC 1851 | 0.007 | 0.005 | 0.025 | 0.006 | -1.18 | | | 5.45 | 6.11 |
| NGC 1904 | | | | | -1.60 | 0.013 | 0.015 | 5.23 | 6.08 |
| NGC 2298 | -0.003 | 0.009 | 0.011 | 0.012 | -1.92 | | | 4.65 | 5.64 |
| NGC 2419 | | | 0.19 | | -2.15 | | | 6.09 | 6.40 |
| NGC 2808 | 0.048 | 0.005 | 0.124 | 0.007 | -1.14 | 0.070 | 0.018 | 5.91 | 6.36 |
| Pal 3 | | | | | -1.63 | | | 4.36 | 4.70 |
| NGC 3201 | -0.001 | 0.013 | 0.028 | 0.032 | -1.59 | -0.026 | 0.013 | 5.12 | 5.51 |
| Pal 4 | | | | | -1.41 | | | 4.43 | 4.80 |
| NGC 4147 | | | | | -1.80 | | | 4.50 | 5.56 |
| NGC 4372 | | | | | -2.17 | | | 5.34 | 5.81 |
| Rup 106 | | | | | -1.68 | | | 4.57 | 5.16 |
| NGC 4590 | 0.007 | 0.009 | 0.012 | 0.009 | -2.23 | -0.021 | 0.018 | 5.09 | 5.48 |
| NGC 4833 | 0.016 | 0.008 | 0.051 | 0.009 | -1.85 | | | 5.24 | 6.05 |
| NGC 5024 | 0.013 | 0.007 | 0.044 | 0.008 | -2.10 | | | 5.53 | 5.88 |
| NGC 5053 | -0.002 | 0.013 | 0.004 | 0.025 | -2.27 | | | 4.75 | 5.20 |
| NGC 5139 | 0.033 | 0.006 | 0.090 | 0.010 | -1.53 | | | 6.53 | 6.86 |
| NGC 5272 | 0.016 | 0.005 | 0.041 | 0.009 | -1.50 | | | 5.57 | 5.94 |
| NGC 5286 | 0.007 | 0.006 | 0.044 | 0.004 | -1.69 | | | 5.58 | 6.11 |
| NGC 5466 | 0.002 | 0.017 | 0.007 | 0.024 | -1.98 | | | 4.64 | 5.12 |
| NGC 5634 | | | | | -1.88 | | | 5.33 | 5.77 |
| NGC 5694 | | | | | -1.98 | | | 5.56 | 5.92 |
| IC 4499 | 0.004 | 0.006 | 0.017 | 0.008 | -1.53 | | | 5.08 | 5.50 |
| NGC 5824 | | | | | -1.91 | | | 5.87 | 6.19 |
| Pal 5 | | | | | -1.41 | | | 4.22 | 4.86 |
| NGC 5897 | | | | | -1.90 | | | 5.22 | 5.77 |
| NGC 5904 | 0.012 | 0.004 | 0.037 | 0.007 | -1.29 | -0.001 | 0.010 | 5.56 | 5.96 |
| NGC 5927 | 0.011 | 0.004 | 0.055 | 0.015 | -0.49 | | | 5.40 | 5.83 |
| NGC 5946 | | | | | -1.29 | | | 5.06 | 6.02 |
| NGC 5986 | 0.005 | 0.006 | 0.031 | 0.012 | -1.59 | | | 5.52 | 6.20 |
| Lynga 7 | | | | | -1.01 | | | 5.00 | 5.72 |
| Pal 14 | | | | | -1.41 | | | 4.19 | 5.07 |
| NGC 6093 | 0.011 | 0.008 | 0.027 | 0.012 | -1.75 | | | 5.44 | 6.33 |
| NGC 6101 | 0.005 | 0.010 | 0.017 | 0.011 | -1.98 | | | 5.10 | 5.47 |
| NGC 6121 | 0.009 | 0.006 | 0.014 | 0.006 | -1.16 | 0.008 | 0.012 | 4.95 | 6.03 |
| NGC 6139 | | | | | -1.65 | | | 5.53 | 6.07 |
| NGC 6144 | 0.009 | 0.011 | 0.017 | 0.013 | -1.76 | | | 4.72 | 5.61 |
| Ter 3 | | | | | -0.74 | | | 4.70 | 5.88 |

Table 7 Cont...

| Name | dY _{2g1G} | err | dYmax | err | [Fe/H] | d[Fe/H] | err | Log (M _{fin}) | Log (M _{in}) |
|----------|--------------------|-------|-------|-------|--------|---------|-------|----------------------------|---------------------------|
| NGC 6171 | 0.019 | 0.011 | 0.024 | 0.014 | -1.02 | 0.018 | 0.025 | 4.94 | 5.86 |
| 1636-283 | | | | | -1.50 | | | | |
| NGC 6205 | 0.020 | 0.004 | 0.052 | 0.004 | -1.53 | | | 5.66 | 6.11 |
| NGC 6218 | 0.009 | 0.007 | 0.011 | 0.011 | -1.37 | 0.000 | 0.009 | 4.90 | 5.63 |
| NGC 6229 | | | | | -1.47 | | | 5.46 | 6.02 |
| NGC 6235 | | | | | -1.28 | | | 5.04 | 5.49 |
| NGC 6254 | 0.006 | 0.008 | 0.029 | 0.011 | -1.56 | -0.002 | 0.015 | 5.27 | 5.83 |
| Pal 15 | | | | | -2.07 | | | 4.62 | 5.62 |
| NGC 6266 | | | | | -1.18 | | | 5.82 | 6.29 |
| NGC 6273 | | | | | -1.74 | | | 5.81 | 6.27 |
| NGC 6284 | | | | | -1.26 | | | 5.39 | 5.96 |
| NGC 6287 | | | | | -2.10 | | | 5.12 | 5.85 |
| NGC 6304 | 0.008 | 0.005 | 0.025 | 0.006 | -0.45 | | | 5.16 | 5.80 |
| NGC 6316 | | | | | -0.45 | | | 5.57 | 6.12 |
| NGC 6333 | | | | | -1.77 | | | 5.48 | 6.05 |
| NGC 6341 | 0.022 | 0.004 | 0.039 | 0.006 | -2.31 | | | 5.49 | 6.09 |
| NGC 6342 | | | | | -0.55 | | | 4.78 | 5.89 |
| NGC 6352 | 0.019 | 0.014 | 0.027 | 0.006 | -0.64 | | | 4.78 | 5.56 |
| NGC 6356 | | | | | -0.40 | | | 5.57 | 6.04 |
| IC 1257 | | | | | -1.70 | | | 4.80 | 5.64 |
| NGC 6362 | 0.003 | 0.011 | 0.004 | 0.011 | -0.99 | | | 5.05 | 5.67 |
| NGC 6366 | 0.022 | 0.010 | 0.011 | 0.015 | -0.59 | | | 4.70 | 5.51 |
| Ter 4 | | | | | -1.41 | | | 4.88 | 6.19 |
| Liller 1 | | | | | -0.33 | | | 5.81 | 6.49 |
| NGC 6380 | | | | | -0.75 | | | 5.48 | 6.32 |
| Ter 2 | | | | | -0.70 | | | 4.52 | 6.35 |
| NGC 6388 | 0.019 | 0.007 | 0.067 | 0.009 | -0.55 | 0.038 | 0.042 | 6.02 | 6.42 |
| NGC 6397 | 0.006 | 0.009 | 0.008 | 0.011 | -2.02 | | | 4.94 | 5.60 |
| NGC 6401 | | | | | -1.02 | | | 5.45 | 6.20 |
| NGC 6402 | | | | | -1.28 | 0.029 | 0.021 | 5.87 | 6.38 |
| Pal 6 | | | | | -0.91 | | | 5.13 | 6.24 |
| NGC 6426 | | | | | -2.15 | | | 4.84 | 5.19 |
| Ter 5 | | | | | -0.23 | | | 5.59 | 6.13 |
| NGC 6440 | | | | | -0.36 | | | 5.58 | 6.37 |
| NGC 6441 | 0.029 | 0.006 | 0.081 | 0.022 | -0.46 | | | 6.06 | 6.46 |
| UKS 1 | | | | | -0.64 | | | 4.88 | 6.29 |
| NGC 6496 | 0.009 | 0.011 | 0.021 | 0.006 | -0.46 | | | 4.63 | 5.29 |
| Djorg 2 | | | | | -0.65 | | | 4.79 | 5.96 |
| NGC 6517 | | | | | -1.23 | | | 5.56 | 6.26 |
| Ter 10 | | | | | -1.79 | | | 4.72 | 5.88 |
| NGC 6528 | | | | | -0.11 | | | 4.97 | 6.19 |
| NGC 6535 | 0.003 | 0.021 | 0.003 | 0.022 | -1.79 | | | 3.97 | 5.77 |

Table 7 Cont...

| Name | dY _{2g1G} | err | dYmax | err | [Fe/H] | d[Fe/H] | err | Log (M _{fin}) | Log (M _{in}) |
|----------|--------------------|-------|-------|-------|--------|---------|-------|----------------------------|---------------------------|
| NGC 6541 | 0.024 | 0.005 | 0.045 | 0.006 | -1.81 | | | 5.39 | 5.95 |
| NGC 6544 | | | | | -1.40 | | | 5.06 | 6.09 |
| NGC 6553 | | | | | -0.18 | | | 5.52 | 6.07 |
| IC 1276 | | | | | -0.75 | | | 4.96 | 5.55 |
| Ter 12 | | | | | -0.50 | | | 3.13 | 5.18 |
| NGC 6569 | | | | | -0.76 | | | 5.36 | 5.96 |
| NGC 6584 | 0.0 | 0.007 | 0.015 | 0.011 | -1.50 | | | 5.23 | 5.84 |
| NGC 6624 | 0.010 | 0.004 | 0.022 | 0.003 | -0.44 | | | 4.88 | 6.18 |
| NGC 6626 | | | | | -1.32 | | | 5.47 | 6.21 |
| NGC 6637 | 0.004 | 0.006 | 0.011 | 0.005 | -0.64 | | | 5.16 | 6.18 |
| NGC 6638 | | | | | -0.95 | | | 5.26 | 6.27 |
| NGC 6642 | | | | | -1.26 | | | 4.58 | 6.27 |
| NGC 6652 | 0.008 | 0.007 | 0.017 | 0.011 | -0.81 | | | 4.79 | 6.19 |
| NGC 6656 | 0.005 | 0.008 | 0.041 | 0.012 | -1.70 | | | 5.60 | 6.01 |
| Pal 8 | | | | | -0.37 | | | 4.75 | 5.61 |
| NGC 6681 | 0.009 | 0.008 | 0.029 | 0.015 | -1.62 | | | 5.06 | 5.94 |
| NGC 6712 | | | | | -1.02 | | | 5.07 | 6.21 |
| NGC 6715 | 0.012 | 0.003 | 0.052 | 0.012 | -1.49 | | | 6.19 | 6.51 |
| NGC 6717 | 0.003 | 0.006 | 0.003 | 0.009 | -1.26 | | | 4.24 | 5.87 |
| NGC 6723 | 0.005 | 0.006 | 0.024 | 0.007 | -1.10 | | | 5.22 | 5.85 |
| NGC 6749 | | | | | -1.60 | | | 4.90 | 5.68 |
| NGC 6752 | 0.015 | 0.005 | 0.042 | 0.004 | -1.54 | -0.014 | 0.014 | 5.36 | 5.83 |
| NGC 6760 | | | | | -0.40 | | | 5.43 | 5.92 |
| NGC 6779 | 0.011 | 0.007 | 0.031 | 0.008 | -1.98 | | | 5.18 | 6.01 |
| Ter 7 | | | | | -0.32 | | | 4.31 | 4.75 |
| Pal 10 | | | | | -0.10 | | | 4.74 | 5.38 |
| Arp 2 | | | | | -1.75 | | | 4.56 | 4.98 |
| NGC 6809 | 0.014 | 0.008 | 0.026 | 0.015 | -1.94 | -0.009 | 0.013 | 5.27 | 5.88 |
| Ter 8 | | | | | -2.16 | | | 4.80 | 5.18 |
| Pal 11 | | | | | -0.40 | | | 4.78 | 5.34 |
| NGC 6838 | 0.005 | 0.009 | 0.024 | 0.010 | -0.78 | -0.005 | 0.016 | 4.72 | 5.32 |
| NGC 6864 | | | | | -1.29 | | | 5.60 | 6.07 |
| NGC 6934 | 0.006 | 0.003 | 0.018 | 0.004 | -1.47 | | | 5.25 | 5.74 |
| NGC 6981 | 0.011 | 0.006 | 0.017 | 0.006 | -1.42 | | | 4.87 | 5.88 |
| NGC 7006 | | | | | -1.52 | | | 5.10 | 5.72 |
| NGC 7078 | 0.021 | 0.009 | 0.069 | 0.006 | -2.37 | -0.008 | 0.022 | 5.69 | 6.08 |
| NGC 7089 | 0.013 | 0.005 | 0.052 | 0.009 | -1.65 | | | 5.70 | 6.38 |
| NGC 7099 | 0.015 | 0.010 | 0.022 | 0.010 | -2.27 | -0.027 | 0.020 | 5.11 | 5.79 |
| Pal 12 | | | | | -0.85 | | | 3.76 | 4.33 |
| Pal 13 | | | | | -1.88 | | | 3.49 | 4.36 |
| NGC 7492 | | | | | -1.78 | | | 4.51 | 5.25 |

Table 8 Additional parameters for selected GCs

| Name | IQR [O/Na] | IQR source | IQR [Al/Mg] | dRGB | err | f(FG) | err | GC type | δ [Al/Mg] |
|----------|---------------|---------------|----------------|-------|-------|-------|-------|------------|---------------------|
| NGC 104 | 0.472 | 1 | 0.091 | 0.369 | 0.009 | 0.175 | 0.009 | 1 | 0.3 |
| NGC 288 | 0.776 | 1 | 0.059 | 0.276 | 0.008 | 0.542 | 0.031 | 1 | 0.2 |
| NGC 362 | 0.644 | 1 | 0.405 | 0.275 | 0.005 | 0.279 | 0.015 | 2 | 0.4 |
| NGC 1261 | | | | 0.29 | 0.01 | 0.359 | 0.016 | 2 | |
| Eridanus | | | | | | | | | |
| Pal 2 | | | | | | | | | |
| NGC 1851 | 0.693 | 1 | 0.45 | 0.342 | 0.005 | 0.264 | 0.015 | 2 | 0.4 |
| NGC 1904 | 0.759 | 1 | 0.438 | | | | | | |
| NGC 2298 | | | | 0.243 | 0.017 | 0.37 | 0.037 | 1 | |
| NGC 2419 | | | | | | 0.37 | 0.01 | | |
| NGC 2808 | 0.999 | 1 | 0.935 | 0.457 | 0.009 | 0.232 | 0.014 | 1 | 1.25 |
| Pal 3 | | | | | | | | | |
| NGC 3201 | 0.634 | 1 | 0.383 | 0.292 | 0.016 | 0.436 | 0.036 | 1 | 0.5 |
| Pal 4 | | | | | | | | | |
| NGC 4147 | 0.560 | 2 | | | | | | | |
| NGC 4372 | 0.390 | 3 | | | | | | | |
| Rup 106 | 0.160 | 28 | | | | 1.0 | 0.1 | | |
| NGC 4590 | 0.372 | 1 | 0.274 | 0.132 | 0.007 | 0.381 | 0.024 | 1 | 0.3 |
| NGC 4833 | 0.945 | 1 | 0.81 | 0.26 | 0.008 | 0.362 | 0.025 | 1 | 0.65 |
| NGC 5024 | 0.400 | 4 | 0.8 | 0.209 | 0.005 | 0.328 | 0.02 | 1 | 0.5 |
| NGC 5053 | 0.950 | 4 | | 0.102 | 0.013 | 0.544 | 0.062 | 1 | 1.1 |
| NGC 5139 | 1.200 | 5 | | 0.39 | 0.01 | 0.086 | 0.01 | 2 | 0.85 |
| NGC 5272 | 0.610 | 6 | 0.9 | 0.279 | 0.007 | 0.305 | 0.014 | 1 | 0.55 |
| NGC 5286 | 0.700 | 7 | | 0.303 | 0.007 | 0.342 | 0.015 | 2 | |
| NGC 5466 | | | 0.4 | 0.141 | 0.016 | 0.467 | 0.063 | 1 | 0.5 |
| NGC 5634 | 0.756 | 1 | 0.44 | | | | | | |
| NGC 5694 | 0.260 | 9 | 0.2 | | | | | | |
| IC 4499 | | | | | | | | | |
| NGC 5824 | | 30 | 0.92 | | | | | | |
| Pal 5 | | | | | | | | | |
| NGC 5897 | 0.620 | 11 | | 0.149 | 0.008 | 0.547 | 0.042 | 1 | |
| NGC 5904 | 0.741 | 1 | 0.541 | 0.332 | 0.013 | 0.235 | 0.013 | 1 | 0.6 |
| NGC 5927 | 0.600 | 10 | 0.1 | 0.422 | 0.02 | | | | 0.1 |
| NGC 5946 | | | | | | | | | |
| NGC 5986 | 0.580 | 14 | 0.6 | 0.294 | 0.008 | 0.246 | 0.012 | 1 | 0.65 |
| Lynga 7 | | | | | | | | | |
| Pal 14 | | | | | | | | | |
| NGC 6093 | 0.784 | 1 | 0.56 | 0.305 | 0.015 | 0.351 | 0.029 | 1 | 0.5 |
| NGC 6101 | | | | 0.14 | 0.009 | 0.654 | 0.032 | 1 | |
| NGC 6121 | 0.373 | 1 | 0.18 | 0.27 | 0.012 | 0.285 | 0.037 | 1 | 0.0 |
| NGC 6139 | 0.647 | 1 | 0.436 | | | | | | |
| NGC 6144 | | | | 0.21 | 0.012 | 0.444 | 0.037 | 1 | |

Table 8 Cont...

| Name | IQR [O/Na] | IQR source | IQR [Al/Mg] | dRGB | err | f(FG) | err | GC type | δ [Al/Mg] |
|----------|---------------|---------------|----------------|-------|-------|-------|-------|------------|---------------------|
| Ter 3 | | | | | | | | | |
| NGC 6171 | 0.522 | 1 | 0.1 | 0.351 | 0.017 | 0.397 | 0.031 | 1 | 0.0 |
| 1636-283 | | | | | | | | | |
| NGC 6205 | 0.890 | 6 | 1.1 | 0.291 | 0.006 | 0.184 | 0.013 | 1 | 0.9 |
| NGC 6218 | 0.863 | 1 | 0.271 | 0.274 | 0.009 | 0.4 | 0.029 | 1 | 0.3 |
| NGC 6229 | 0.810 | 13 | | | | | | | |
| NGC 6235 | | | | | | | | | |
| NGC 6254 | 0.565 | 1 | 0.75 | 0.31 | 0.007 | 0.364 | 0.028 | 1 | 0.6 |
| Pal 15 | | | | | | | | | |
| NGC 6266 | 1.160 | 16 | | | | | | | |
| NGC 6273 | | 15 | 0.32 | | | | | | |
| NGC 6284 | | | | | | | | | |
| NGC 6287 | | | | | | | | | |
| NGC 6304 | | | | 0.32 | 0.024 | | | | |
| NGC 6316 | | | | | | | | | |
| NGC 6333 | | | | | | | | | |
| NGC 6341 | | | 0.9 | 0.177 | 0.005 | 0.304 | 0.015 | 1 | 0.9 |
| NGC 6342 | | | | | | | | | |
| NGC 6352 | | 17 | 0.14 | 0.395 | 0.015 | 0.474 | 0.035 | 0 | |
| NGC 6356 | | | | | | | | | |
| IC 1257 | | | | | | | | | |
| NGC 6362 | 0.280 | 18 | 0.11 | 0.292 | 0.011 | 0.574 | 0.035 | 1 | 0.0 |
| NGC 6366 | 0.280 | 12 | | 0.291 | 0.064 | 0.418 | 0.045 | 1 | 0.15 |
| Ter 4 | | | | | | | | | |
| Liller 1 | | | | | | | | | |
| NGC 6380 | | | | | | | | | |
| Ter 2 | | | | | | | | | |
| NGC 6388 | 0.644 | 1 | 0.529 | 0.494 | 0.01 | 0.245 | 0.01 | 2 | 0.55 |
| NGC 6397 | 0.274 | 1 | | 0.117 | 0.023 | 0.345 | 0.036 | 1 | 0.1 |
| NGC 6401 | | | | | | | | | |
| NGC 6402 | 0.525 | 33 | 0.270 | | | | | | |
| Pal 6 | | | | | | | | | |
| NGC 6426 | | | | | | | | | |
| Ter 5 | | | | | | | | | |
| NGC 6440 | 0.370 | 19 | 0.41 | | | | | | |
| NGC 6441 | 0.660 | 1 | | 0.512 | 0.015 | | | | 0.2 |
| UKS 1 | | | | | | | | | |
| NGC 6496 | | | | 0.331 | 0.038 | 0.674 | 0.035 | 1 | |
| Djorg 2 | | | | | | | | | |
| NGC 6517 | | | | | | | | | |
| Ter 10 | | | | | | | | | |
| NGC 6528 | 0.650 | 29 | 0.14 | | | | | | |

Table 9 Data for extra-galactic massive clusters

| Cluster | Age Gyr | [Fe/H] | $\log M/M_{\odot}$ | FG/tot | dCUNBI | d(C/N) | IQR(Na/O) | Source |
|---------------|------------|--------|--------------------|--------|--------|--------|-----------|---|
| SMC-Kron 3 | 6.5 | -1.08 | 5.17 | 0.68 | | 0.99 | | Hollyhead et al. (2018) |
| SMC-NGC 121 | 10.5 | -1.46 | 5.50 | 0.70 | 0.14 | | | Niederhofer et al. (2017b) Dalessandro et al. (2016) |
| SMC-Lindsay 1 | 7.5 | -1.14 | 5.28 | 0.70 | 0.08 | | | Niederhofer et al. (2017a) Hollyhead et al. (2017) |
| SMC-NGC 339 | 6.0 | -1.12 | 4.96 | 0.59 | 0.08 | | | Niederhofer et al. (2017a) |
| SMC-NGC 416 | 6.0 | -1.00 | 5.24 | 0.47 | 0.12 | | | Niederhofer et al. (2017a) |
| SMC-NGC 419 | 1.5 | -0.70 | 5.23 | 1.00 | 0.00 | | | Martocchia et al. (2017) |
| LMC-NGC 1783 | 1.8 | -0.36 | 5.26 | 1.00 | | | 1.20 | Zhang et al. (2018) |
| LMC-NGC 1786 | 13.4 | -1.87 | 5.57 | 0.42 | | | 1.20 | Mucciarelli et al. (2009) |
| LMC-NGC 1806 | 1.7 | -0.30 | 5.01 | 1.00 | 0.00 | | | Mucciarelli et al. (2014a) |
| LMC-NGC 1978 | 1.9 | -0.38 | 5.33 | 0.80 | 0.06 | | | Martocchia et al. (2018b) |
| LMC-NGC 2210 | 13.4 | -1.63 | 5.48 | 0.40 | | | 0.78 | Mucciarelli et al. (2009) |
| LMC-NGC 2257 | 13.4 | -1.63 | 5.41 | 0.33 | | | 0.51 | Mucciarelli et al. (2009) |
| LMC-Hodge 6 | 2.0 | -0.30 | 4.90 | 0.87 | | | | Hollyhead et al. (2019) |
| LMC-Hodge 11 | 13.4 | -2.06 | 5.63 | | | | | Mateluna et al. (2012) |

Table 10 Data for MW open clusters (GES is GAIA-ESO Survey)

| Cluster | M_J | $\log M$ (M_{\odot}) | age (Gyr) | [Fe/H] | Spectr. ref. |
|--------------|--------|-----------------------------|--------------|--------|---|
| Berkeley39 | -5.071 | | 6.5 | -0.20 | Bragaglia et al. (2012) |
| Berkeley81 | -5.624 | | 1 | +0.23 | Magrini et al. (2015) (GES) |
| Collinder261 | -6.211 | | 6 | -0.03 | MacLean et al. (2015) |
| IC4756 | -4.535 | 3.428 | 0.8 | -0.02 | Bagdonas et al. (2018) |
| NGC 2360 | -5.475 | 2.980 | 1.1 | -0.07 | Peña Suárez et al. (2018) |
| NGC 2420 | -5.435 | | 2 | -0.16 | Souto et al. (2016) (APOGEE) |
| NGC 2682 | -5.025 | 2.446 | 4 | +0.03 | MacLean et al. (2015) |
| NGC 3114 | -5.459 | 3.247 | 0.16 | -0.01 | Santrich et al. (2013) |
| NGC 3680 | -4.077 | 2.124 | 1.8 | -0.06 | Peña Suárez et al. (2018) |
| NGC 5822 | -5.346 | 3.519 | 0.9 | -0.09 | Peña Suárez et al. (2018) |
| NGC 6134 | -4.986 | | 0.9 | +0.15 | Mikolaitis et al. (2010) |
| NGC 6705 | -5.295 | | 0.3 | +0.10 | Cantat-Gaudin et al. (2014) (GES) |
| NGC 6791 | -7.298 | 3.700 | 8 | +0.40 | Bragaglia et al. (2014) ; Villanova et al. (2018) |
| NGC 6802 | -5.139 | | 0.9 | +0.10 | Tang et al. (2017) (GES) |
| NGC 6940 | -6.612 | 2.770 | 1.1 | +0.04 | Böcek Topcu et al. (2016) |
| NGC 752 | -4.198 | 3.440 | 1.6 | -0.02 | MacLean et al. (2015) |
| NGC 7789 | -6.789 | 3.922 | 1.6 | +0.03 | MacLean et al. (2015) |
| Pismis18 | -7.306 | | 0.7 | +0.23 | Hatzidimitriou et al. (2019) (GES) |
| Praesepe | -3.317 | 3.367 | 0.73 | +0.13 | MacLean et al. (2015) |
| Ruprecht147 | -3.489 | 2.148 | 2.5 | +0.08 | Bragaglia et al. (2018) |
| Trumpler20 | -7.40 | | 1.5 | +0.17 | Donati et al. (2014) (GES) |
| Trumpler23 | -5.129 | 3.0 | 0.8 | +0.14 | Overbeek et al. (2017) (GES) |

Notes: M_J and $\log M$ from [Piskunov et al. \(2008\)](#); $\log M$ for NGC 6791 based on $5000 M_{\odot}$ in [Platais et al. \(2011\)](#).